ABSTRACT

Title of dissertation: THE DIFFERENTIAL RADIAL CAPILLARY ACTION OF LIGAND ASSAY ENABLES SYSTEMATIC IDENTIFICATION AND CHARACTERIZATION OF LIGAND BINDING INTERACTIONS WITH PROTEINS AND NUCLEIC ACIDS

Kevin Gerrit Roelofs, Doctor of Philosophy, 2014

Dissertation directed by: Assoc. Professor Vincent T. Lee
Department of Cell Biology and Molecular Genetics

Cyclic di-GMP (cdiGMP) is a ubiquitous prokaryotic nucleotide signaling molecule that regulates important bacterial processes, including biofilm formation, motility, and virulence. The differential radial capillary action of ligand assay (DRaCALA) was developed to determine protein-ligand interactions and provide insight into the mechanism of cdiGMP signal transduction. DRaCALA is based on the ability of nitrocellulose membranes to separate free ligand from bound protein-ligand complexes resulting in precise measurements of the fraction of bound ligand. The principle of DRaCALA was demonstrated by detection of 3 radiolabeled nucleotides binding to their cognate receptors. DRaCALA also enabled the determination of affinity, specificity, and kinetics of cdiGMP-binding to Alg44. A unique feature of DRaCALA is the ability to determine specific binding interactions to heterologously expressed proteins in whole cell lysates, suggesting that individual open reading frames could be screened for the expression of a cdiGMP-binding protein. DRaCALA was applied on a genome-wide

scale to systematically screen protein products of over 98% of *Vibrio cholerae* open reading frames for cdiGMP-binding activity. The DRaCALA ORFeome screen identified 5 of 10 previously described cdiGMP-binding proteins, 19 proteins with predicted cdiGMP-binding domains, and 6 novel putative cdiGMP-binding proteins lacking a defined cdiGMP-binding site. Direct cdiGMP-binding was demonstrated for the T2SE ATPase MshE, and cdiGMP-binding activity was observed for a *Pseudomonas aeruginosa* homolog PA14_29490. These results suggest that cdiGMP-binding may be a conserved feature of a subset of T2SE ATPases that regulate type IV pili and type II secretion. Finally, the applications of DRaCALA were extended for the determination of protein binding to nucleotide polymers of DNA and RNA and cdiGMP-binding to a RNA aptamer. In total these studies report the development of DRaCALA as a novel biochemical assay and its use in the systematic identification and characterization of protein-ligand interactions.

THE DIFFERENTIAL RADIAL CAPILLARY ACTION OF LIGAND ASSAY ENABLES SYSTEMATIC IDENTIFICATION AND CHARACTERIZATION OF LIGAND BINDING INTERACTIONS WITH PROTEINS AND NUCLEIC ACIDS

by

Kevin Gerrit Roelofs

Dissertation submitted to the Faculty of the Graduate School of the
University of Maryland, College Park in partial fulfillment
of the requirements for the degree of
Doctor of Philosophy
2014

Advisory Committee:

Assoc. Professor Vincent Lee, Chair
Assoc. Professor Kevin McIver
Assoc. Professor Richard Stewart
Professor Daniel Stein
Professor Philip DeShong, Dean's Representative

Dedication: To my father Mark Roelofs, my mother Elizabeth McCord, my sisters Katie and Rebecca Roelofs and my younger brother Sean Roelofs, thank you for supporting me in all my endeavors. I would also like to thank my mentor Dr. Vincent Lee and members of the Lee Laboratory who have taught and inspired me.

Acknowledgements: I would like to acknowledge Greg Donaldson for his contributions to the development of DRaCALA, which are highlighted in Chapter 4. I would also like to thank Dr. Herman O. Sintim and his former graduate student Jingxin Wang for their contributions of reagents for the development of DRaCALA as indicated in Chapter 2.

Table of Contents **Page #**

List of Figures Page

Chapter 1

Chapter 2

Chapter 3

Chapter 4

List of Tables

Chapter 3

Chapter 4

Appendix A

List of Abbreviations

AC: adenlyate cyclase
AKAP: A-kinase anchoring protein
ATP: adenosine triphosphate
B_C: cdiGMP bound in the presence of unlabeled cdiGMP
B_G: cdiGMP bound in the presence of unlabeled GTP
CRP: cyclic AMP receptor protein
cdiAMP: cyclic di-adenosine monophosphate
cdiGMP: cyclic di-guanosine monophosphate
cAMP: cyclic adenosine monophosphate
cGMP: cyclic guanosine monophosphate
ChIP-chip: chromatin immunoprecipitation on a microarray chip
ChIP-seq: sequencing of chromatin immunoprecipitation
DRaCALA: Differential Radial Capillary Action of Ligand Assay
DGC: diguanylate cyclase
EDTA: ethylenediaminetetraacetic acid
EPAC: exchange protein directly activated by cAMP
EPS: exopolysaccharides
F_B: fraction bound
GPCR: G-coupled protein receptor
His-ORF: histidine fusion to an open reading frame
His-MBP-ORF: histidine-maltose binding protein fusion to an open reading frame
I-site: allosteric inhibitory binding site for cdiGMP in GGDEF domains
ITC: isothermal calorimetry
K_d: dissociation constant
k_{off}: dissociation rate
LC-MS: liquid chromatography-mass spectrometry
MBP: maltose binding protein
ORF: open reading frame
ORFeome: ORF library containing a majority of ORFs from a genome
polyP: polymers of inorganic phosphate
PAGE: polyacrylamide gel electrophoresis
PCR: polymerase chain reaction
PDE: phosphodiesterase
PNK: polynucleotide kinase
PKA: protein kinase A
PSL: photostimulated luminescence
(p)ppGpp: guanosine pentaphosphate
SD: standard deviation
SDS: sodium dodecyl sulfate
SE: standard error
SPR: surface plasmon resonance
SSC: saline sodium citrate
T2SE ATPases: hexameric ATPases regulating Type IV pili or Type II secretion
T3SS: Type 3 secretion system

TBE: tris borate EDTA
TLC: thin layer chromatography
VC ORF: *Vibrio cholerae* open reading frame
VPS: *Vibrio* Polysaccharide
UTR: untranslated region

Chapter 1: Introduction

1.1 Low Molecular Weight Molecules are Biological Signals

Living organisms rely on low molecular weight signaling molecules to regulate critical cellular processes. These signaling molecules are produced from metabolic precursors, but are primarily used for signal transduction. For example, steroid hormones such as testosterone and estradiol are produced from cholesterol, neurotransmitters dopamine and serotonin are modified amino acids, and cyclic nucleotides such as cAMP and cGMP are synthesized from ATP and GTP precursors (1-3). These molecules can mediate inter- or intra-cellular signaling depending on their ability to cross cell membranes. Steroid hormones can passively diffuse across cellular membranes to bind cytosolic receptors, while membrane-impermeable neurotransmitters are actively secreted to bind cell-surface receptors. In contrast, cyclic nucleotides are generally not transported across cell membranes and therefore typically signal through intracellular receptors.

Signaling by these molecules regulates important, yet diverse, biological processes such as gender determination by steroid hormones, cognitive reward seeking by dopamine, and preferential carbon metabolite utilization in *E. coli* (4-6). As a result of these powerful regulatory activities, low molecular weight signaling pathways are targets for pharmaceutical intervention. The amount of signaling molecule can be manipulated as in the case of birth control through ingestion of progestin and estradiol, or manipulating signaling metabolism as in the prevention of cGMP degradation by Viagra (7,8). Alternatively, molecular analogs can alter the activity of signal receptors such as inhibition of the NMDA receptor by ketamine (9). Elucidating the molecular targets of signaling by low molecular weight molecules is critical to our understanding of biological

regulation, signal transduction, and the rational design of pharmaceuticals that target these processes.

1.1.1 Architecture of Signaling by Low Molecular Weight Molecules

Signaling by low molecular weight molecules involves four steps that are present in all signaling modules: 1) signal generation, 2) signal binding to effector, 3) allosteric regulation of effector activity, and 4) signal elimination (Figure 1). First, a signal is generated by the synthesis or release of a low molecular weight signaling molecule. The signaling molecule must then bind to an effector molecule to regulate cellular activity. Effectors are genomically-encoded proteins or RNAs with a biological activity that is allosterically regulated by ligand binding. Upon binding at the allosteric site, a conformational change is transduced through the structure of the effector molecule to regulate its biological output. In the final step, elimination of the signaling molecule is required to allow dynamic response to further signal generation. This can be accomplished by catalytic inactivation of the signaling molecule or sequestration of the signaling molecule from cells or subcellular compartments. Each of the four processes listed above are universal to signaling by low molecular weight molecules and define the minimal components of a signaling module.

1.2 A Minimal Signaling Module: cAMP Regulation of Carbon Catabolite Utilization in *E. coli*

Cyclic adenosine monophosphate (cAMP) is one of the most well-characterized low molecular weight signaling molecules with regulatory activities in prokaryotes and eukaryotes. In *Escherichia coli*, cAMP regulates the preferential catabolism of glucose over other

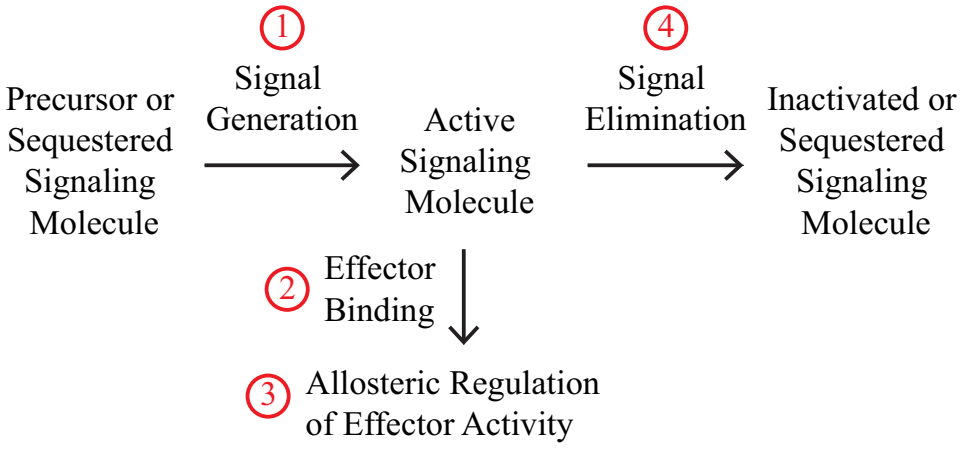

Figure 1. Architecture of signaling by low molecular weight molecules. Signaling molecules are (1) generated, (2) bind effectors, (3) allosterically regulate effector activity, and (4) are eliminated by sequestration or chemical modification.

carbon sources such as lactose (Figure 2) (10). When present in the environment, glucose is imported by EII^{Glc} and simultaneously phosphorylated by phosphotransfer from the $EIIA^{Glc}$ subunit (11). In the absence of glucose as a substrate for phosphotransfer, $EIIA^{Glc}$ remains phosphorylated and $EIIA^{Glc}$-P interacts with the *E. coli* adenlyate cyclase (AC) to activate cAMP synthesis (12,13). Through this mechanism, cAMP synthesis acts as a signal for decreasing glucose availability. cAMP has one well-characterized effector in *E. coli* called the cAMP receptor protein (CRP) that specifically binds cAMP with high affinity (14). Binding to cAMP allosterically promotes CRP dimerization and increases its affinity for specific regulatory DNA sequences called CAP sites (15). CAP sites are found in the promoters of the *lac, gal,* and *mal* utilization operons, allowing CRP to regulate transcription of these operons (16). In the presence of high glucose, cAMP is not generated. As a consequence, CRP does not dimerize and bind CAP sites, thereby decreasing transcription from alternative carbon catabolite utilization

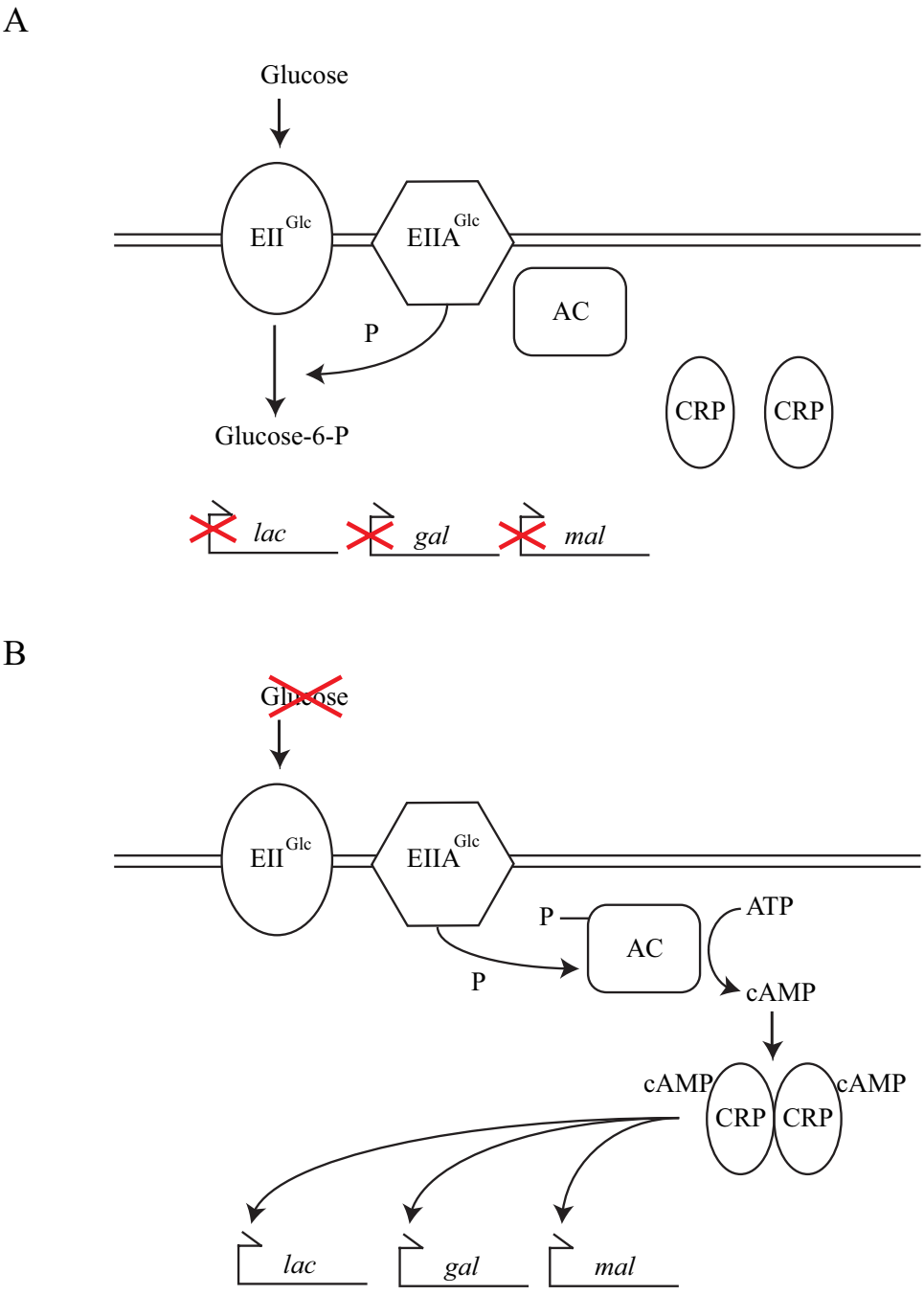

Figure 2. cAMP-dependent carbon catabolite regulation in *E. coli*. (A) In the presence of glucose, $EIIA^{Glc}$ phosphorylates glucose during import into the cell. (B) In the absence of glucose, $EIIA^{Glc}$ phosphorylates adenylcate cyclase (AC), which then produces cAMP. cAMP binds cAMP receptor protein (CRP), inducing dimerization and transcritpion of operons encoding genes for alternative carbon utilization pathways.

operons and prioritizing glucose catabolism (17). As glucose levels fall, cAMP will be synthesized, bind to CRP, and promote transcription of genes for non-glucose carbon catabolite utilization (18,19). To maintain a dynamic response to glucose availability, *E. coli* must be able to remove cAMP produced from previous periods of low glucose. Low intracellular levels of cAMP are maintained by a cAMP-specific phosphodiesterase (PDE) CpdA and active transport of cAMP from the cytoplasm by TolC (20,21). Thus cAMP signaling in *E. coli* demonstrates the four minimal components of a biological signaling module including: 1) signal generation by adenylate cyclase synthesis of cAMP, 2) signal recognition by cAMP binding to CRP, 3) signal output through increased affinity of CRP to CAP sites, and 4) signal elimination through enzymatic degradation and export from the cytosol (Figure 3).

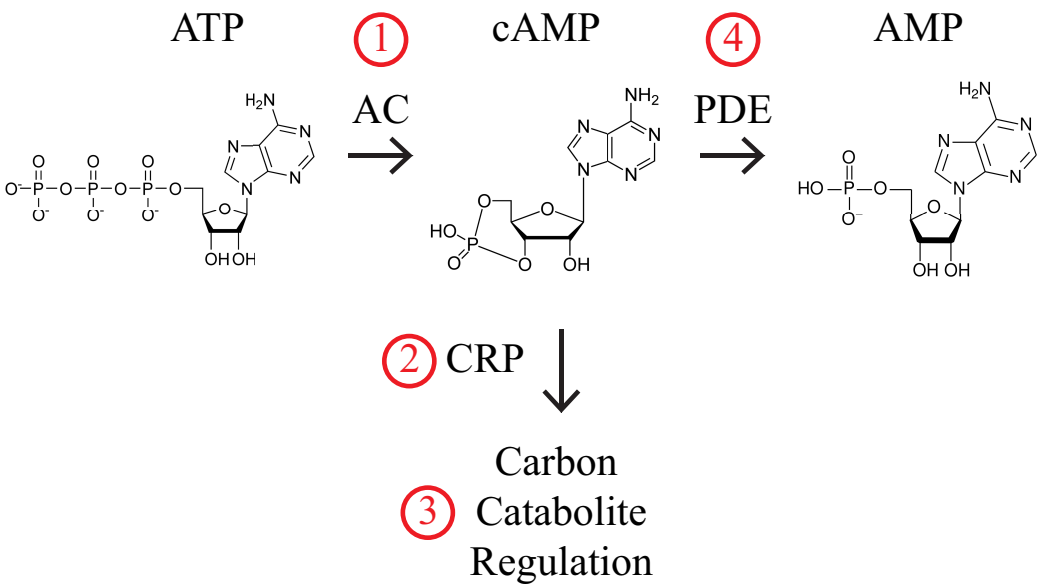

Figure 3. Architecture of cAMP signaling in *E. coli.* In *E. coli,* cAMP is (1) synthesized by adenylate cyclase (AC) from an ATP precursor, (2) binds CRP, (3) regulates carbon catabolism utilization, and (4) is degraded to AMP by a phosphodiesterase (PDE).

1.3 Complexity in Eukaryotic cAMP Signaling

In eukaryotic systems, the architecture of cAMP signaling has increased complexity. Complexity is a result of multiple ACs, cAMP effector proteins, regulatory targets, and PDEs. Humans encode at least 9 membrane bound ACs as well as a soluble AC, which are regulated both transcriptionally and post-translationally (22). AC expression is differentially-regulated in tissues, although the molecular mechanisms of differential expression are not well characterized. The most common mechanism of post-translational AC regulation is through the activity of G-protein-coupled receptors (GPCRs) (23). GPCRs respond to environmental signals by releasing a trimeric complex of regulatory G-protein subunits. G-protein α-subunits can either stimulate or inhibit AC activity, while the G-protein β/γ heterodimers are potent inhibitors of specific ACs (24-26). In addition to GPCR regulation, AC activity can be inhibited through phosphorylation by several kinases, including a cAMP-dependent protein kinase A providing a mechanism of feedback inhibition (27). The presence of multiple ACs that are individually regulated by different mechanisms creates complex cAMP signal production in eukaryotes.

There is additional complexity in cAMP signaling due to the presence of multiple cAMP-dependent effector molecules (Figure 4). The most well-studied effector of eukaryotic cAMP signals is the cAMP-dependent protein kinase A (PKA). In its inactive form, PKA exists as a heterotetramer composed of a regulatory homodimers and two catalytic subunits containing kinase activity (28). cAMP binding to the regulatory subunits of PKA causes

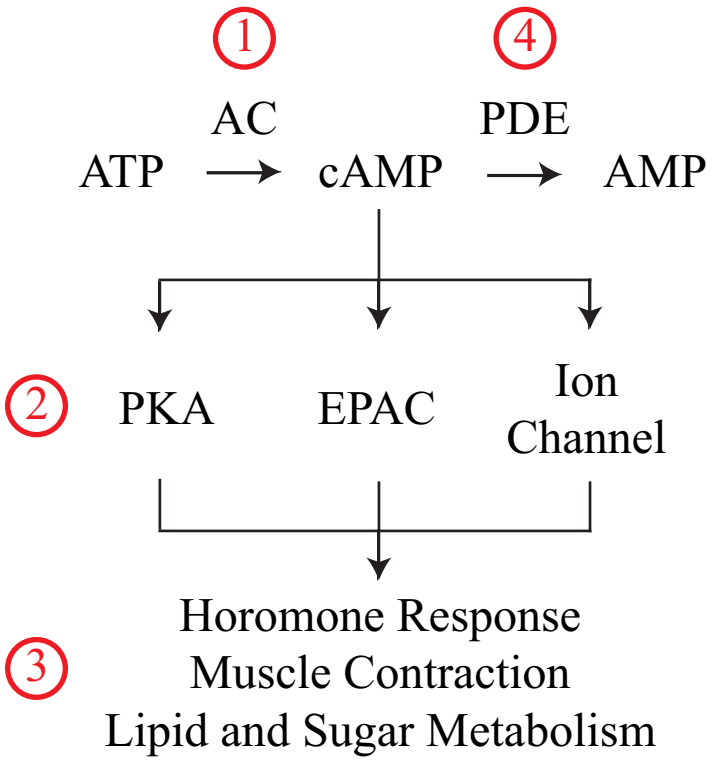

Figure 4. Architecture of cAMP signaling in eukaryotes. In eukaryotes, cAMP is (1) synthesized by multiple isoforms of adenylate cyclase (AC), (2) binds multiple effector types, (3) regulates diverse cellular processes, and (4) is degraded by multiple phosphodiesterase isoforms (PDE).

release of the active catalytic monomers, which can then phosphorylate target proteins to regulate cellular activity (29). Multiple isoforms of PKA exist based on the differential expression of 3 genes encoding catalytic subunits and 4 genes encoding regulatory subunits, each of which are subject to post-transcriptional splicing creating multiple subunit splice variants (30-38). Furthermore, catalytic and regulatory subunits are differentially assembled into PKA tetramers, providing a large variety of PKA isoforms (39). The multitude of PKA isoforms created by transcriptional, post-transcriptional, and post-translational regulation creates complexity in cAMP regulation of PKA activity.

In addition to PKA, two other classes of eukaryotic cAMP effectors have been described, including a guanine exchange factor protein directly activated by cAMP (EPAC or cAMP-GEF) and cAMP-gated ion channels. EPACs were discovered as a result of the PKA-independent cAMP-dependent regulation of the Rap1small GTPase (40). EPACs activate the small GTPases Rap1 and Rap2 by promoting the exchange of GDP for GTP and allowing regulation of further downstream protein effectors (41). For example, regulation of Rap signaling by cAMP-dependent EPACs is required for maintenance of cellular adhesion and tight junction localization (42). cAMP-gated ion channels are a third class of cAMP-dependent effectors, which are involved in sensory and neural processes such as olfactory perception (43). From these examples, it is apparent that different cAMP effectors have different effector mechanisms including enzymatic phosphorylation, protein-protein interactions, and ion flux that provide a complex set of outputs for cAMP signaling.

In eukaryotic systems, cAMP degradation is accomplished by multiple PDEs with specific regulatory features. Mammalian PDEs fall into 8 structure/function families of

which the Class-4 PDEs are specific for cAMP and account for the majority of cAMP PDE activity in mammalian cells (44). Class-4 PDEs are generated from 4 genetic loci with differential splicing leading to the production of at least 20 PDE isoforms with different N-terminal and C-terminal regulatory domains flanking a conserved catalytic domain (45). PDE activity of different isoforms is regulated by multiple mechanisms including phosphorylation by ERK MAP-kinase or PKA and binding to phosphatidic acid (46-48). The presence of multiple differentially-regulated PDE isoforms provides complexity in eukaryotic cAMP signal degradation.

cAMP signaling components are regulated to create specific interactions between ACs, effectors, and PDEs. Signaling specificity can be achieved by expression of subsets of ACs, effectors, and PDEs in different cells or tissues. For example, a soluble AC activated by bicarbonate is expressed only in the testes, providing a unique cAMP signaling response to bicarbonate concentrations (49). Signaling specificity of co-expressed ACs, effectors, and PDEs can also be achieved by subcellular localization. In one example, a class of structurally diverse proteins called A-kinase anchoring proteins (AKAPs) localizes specific AC, PKA and PDE proteins to create localized signaling modules (50). In cardiac myocytes, muscle-specific AKAP (mAKAP) directly binds AC5, a specific PKA isoform, and a isoform of PDE4 to regulate opening of a calcium channel (51-53). Genetic ablation of the mAKAP binding site prevents proper PKA localization and regulation, resulting in decreased PKA activity and improper regulation of the calcium channel. A result of localization of signaling components is the production of localized differences in cAMP concentration. FRET sensors have revealed the presence of sub-cellular cAMP concentration gradients in cardiac myocytes that are

dependent upon the activity of PDEs (54). Activity of specific cAMP effectors could be regulated by their subcellular localization with respect to high and low cAMP concentrations (55). Thus, in addition to the large number of eukaryotic cAMP signaling components, differential expression and subcellular localization creates further complexity in eukaryotic cAMP signaling.

1.3.1 Complexity in Prokaryotic cAMP Signaling

The identification of multiple ACs, effectors, and PDEs in bacterial genomes suggests that prokaryotes may also posesses complex cAMP signaling networks. *Pseudomonas aeruginosa* encodes 2 intracellular ACs, CyaA and CyaB, that produce cAMP to regulate expression of virulence factors (56). A third AC, ExoY, is injected into eukaryotic cells by a type III secretion system to target eukaryotic cAMP-dependent processes (57). cAMP production by CyaA and CyaB targets a single cAMP effector, a CRP homolog called Vfr (58,59). Unlike the CRP of *E. coli*, Vfr appears to regulate virulence factor production rather than carbon catabolite utilization in *P. aeruginosa* (60). Regulation of CyaA and CyaB activity are not fully understood, but the presence of two cyclases suggests that *P. aeruginosa* may generate cAMP in response to multiple inputs.

In *Mycobacteria tuberculosis,* a complex cAMP signaling system containing multiple ACs and cAMP effectors was discovered by *in silico* prediction of cyclic nucleotide monophosphate binding domains and cyclases (61). Of the 16 predicted ACs, 10 have been demonstrated to synthesize cAMP in response to distinct environmental cues including fatty acids, pH, bicarbonate, and growth in macrophages (62). In addition to the cyclases, 10 cAMP binding proteins have been predicted, although only CRP_{Mt} and a lysine acetyl transferase (KAT_{Mt}) have been shown empirically to directly bind cAMP

(63,64). A second CRP ortholog (CMR) with a predicted cAMP binding site regulates transcription in a cAMP-dependent manner, although direct binding has not been demonstrated (65). CMR and CRP_{Mt} bind distinct regulatory DNA sites allowing CMR to regulate a specific set of genes, which may explain the requirement for CMR but not CRP_{Mt} during *M. tuberculosis* growth in macrophages (66). In contrast to the multiplicity of ACs and effectors, only one PDE has been identified in *M. tuberculosis* (67). However, *M. tuberculosis* can export cAMP, providing an alternative mechanism for signal elimination (68). Indeed, cAMP levels increase 50-fold upon passage in macrophages, and cAMP is directly exported into macrophages to disrupt immune signaling (69,70). In total, these studies describe a complex cAMP signaling system containing multiple cyclases, multiple cAMP binding proteins with different regulatory activities, and multiple cAMP removal mechanisms.

1.4 Discovery of a Cyclic di-Nucleotide Signaling Molecule in Prokaryotes

Bis-(3',5')-cyclic-dimeric-guanosine monophosphate or cyclic di-GMP (cdiGMP) is a cyclic di-nucleotide signaling molecule in prokaryotes. Unlike cAMP and cGMP which are monomers, cdiGMP is composed of two guanosine monophosphates joined through phosphodiester bonds between the C-3 and C-5 hydroxyl groups of their ribose (71). The unique cyclic di-nucleotide was initially identified as an activator of cellulose synthase in membrane preparations of *Gluconacetobacter xylinus* (Figure 5) (72). Addition of GTP to membrane preparations from *G. xylinus* induced cdiGMP synthesis by a diguanylate cyclase (DGC). Addition of purified cdiGMP to these membrane preparations was shown to allosterically enhance the rate of cellulose polymerization by direct interactions with cellulose synthase (73,74). In addition to DGC

activity, the original membrane preps contained cdiGMP specific PDE activity. PDE activity sequentially hydrolyzed both phosphodiester bonds, producing a linear pGpG intermediate, which was subsequently hydrolyzed to 2 GMP (72). These early studies described the minimal components of a cdiGMP signaling module composed of synthesis by DGC, effector binding, allosteric regulation of effector activity, and subsequent removal by PDE.

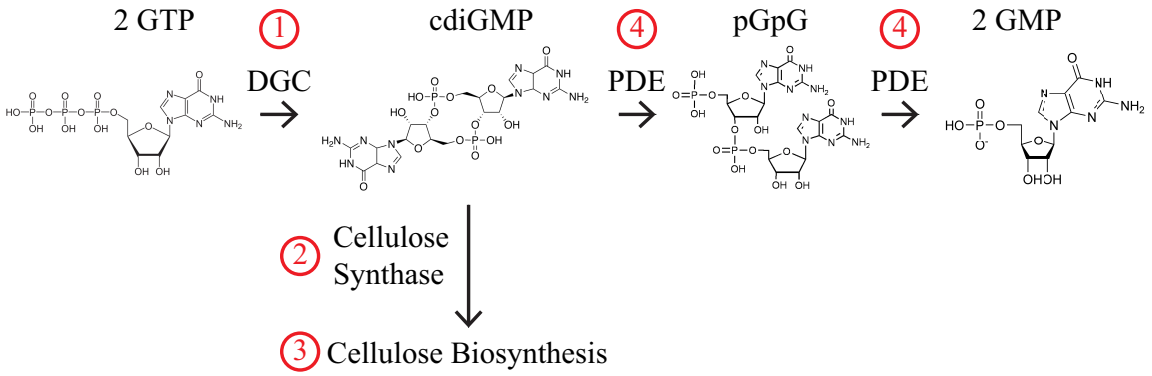

Figure 5. Architecture of cdiGMP signaling. cdiGMP is (1) synthesized from 2GTP by diguanylate cyclases (DGC), (2) binds cellulose synthase, (3) upregulates cellulose biosynthesis, and (4) is degraded to pGpG and subsequently 2GMP.

1.4.1 GGDEF Domains Catalyze cdiGMP Synthesis

Studies of cdiGMP signaling have been greatly aided by the identification of a conserved GGDEF domain required for cdiGMP synthesis. Initial experiments to identify genes that regulate DGC activity in *G. xylinus* identified several genes encoding proteins with GGDEF domains (75). Alignment of GGDEF domains with adenlyate cyclases of *Mycobacteria* revealed conservation of secondary structure motifs, suggesting GGDEFs may also have nucleotide cyclase activity (76). Direct cdiGMP synthesis by a GGDEF-domain protein was demonstrated using purified PleD from *Caulobacter crescentus* (77).

PleD was found to catalyze cdiGMP formation from GTP *in vitro*, and mutation of the conserved GGDEF residues abolished cdiGMP synthesis. Numerous proteins containing GGDEF domains have now been shown to have DGC activity and no other source of cdiGMP synthesis has been identified, suggesting that cdiGMP synthesis is accomplished only by GGDEF domains (78).

The ability to identify DGCs based on the presence of a GGDEF domain has enabled systematic genetic and biochemical analysis of DGC activity. Surprisingly, individual organisms can encode dozens of GGDEF-domain proteins, including 41 in *Vibrio cholerae* and 33 in *P. aeruginosa* (79). Systematic analyses of GGDEF-domain proteins in *P. aeruginosa*, *Salmonella typhimurium, E. coli,* and *V. cholerae* has revealed that a majority of proteins containing a GGDEF domain are active DGCs and can contribute to regulation of cdiGMP-dependent phenotypes *in vivo* (80-83). Interestingly, the production of cdiGMP by individual DGCs was not absolutely correlated with regulation of cdiGMP-dependent phenotypes. For example, PA2870 and PA3343 of *P. aeruginosa* produced high levels of cdiGMP, but failed to upregulate cdiGMP-dependent biofilm formation, suggesting that individual DGCs may target specific effectors (80). The presence of numerous DGCs with varying enzymatic activity and specific cellular targets creates complex cdiGMP signaling in prokaryotes.

Structural studies have revealed the mechanism of cdiGMP synthesis by GGDEF domains and identified a conserved regulatory motif required for feedback inhibition of DGC activity by cdiGMP. Crystallization of the PleD protein revealed a dimer structure with conserved GGDEF residues binding and positioning two GTP molecules at the catalytic GGDEF domain interface for condensation to cdiGMP (84). This suggests that

DGC activity requires dimerization, which is supported by the finding that only dimer fractions of PleD contain DGC activity (85). In addition to revealing a catalytic mechanism for cdiGMP, the crystal structure of PleD revealed bound cdiGMP at an allosteric inhibitory site (I-site) (84). Sequence alignment of residues in the I-site revealed a conserved RxxD motif that is present in the majority of GGDEF-domain proteins, especially those with conserved residues for cdiGMP catalysis (86). Systematic mutation of the RxxD motif of PleD demonstrated that the conserved arginine and aspartate residues of the RxxD motif are required for cdiGMP-binding and feedback inhibition (86). Thus, activation of cyclase activity by dimerization and product inhibition through cdiGMP-binding at the I-site appear to be conserved regulatory features of DGCs.

DGC activity can also be regulated by N-terminal domains that effect dimerization or the positioning of GGDEF domains. PleD contains an N-terminal REC domain that is phosphorylated to promote dimerization and activate cdiGMP synthesis (77,85). The structure of PleD was solved after modification with BeF_3^-, which mimics aspartate phosphorylation of REC domains (87). This structure confirmed that PleD dimers are stabilized by phosphorylation-dependent N-terminal REC domain interactions (88). A similar regulatory mechanism has been described for WspR in which DGC activity is upregulated by phosphorylation-dependent dimerization of its N-terminal REC (89-91). In addition to regulation of dimerization, N-terminal domains may affect the tertiary structure of GGDEF domains to regulate DGC activity. DgcZ (YdeH) of *E. coli* is a constitutive dimer with an N-terminal zinc binding domain (92). A crystal structure of DgcZ shows that zinc binding prevents proper positioning of the GTP molecules at the

dimer interface (93). Thus, N-terminal domains can regulate DGC activity through a variety of mechanisms including dimerization and ligand binding. The combination of multiple DGCs with unique N-terminal regulatory domains creates a high level of complexity in cdiGMP signal production.

1.4.2 EAL and HD-GYP Domains Catalyze cdiGMP Hydrolysis

Early genetic and biochemical studies of cdiGMP metabolism demonstrated that EAL-domain proteins decreased cellular cdiGMP levels and repressed cdiGMP-dependent phenotypes in multiple organisms (75,94). The purified EAL-domain protein VieA of *V. cholerae* was shown to directly hydrolyze cdiGMP in a manner that depended on the conserved glutamate residue of the EAL motif (95). VieA can hydrolyze both phosphodiester bonds of cdiGMP to produce linear pGpG and subsequently 2 GMP. However, pGpG formation is several orders of magnitude faster than GMP production, indicating that pGpG may be the physiologically relevant product of EAL-domain proteins (95). Rapid hydrolysis of cdiGMP to pGpG has now been demonstrated for numerous EAL-domain proteins, indicating that cdiGMP hydrolysis is a conserved feature of EAL domains (80,95-98).

Structural studies have revealed that EAL domains function as dimers with inter- and intra-molecular domain interactions regulating catalytic activity. Blrp1 of *Klebsiella pneumonia* encodes an N-terminal blue light-responsive BLUF domain and a C-terminal EAL domain (99). Blue light induces structural changes in the BLUF domain that are transmitted to the EAL domain, specifically affecting conserved alpha helices at the EAL-EAL dimer interface. Interactions between the EAL domains reciprocally repositions the catalytic divalent cation clusters of each other's active sites, thereby

promoting PDE activity. Regulation of PDE activity through the EAL dimer interface has also been demonstrated for YahA of *E. coli* (98). Isolated EAL domains of YahA are normally monomers that can form dimers at high concentrations that activates PDE activity (100). cdiGMP-binding at the active site causes changes in the structure of the EAL domain dimer interface, thereby promoting dimerization and PDE activity in the presence of the cdiGMP substrate. Thus, EAL domain PDE activity is reciprocally regulated by a conserved EAL-EAL dimer interface. The inter-domain interactions can be regulated by N-terminal signaling domains or substrate-dependent dimerization, creating complex regulation of cdiGMP hydrolysis by EAL domains.

The HD-GYP domain, a subclass of the HD family of metal-dependent phosphohydrolases, defines a second class of cdiGMP specific PDE proteins. In contrast to EAL domains, HD-GYP domains efficiently hydrolyze both phosphodiester bonds of cdiGMP and therefore produce 2 GMP as the major product (101,102). Regulation of HD-GYP domain PDE activity is not well characterized, although several mechanisms have been proposed. HD-GYP domains are often paired with signal receiver domains such as REC, GAF and PAS, suggesting that PDE activity could be regulated by the activity of associated domains (79). Indeed, the prototypical HD-GYP domain protein RpfG contains an N-terminal REC domain that, in the absence of phosphorylation, inhibits cdiGMP-binding at the active site (101,103). Alternatively, a recent report has described an HD-GYP domain protein from *V. cholerae* that is active in the presence of reduced ferrous iron, but not oxidized ferric iron (104). This suggests that PDE activity could be regulated by redox activity. A crystal structure of a catalytically-active HD-GYP protein *Pm*GH of *Persephonella marina* was recently solved, revealing a possible

mechanism for PDE activity (105). The authors proposed a two step model. First cdiGMP is linearized to pGpG, which is then rotated in the active site for hydrolysis of the second phosphodiester bond. Although not as numerous or well-characterized as the EAL domain PDEs, HD-GYP domains define a second class of cdiGMP PDEs with distinct mechanistic features creating further complexity in cdiGMP elimination.

1.4.3 Enzymes Containing Both GGDEF and EAL Domains

One further aspect of complexity in cdiGMP metabolism is the common occurrence of both GGDEF and EAL domains in a single hybrid protein. Bioinformatic analysis has revealed that 68% of EAL domains are associated with a GGDEF domain, and 40% of GGDEF-domain proteins also contain an EAL domain (106). One possibility for these hybrid GGDEF/EAL-domain proteins is that one or both domains may be inactive, thereby preventing paradoxical biochemical activities. Analysis of catalytic residue conservation in hybrid GGDEF/EAL-domain proteins suggests that PDE activity is typically conserved while approximately 40% of GGDEF domains in hybrid proteins lack catalytic residues for DGC activity (106). In *C. crescentus,* CC3396 was shown to contain a degenerate GGDEF domain that retained GTP binding at the active site, but lacked DGC activity (96). Instead, GTP binding to the GGDEF domain promoted PDE activity of the C-terminal EAL domain, providing a potential mechanism of PDE regulation in response to cellular GTP levels. Another possibility is that both DGC and PDE activity are retained, but differentially-regulated. Several examples of bi-functional DGC/PDE enzymes have been described, including ScrC in *Vibrio parahaemolyticus* and BphG1 in *Rhodobacter sphaeroides* (107,108). The opposing DGC and PDE activities of ScrC and BphG1 are regulated by different mechanisms. ScrC is encoded in an operon

that also produces ScrA and ScrB. In the absence of ScrAB, ScrC demonstrates DGC activity, but in the presence of ScrAB, ScrC has PDE activity, providing dynamic switching between DGC and PDE activity (107). In contrast, BphG1 is a constitutive PDE with N-terminal red-light sensing and GGDEF domains. When expressed in *E. coli,* BphG1 was shown to be proteolytically cleaved resulting in the separation of the N-terminal GGDEF and C-terminal EAL domains (108). The remaining N-terminal fragment possessed DGC activity that was strongly upregulated by exposure to red light. These results suggests a potential mechanism for irreversible transition from PDE to DGC activity, although endogenous proteolysis of ScrC has not been demonstrated in *R. sphaeroides*. In summary, proteins encoding GGDEF and EAL domains can exhibit both DGC or PDE activity, and these enzymatic activities are subject to a variety of regulatory mechanisms, creating further complexity in cdiGMP metabolism.

1.4.4 cdiGMP Effectors with Conserved Binding Sites

The identification of cdiGMP effectors with conserved cdiGMP-binding domains has revealed the cellular targets and molecular mechanisms of cdiGMP regulated phenotypes (Figure 6). The I-site of GGDEF domains represents the first conserved cdiGMP-binding site identified for cdiGMP effectors. In catalytically-competent DGCs, the I-site binding provides feedback inhibition of cyclase activity (86). PopA of *C. crescentus* contains a GGDEF domain but lacks the conserved glycine and glutamate residues required for cdiGMP synthesis (109). However, purified PopA retains the ability to bind cdiGMP with high affinity at the I-site. The same study showed that PopA is sequestered to the cell poll to regulate *C. crescentus* cell cycle progression in a cdiGMP-dependent manner. Mutation of PopA's RxxD motif prevents PopA localization and

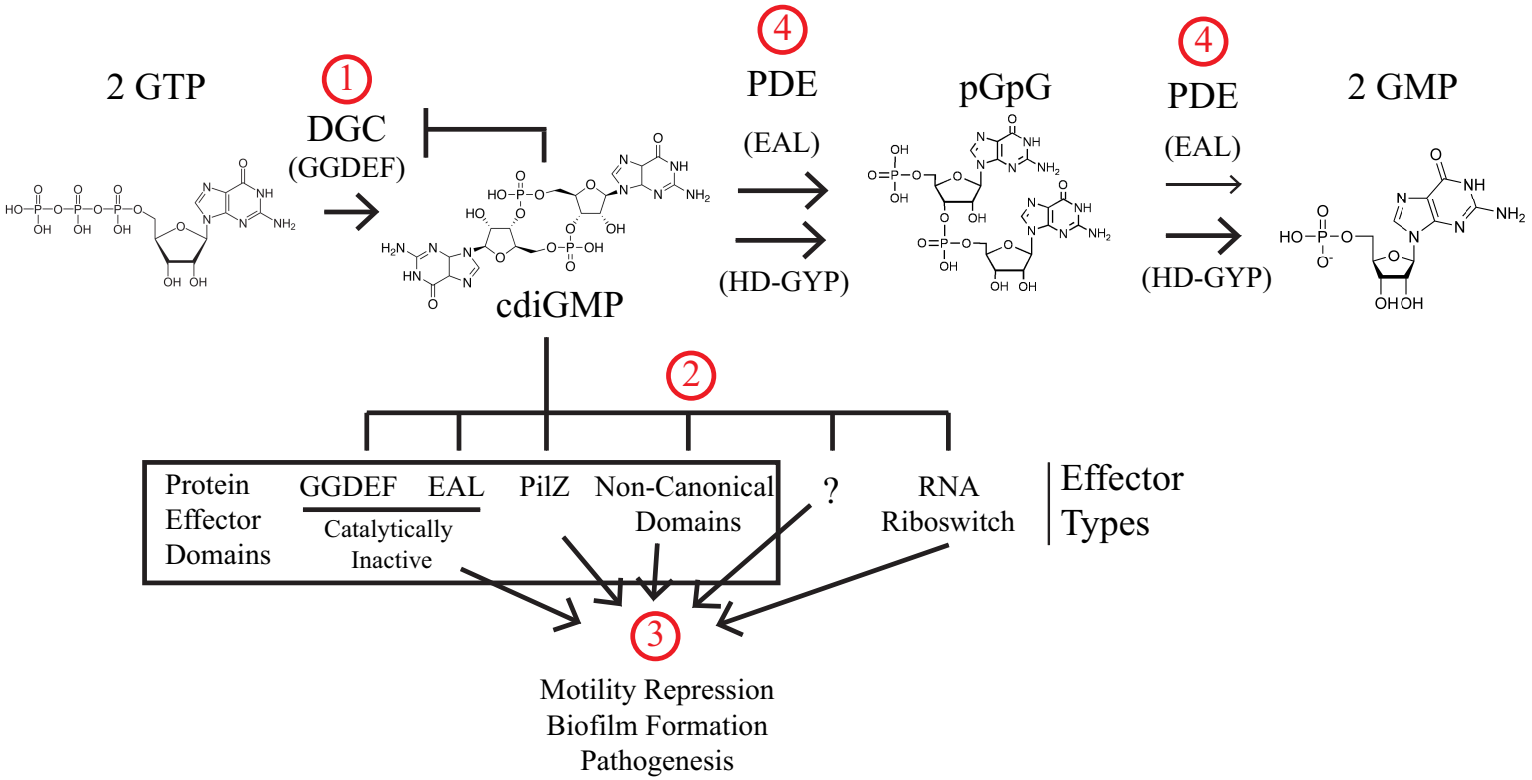

Figure 6. Complexity in cdiGMP signaling. cdiGMP is produced by DGCs and binds to I-sites to provide feedback inhibition. Multiple effector types bind cdiGMP, some with conserved binding sites, to regulate diverse cellular processes. Finally, cdiGMP is eliminated by PDEs containing either EAL or HD-GYP domains, which preferentially produce pGpG or 2GMP respectively.

cdiGMP-dependent cell cycle progression, demonstrating that PopA is a cdiGMP effector. Several other degenerate GGDEF-domain proteins have been identified that retain high-affinity cdiGMP-binding to regulate protein function, demonstrating that GGDEF domains that retain the RxxD motif in the I-site are a conserved class of cdiGMP effectors (110,111).

In addition to the I-site of GGDEF domains, catalytically inactive EAL domains that retain cdiGMP-binding represent a second class of cdiGMP effectors with a conserved cdiGMP-binding domain. The *P. aeruginosa* protein FimX contains a GGDEF and EAL domain, but lacks conserved residues for catalysis in both domains (112,113). Further studies revealed that FimX binds cdiGMP with high affinity and that binding is dependent on the EVL residues of the EAL domain (114,115). FimX was first studied for its role in assembly of type IV pili at cell poles (116). A Δ*fimX* mutant is unable to assemble type IV pili, which can be complemented by expression of wild type FimX, but not the non-binding EVL motif mutant (112). This suggests that cdiGMP-binding to FimX is essential for regulation of type IV pili biogenesis in *P. aeruginosa*. Several other proteins that bind cdiGMP with a non-catalytic EAL domain have been described, including LapD of *P. fluorescens* and YkuI of *B. subtilis* (117,118). Genetic and structural studies have demonstrated that cdiGMP-binding to the cytoplasmic EAL domain of LapD regulates proteolysis of a cell-surface adhesin (119,120). In total, these studies demonstrate that EAL domains lacking catalytic activity can be re-purposed as high affinity cdiGMP effectors with diverse regulatory functions.

The PilZ domain defines a third class of cdiGMP effectors that utilize a conserved cdiGMP-binding domain. In a seminal bioinformatic study, Amikam and Galperin

predicted that PilZ domains would bind cdiGMP based on PSI-BLAST identification of the PilZ domain in prokaryotic cellulose synthase (121). Notably, PilZ domains were absent in the closely related cellulose synthases of eukaryotes that lack cdiGMP regulation. After this report, the PilZ domain protein YcgR of *E. coli* was purified and shown to bind cdiGMP with high affinity in a manner that required conserved residues of the PilZ domain (122). YcgR had previously been characterized as a regulator of flagellar motility in *E. coli*, and genetic manipulation of DGCs and PDEs in *S. typhimurium* had revealed that flagellar motility was a cdiGMP-dependent phenotype (123,124). Deletion of the PDE YahA repressed flagellar motility in *E. coli,* and subsequent deletion of YcgR restored flagellar motility, suggesting that YcgR repressed flagellar motility in response to increasing cdiGMP concentrations. Complementation of a Δ*yahA* Δ*ycgR E. coli* strain with a cdiGMP-binding deficient *ycgR* allele failed to repress swimming motility, demonstrating that YcgR is a cdiGMP effector that binds cdiGMP using conserved residues of the PilZ domain (122). The ability to identify PilZ domains from primary sequence has since enabled the identification and characterization of numerous cdiGMP effectors in many organisms. For example, a PilZ domain was identified in the Alg44 protein that regulates alginate biosynthesis in *P. aeruginosa* (125). cdiGMP-binding to purified Alg44 required conserved residues in the PilZ domain and mutation of these residues abolished alginate biosynthesis *in vivo* (126). Similar results have been reported for numerous PilZ domain proteins, demonstrating that cdiGMP-binding and regulation of cdiGMP-dependent phenotypes are conserved features of PilZ domain proteins (127-135).

In addition to three classes of cdiGMP protein effectors with conserved binding domains, two classes of cdiGMP-binding RNA riboswitches have been described. Riboswitches are structured RNA, typically found in 5' UTRs, that bind low molecular weight molecules to regulate gene expression (136,137). Class-I cdiGMP-binding riboswitches contain a GEMM motif and are widely distributed among proteobacteria (138). A Class-I cdiGMP-binding riboswitch from *Clostridium difficile* placed upstream of a β-galactosidase reporter was shown to regulate gene expression in response to changes in cellular cdiGMP concentrations (138). Class-2 cdiGMP riboswitches are mostly found in *Clostridia*, and are structurally distinct from Class-1 riboswitches, suggesting that they evolved independently (139). Intriguingly, the target sequence of a self-splicing ribozyme containing a Class-2 riboswitch was altered by cdiGMP-binding (139). A self-splicing ribozyme is a structured RNA molecule that can catalyze endonuclease cleavage and subsequent re-ligation of its own RNA strand (140). In the absence of cdiGMP, the ribozyme splicing removes 4 nucleotides of a putative ribosome binding site. cdiGMP-binding causes the ribozyme to splice upstream of the ribosome binding site, providing a potential mechanism for cdiGMP-dependent regulation of protein translation. Since their discovery the structure and biochemistry of these cdiGMP riboswitches has been intensely studied (141-147), but relatively little is known about their role in the regulation of cdiGMP-dependent phenotypes.

The I-sites of GGDEF domains, catalytically inactive EAL domains, PilZ domains, and RNA riboswitches all contain conserved motifs for binding cdiGMP. Bioinformatic identification of these motifs from primary nucleotide sequence has enabled identification and characterization of numerous cdiGMP effectors revealing the

cellular targets and molecular mechanisms of cdiGMP-regulated phenotypes. However, not all cdiGMP-dependent phenotypes are regulated by effectors containing these conserved binding domains.

1.4.5 cdiGMP Effectors Lacking Conserved Binding Domains

Genetic and biochemical investigation of cdiGMP regulated phenotypes have identified cdiGMP effectors lacking conserved cdiGMP-binding domains. For example, a *P. aeruginosa* Δ*fleQ* mutant resulted in a rugose or rough colony morphology, which was indicative of increased PEL or PSL production (148-150). Alginate and cellulose production had previously been described as cdiGMP-dependent phenotypes, suggesting that FleQ may be required for cdiGMP-dependent exopolysaccharides (EPS) biosynthesis. FleQ was purified and shown to bind cdiGMP directly and transcriptional reporters of the *pel* and *psl* biosynthetic operons were shown to be upregulated in a *fleQ* mutant (148). Purified FleQ was shown to bind to the *pel* promoter *in vitro,* and the presence of cdiGMP in EMSA experiments prevented FleQ from binding the *pel* promoter (148). These studies suggested that cdiGMP-binding to FleQ prevents binding to the *pel* promoter, thus relieving transcriptional repression of the *pel* operon. However, DNAse footprinting studies have revealed a more complex mechanism of cdiGMP-dependent FleQ regulation. In the absence of cdiGMP, FleQ binds at two sites in the *pel* promoter and FleQ interactions with FleN produce a bend in the DNA of the *pel* promoter that is proposed to inhibit transcription initiation (151). In the presence of cdiGMP, FleQ remains bound to the *pel* promoter, but the DNA is no longer bent and cdiGMP bound FleQ activity switches from a repressor to a transcriptional activator (151). Furthermore, cdiGMP and FleN have been shown to regulate ATPase activity of

FleQ, which in homologous transcription factors regulates sigma factor-dependent transcription initiation (152). In total these studies suggest that transcriptional regulation by FleQ requires multiple regulatory factors, including FleN and cdiGMP. FleQ represents the first description of a cdiGMP-dependent transcription factor lacking a defined cdiGMP-binding domain, and its identification based on the regulation of cdiGMP-dependent phenotypes represents a general approach for the identification of cdiGMP effectors.

Biosynthesis of the PEL polysaccharide requires the 7-gene *pel* operon that is transcriptionally regulated by both cdiGMP-binding to FleQ and a RetS-dependent signaling pathway (148,153). Despite similar transcriptional induction of *pel*, biosynthesis of PEL via the RetS pathway was significantly reduced in comparison to regulation by cdiGMP (154). This suggested there may be cdiGMP-dependent post-transcriptional regulation of PEL biosynthesis, but no cdiGMP-binding domains could be identified in Pel proteins. Purification of the 7 proteins of the *pel* operon and subsequent biochemical analysis revealed that PelD specifically bound cdiGMP with high affinity (154). Alignment of PelD homologs revealed a RxxD motif similar to the I-site of GGDEF domains and conserved secondary structural features between PelD and the DGC PleD. Mutation of the RxxD motif prevented cdiGMP-binding *in vitro* and cdiGMP-binding mutants failed to complement PEL biosynthesis in a *pelD* mutant strain, suggesting that PelD is a cdiGMP effector (154). While PelD lacks a recognizable GGDEF domain based on primary sequence information, crystallization has revealed that the C-terminus adopts a similar structure to GGDEF domains of active DGCs with alterations of several conserved secondary structures (155,156). Thus, PelD probably

evolved from a degenerate DGC that maintained structural features of the GGDEF domain and the RxxD I-site motif to bind cdiGMP and thereby regulate PEL biosynthesis.

In addition to PelD and FleQ, several other cdiGMP-dependent transcription factors have been identified that lack a canonical cdiGMP-binding domain. A CRP-like transcription factor (Clp) has been identified in *X. campestris* (157). Both Clp and cdiGMP were known to regulate pathogenesis of *X. campestris*, and *X. campestris* lacked an adenylate cyclase, suggesting that Clp did not respond to cAMP (158,159). Purification and biochemical analysis of Clp revealed high affinity cdiGMP-binding that regulated Clp binding to DNA binding, demonstrating that Clp is a cdiGMP effector. In addition to Clp, three cdiGMP-binding transcription factors have been identified in *V. cholerae.* A FleQ homolog FlrA, was recently shown to bind cdiGMP and regulate flagellar transcription in *V. cholerae* (160). Similar to PEL regulation in *P. aeruginosa,* cdiGMP regulates transcription of the *Vibrio* Polysaccharide (VPS) biosynthetic operon *vps,* but in contrast to FleQ, loss of *flrA* does not affect cdiGMP-dependent *vps* transcription (160-164). Instead, cdiGMP-dependent *vps* transcription is mediated by VpsR and VpsT, which were shown to bind cdiGMP after the discovery of their regulatory role in *vps* transcription (165,166). Interestingly, FleQ, VpsR, and FlrA are all members of the NtrC family of enhancer-binding proteins containing a N-terminal Rec domain, a central AAA+ ATPase domain, and a C-terminal DNA binding domain (167). For both FleQ and FlrA, cdiGMP-binding requires residues in the AAA+ ATPase domain, while the location of cdiGMP-binding to VpsR has not been investigated (152,160,165). These results suggest that there may be a conserved cdiGMP-binding site

among the NtrC family of enhancer-binding proteins, but conserved residues required for cdiGMP-binding have yet to be reported.

The identification of cdiGMP-dependent phenotypes that are not regulated by known cdiGMP effectors suggests that more cdiGMP effectors await discovery. For example, a single PilZ-domain protein PlzA has been described for the causitive agent of lyme disease, *Borrelia burgdorferi*. *B. burgdorferi* encodes a single DGC Rrp1 that is required for survival in the tick vector, but the only known cdiGMP effector PlzA is not required for surivival (168-171). Thus, it appears that in addition to PlzA, the cdiGMP signal from Rrp1 must have another unidentified effector in *B. burgdorferi*. Similarly in *V. cholerae,* cdiGMP regulates a number of phenotypes, including transcription of *ctxAB* encoding cholera toxin (172). PDE activity of VieA has been shown to reduce cellular cdiGMP levels that results in the expression of *ctxAB* (173). However, genetic studies have indicated that neither the three cdiGMP-binding transcription factors nor the five PilZ domain proteins of *V. cholerae* are required for cdiGMP-dependent repression of *ctxAB* transcription (95,127,165). In addition to *ctxAB,* several other cdiGMP-dependent promoters have been described that are not regulated by a known cdiGMP-dependent effector in *Vibrio cholerae* (160). These studies indicate that known cdiGMP effectors are not sufficient to explain observed cdiGMP-dependent phenotypes suggesting that more effectors remain to be discovered.

In subsequent chapters, I will describe the differential radial capillary action of ligand assay (DRaCALA) as a novel biochemical assay of protein-ligand interactions. In Chapter 2, I will show that DRaCALA can detect specific binding between proteins and nucleotides. DRaCALA can determine specificity, affinity, and kinetics of purified

protein ligand interactions and detect specific cdiGMP-binding to heterologously expressed proteins in *E. coli* whole cell lysates. In Chapter 3, DRaCALA will be used to screen a *Vibrio cholerae* open reading frame library to systematically identify cdiGMP-binding proteins with positive hits encoding both characterized and novel cdiGMP-binding proteins. Finally, Chapter 4 extends DRaCALA beyond protein interactions with small RNA oligonucleotides by demonstrating its ability to determine protein-DNA, protein-RNA, and RNA-ligand binding interactions. Overall, this dissertation describes the DRaCALA assay and its varied uses in exploring the genetic and molecular basis of biological regulation by nucleotide signaling molecules.

Copyright Notice

Chapter 2: Differential Radial Capillary Action of Ligand Assay for High-throughput Detection of Protein-Metabolite Interactions

2.1 Introduction

Interactions of low molecular weight ligands with protein receptors are critical in biological signaling both between cells and within individual cells. Examples of intercellular signaling include quorum signaling in bacteria, hormone and neurotransmitter responses in endocrine systems of animals, and auxin and abscisic acid regulation in plants (174). Intracellular signaling also involves regulatory protein binding molecules such as secondary signaling molecules (*e.g.* cAMP, cGMP, calcium and cyclic-di-GMP (cdiGMP) (97,175). In fact, nucleotide receptors are often targets for therapeutic intervention (176). Thus, these protein-ligand interactions have important implications in modern drug design and use. As each protein-ligand interaction pair may

represent a possible therapeutic intervention, there is an urgent need to collect qualitative and quantitative functional metabolomic data for protein-ligand interaction in a high throughput manner. Current efforts in metabolomics are directed at cataloging the presence of various metabolites through mass spectrometric analysis of biological samples (177-180). However, this approach lacks the ability to confirm interactions with protein partners, and therefore fails to reveal functional significance. Thus, the study of the interactions of a specific metabolite with all available cellular proteins, which we term "metabolite interactomics," has been limited by the available assay systems. Current assays for specific protein-ligand interactions, including equilibrium dialysis, filter-binding assays, ultracentrifugation, isothermal calorimetry (ITC), surface plasmon resonance, and many other assays (181-186), are not high throughput because they are limited by sample processing time, equipment requirements, and assay-specific manipulations. Protein array technology requires purified proteins fixed on solid support (187). Although protein array technology is feasible and quite powerful (188-190), large-scale protein purification is limited by individual protein characteristics that often hinder isolation of functionally active proteins. Currently, protein array technology is limited to only a few laboratories capable of performing mass parallel purification of functional proteins and arraying them. To bypass such constraints of existing assays, we have developed a high-throughput differential radial capillary action of ligand assay (DRaCALA) that can be used to detect binding and to quantitate the fraction of a small-molecule ligand that is bound to a protein of interest. DRaCALA is rapid and quantitative, and it allows detection of protein-ligand interactions for both purified proteins and proteins expressed in whole cells, thus bypassing the requirement for protein

purification. Unlike most comparable protein-ligand detection systems, DRaCALA does not require a wash step; thus, the total ligand available to protein is quantifiable, resulting in an accurate, simple, and precise measure of the fraction of ligand bound.

2.2 Principle of DRaCALA

DRaCALA exploits the ability of nitrocellulose membranes to sequester proteins preferentially over small molecule ligands. When a mixture of protein and radiolabeled ligand is spotted onto a dry nitrocellulose membrane, protein and bound ligand are immobilized at the site of contact, whereas free ligand is mobilized by capillary action with the liquid phase (Figure 7A). DRaCALA is a rapid assay because the capillary action can be completed in less than 5 s. Also, since DRaCALA does not use a wash step, the pattern of ligand migration allows rapid detection of both the total ligand and the ligand sequestered by proteins. Capillary action distributes the unbound ligand throughout the mobile phase, the calculation for the fraction bound (F_B) must correct for this background (see below for edge effects at the solvent front and annulation of the protein). Therefore, F_B is defined by the equation in Figure 7B, where I_{inner} is the intensity of signal in the area with protein (inner circle) and I_{total} is the intensity of total signal of the entire sample (outer circle). The I_{inner} signal consists of both ligand bound to protein and unbound ligand that has not mobilized beyond the area of the inner circle, which we define as $I_{background}$. $I_{background}$ can be calculated by subtracting the I_{inner} from the total ligand I_{total} and adjusting for the relative areas of the inner (A_{inner}) and outer (A_{total}) circles (Figure 7B). For free ligand alone, the signal for the ligand is not sequestered, and therefore has a baseline F_B of 0.01 ± 0.04 (Figure 8A), whereas protein alone does not mobilize on nitrocellulose (Figure 8B). Herein, we demonstrate the uses of DRaCALA

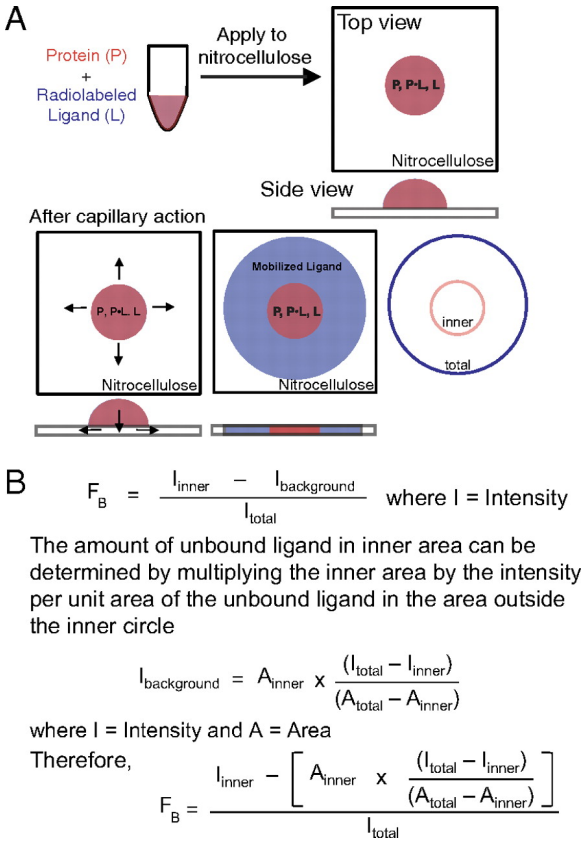

Figure 7. Principle of DRaCALA. (A) Schematic representation of DRaCALA assay on application of protein-ligand mixture onto nitrocellulose and capillary action. Protein (P), ligand (L), and protein–ligand complex (P•L) distribution during the assay is shown. (B) Equations are used to analyze DRaCALA data for F_B for purified proteins. An explanation of the apparent edge effect at the capillary migration front is provided in Figure 12.

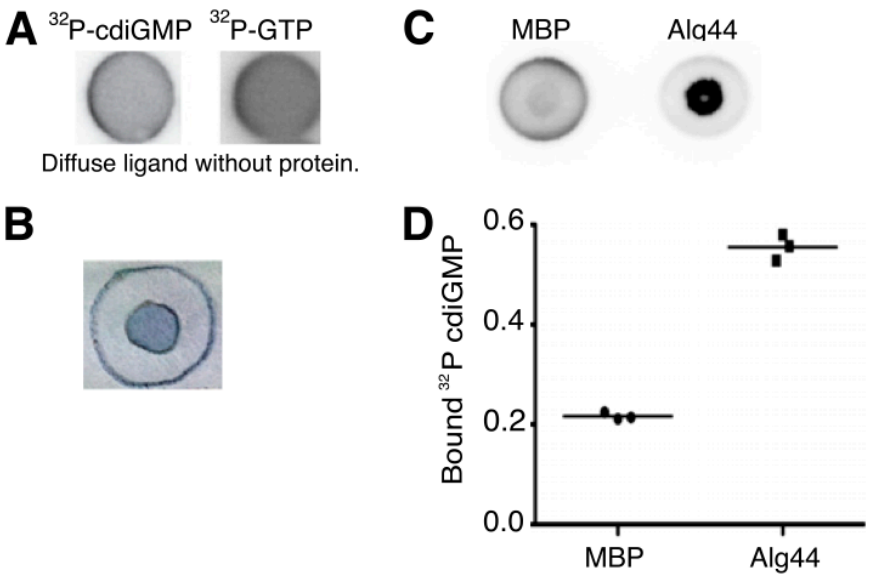

Figure 8. Proof of principle for DRaCALA. (A) Ligand distribution in the absence of protein when spotted on nitrocellulose. (B) Coomassie-stained MBP immobilized on nitrocellulose. Pencil marks were drawn before staining to indicate the darker protein spot and total capillary action. (C) DRaCALA image of *E. coli* BL21(DE3) whole-cell lysates overexpressing MBP or MBP-Alg44$_{PilZ}$ incubated with 8 nM ^{32}P-cdiGMP and spotted onto nitrocellulose. (D) Graph of DRaCALA spots from Figure 8C.

for rapid detection of metabolite binding to proteins and describe potential uses for identification of unknown interactions and pharmaceutical screening of protein agonists and antagonists.

2.3 DRaCALA Detection of Protein-Ligand Interactions

The principle of DRaCALA was illustrated by measuring ligand binding to known nucleotide binding proteins: *Pseudomonas aeruginosa* $Alg44_{PilZ}$ binds cdiGMP (191), *Escherichia coli* cyclic AMP receptor protein (CRP) binds cAMP (14,192), and *E. coli* nitrogen regulator B (NtrB) binds ATP (193). Radiolabeled ligands were incubated with each of the proteins, and the mixtures were spotted on a nitrocellulose membrane. After spreading by capillary action, membranes were dried and quantitated using a phosphorimager. Maltose binding protein (MBP), which does not bind to any of these small molecules, was used as a control. As expected, each of the radiolabel signals from MBP mixtures was distributed by capillary action (Figure 9A). CRP specifically bound cAMP, as demonstrated by the sequestration of the signal, but it did not bind cdiGMP or ATP (14,192) (Figure 9A). NtrB bound ATP, but not cdiGMP or cAMP (193) (Figure 9A). Similarly, $Alg44_{PilZ}$ bound cdiGMP, but not cAMP or ATP (191) (Figure 9A). The specificity of $Alg44_{PilZ}$ binding to cdiGMP was further tested by competition with excess unlabeled nucleotides (400-fold molar excess relative to the $Alg44_{PilZ}$ protein). $Alg44_{PilZ}$ binding to ^{32}P-cdiGMP was abolished by cdiGMP but not by cGMP, GMP, GDP, GTP, ATP, CTP, or UTP as was previously described (Figure 9B). Unlabeled cdiGMP was synthesized by Dr. Herman Sintim and Jingxin Wang. The F_B for cdiGMP was 0.47 ± 0.01, which was reversed by competition with unlabeled cdiGMP to the background level of 0.03 ± 0.01 (Figure 9C).

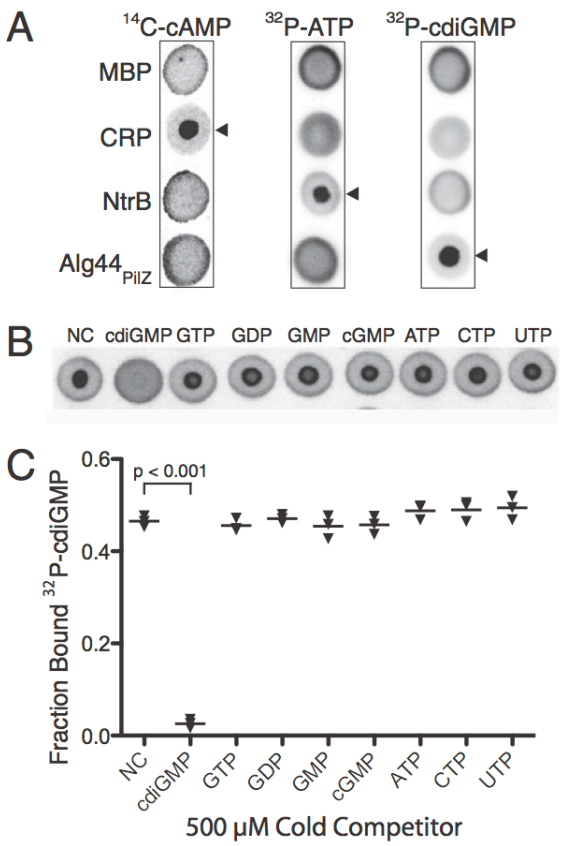

Figure 9. Detection of specific protein-ligand interactions by DRaCALA. (A) DRaCALA images of interactions between purified proteins (20 µM) incubated with 500 nM ^{14}C-cAMP, 4 nM ^{32}P-ATP, or 4 nM ^{32}P-cdiGMP. Protein- ligand mixtures were spotted on nitrocellulose and allowed to dry before imaging using a Fuji FLA7100 PhosphorImager. Cognate protein-nucleotide combinations are indicated by arrowheads. MBP was used as a negative control. (B) DRaCALA images of competition assays assessing the ability of 1 mM indicated cold nucleotides to compete with binding interactions be- tween 4 nM ^{32}P-cdiGMP and 2.5 µM HisMBP-Alg44$_{PilZ}$. (C) Graph of F_B for each sample in Figure 9B, with averages indicated by a horizontal bar. NC, no competitor. P values were determined by a Student t test for significant differences compared with the NC control for three independent experiments. The I_{total} of each DRaCALA spot in Figure 9 A and B is provided in Table 9 and Table 10 (see Appendix A), respectively. Unlabeled cdiGMP was synthesized by Dr. Herman Sintim and Jingxin Wang.

2.4 Use of DRaCALA to Quantitate Protein-Ligand Interactions

In addition to qualitative assessments of specific protein-ligand interactions, DRaCALA is useful for quantitating biochemical parameters, including the dissociation constant (K_d) and the dissociation rate (k_{off}). The K_d can be measured by altering either the protein or ligand concentration in titration experiments; because DRaCALA detects only the ligand mobility, ligand concentrations are always held constant. As an example, the K_d of $Alg44_{PilZ}$ binding to cdiGMP was determined by analyzing mixtures of 4 nM ^{32}P-cdiGMP with 0.006–100 μM $Alg44_{PilZ}$ (Figure 10A). At concentrations of protein above the K_d, the F_B approaches saturation; this binding decreases as the $Alg44_{PilZ}$ concentration is decreased, reaching a level indistinguishable from background at the lowest protein concentrations. Analysis of this binding curve indicated that $K_d = 1.6 \pm 0.1$ μM, which is in reasonable agreement with our previously reported value of 5.6 μM determined by ITC (191) (Figure 10B). Application of identical samples to the dot blot apparatus for a vacuum-mediated filter-binding assay resulted in problems associated with high protein concentrations and, as a consequence, difficulty in assessing saturation of binding (Figure 11). Because the assay is completed in less than 5 s, DRaCALA can also be used to determine the k_{off} for those protein–ligand complexes with slower off rates. The k_{off} was determined for cdiGMP and $Alg44_{PilZ}$ by spotting at the indicated time points after the addition of 1 mM unlabeled cdiGMP to a preincubated mixture of $Alg44_{PilZ}$ and ^{32}P-cdiGMP (Figure 10C). The fractions bound were plotted against time and analyzed by nonlinear regression, which yielded a k_{off} of 0.017 ± 0.002 s^{-1}, corresponding to a $t_{1/2}$ of 35.6 ± 10.7 s (Figure 10D). The binding of ^{32}P-cdiGMP to $Alg44_{PilZ}$ was completely competed away by 1 mM unlabeled cdiGMP within 90 s.

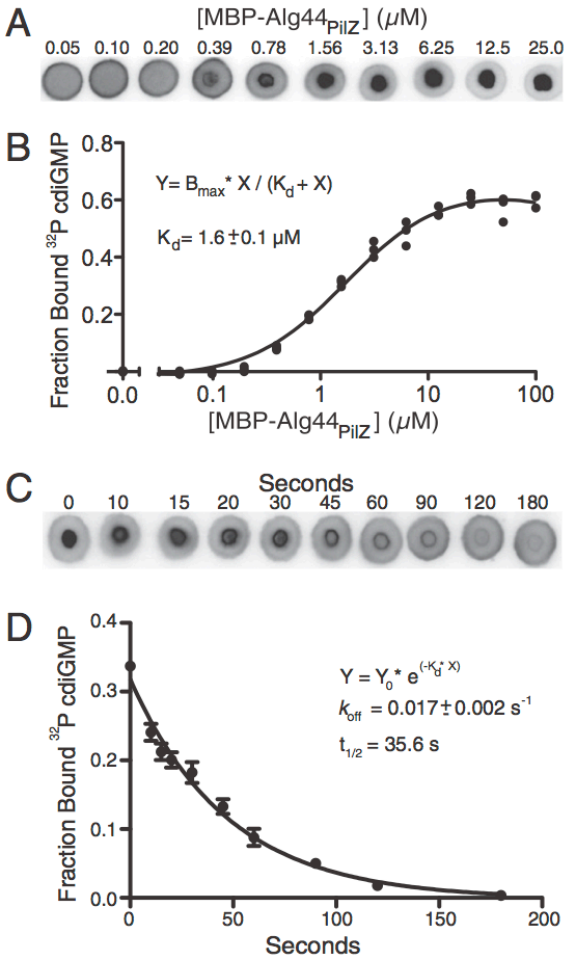

Figure 10. Determination of K_d and k_{off} by DRaCALA. (A) DRaCALA images were used for K_d determination for the interaction of $Alg44_{PilZ}$ and cdiGMP. His-MBP-$Alg44_{PilZ}$ was varied from 100 μM to 6 nM, and the ^{32}P-cdiGMP was held constant at 4 nM. Representative images of six sets of DRaCALA experiments are shown for 40 nM to 25 μM Alg44 protein. (B) F_B from data in A were plotted as a function of [MBP-$Alg44_{PilZ}$], and the best-fit line was determined by nonlinear regression using the indicated equation. A no-protein control was also plotted. The fitting program varied both K_d and B_{max} to obtain the best fit, indicated by the solid line. (C) k_{off} was determined by spotting protein-ligand mixtures onto nitrocellulose at various times after the addition of 1 mM cold cdiGMP to a mixture of 4 nM ^{32}P-cdiGMP and HisMBP-$Alg44_{PilZ}$. (D) Time course of decrease of F_B from analysis of the data in C was fitted to a single exponential decay, indicating k_{off}. The I_{total} of each DRaCALA spot in Figure 10 A and C is provided in Table 11 and Table 12 (see Appendix A), respectively. Unlabeled cdiGMP was synthesized by Dr. Herman Sintim and Jingxin Wang.

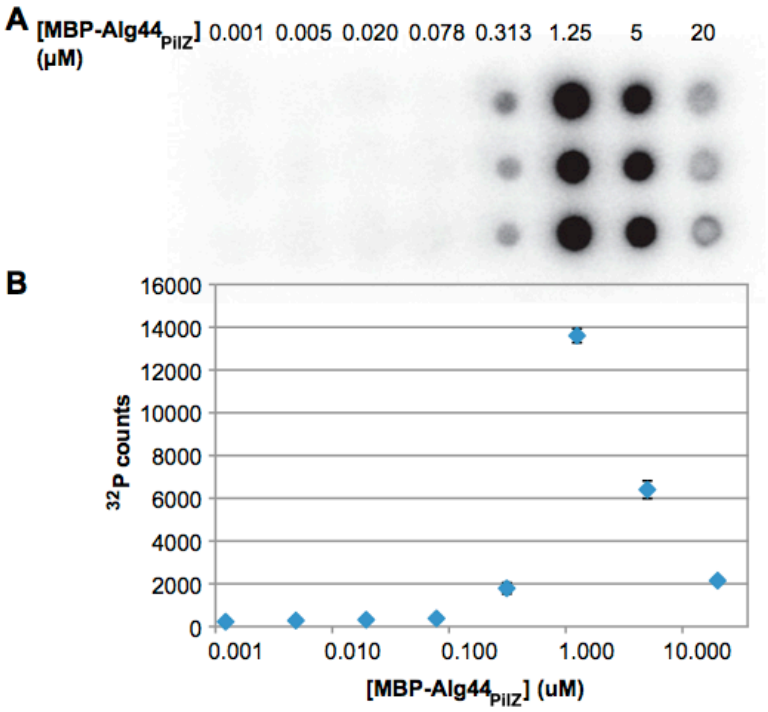

Figure 11. Dot-blot analysis of cdiGMP-binding to Alg44PilZ. MBP-Alg44$_{PilZ}$ at the indicated concentration was mixed with 4 nM ^{32}P-cdiGMP and incubated for 10 min. Samples were applied to the dot apparatus and washed with 10 mM Tris (pH 8.0) and 100 mM KCl. The filter was dried and exposed to the phosphorimager screen. (A) Image of the dot-blot experiment performed in triplicate. (B) ^{32}P counts graphed against each concentration of Alg44$_{PilZ}$.

Occasionally, we observed an increased signal at the leading edge of the capillary action and in the protein portion of the DRaCALA spot. Both edge and annulation effects are explained in Figure 12. The edge effect is attributable to evaporation of the solvent during the time of the experiment, and it is dependent on the humidity of the local environment around the nitrocellulose support. The evaporation results in a smaller total area (A_{total} observed in Figure 12A) and leads to an increased value in the calculated $I_{background}$. As a secondary correction for the edge effect, the F_B determined for spotted ligand in the absence of protein can be subtracted from all samples in parallel (Figure 12B). The annulation effect does not alter the F_B calculation (Figure 12C). Results from these experiments demonstrate the utility of DRaCALA for rapid and precise quantitation of biochemical parameters.

2.5 DRaCALA Detection of Ligand-Binding Proteins in Whole Cells

A major limitation of most biochemical assays is the requirement for purified protein. We asked whether DRaCALA could be applied to crude extracts to overcome this limitation. $Alg44_{PilZ}$ binding to cdiGMP requires a number of conserved residues, including R17, R21, D44, and S46, in the PilZ domain of the protein (191). *E. coli* BL21(DE3) expressing $Alg44_{PilZ}$ and variants with R21A, D44A, S46A, and R17A/R21A substitutions were lysed and tested for binding to cdiGMP using DRaCALA. Protein extracts from *E. coli* expressing MBP alone did not bind cdiGMP (Figure 8 C and D). Only the whole-cell lysates from *E. coli* expressing WT $Alg44_{PilZ}$ sequestered ^{32}P-cdiGMP (Figure 13A). Specificity of ^{32}P-cdiGMP sequestration in the background of all other cellular macromolecules was demonstrated by competition with 1 mM unlabeled specific competitor cdiGMP or the nonspecific competitor GTP. A significant difference

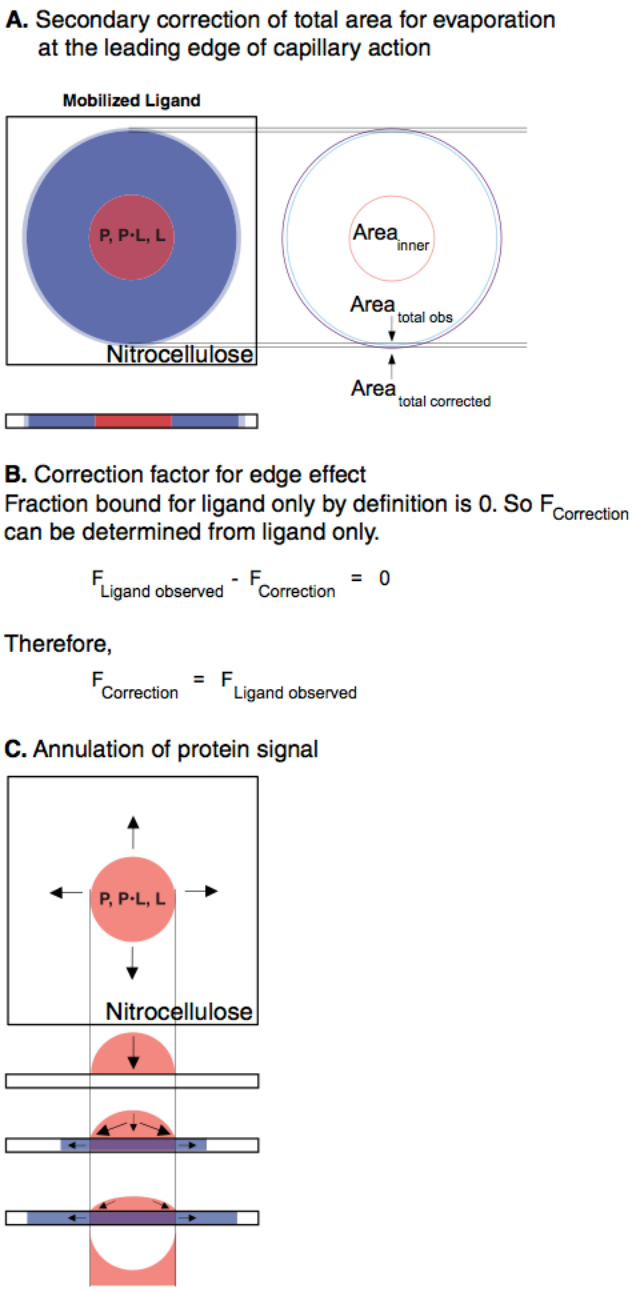

Figure 12. Edge and annulation effects of DRaCALA. (A) Schematic for the basis of the edge effect attributable to evaporation. obs, observed. (B) Correction factor for the edge effect. (C) Schematic indicating the basis of the annulation of the protein signal. P, protein; L, ligand; P•L, protein–ligand complex.

between the bound fractions for cdiGMP or GTP competition experiments was detected for the WT $Alg44_{PilZ}$ but not for the PilZ domain mutants (Figure 13 A and B). The results from whole-cell lysates are in agreement with the results obtained with purified proteins (191) (Figure 13B). The sensitivity of DRaCALA detection of MBP-$Alg44_{PilZ}$ binding to cdiGMP was tested by testing serial dilutions of purified protein alone or in the presence of BL21(DE3) whole-cell lysates. The results show that the binding of cdiGMP by MBP- $Alg44_{PilZ}$ is not affected by the presence of cellular proteins (Figure 13C). Furthermore, serial dilution of extracts from BL21(DE3) cells expressing MBP-$Alg44_{PilZ}$ also resulted in a similar binding curve for comparable levels of MBP-$Alg44_{PilZ}$ proteins (Figure 13C and Figure 14). A common problem during expression of heterologous protein in a foreign host is that the protein is often insoluble and forms inclusion bodies. Expression of both $Alg44_{PilZ}$ and PelD without the MBP tag resulted in insoluble proteins (Figure 15A). We tested the whole-cell extracts with soluble and insoluble proteins and found that either form of the protein can specifically sequester cdiGMP by DRaCALA (Figure 15 B and C). Serial dilution of the whole-cell extracts reduced cdiGMP sequestration to background levels for BL21 whole-cell extracts (Figure 15D). The ability to detect protein-ligand interactions in whole-cell lysates makes DRaCALA amenable to high-throughput analysis of whole-cell lysates for the presence of ligand-binding proteins.

2.6 DRaCALA Detection of cdiGMP-Binding Proteins in Diverse Prokaryotic and Eukaryotic Organisms

The applicability of DRaCALA to high-throughput metabolite interactomics was demonstrated by screening for binding proteins of an important secondary signaling

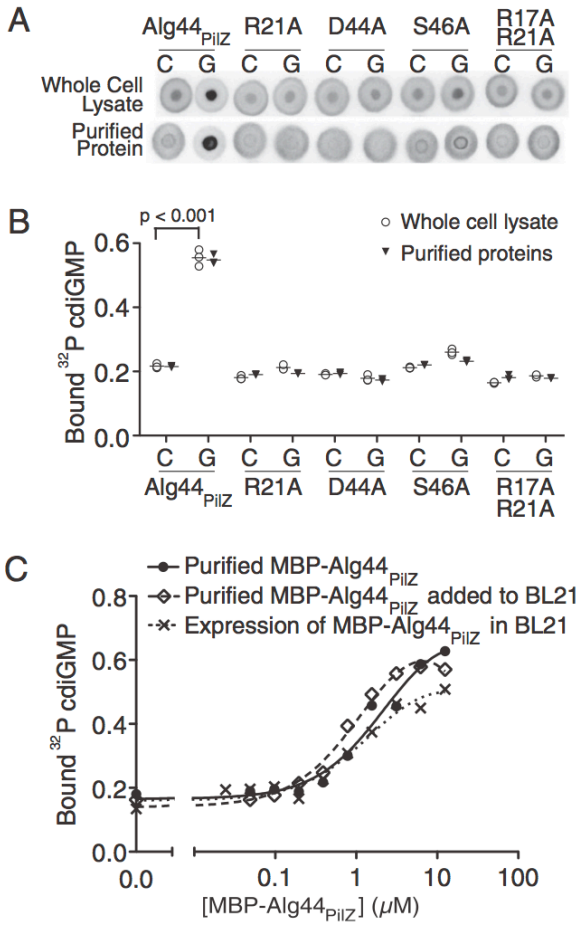

Figure 13. Detection of specific protein-ligand interaction in whole-cell lysates by DRaCALA. (A) Images of $Alg44_{PilZ}$ interaction with 4 nM ^{32}P-cdiGMP and either 1 mM cold cdiGMP or GTP with purified proteins or when expressed in E. coli BL21(DE3). C, cdiGMP; G, GTP. (B) Graph of ^{32}P-cdiGMP-binding by whole-cell lysate samples (open circles) and purified proteins (triangles) in Figure 13A, with the average indicated by a horizontal bar. P values were determined by a Student t-test for significant differences compared with the no-competitor control for three independent experiments. The I_{total} of each DRaCALA spot in Figure 13B is provided in Table 13 and Table 14 (see Appendix A). Unlabeled cdiGMP was synthesized by Dr. Herman Sintim and Jingxin Wang. (C) Graph of ^{32}P-cdiGMP-binding by purified MBP-$Alg44_{PilZ}$, purified MBP- $Alg44_{PilZ}$ added to BL21 whole-cell lysates, and whole-cell lysates of BL21(DE3) overexpressing MBP- $Alg44_{PilZ}$. Protein concentrations were determined by separation on SDS/PAGE and staining with Coomassie blue (Figure 14).

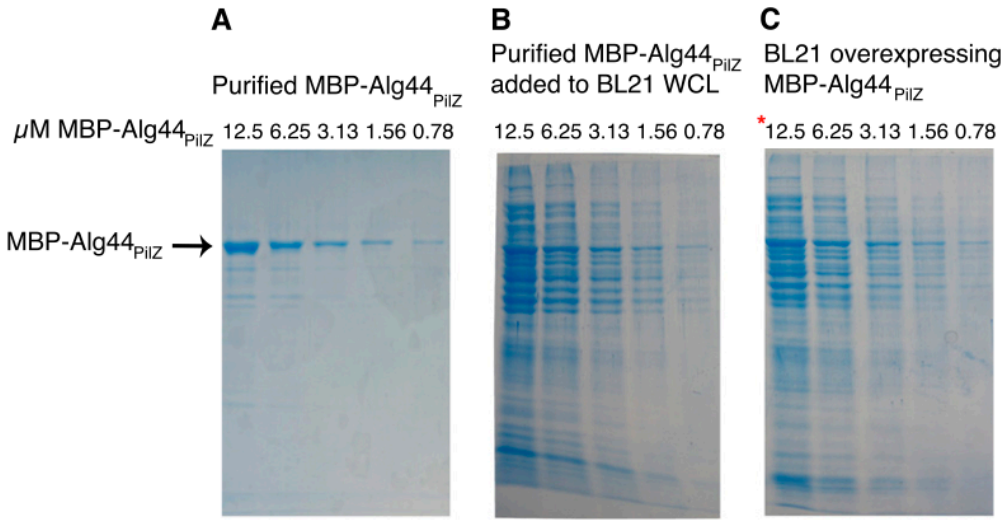

Figure 14. Protein pattern of purified and expressed MBP-Alg44PilZ. Coomassie-stained PAGE of two-fold serial dilutions of MBP-Alg44$_{PilZ}$ as a purified protein in cdiGMP-binding buffer (A), a purified protein added to BL21 whole cell lysate (B), or an overexpressed protein in BL21 cells (C). whole cell lysate, whole-cell lysate. The protein concentration for the purified protein in A and B was determined as described in 2.8 Materials and Methods. The protein concentrations of the MBP-Alg44$_{PilZ}$ in whole-cell lysates in C were estimated based on comparison with A and B.

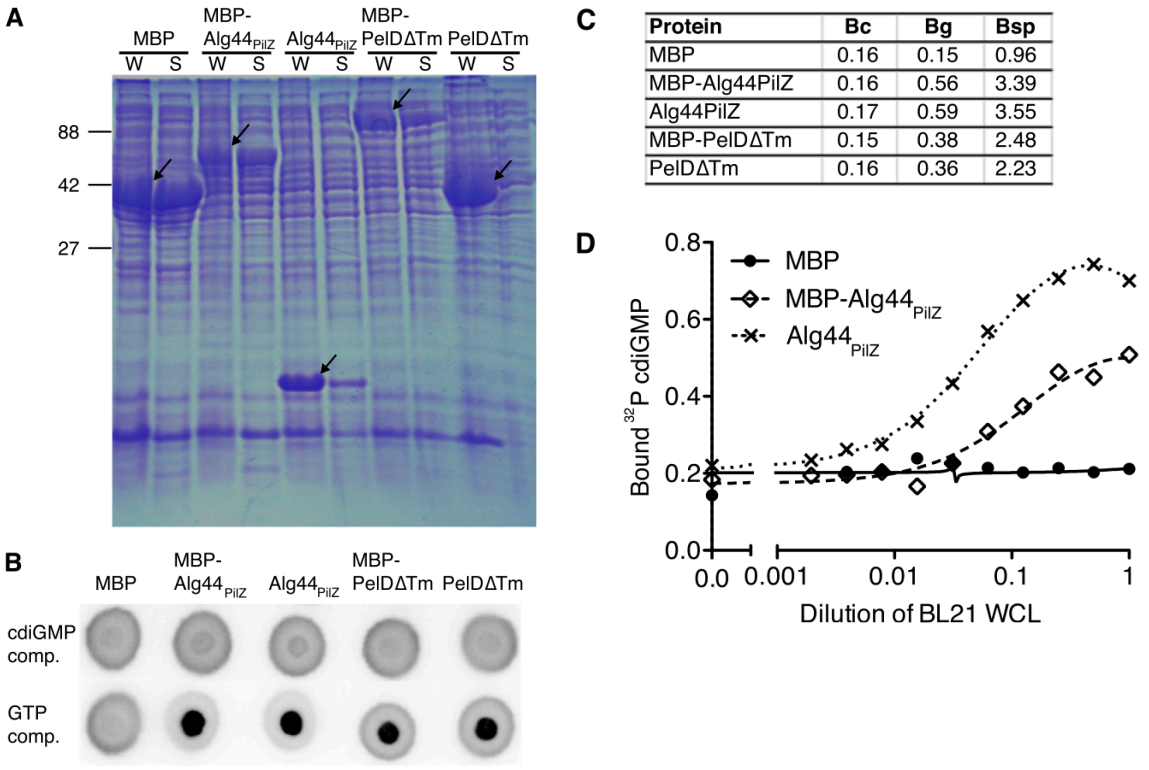

Protein	Bc	Bg	Bsp
MBP	0.16	0.15	0.96
MBP-Alg44PilZ	0.16	0.56	3.39
Alg44PilZ	0.17	0.59	3.55
MBP-PelDΔTm	0.15	0.38	2.48
PelDΔTm	0.16	0.36	2.23

Figure 15. Binding of cdiGMP to whole-cell lysates expressing soluble or insoluble cdiGMP-binding proteins. (A) BL21(DE3) cells expressing the indicated proteins were analyzed by PAGE and Coomassie staining of whole-cell (WC) and soluble (S) fractions. Arrows indicate the overexpressed protein of the correct molecular weight in whole-cell lysates. Molecular weights of proteins are indicated on the left in kilodaltons. (B) Spots of BL21 cells overexpressing the indicated proteins were assayed for ^{32}P-cdiGMP-binding by DRaCALA when competed (comp.) with unlabeled cdiGMP or GTP as indicated. Unlabeled cdiGMP was synthesized by Dr. Herman Sintim and Jingxin Wang. (C) Quantification of the data shown in B. (D) Binding of ^{32}P-cdiGMP to various dilutions of lysates of BL21(DE3) cells expressing the indicated proteins.

dinucleotide, cdiGMP. Recent findings have identified cdiGMP as the signaling molecule that controls biofilm formation, motility, and a number of other bacterial functions (97,175,194-196). Although the enzymes known to synthesize and degrade cdiGMP are restricted to bacteria, there are questions as to which bacterial species express cdiGMP-binding proteins. cdiGMP has also proven to be useful as an adjuvant during immunization to enhance the mammalian immune response (197), which suggests that there may be cdiGMP-binding proteins in higher eukaryotes. We used DRaCALA to test 191 strains of *P. aeruginosa* and a panel of 61 other species in a 96-well plate format. As a control for specificity, each extract was tested for binding to the labeled ligand by competition with the unlabeled specific or nonspecific ligand. As in the example of whole-cell lysates of *E. coli*, unlabeled GTP competitor was used to detect specific ^{32}P-cdiGMP-binding [bound during GTP competition (B_G)] and unlabeled cdiGMP competitor was used to detect nonspecific 32P-cdiGMP-binding [bound during cdiGMP competition (B_C)] (Figure 16A). The ratio of B_G to B_C is called specific binding (B_{Sp}). The limit of nonspecific binding was calculated by adding 2 SDs to the average B_C, resulting in a conservative cutoff value for a positive B_{Sp} value of 1.17 (Figure 16A and Table 15 (see Appendix A)). Of the 191 *P. aeruginosa* isolated from various sources, 184 (96%) displayed a positive B_{Sp} value greater than 1.17 (96 samples shown in Figure 16B and all data presented in Table 15 (see Appendix A)). These results suggest that most *P. aeruginosa* strains express detectable levels of cdiGMP-binding proteins. When strains isolated from different sources were analyzed for cdiGMP-binding, all groups had an average B_{Sp} value greater than 1.48, suggesting that cdiGMP signaling is retained (Figure 17 and Table 15 (see Appendix A)). The range of cell lysate concentrations required for

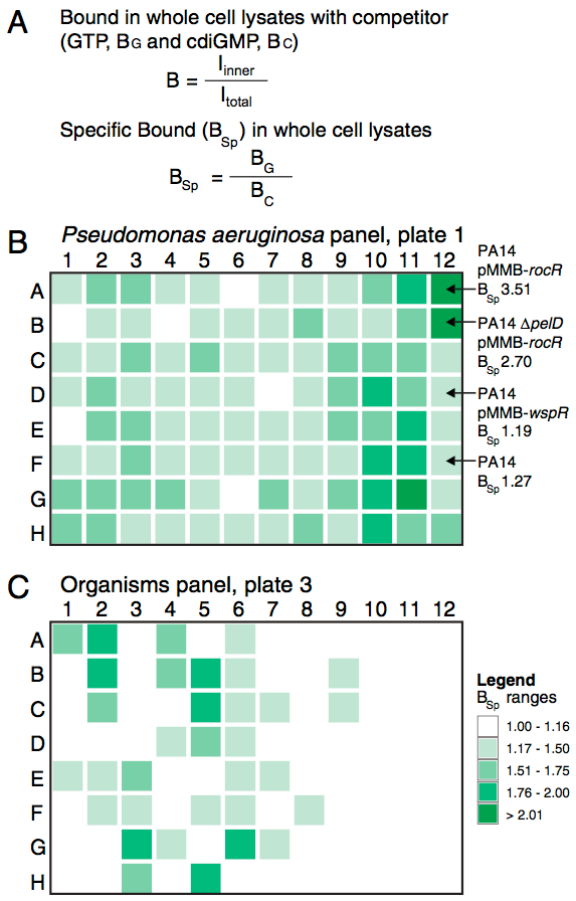

Figure 16. Analysis of cdiGMP-binding proteins in various organisms. B_{Sp} values of whole-cell lysates are shown as a heat map using the range indicated in the legend. (A) Equations used to analyze DRaCALA data for B_{Sp} for whole-cell lysates or tissue extracts. (B) Plate 1 is the analysis of cdiGMP-binding by lysates from P. aeruginosa isolates. Specific strains discussed in the text are indicated by arrows. Sources of all strains in plates 1 and 2, as well as the raw data for each lysate, are shown in Table 15 (see Appendix A). (C) Plate 3 is the analysis of cdiGMP-binding by lysates from various organisms. Plate numbers, column numbers, and row letters correspond to the strains and organisms listed in Table 15 and Table 16 (see Appendix A). Unlabeled cdiGMP was synthesized by Dr. Herman Sintim and Jingxin Wang.

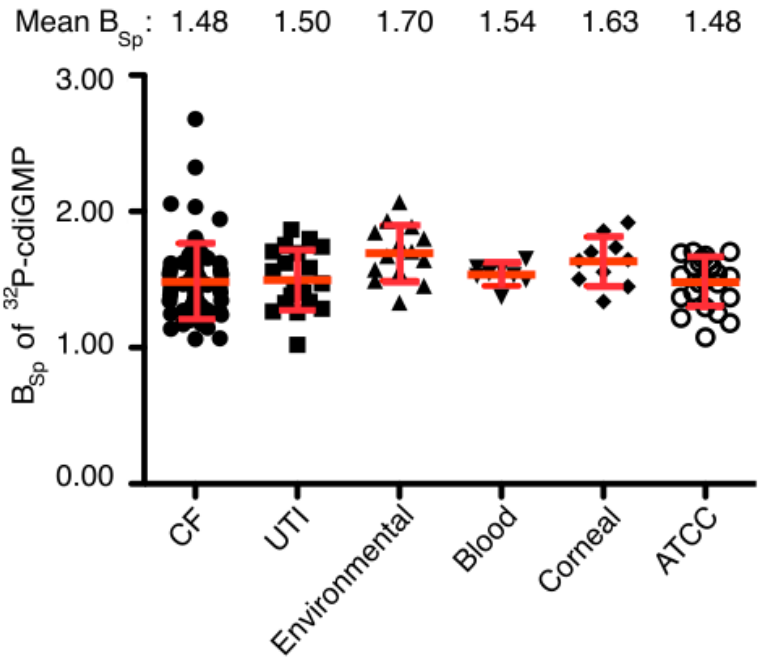

Figure 17. B_{Sp} distribution of P. aeruginosa strains from different sources. B_{Sp} values of ^{32}P-cdiGMP for P. aeruginosa isolates of different origins, with mean and SD, are shown. The mean ± SD is noted above each group; no significant differences were observed. CF, cystic fibrosis; UTI, urinary tract infection; ATCC, American Type Culture Collection.

consistent signal detection was tested by diluting cell extracts to 10–60 absorbance (280 nm) units in intervals of 10. Each lysate dilution yielded similar B_{Sp} values, suggesting that this range of cell lysate concentration provides a reliable readout for the detection of cdiGMP-binding (Figure 18).

One potential complicating factor is the effect of cdiGMP metabolism and endogenous cdiGMP levels on the DRaCALA readout. Extracts of the laboratory *P. aeruginosa* strain PA14 overexpressing either the PDE RocR (198) or the DGC WspR (89) were tested for their ability to bind cdiGMP. WT PA14 showed a B_{Sp} value of 1.27 indicating that cdiGMP-binding proteins are not fully occupied by endogenous cdiGMP consistent with what is expected for signaling systems (F12 of plate 1 of Figure 16B and Table 15 (see Appendix A)). Increasing the cellular cdiGMP concentration through WspR overexpression decreased the B_{Sp} value to 1.19 (D12 of Figure 16B and Table 15 (see Appendix A)). Reducing cellular cdiGMP through RocR overexpression increased the B_{Sp} value to 3.51 (A12 in Figure 16B and Table 15 (see Appendix A)). The amount of cdiGMP sequestered by a whole-cell extract should reflect the amount and affinity of the binding proteins present. This was tested by overexpression of RocR in the PA14*ΔpelD* background, which lacks the cdiGMP-binding protein PelD (199). Without PelD, the B_{Sp} value was reduced to 2.70 (B12 in Figure 16B and Table 15 (see Appendix A)), indicating that PelD is an important binding protein for cdiGMP and that other proteins also bind cdiGMP (191,199). These results indicate that endogenous cdiGMP metabolism affects but does not abolish the ability of DRaCALA to detect cdiGMP-binding proteins.

cdiGMP signaling occurs in a wide variety of bacterial species but is not known to be present in Eukarya (200). We tested 54 bacterial species from 37 genus and 7

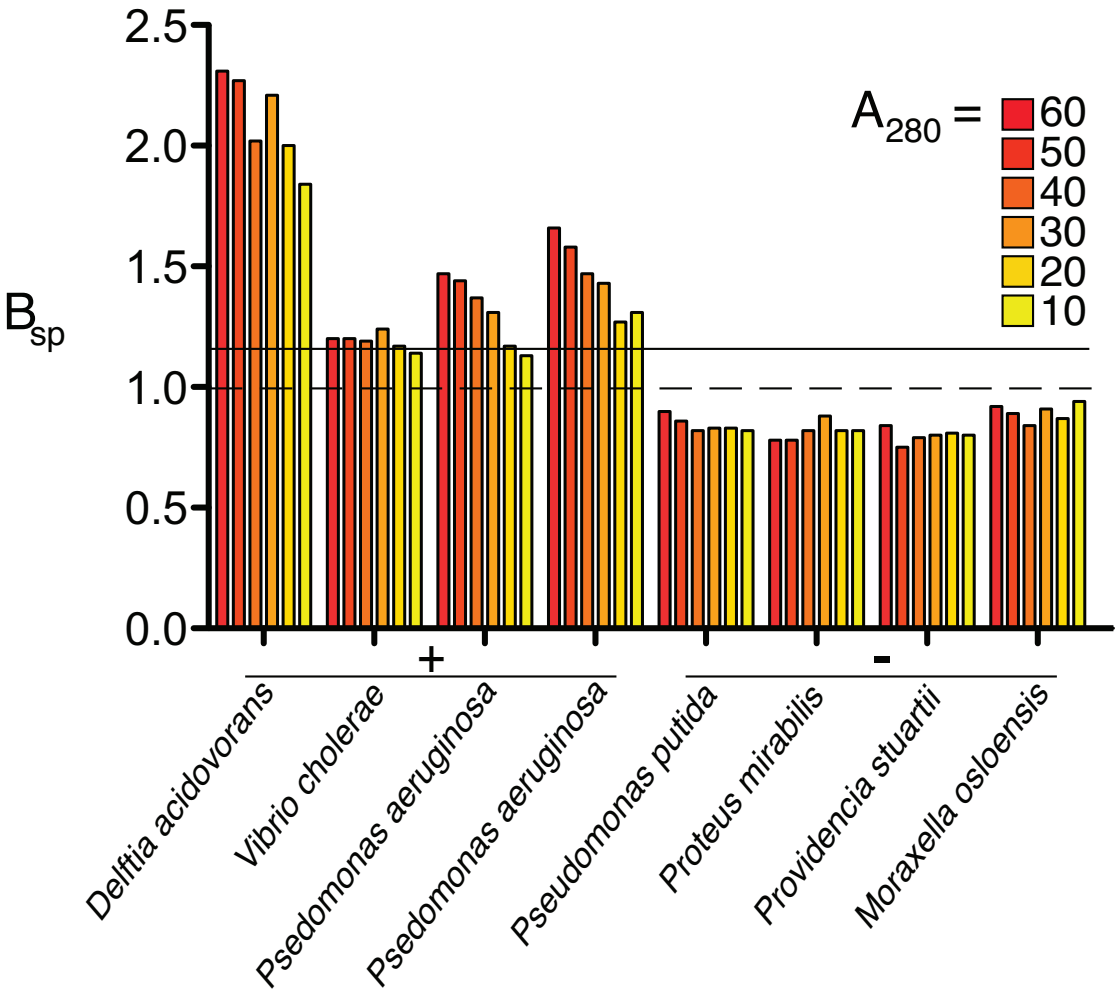

Figure 18. Effect of Dilution on Organism Whole Cell Lysate Binding. The effect of whole cell lysate A_{280} on organism B_{sp} was examined for eight representative strains examined in Figure 16. Four strains displaying a positive B_{sp} *Delftia acidovorans* (3_A12), *Vibrio cholerae* (3_A2), *Pseudomonas aeruginosa* (1_A10), *Pseudomonas aeruginosa* (1_D10) and four strains displaying a negative B_{sp} *Pseudomonas putida* (3_B3), *Proteus mirabilis* (3_C3), *Providencia stuartii* (3_C4), *Moraxella osloensis* (3_F4) were diluted to have A_{280} = 60, 50, 40, 30, 20, or 10 as assessed by NanoDrop. The dotted line indicates the cutoff for specific binding of the whole cell lysate for cdiGMP, while the solid line indicates the positive cutoff for specific binding indicative of the presence of a cdiGMP-binding protein.

eukaryotic species, including protozoa, fungi, nematodes, plants, and mammals. Of the 82 tested bacteria strains, 31 (38%) displayed a B_{Sp} value greater than 1.17. Included in the 31 positive samples are 21 species for which functional cdiGMP signaling has yet to be demonstrated, of which 4 species, *Serratia marcescens, Pseudomonas alcaligenes, Pseudomonas diminuta, and Brevundimonas vesicularis*, have not yet been sequenced (Figure 16C and Table 15 (see Appendix A)). We tested 6 bacterial species with sequenced genomes that do not have annotated DGCs, and all of them failed to sequester cdiGMP above the threshold. We also tested 8 eukaryotic species, none of which have annotated DGCs. Whole-cell extracts of protozoa, fungi, and nematodes displayed a B_{Sp} value below 1.17, indicating that cdiGMP-binding proteins are absent or below the limit of detection. Mammalian tissue extracts from rodent and human cell lines displayed high nonspecific binding with BC values greater than 3 SDs above the average B_C value (> 0.233; F6, E12, G12, and H12 in Figure 16C and Table S2.8). Furthermore, the nonspecific binding was eliminated after three twofold dilutions of these tissue extracts, indicating that mammalian tissues may contain receptors with low affinity or low abundance. Only positive B_{Sp} results from DRaCALA can be interpreted for utilization of cdiGMP signaling. As a result, DRaCALA is most effective in whole-cell extracts with low nonspecific binding. Utilization of DRaCALA in a high-throughput format has expanded our knowledge of the bacterial organisms harboring cdiGMP-binding proteins and confirmed the absence of abundant high-affinity cdiGMP-binding proteins in eukaryotes.

2.7 Discussion

In this work, we have developed and characterized DRaCALA as a rapid and

precise method for quantitatively measuring protein-ligand interactions. We show the utility of DRaCALA by using the example of cdiGMP-binding to $Alg44_{PilZ}$ as a proof of principle. The dissociation constant of 1.6 μM obtained by DRaCALA is similar to those obtained in previous studies using filter binding, ITC, and surface plasmon resonance assays (191,199). Previous studies of the dissociation rate of cdiGMP from $Alg44_{PilZ}$ were based on saturating the protein with radiolabeled cdiGMP and separating the protein–ligand complex from unbound cdiGMP over a Sephadex column. The $t_{1/2}$ of the complex was estimated by filter binding as 5 min, in contrast to 35.6 ± 10.7 s as detected by DRaCALA. This discrepancy is likely attributable to two key differences between the two assays. First, DRaCALA is able to quantify the total signal directly in each sample. Because of the various separation steps required for the filter-binding assay, the total ligand in each sample is just assumed to be equivalent. For DRaCALA, the total signal of labeled ligand is known for each individual sample, therefore eliminating the need to assume that the total signal is equivalent. The ability to detect the total signal and F_B significantly increases the precision of the measurement and reduces the error incurred from pipetting and other physical manipulations. Second, the processing times of the assays are dramatically different. The filter assay involved binding, separation of bound ligand from free ligand, filter binding, and the associated wash time, requiring at least 5 to 10 min of processing time. DRaCALA directly assays the binding without prior processing or the subsequent wash steps. As a result, DRaCALA can be completed within 5 to 30 s, depending on the volume of the sample spotted. Because all binding interactions have off-rates, the speed of the assay is critical to capture accurate data. Other techniques for determining biochemical interaction are also available, such as ITC

or surface plasmon resonance; however, these techniques require dedicated specialized instrumentation and individual processing of samples, resulting in longer assay time and lower throughput. An important feature of DRaCALA is that it will make biochemical approaches accessible to molecular and cellular biologists interested in precise and simple measurements of interactions between protein-ligand pairs of interest. The ability to determine k_{off}, in addition to K_d, allows calculation of the on-rate. Differences in the k_{off} can be useful in understanding biological processes, because interactions with similar affinities can result in distinct biological outputs.

As protein concentrations increase, fraction bound of the labeled ligand eventually saturates, with some fraction of the label unable to be immobilized by increasing protein concentration. There are three potential factors that contribute to the amount of label that cannot be immobilized in DRaCALA assays. First, some label may not be associated with the desired ligand. For example, during synthesis of ^{32}P-cdiGMP, approximately 1 – 4 % of radiolabel is not associated with cdiGMP when assayed by thin layer chromatography. Second, labeled ligands may degrade over time and lose their ability to interact with cognate binding proteins. Label that is not associated with the appropriate ligand cannot be immobilized in the DRaCALA assay and likely contributes to saturating fraction bound < 1.0. A third potential factor affecting maximum fraction bound is that labeled ligands can dissociate from proteins during the DRaCALA assay time. During the time that liquid drops are wicked into the membrane, bound ligand can dissociate from immobilized protein. Ligand that dissociates during wicking will be mobilized away from the protein, thereby systematically reducing apparent fraction bound. The magnitude of this effect is expected to decrease with slower off-rates.

Supporting this idea, protein-ligand interactions with slow off-rates, such as the biotin-streptavidin interaction presented in Chapter 4 with a half-life of 112 h achieves an apparent fraction bound close to 1.0. In contrast, the Alg44-cdiGMP complex has a half-life of approximately 35 s, which is on the same scale as the time of the DRaCALA assay (5 - 10 s), and achieves a maximum fraction bound of approximately 0.6. Thus, protein-ligand interactions with off-rates that are faster or of the same magnitude as the assay time will have systematically decreased apparent fraction bound. Variations in maximum fraction bound likely do not affect quantification of dissociation constants and dissociation rates. Linear regression models used to determine these parameters do not assume a maximum fraction bound of 1.0 and measurements of protein-ligand interactions with Alg44 (Chapter 2) and CRP (Chapter 4) closely match previous observations.

The principle of DRaCALA should be universally applicable to any system in which the ligand can be mobilized by capillary action in conjunction with a solid support capable of sequestering the macromolecule. Thus, the choice of the support, the solvent composition of the mobile phase, and the specific properties of the ligand can be altered to enhance the effectiveness of DRaCALA for various protein-ligand systems. In this paper, we have described the application of DRaCALA only for radiolabeled ligands; however, the principle of the assay should also apply to fluorescently labeled ligands. The solid support could also be changed to sequester other macromolecules based on their unique chemical properties. For example, nucleic acids can be retained by DEAE-cellulose (183). The solvent composition could also be changed to alter the chemical properties of the mobile phase. Detergents, salts, and other agents may be added to alter

the relative behavior of the protein and ligand on the solid support.

Studies of numerous systems involving low molecular weight biological ligands and receptor macromolecules can benefit from DRaCALA, including nucleotide derivatives, amino acid derivatives, metal ions, sugars, and other small signaling molecules. The function of biological ligands can be specific to subset of organisms that produce or use these molecules. To identify biological samples that may be enriched in a specific ligand-binding protein, a similar approach to the screen for cdiGMP-binding proteins (Figure 16C) can be taken to identify model organisms for study of the ligand of interest. Alternatively, expression of ligand-binding proteins may be regulated. DRaCALA provides a method for rapidly screening a single organism grown in different conditions, as in phenotypic arrays, and a test for ligand binding activity.

The systematic identification of protein receptors for each of these small molecular ligands will allow for a comprehensive understanding of the biological effect of these signaling molecules, and DRaCALA offers a high-throughput platform that should greatly facilitate this process. Furthermore, the ability of DRaCALA to detect ligand binding in whole-cell extracts should allow for systematic screening of whole-genome ORF libraries (ORFeomes) for proteins that bind various small molecules. Although the binding proteins have been overexpressed, the key parameter for detection is that the cellular concentration of expressed protein is greater than the K_d for the ligand. For proteins with low affinities, these interactions will be difficult to detect in whole cells similar to purified systems. DRaCALA is scalable, and it has been performed using both a standard single-channel pipette and an eight-channel multichannel pipette with equal precision and accuracy. Thus, DRaCALA could be easily adapted for high-throughput

applications by using a 96-well pin tool in combination with standard robotics. The volume required for the DRaCALA assay can be further reduced to allow for screening using the 384-well format. A current limitation of the whole cell-based DRaCALA system is the requirement to identify a cell that has low background expression of proteins that bind the ligand of interest. This problem can be solved using protein array technology (187-189,201,202). However, high-volume parallel protein purification requires specialized equipment, and it is difficult to assess the stability and functionality of all proteins on the chip. Nonetheless, DRaCALA and protein arrays can be viewed as complementary technologies. This is analogous to the identification of protein-protein interactions using the genetic/molecular biology approach of the yeast two-hybrid assay (203), which is complementary to the biochemical approach of mass spectrometric identification of co-precipitated proteins. An important advantage of DRaCALA is that insoluble proteins appear to have a similar behavior as soluble protein in whole-cell lysates, thus avoiding purification problems associated with insoluble proteins.

Development of DRaCALA as a high-throughput assay for the detection of protein-ligand interactions will be useful for identifying new targets for pharmaceutical intervention. To this end, DRaCALA might be used initially as a screening tool to identify new interaction pairs and then in a second round of DRaCALA to identify inhibitors that prevent the interaction. Labeling of the identified specific inhibitor would then allow for rapid sequential screening for even more potent molecules that can displace the original inhibitor. Our results show that DRaCALA can be developed as a platform to enable critical advances in metabolite interactomics and therapeutic intervention.

2.8 Materials and Methods

Protein purification

pBAD-CRP was a generous gift from Dr. Sankar Adhya, and purified NtrB was a generous gift from Dr. Richard Stewart. *E. coli* strain BL21(DE3) harboring a modified pET19 expression vector (pVL847) expressing an N-terminal histidine-MBP-Alg44 were induced for 6 hours at 30 ˚C with 1mM IPTG. Induced bacteria were collected by centrifugation and resuspended in His Buffer A (10 mM Tris, 100 mM NaCl and 25 mM imidazole, pH8.0) and frozen at -80 ˚C until purification. After addition of DNase, lysozyme and PMSF (1 mM final concentation), thawed bacteria were lysed by sonication. Insoluble material was removed by centrifugation and the His-fusion protein was purified from the clarified whole cell lysate by separation over an Ni-NTA column. Proteins were subsequently purified and concentrated using anion exchange to a concentration of at least 100 μM, supplemented with 25% glycerol, and frozen at -80 °C until thawed for use.

Detailed Protein Purification

*His affinity purification***:** Clarified whole cell lysates were loaded onto a 10mL column containing Ni-Nta resin. The Ni-NTA column was washed with 120mL of His Buffer A to remove non-specifically bound proteins. Elution of the His-tagged protein was accomplished by linearly increasing the imidazole concentration from 25 to 250 mM over 30mL. Eluted proteins were pooled and dialysed twice against 40 volumes of 100 mM NaCl, 10 mM Tris pH = 8.0.

Anion exchange purification: The dialyzed eluent from Ni-NTA was loaded onto an 5 mL Q-Sepharose anion exchange column, followed by a wash of 120 mL of 10 mM

Tris pH = 8.0 and 100 mM NaCl. Proteins were eluted by linearly increasing the concentration of NaCl from 100 mM to 500 mM over an 80 mL volume. Eluent fractions containing the protein of interest were pooled, dialysed twice against 40 volumes of 100 mM NaCl, 10 mM Tris pH = 8.0, supplemented with 25% glycerol, and frozen at -80°C until thawed for use. Protein concentration was determined by absorbance 280 nm and calculated using predicted extinction co-efficient as determined by ProtParam program at the ExPASy website (http://expasy.org/tools/protparam.html).

Radiolabeled nucleotides

^{14}C labeled cAMP, γ-^{32}P labeled ATP, α-^{32}P labeled GTP were purchased from Perkin Elmer. cdiGMP was synthesized from α-^{32}P labeled GTP by incubating overnight in 1X cdiGMP-binding Buffer with a constitutively active diguanylate cyclase WspR(D70E). Purity of cdiGMP was assessed by TLC and was greater than 98%.

Differential Radial Capillary Assays

20 µl of protein or whole-cell lysates in 1x cdiGMP-binding buffer was mixed with 4 nM of radiolabeled nucleotide and allowed to incubate for 10 minutes at room temperature. Radiolabeled nucleotide was competed away by cold nucleotides in concentrations and for times indicated. 2-5 µl drops of these solutions were placed on dry, untreated nitrocellulose (GE Healthcare) in triplicate and allowed to dry completely before quantification. An FLA7100 Fujifilm Life Science Phosphorimager was used to detect luminescence following a 5-minute exposure of blotted nitrocellulose to phosphorimager film. Data was quantified using Fujifilm Multi Gauge software v3.0.

Whole-cell lysate preparation

BL21(DE3) cells expressing pVL847 (MBP), pVL882 (MBP-Alg44) or Alg44 point mutations were induced for overexpression with 100 μM IPTG. All bacterial samples and eukaryotic tissue were collected and resuspended in one-tenth volume of 1X cdiGMP-binding Buffer (100 mM KCl, 5 mM $MgCl_2$, 100 mM Tris, pH = 8.0 and 100 μM PMSF). Bacterial samples were also supplemented with lysozyme and DNase. Cells were lysed by two 10-second sonication pulses with 1 minute recovery on ice or by bead beating using the Q-Bio lysis system. Extracts were flash frozen in liquid nitrogen and stored at -80 ˚C. After thawing, 10 μL of whole cell lysates were incubated with 8 nM ^{32}P-cdiGMP for 45 seconds prior to spotting 2 μL drops on nitrocellulose using an 8-channel pipette.

Detailed Whole-cell lysate preparation

Samples from Figure 16B and Table 15 (see Appendix A) excepting those listed below, were grown in LB broth at 37 ˚C with 200 rpm shaking. Samples 75, 90, 91 were grown on YPD plates at 30 ˚C; 74 on TSB plate in anaerobic chamber at 37 ˚C; 16, 58, 67, 70, 79 in TSB broth at 37 ˚C; 83, 84, 85, 86 in THB broth at 37 ˚C; 20, 42, 46, 50, 89 are tissue samples; 51 in Marine Media at 30 ˚C with shaking; 37 in LB broth supplemented with 1 M NaCl; 5, 6, 7, 49, 63 in LB broth at 30 ˚C; 93, 94, 95, 96 in DMEM F12 from Gibco (Catalog # 10565) supplemented with 10% FBS, 1& Penn/Strep, and 1% glutamine; 92 in a 50/50 mixture of Sigma Media 199 (Catalog #M7528) and Sigma Schneider's Complete Media (Catalog #S0146) supplemented with 10%FBS, 1% glutamine, and 1% Penn/Strep; Sample 3G_11 *Mycobacterium smegmatis* (strain mc2 155) was grown in modified 7H9 medium (DIFCO) as previously described (204);

Samples 3H_10 and 3A_11 *Neisseria gonorrhoeae* and 3B_11 *Neisseria sicca* were grown in phosphate-buffered gonococcal medium (Difco) supplemented with 20 mM d-glucose and growth supplements in broth with addition of 0.042% $NaHCO_3$ in a CO_2 incubator at 37°C (205).

All bacterial samples were collected by centrifugation and all tissues were collected by dissection and resuspended in one-tenth volume of 1X cdiGMP-binding Buffer (100 mM KCl, 5 mM $MgCl_2$, 100 mM Tris, pH = 8.0 and 100 μM PMSF). Bacterial samples were also supplemented with lysozyme and DNase. Cells were lysed by two 10-second sonication pulses with 1 minute recovery on ice or by bead beating using the Q-Bio lysis system. Extracts were flash frozen in liquid nitrogen and stored at -80 ˚C. After thawing, 10 μL of whole cell lysates were incubated with 8 nM ^{32}P-cdiGMP for 45 seconds prior to spotting 2 μL drops on nitrocellulose using an 8-channel pipette.

Chapter 3: Systematic Identification of Cyclic di-GMP Binding Proteins in *Vibrio cholerae*

3.1 Introduction

Cyclic di-GMP (cdiGMP) is a ubiquitous prokaryotic nucleotide second messenger produced by members of every major bacterial phylum to regulate diverse cellular processes (78,206). cdiGMP is synthesized by diguanylate cyclases (DGCs), which encode a conserved GGDEF domain, and degraded by phosphodiesterases (PDEs) that contain either an EAL or HD-GYP domain (84,95,101). Individual organisms can encode dozens of DGCs and PDEs creating complex regulation of cdiGMP metabolism (79). Genetic manipulation of DGCs and PDEs has revealed numerous cdiGMP-dependent phenotypes including biofilm formation, motility, cell cycle progression, and pathogenesis (94,124,173,207). The cdiGMP signal is sensed by protein and RNA effectors that bind cdiGMP to allosterically regulate effector activity. To understand how cdiGMP regulates these phenotypes, considerable effort has been spent identifying the cellular effectors of cdiGMP signaling.

cdiGMP effector proteins have been identified by bioinformatic, biochemical, and genetic approaches. Bioinformatics can identify proteins with conserved cdiGMP-binding domains, including the PilZ domain, the I-sites of GGDEF domains, and non-catalytic EAL domains that retain cdiGMP-binding activity (106,121). However, several cdiGMP effectors that lack a recognizable cdiGMP-binding domain have been identified by biochemical and genetic approaches. Genetic experiments can identify target proteins required for cdiGMP-dependent phenotypes, which can be subsequently purified and assayed for cdiGMP-binding (148,154). While this approach has been successful, several

constraints prevent the systematic identification of cdiGMP effectors. First, not all cdiGMP effectors display a phenotype under laboratory conditions. Second, cdiGMP-dependent phenotypes can be complex with multiple effectors and regulation by specific DGCs and PDES. Finally, biochemical approaches for cdiGMP-binding protein identification rely on affinity pull down of endogenously expressed proteins or systematic purification of individual genomically-encoded proteins (187,208). However, not all cdiGMP-binding proteins are expressed in laboratory conditions and not all are able to be purified.

We have developed a differential radial capillary action of ligand assay (DRaCALA) and demonstrated its ability to detect cdiGMP-binding proteins when expressed at levels that exceed the dissociation constant of their respective complexes with cdiGMP in *E. coli* whole cell lysates (209). DRaCALA provides a rapid biochemical assay suitable for determining if an individual open reading frame (ORF) encodes a cdiGMP-binding protein. Overexpressing all annotated ORFs from a sequenced organism and testing each one for cdiGMP-binding activity provides a systematic approach to identifying cdiGMP binding proteins. This approach does not require protein purification, overcomes potentially low endogenous protein expression by driving the expression of individual proteins in a heterologous system, and provides a direct measure of cdiGMP binding instead of observing a cdiGMP-dependent phenotype. Several libraries representing the majority of genomically-encoded ORFs (ORFeomes) have been constructed for prokaryotic organisms that contain a cdiGMP signaling system (210-213). A *Vibiro cholerae O1 El Tor N16961* library contains >98% of sequenced ORFs and thus represents the majority of genomically-encoded proteins of *V. cholerae(213). V. cholerae*

represents a model system for the study of complex cdiGMP signaling with genes encoding 41 GGDEF, 22 EAL, 9 HD-GYP, and 6 PilZ domains as well as 3 cdiGMP-dependent transcription factors (79,127,160,165,166). However, several cdiGMP-dependent phenotypes including expression of cholera toxin are not regulated by known cdiGMP-binding proteins, suggesting that more remain to be discovered (172).

Here we report the use of the DRaCALA screening to systematically identify cdiGMP-binding proteins from two *V. cholerae* protein expression libraries. Of these, we show that purified MshE binds cdiGMP and expression of a homologous ATPase PA14_29490 from *P. aeruginosa* also increases cdiGMP-binding in whole cell lysate. These results demonstrate the utility of a DRaCALA ORFeome screen for the identification of cdiGMP-binding proteins and suggest an expanded repertoire of cdiGMP regulated processes in *V. cholerae*.

3.2 Systematic Identification of cdiGMP-binding Proteins in *Vibrio cholerae*

We sought to systematically identify protein effectors of cdiGMP by individually testing *Vibrio cholerae* ORFs (VC ORFs) in *E. coli* whole cell lysates for ^{32}P-cdiGMP-binding activity by DRaCALA. To overexpress the protein products of *V. cholerae* ORFs, we mobilized 3812 unique ORFs from the *V. cholerae* O1 El Tor N16961 ORFeome into Gateway-compatible protein expression vectors (Figure 19) (214). To increase the probability of expressing proteins above their dissociation constant, we created two protein expression libraries producing either N-terminal histidine (His-ORF) or his-maltose binding protein (His-MBP-ORF) fusions. MBP fusions have been shown to increase protein solubility enabling a higher level of protein accumulation during overexpression (215). *E. coli* expressing individual ORF fusions were pooled by

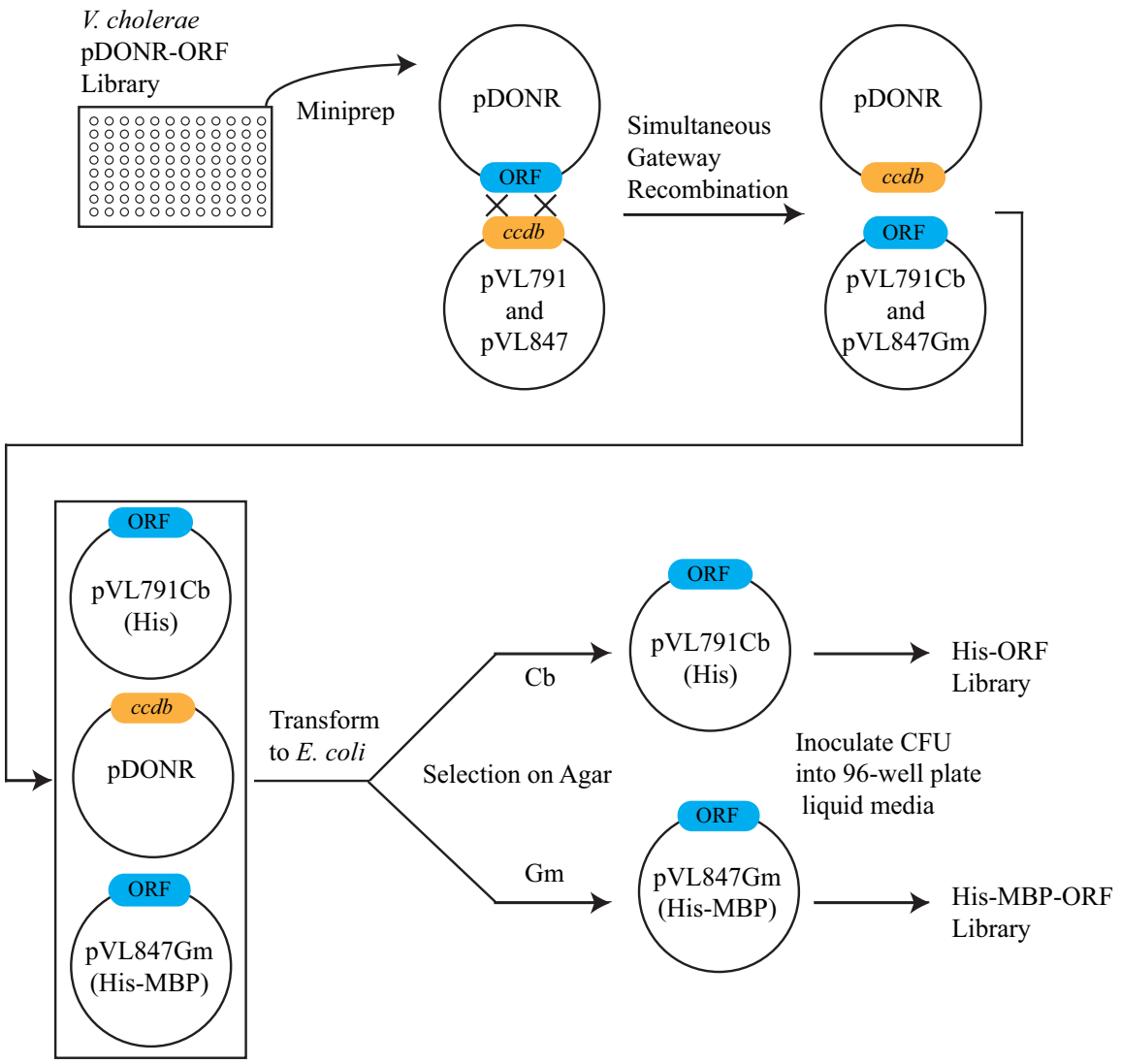

Figure 19. Construction of *Vibrio cholerae* open reading frame expression libraries. The *V. cholerae* pDONR-ORF plasmids were miniprepped and recombined with pVL791Cb and pVL847Gm expression plasmids containing a Gateway destination casette with the *ccdB* counter-selection cell death gene. These reactions were transformed to *E. coli* expression strain and recombinants were selected on LB Agar plates containing carbenicillin or getamycin. Multiple CFU from agar plates were inoculated into liquid media in 96-well plates to create His-ORF and His-MBP-ORF libraries for DRaCALA screening.

streaking pipette tips through multiple transformants to facillitate inoculation of 96-well microtiter plates to create the His-ORF and His-MBP-ORF libraries. Multiple clones of individual recombination reactions and transformations were pooled to expedite inoculation of liquid culture from agar-selected transformants. To determine if proteins were overexpressed, ~600 whole cell lysates were examined by PAGE with coomassie staining for the presence of an overexpressed protein band of the appropriate size. Approximately 50% of His-ORF and 75% of His-MBP-ORF fusions were identified by PAGE for a combined estimated coverage of 81% (data not shown). This is likely a conservative estimate of ORF coverage as DRaCALA can detect high affinity interactions in the absence of observable protein expression by coomassie staining.

To identify ORFs encoding cdiGMP-binding proteins, we analyzed whole cell lysates from His-ORF and His-MBP-ORF libraries by DRaCALA. We assume that the majority VC ORFs do not encode a cdiGMP-binding protein and therefore most whole cell lysates will demonstrate a background level of binding due to the presence of an endogenous cdiGMP signaling system in *E. coli*. To identify ORFs that significantly elevated fraction bound ^{32}P-cdiGMP, we created a positive cutoff three standard deviations above the mean fraction bound of a 96-well plate of whole cell lysates. Positive ORFs were iteratively removed from calculations of mean and standard deviation, thereby decreasing the positive cutoff for individual plates until no additional positives were identified. This method provided different positive cutoffs for plates with different levels of background cdiGMP-binding and was able to identify PelD as a positive control in each plate. Based on this analysis, our primary screen identified 55

His-ORF and 47 His-MBP-ORF fusions whose expression significantly increased ^{32}P-cdiGMP in *E. coli* whole cell lysates (Table 17 in Appendix A).

Our primary screen of the VC ORF expression libraries may have identified false positives due to cross-contamination or random variation in whole cell lysate composition. Each primary screen whole cell lysate was generated from a pool of CFU expressing a single VC ORF inoculated into liquid culture. We deconvoluted this pool by testing 8 single colonies for cdiGMP-binding and verified ORF size by colony PCR. Typically, all clones from a given ORF produced either positive or negative fraction bound ^{32}P-cdiGMP, although several instances of cross-contamination were identified by PCR. In total 23 His-ORFs and 21 His-MBP-ORFs (28 unique ORFs total) were identified that produced at least 7 of 8 whole cell lysates with significantly increased cdiGMP-binding and a PCR product of the correct size (Figure 20, Table 1).

To determine if cdiGMP-binding is specific, DRaCALA was performed on whole cell lysates generated from a sequence-validated clone in the presence of specific and non-specific unlabeled guanosine inhibitors (Table 2). Unlabeled cdiGMP significantly reduced ^{32}P-cdiGMP-binding for all positive ORFs with the exception of His-MBP-VCA0071 and His-MBP-VC2370, which did not significantly increase cdiGMP-binding in this assay. In contrast to cdiGMP competitor, unlabeled GTP and cGMP did not compete with ^{32}P-cdiGMP-binding and for several proteins containing EAL domains, increased the fraction bound of ^{32}P-cdiGMP. The lack of significant 32P-cdiGMP-binding by VCA0071 and VC2370 in this particular assay may reflect decreased protein expression or other differences in whole cell lysate composition. In total, these results suggest that most positive VC ORFs express a protein product that specifically binds

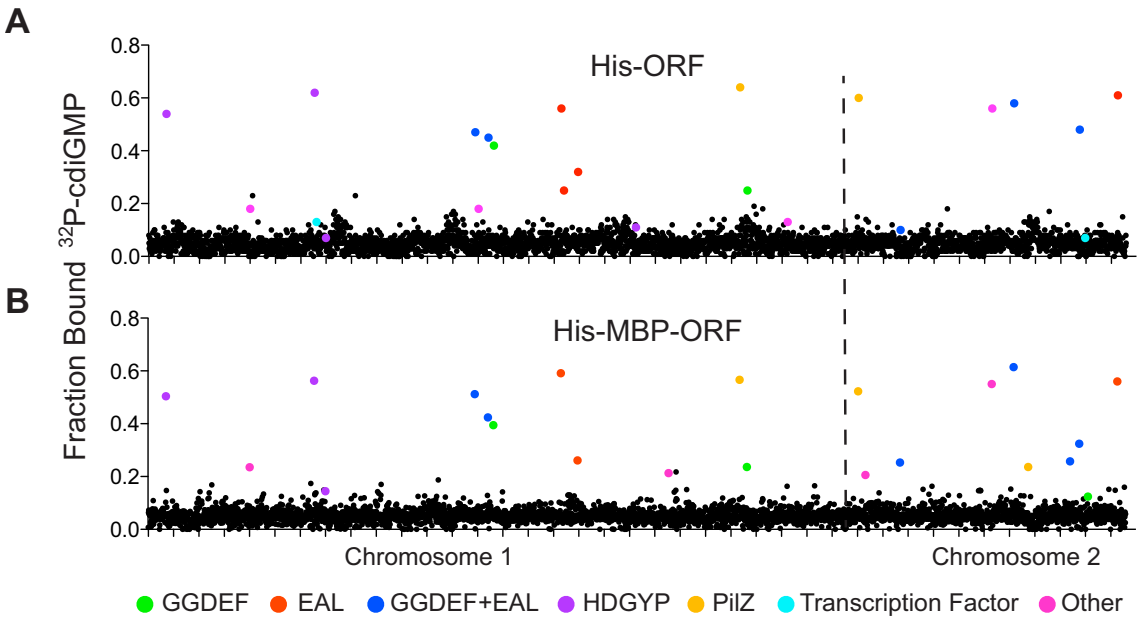

Figure 20. **Primary DRaCALA screen of *Vibrio cholerae* ORF libraries.** Graph of average fraction bound ^{32}P-cdiGMP vs. individual *V. cholerae* (A) His-ORFs and (B) His-MBP-ORFs overexpressed in *E. coli* whole cell lysates. ORFs are arranged by VC gene number along the X-axis. Validated positive ORFs are indicated by color and classified by type of cdiGMP-binding protein. Other refers to proteins that have not been predicted or demonstrated to bind cdiGMP.

Table 1. Fraction bound of whole cell lysate from secondary screen of positive ORFs. Table of fraction bound ^{32}P-cdiGMP generated by individual clones of *V.c.* ORFs identified as positive in primary screen. The cutoff for positive binding in this assay was at least 3 standard deviations above the average fraction bound for a set of 8 vector control clones. Clones with positive fraction bound are highlighted in green.

His-ORF	CFU 1	CFU 2	CFU 3	CFU 4	CFU 5	CFU 6	CFU 7	CFU 8
VC0072	0.48	0.42	0.48	0.43	0.42	0.42	0.46	0.43
VC0405	0.30	0.24	0.28	0.15	0.19	0.23	0.23	0.24
VC0658	0.52	0.53	0.56	0.54	0.55	0.56	0.52	0.51
VC0665	0.21	0.21	0.17	0.11	0.16	0.17	0.22	0.19
VC0703	0.14	0.14	0.12	0.11	0.12	0.14	0.19	0.14
`VC1295	0.43	0.43	0.51	0.46	0.46	0.50	0.47	0.49
VC1308	0.16	0.11	0.23	0.08	0.13	0.17	0.12	0.18
VC1348	0.42	0.46	0.44	0.46	0.47	0.43	0.45	0.44
VC1370	0.32	0.34	0.42	0.41	0.38	0.41	0.43	0.35
VC1641	0.53	0.53	0.57	0.56	0.57	0.58	0.59	0.53
VC1652	0.30	0.29	0.32	0.33	0.34	0.34	0.35	0.30
VC1710	0.35	0.38	0.44	0.43	0.42	0.44	0.40	0.36
VC1934	0.12	0.11	0.11	0.11	0.10	0.08	0.10	0.10
VC2344	0.56	0.52	0.58	0.56	0.57	0.56	0.54	0.55
VC2370	0.21	0.17	0.26	0.19	0.17	0.19	0.23	0.23
VC2529	0.14	0.16	0.13	0.12	0.13	0.11	0.14	0.16
VCA0042	0.57	0.53	0.55	0.58	0.59	0.59	0.58	0.58
VCA0210	0.18	0.16	0.17	0.19	0.17	0.20	0.18	0.18
VCA0593	0.64	0.61	0.51	0.53	0.56	0.65	0.61	0.63
VCA0681	No Growth	0.53	0.57	0.58	0.59	0.59	0.55	0.56
VCA0931	0.28	0.20	0.38	0.38	0.37	0.40	0.39	0.37
VCA0952	0.11	0.10	0.10	0.10	0.10	0.13	0.13	0.11
VCA1083	0.55	0.51	0.50	0.52	0.49	0.53	0.53	0.55
His-MBP-ORF								
VC0072	0.51	0.50	0.49	0.49	0.47	0.47	0.48	0.46
VC0405	0.22	0.17	0.19	0.16	0.12	0.14	0.16	0.16
VC0658	0.55	0.51	0.52	0.50	0.48	0.50	0.50	0.48
VC0703	0.16	0.15	0.19	0.16	0.16	0.13	0.14	0.12
VC1295	0.56	0.55	0.55	0.57	0.58	0.50	0.53	0.51
VC1348	0.55	0.54	0.54	0.55	0.55	0.52	0.52	0.52
VC1370	0.17	0.19	0.26	0.20	0.21	0.19	0.24	0.21
VC1641	0.51	0.48	0.50	0.48	0.49	0.50	0.53	0.50
VC1710	0.37	0.30	0.35	0.35	0.38	0.37	0.37	0.35
VC2066	0.21	0.16	0.16	0.12	0.17	0.14	0.15	0.17
VC2344	0.53	0.47	0.51	0.50	0.47	0.49	0.50	0.49
VC2370	0.30	0.27	0.28	0.25	0.24	0.25	0.22	0.23
VCA0042	0.43	0.42	0.46	0.44	0.42	0.46	0.46	0.44
VCA0071	0.14	0.13	0.15	0.13	0.15	0.14	0.16	0.15
VCA0210	0.31	0.27	0.26	0.30	0.32	0.28	0.28	0.24
VCA0593	0.54	0.53	0.50	0.40	0.46	0.48	0.54	0.46
VCA0681	0.56	0.49	0.47	0.51	0.50	0.50	0.51	0.52
VCA0735	0.25	0.28	0.28	0.29	0.30	0.27	0.31	0.36
VCA0931	0.40	0.40	0.39	0.38	0.38	0.39	0.36	0.36
VCA0965	0.25	0.21	0.23	0.25	0.27	0.20	0.19	0.21
VCA1083	0.57	0.54	0.55	0.52	0.53	0.50	0.50	0.49

Table 2. Validated cdiGMP-binding ORFs from *V. cholerae* ORFeome.

VC Gene #	His-ORF				His-MBP-ORF				Protein (cdiGMP-binding domain)	Reference for cdiGMP-binding[4]
	NC	cdiGMP[1]	cGMP[2]	GTP[3]	NC	cdiGMP[1]	cGMP[2]	GTP[3]		
VC0405	0.29	0.07***	0.30***	0.39***	0.36	0.03 ***	0.32***	0.38***	MshE	N/A
VC1308	0.34	0.06***	0.26***	0.35***	-	-	-	-	TyrR	N/A
VC2066	-	-	-	-	0.12	0.02 ***	0.08**	0.12***	FliA	N/A
VC2529	0.08	0.01***	0.07*	0.09***	-	-	-	-	RpoN	N/A
VCA0071	-	-	-	-	0.05	0.02	0.05	0.05	PstC	N/A
VCA0593	0.55	0.02 ***	0.62***	0.61***	0.53	0.03 ***	0.59***	0.57***	hypothetical protein	N/A
VC0665	0.15	0.02 ***	0.15***	0.14***	-	-	-	-	VpsR	(165)
VCA0952	0.17	0.04 ***	0.18***	0.24***	-	-	-	-	VpsT	(166)
VCA0042	0.58	0.03 ***	0.65***	0.61***	0.48	0.07 ***	0.50***	0.52***	PlzD (PilZ)	(127)
VC2344	0.57	0.04 ***	0.61***	0.62***	0.53	0.03 ***	0.55***	0.55***	PlzC (PilZ)	(127)
VCA0735	-	-	-	-	0.28	0.03 ***	0.27***	0.31***	PlzE (PilZ)	(127)
VC1370	0.45	0.03 ***	0.51***	0.47***	0.30	0.02 ***	0.34***	0.37***	(GGDEF)	N/A
VC2370	0.16	0.04 ***	0.20***	0.15***	0.07	0.04	0.13**	0.08***	(GGDEF)	N/A
VCA0965	-	-	-	-	0.17	0.02 ***	0.14***	0.13***	CdgF (GGDEF)	DGC (216)
VC0658	0.55	0.02 ***	0.60***	0.61***	0.56	0.02 ***	0.58***	0.59***	(GGDEF + EAL)	N/A
VC0072	0.36	0.00 ***	0.49***	0.48***	0.47	0.02 ***	0.51***	0.55***	(GGDEF + EAL)	N/A
VC0703	0.19	0.05 ***	0.19***	0.23***	0.23	0.01 ***	0.19***	0.20***	MbaA (GGDEF + EAL)	N/A
VC1934	0.24	0.02 ***	0.21***	0.22***	-	-	-	-	(GGDEF + EAL)	N/A
VC1641	0.58	0.02 ***	0.66***	0.63***	0.30	0.04 ***	0.32***	0.36***	(EAL)	N/A
VC1710	0.42	0.06 ***	0.50***	0.58***	0.42	0.02 ***	0.47***	0.56***	(EAL)	N/A
VCA1083	0.57	0.04 ***	0.64***	0.61***	0.53	0.04 ***	0.53***	0.58***	(EAL)	N/A
VC1652	0.36	0.08 ***	0.47***	0.52***	-	-	-	-	VieA (EAL)	PDE (95)
VCA0681	0.51	0.01 ***	0.50***	0.58***	0.50	0.01 ***	0.48***	0.55***	(HD-GYP)	PDE (217)
VCA0210	0.17	0.03 ***	0.17***	0.15***	0.33	0.04 ***	0.41***	0.34***	(HD-GYP)	N/A
VC1295	0.46	0.02 ***	0.55***	0.52***	0.51	0.02 ***	0.55***	0.57***	(HD-GYP)	N/A
VCA0931	0.33	0.01 ***	0.36***	0.42***	0.36	0.02 ***	0.41***	0.48***	(HD-GYP)	N/A
VC1348	0.49	0.02 ***	0.55***	0.52***	0.54	0.02 ***	0.54***	0.56***	(HD-GYP)	N/A
VCA0895	-	-	-	-	0.28	0.01 ***	0.27***	0.26***	(HD-GYP)	N/A

[1]Two-way ANOVA of Fb cdiGMP vs. No Competitor (NC). [2] Two-way ANOVA of Fb cdiGMP vs. cGMP. [3] Two-way ANOVA of Fb cdiGMP vs. GTP. * = $p < 0.05$, ** = $p < 0.01$, *** = $p < 0.001$, No asterisk = $p > 0.05$. [4] Binding and enzymatic activity is deemed positive if activity has been demonstrated for the purified protein or if mutation of residues required for cdiGMP-binding or enyzmatic activity regulate a cdiGMP-dependent phenotype. DGC = diguanylate cyclase activity reported, PDE = phosphodiesterase activity reported.

cdiGMP, and that guanosine nucleotides may regulate the availability or affinity of some cdiGMP-binding sites (96).

3.3 Positive ORFs Encode cdiGMP-binding Proteins

Several *V. cholerae* proteins have been predicted or demonstrated to have cdiGMP binding activity and some of these proteins were among the validated positive ORFs (Table 3, Table 4). Four cdiGMP-binding domains can be predicted from sequence information including the I-site of GGDEF domains, PilZ domain proteins, and the active sites of EAL and HD-GYP domains. In addition to genes with conserved cdiGMP-binding domains, 3 cdiGMP-binding transcription factors lacking a defined cdiGMP-binding domain have been described and are present in the *V. cholerae* ORFeome (160,165,166). The ability of the DRaCALA ORFeome screen to identify cdiGMP-binding proteins can be assessed by the hit rate of ORFs encoding predicted and empirically demonstrated cdiGMP-binding activity.

GGDEF Domain Proteins

The *V. cholerae* ORFeome contains 38 of 41 genes encoding a GGDEF domain (excluding VCA1082, VC1376, and VC0398), with 9 of 10 genes encoding both a GGDEF and EAL domain (excluding VC0398). The RxxD motif required for cdiGMP-binding is conserved in 10 of these genes, but cdiGMP binding has not been demonstrated for their protein products (86). 3 of 10 GGDEF domains with a conserved RxxD motif were identified as positive ORFs, suggesting that these proteins have cdiGMP-binding activity (Table 1, Table 3). The remaining 7 GGDEF domain ORFs may either lack cdiGMP-binding activity, not have been expressed, or produce unlabeled cdiGMP which can compete radiolabeled cdiGMP from cdiGMP-binding proteins.

Table 3. Hit rate of VC ORFs encoding proteins with predicted cdiGMP-binding domains. This table lists proteins with conserved domains predicted to bind cdiGMP. Residues required for cdiGMP-binding are defined for GGDEF (86), EAL (218), HD-GYP (79), and PilZ (127) domains.

	Number in Genome	Contains Conserved Resiudes for cdiGMP-binding	Conserved Binding Residues and Present in ORFeome	Number Identified by ORFeome Screen
GGDEF only	31	11	10	3 (30%)
EAL only	12	11	10	4 (40%
GGDEF+EAL	10	9	9	4 (44%)
HD-GYP	9	7	7	6 (86%)
PilZ	5	4	4	3 (75%)
Total	67	42	40	20 (50%)

Table 4. Hit rate of VC ORFs encoding proteins with demonstrated cdiGMP-binding activity. This table lists proteins that have been purified and shown to bind cdiGMP directly. References for PDE (EAL) (94,219-222), (HD-GYP) (217), and cdiGMP-binding (PilZ) (127) and transcription factors (160,165,166).

	Present in Genome	Present in ORFeome	Identified in ORFeome Screen
GGDEF only	0	N/A	N/A
EAL only	4	4	1
GGDEF+EAL	1	1	0
HD-GYP	1	1	1
PilZ	2	2	2
Transcription Factors	3	3	2
Total	11	11	6 (55%)

EAL Domain Proteins

The *V. cholerae* ORFeome contains 20 of 22 genes encoding a EAL domain (excluding VCA0536 and VC0398). Residues required for PDE activity are completely conserved in 19 of 20 EAL domains (excluding VCA1083), which predicts that the protein products of these genes may bind cdiGMP. The EAL domain of VCA1083 encodes a serine instead of the conserved glutamate corresponding to residue 208 of *P. aeruginosa* RocR, but is annotated as a pseudogene in NCBI and is likely not expressed in *V. cholerae* (218). 6 of 19 EAL domains with conserved active were identified as positive ORFs (Table 3). 4 of the positive ORFs with EAL domains also contain a GGDEF domain, but none retained the conserved RxxD motif, suggesting that cdiGMP-binding activity is due to binding at the EAL domain active site. VCA1083 was also identified as positive, suggesting the protein product of this pseudogene retains cdiGMP-binding activity. Of the 19 EAL domains with predicted cdiGMP-binding activity, 5 have been demonstrated to have PDE activity, including VC1652 (VieA), VC0130 (CdpA), VC1592, VC1086, and VC0137 (CdgJ) (95,218-222). Positive ORFs containing EAL domains include 1 of these 5 EAL domain proteins (VieA). EAL-domain proteins that were not identified may not bind cdiGMP, not be sufficiently expressed, or hydrolyze cdiGMP to pGpG before DRaCALA is complete. These results suggest that some, but not all cdiGMP-binding EAL-domain proteins were identified by this screen.

HD-GYP Domain Proteins

The *V. cholerae* ORFeome contains 9 out of 9 *V. cholerae* proteins with an HD-GYP domain, of which only VCA0681 has been purified and shown to have PDE activity (217). HD-GYP domains require conserved residues for PDE activity and these residues

are conserved in 7 of 9 HD-GYP domains (excluding VC1087 and VC2497) (206,217). Positive ORFs include 6 of 7 ORFs encoding HD-GYP domains with conserved residues for PDE activity, including VCA0681 with demonstrated binding activity. Thus, most HD-GYP domain proteins with predicted PDE activity were identified by the DRaCALA ORFeome screen.

PilZ Domain Proteins

The *V. cholerae* ORFeome contains 5 of 5 *V. cholerae* genes encoding PilZ domain proteins. 4 of 5 PilZ proteins contain the the conserved RxxxR and DxSxxG residues required for cdiGMP-binding, with the exception of PlzB (VC1885) (127). A previous study has demonstrated cdiGMP-binding to PlzC (VC2344) and PlzD (VCA0042), but failed to identify cdiGMP-binding for PlzA (VC0697) or PlzE (VCA0735) (127). PlzC and PlzD were identified as positive in both His-ORF and His-MBP-ORF libraries, while PlzE was identified as positive only in the His-MBP-ORF library. CdiGMP-binding was not previously detected for a purified His-PlzE fusion, suggesting that maltose binding protein may be required for cdiGMP-binding activity of heterologously expressed PlzE (127).

CdiGMP Binding Transcription Factors

3 cdiGMP-binding transcription factors lacking a defined cdiGMP-binding domain have been described and are present in the *V. cholerae* ORFeome (160,165,166). Positive ORFs include 2 of the 3 known cdiGMP-binding transcription factors VpsT and VpsR, but not FlrA.

In total, we identified 19 of 40 ORFs with predicted cdiGMP-binding domains (Table 3) and 5 of 10 ORFs encoding proteins with empirically demonstrated cdiGMP-

binding activity (Table 4). These results indicate that positive ORFs encode cdiGMP-binding proteins and that our DRaCALA ORFeome screen positively identified approximately 50% of both predicted and empirically demonstrated cdiGMP-binding proteins.

The DRaCALA screen also revealed 6 positive ORFs encoding proteins that are not predicted to bind cdiGMP. These proteins represent putative new classes of non-canonical cdiGMP-binding proteins. One of these ORFs encodes MshE (VC0405), an ATPase that is required for biogenesis of the MSHA type IV pilus (223). The *msh* operon encodes an uncharacterized GGDEF/EAL-domain protein (VC0398) and the MSHA pilus plays a role in cdiGMP regulated phenotypes including surface attachment, biofilm formation, and host colonization (224-228). This suggests that cdiGMP may regulate the MSHA pilus, possibly through direct binding to MshE. Two other cdiGMP-binding ORFs encode highly conserved sigma factors FliA (sigma28, VC2066) and RpoN (sigma54, VC2529). These sigma factors are highly conserved global transcriptional regulators in multiple organisms and their role in the transcriptional regulation of *V. cholerae* flagellar biosynthesis has been well characterized (229-231). Several enhancer-binding protein transcription factors with cdiGMP-binding activity are predicted to interact with sigma54 including FlrA and FleQ. Furthermore, cdiGMP is known to regulate flagellar transcription in *V. cholerae,* suggesting that these sigma factors may have cdiGMP regulated activities. A fourth positive ORF encodes PstC (VCA0071), a component of a conserved phosphate transport system that is well-studied in *E. coli* (232,233). A genetic screen for suppressors of cdiGMP-dependent repression of *V. cholerae* motility identified 8 unique transposon insertions in PstC, but a direct role of

PstC in cdiGMP-binding was not investigated (221). The fifth positive ORF encodes VCA0593, which is annotated as an exopolyphosphatase-related protein. Exopolyphosphatases hydrolyze polymers of inorganic phosphatase (polyP), and regulation of polyP has been shown to affect cdiGMP-dependent phenotypes including biofilm formation and motility in numerous prokaryotic organisms (234-238). However, VCA0593 has low homology to *E. coli* exoployphosphatase, and is not reciprocal best BLAST hit for *E. coli* exopolyphosphatase in *V. cholerae*, suggesting that VCA0593 may represent a novel class of exopolyphosphatase-related proteins that bind cdiGMP. A final positive ORF encodes TyrR, which is a member of the NtrC class enhancer-binding protein similar to FleQ, FlrA, and VpsR. The identification of these putative cdiGMP-binding proteins as positive ORFs in our DRaCALA ORFeome screen suggests several novel mechanism for cdiGMP-dependent regulation in *V. cholerae.*

To determine if FliA and RpoN bind cdiGMP directly, we purified N-terminal His-MBP fusions of FliA and RpoN. We failed to detect binding to purified FliA and RpoN by DRaCALA, suggesting that cdiGMP-binding activity was lost during purification (Figure 21). This could represent the loss of intrinsic binding activity of FliA and RpoN, or loss of *E. coli* cdiGMP-binding proteins that are removed during purification.

3.4 MshE Specifically Binds cdiGMP with High Affinity

Type IV pili are ubiquitious multi-functional pili that participate in cdiGMP-dependent phenotypes including twitching and swarming motility, biofilm formation, and pathogenesis (112,239-241). Conserved ATPases required for type IV pilus assembly and retraction have been shown to interact with cdiGMP-binding proteins in *P. aeruginosa*

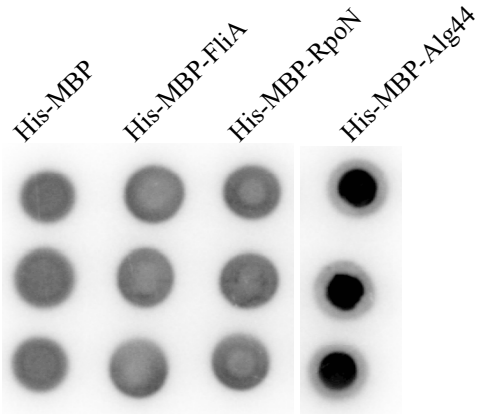

Figure 21. Binding of cdiGMP to purified FliA and RpoN. DRaCALA spots of purified His-MBP, His-MBP-FliA, His-MBP-RpoN, and His-MBP-Alg44 incubated with ^{32}P-cdiGMP.

and *X. campestris*, but direct binding of cdiGMP to T2SE ATPases has not been demonstrated (103,242-244). Identification of the ATPase MshE in both His- and His-MBP-ORF libraries suggested a potential role for cdiGMP in the regulation of the MSHA type IV pilus in *V. cholerae.*

To determine the affinity and specificity of cdiGMP-binding to MshE, we purified His-MBP-MshE and assayed binding to ^{32}P-cdiGMP by DRaCALA. The affinity of cdiGMP-binding to MshE was determined by quantifying fraction bound ^{32}P-cdiGMP to serial dilutions of purified MshE. Non-linear regression analysis of cdiGMP-binding vs. protein concentration using a one site binding model estimated the dissociation constant (K_d) for cdiGMP to be 830 ± 80 nM (Figure 22A). To determine the specificity of cdiGMP-binding to MshE, we measured fraction bound ^{32}P-cdiGMP in the presence of unlabeled nucleotide competitors. ^{32}P-cdiGMP-binding to His-MBP-MshE was significantly decreased by unlabeled cdiGMP and GDP, but not by cGMP, GMP, GTP, ATP, CTP, or UTP (Figure 22B). These results indicate that MshE specifically binds cdiGMP with high affinity.

cdiGMP effector proteins bind cdiGMP to allosterically regulate protein activity. To determine if cdiGMP-binding regulates MshE ATPase activity, purified His-MBP-MshE was incubated with radiolabeled ATP in the presence and absence of cdiGMP and ATP hydrolysis was measured over time by thin layer chromatography. We observed a similar rate of ATP hydrolysis in the presence and absence of cdiGMP, suggesting that cdiGMP binding does not regulate the ATPase activity of purified His-MBP-MshE (Figure 23).

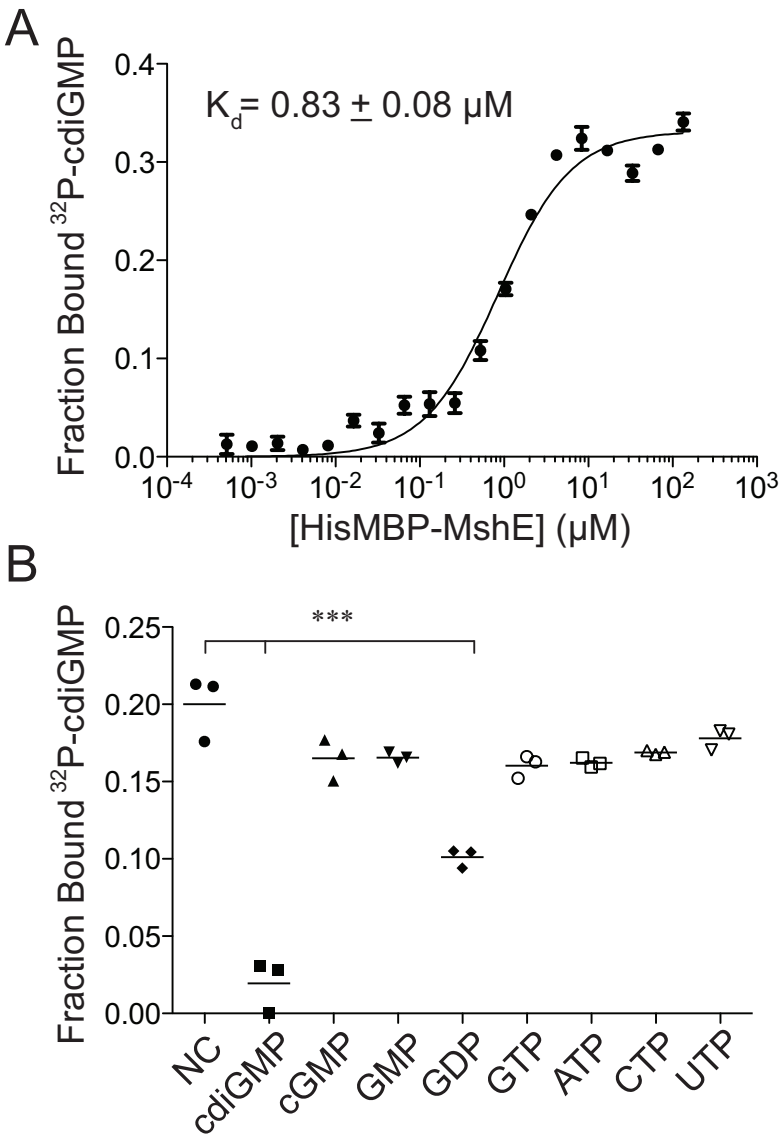

Figure 22. Affinity and specificity of cdiGMP-binding to MshE. (A) Graph of fraction bound ^{32}P-cdiGMP of 2-fold serial dilutions of purified His-MBP-MshE. The dissociation constant (K_d) is indicated. **(B)** Graph of fraction bound ^{32}P-cdiGMP-binding to 4µM His-MBP-MshE in the presence of 1 mM nucleotide competitors. 1-Way ANOVA with Dunnet's Post Test indicates a significant difference in fraction bound for cdGMP and GDP compared to no competitor (NC), * indicates $p < 0.001$.

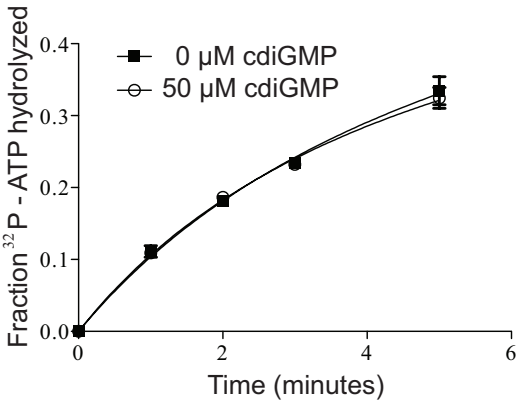

Figure 23. ATPase activity of MshE is not regulated by cdiGMP. (A) Graph of fraction ^{32}P-ATP hydrolyzed over time by 4 µM His-MBP-MshE in the presence and absence of 50 µM unlabeled cdiGMP.

3.5 The N-terminus of MshE Defines a Subset of cdiGMP-binding ATPases that Regulate Type IV Pili and Type II Secretion Systems

MshE belongs to a family of ATPases associated with the biosynthesis and retraction of type IV pili and secretion by type II secretion systems. Although phylogenetically related, these ATPases do not have a common nomenclature and are referred to here as T2SE ATPases based on the common "E" assignment of ATPases among genes encoding type II secretion components (245). To determine if cdiGMP-binding is a conserved feature of T2SE ATPases, we identified homologs of MshE and assayed them for cdiGMP-binding. P-Blast with the full length MshE amino acid sequence identified 5 related ATPases in *V. cholerae* and 8 in *P. aeruginosa,* including several ATPases that regulate type IV pili function (PilB, PilT, and PilU) and type II secretion (GspE, EpsE, and XcpR) (241,246-252). We constructed His-ORF fusions for each *V. cholerae* and *P. aeruginosa* MshE homolog and assayed cdiGMP-binding by DRaCALA in *E. coli* whole cell lysate (Figure 24A). Expression of PA14_29490 significantly increased fraction bound ^{32}P-cdiGMP, suggesting that PA14_29490 is a cdiGMP-binding protein. These results suggest that a subset of T2SE ATPases represented by MshE and PA14_29490 are cdiGMP-binding proteins.

T2SE ATPases encode a N-terminal T2SE domain and a highly conserved C-terminal domain containing the Walker A/B ATPase motif (Figure 25A). To localize the cdiGMP-binding site of MshE, we created N- and C-terminal truncations of MshE (Figure 25B). These truncations were overexpressed as N-terminal His fusion proteins in *E. coli* and assayed for cdiGMP-binding. Expression of each fragment was visualized by coomassie staining of whole cell lysates separated by SDS PAGE (Figure 25C).

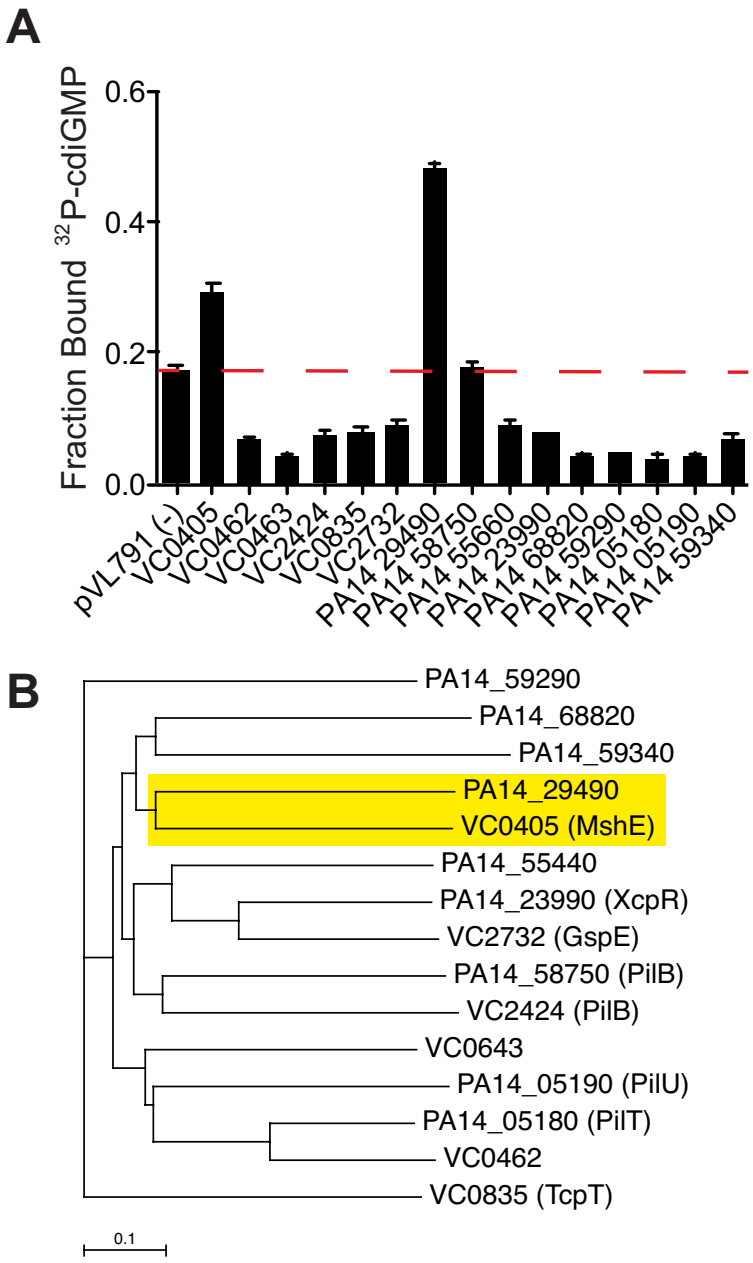

Figure 24. cdiGMP binding to *Vibrio cholerae* and *Pseudomonas aeruginosa* homologs of MshE in whole cell lysate. (A) Graph of fraction bound ^{32}P-cdiGMP of whole cell lysate expressing *Vibrio cholerae* and *Pseudomonas aeruginosa* homologs of MshE. The dashed red line indicates background binding for a vector control strain. **(B)** Clustal-W alignment of the N-terminal fragments of MshE homologs corresponding to residues 1-242 of MshE. The monophyletic cluster of MshE and PA14_29490 is highlighted in yellow.

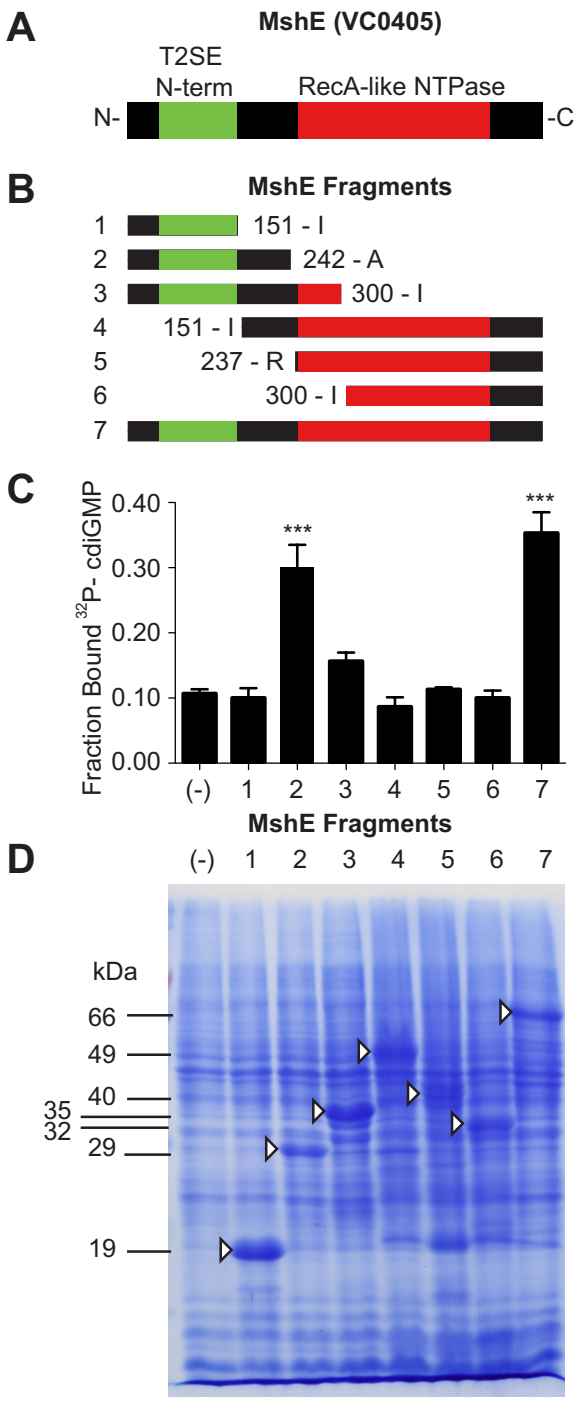

Figure 25. cdiGMP binds to an N-terminal fragment of MshE. (A) Cartoon of conserved domains in MshE. **(B)** Fragments generated for binding analysis are numbered with and the N- and C-terminal amino acid are indicated. **(C)** Fragments of $MshE_{VC}$ were overexpressed in *E. coli* and whole cell lysate was assayed by DRaCALA. **(D)** Image of coomassie-stained PAGE of *E. coli* whole cell lysate analyzed by DRaCALA in (C). Arrowheads indicate overexpressed fragments of MshE and predicted size of protein products is indicated.

DRaCALA of the same lysates demonstrated that fraction bound ^{32}P-cdiGMP was significantly increased in whole cell lysates expressing the N-terminal 242 residues of MshE (Fragment 2) as compared to an empty vector control (Figure 25D). Fragment 3 was also expressed, but failed to significantly elevate fraction bound ^{32}P-cdiGMP despite containing all of Fragment 2. This suggests that the additional amino acids in Fragment 3 may prevent proper folding of a N-terminal cdiGMP-binding site in MshE. In agreement with a previous phylogenetic analysis of T2SE ATPases, Clustal-W alignment of the N-termini of the *P.a.* and *V.c.* MshE homologs revealed a monophyletic cluster for PA14_29490 and MshE (Figure 24B) (245). Thus, the N-terminus of MshE contains a cdiGMP-binding site, and conserved features in the N-terminus of MshE and PA14_29490 may define a subset of cdiGMP-binding T2SE ATPases.

3.6 Identification of Conserved Residues in the N-terminal cdiGMP-binding Fragment of MshE

To determine the specific residues in the N-terminus of MshE that mediate cdiGMP-binding, conserved charged residues were targeted for mutation to alanine. cdiGMP-binding sites in PilZ, GGDEF, EAL, and HD-GYP domains contain charged residues that make contact with the cdiGMP molecule and are required for cdiGMP-binding (86,105,218,253). To identify residues that mediate cdiGMP-binding to MshE, charged residues in the N-terminal 242 amino acids were identified by clustal-W alignment of MshE, PA14_29490, and the top 12 P-BLAST hits of MshE excluding the *Vibrio* genus (Figure 26A). 13 conserved charged residues were identified, including a cluster of 9 residues in the T2SE domain. These 9 residues are conserved in alignments of PilB and GspE homologs that did not bind cdiGMP in our DRaCALA experiments

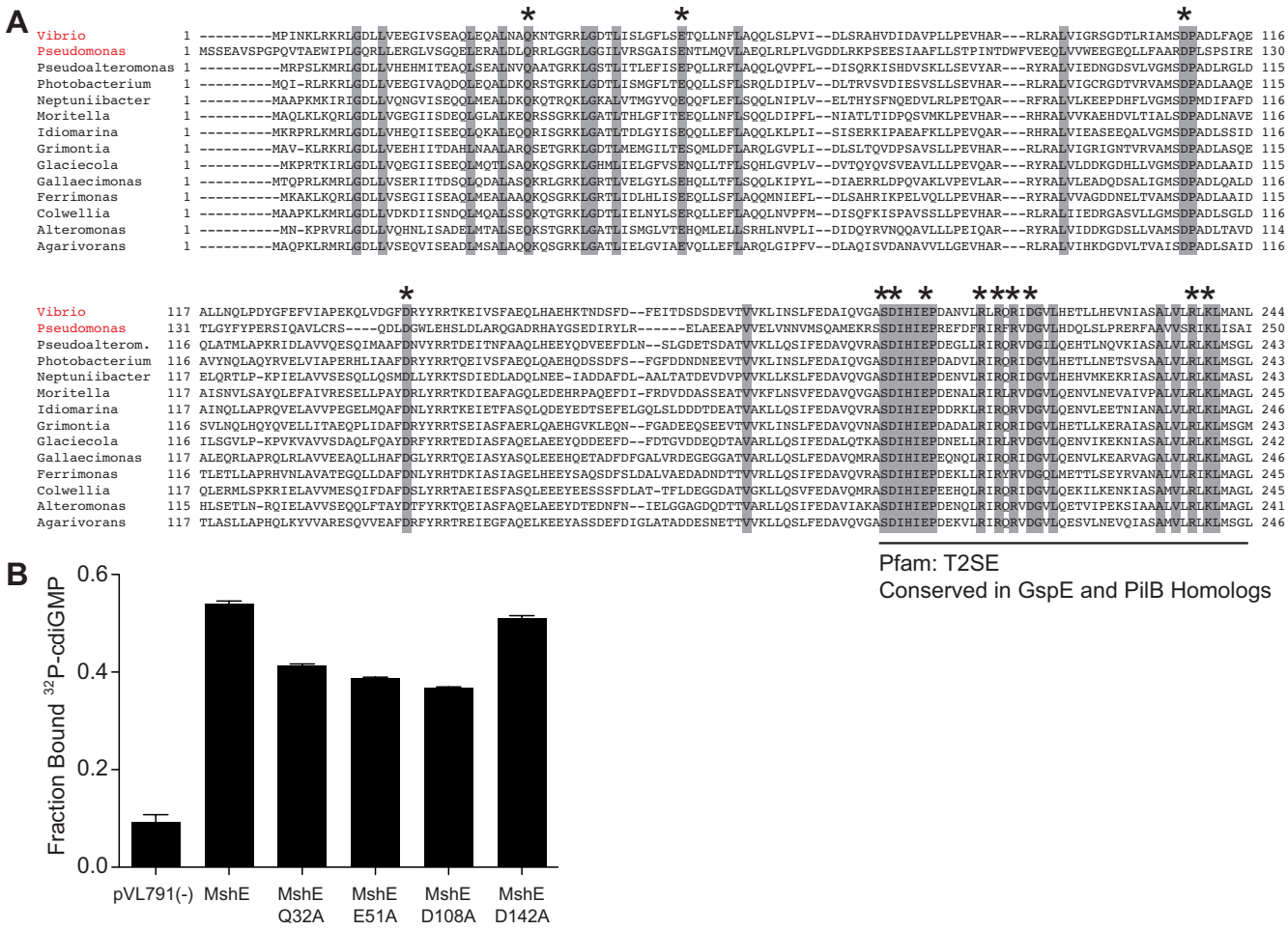

Figure 26. Conserved residues required for cdiGMP-binding by MshE. (A) Clustal-W alignment of amino acid sequences of VC MshE homologs. Grey bars highlight conserved residues. Asterisks indicate charged residues. The cluster of charged residues conserved in alignments of PilB and GspE homologs are indicated by a horizontal line. **(B)** DRaCALA quantification of fraction bound ^{32}P-cdiGMP to whole cell lysates expressing His-MshE wild type and indicated point mutants.

(Figure 25A). Residues required for cdiGMP-binding by T2SE ATPases are probably uniquely conserved in cdiGMP-binding homologs, prompting the elimination of the C-terminal cluster of conserved residues from consideration. Thus, the remaining four charged residues (Q32, E51, D108 and D142) are conserved by MshE and PA14_29490, but not in closely related T2SE ATPases lacking cdiGMP-binding. These residues may be required for cdiGMP-binding.

To test this hypothesis, the mutations Q32A, E51A, D108A, and D142A were introduced into full length MshE. These MshE mutants were expressed as N-terminal His-MshE fusions in *E. coli* and assayed for cdiGMP-binding in whole cell lysates. The mutant alleles displayed decreased cdiGMP-binding compared to wild type *mshE*, but were still able to significantly increase fraction bound ^{32}P-cdiGMP as compared to a vector control (Figure 26B). These results suggest that these residues are not absolutely required for cdiGMP-binding by MshE. However, these experiments are not conclusive about the potential role of these charged residues in cdiGMP-binding by MshE. Mutation of these residues may have subtle effects on the affinity of MshE for cdiGMP which might not be apparent from a single measurement of fraction bound cdiGMP with undefined protein concentrations. Alternatively, MshE may have multiple cdiGMP-binding sites and loss of residues required for cdiGMP-binding at one site may be masked by cdiGMP-binding at a second site. In the future, determining the stoichiometry of cdiGMP-binding to MshE and quantifying the dissociation constant of individual mutants may address these possibilities

3.7 Discussion

Here we have reported the systematic identification of cdiGMP-binding proteins from a *V. cholerae* ORFeome based on a high-throughput biochemical assay of cdiGMP-binding activity. Work in other laboratories has developed several other approaches for identification of protein effectors based on their affinity for signaling molecules. In one approach, an affinity-tagged signaling molecule is used as a molecular bait to "fish out" interacting proteins that are subsequently identified by liquid chromatoraphy-mass spectrometry (LC-MS). For example, biotin-conjugated cyclic di-AMP (cdiAMP) mixed with streptavidin coated beads enabled the pull down and identification of the *S. aureus* cdiAMP binding protein KtrA (254). This approach can identify binding interactions to proteins expressed in their native organism, which may possess unique post-transcriptional and post-translational regulation of protein activity. However, identification of low affinity effectors is limited by wash steps that remove non-specifically bound proteins. To overcome this limitation, the pull-down approach has been modified to include a protein capture step. For example, a cdiGMP capture compound has been developed that contains an aromatic group that forms a highly reactive nitrene upon UV-irradiation. This aromatic group is linked to cdiGMP and biotin via an acyl carrier, and proteins that interact with cdiGMP are irreversibly cross-linked to the capture compound by UV-irradiation (208). Capture compounds allows improved stringency in protein purification, but proteins that interact with cdiGMP, the aromatic group, or the acyl chain may be pulled down by this approach. In total, affinity-pull down approaches enable effector identification from a wide variety of biological samples, but

are not systematic due to the requirement of effector expression under laboratory conditions.

Alternatively, ORF libraries have enabled the systematic overexpression and analysis of individual proteins (255). Most biochemical assays typically require protein purification and thus ORFs are expressed as fusion proteins with affinity tags for purification. For example, a study of the *Saccharomyces cerevisiae* proteome expressed GST-ORF fusions cloned from an open reading frame library, purified proteins in pools, and assayed the pools for various biochemical activities (256). Positive pools were deconvoluted enabling the identification of open reading frames encoding proteins with specific biochemical activity. This approach has been extended by covalently attaching purified proteins to glass slides, enabling the production of high-density protein microarrays that have been used to systematically screen protein-protein and protein-ligand interactions (188,189,257,258). However, both affinity pulldown and screening of purified proteins use chemically modified ligands that may alter protein-ligand interactions. DRaCALA uses radiolabeled probes that are synthesized enzymatically from common radiolabeled precursors such as ATP and GTP. However, not all ligands can be easily radiolabeled and the use of radiolabeled compounds requires specialized equipment and monitoring. DRaCALA can also detect specific binding activity of both soluble and insoluble proteins in whole cell lysate, and thus bypass the requirement for protein purification (Figure 15). While DRaCALA screening of whole cell lysates is rapid, confirmation of direct binding still requires protein purification or identification and mutation of the ligand binding site. In summary, DRaCALA ORFeome screens represent a low-cost, high-throughput method for identifying protein-ligand interactions

that combines systematic protein overexpression with direct detection protein-ligand interactions in whole cell lysate.

A previously reported DRaCALA ORFeome screen identified 3 cdiAMP binding proteins from a *Staphyloccus aureus* His-ORF library. A cdiAMP-based affinity pull down from a *S. aureus* whole cell lysate had previously identified KtrA, suggesting that the other two cdiAMP binding proteins may not have been sufficiently expressed by *S. aureus* for detection by affinity pull-down. However, the cdiAMP binding protein, CpaA, was not present in the *S. aurues* ORFeome, and was thus not identified by DRaCALA screening. CdiAMP signaling is not well-studied and thus the hit rate of the *S. aureus* ORFeome screen was unable to be evaluated.

In this study, several predicted and empirically demonstrated cdiGMP binding proteins from *V. cholerae* were not identified in the ORFeome screen. There are both general and protein-specific reasons that potentially explain why some cdiGMP binding proteins were not identified as positive ORFs. In general, ORFs encoding cdiGMP-binding proteins may not be identified due to insufficient protein expression, improper folding of cdiGMP-binding sites, or low affinity for cdiGMP. We attempted to overcome the limitations of low protein expression and inactive ORF fusions by the use of both His-ORF and His-MBP-ORF libraries. From a total of 28 positive ORFs, 6 were identified exclusively in the His-ORF library and 5 in the His-MBP-ORF library. Thus, screening two ORF libraries improved our detection rate by approximately 20-30% and resulted in a total hit rate of approximately 50% of known and 50% of predicted cdiGMP-binding proteins. In addition to these general issues, proteins with both cdiGMP-binding and DGC activity may be difficult to identify. Previous experiments

with the *P. aeruginosa* DGC WspR indicated that excess cdiGMP decreases fraction bound ^{32}P-cdiGMP, suggesting that DGC activity may have decreased the hit rate of ORFs encoding GGDEF domains (Figure 13A). In total, these results suggest that DRaCALA ORFeome screens are a powerful method for identifying many, but not all genomically-encoded cyclic di-nucleotide binding proteins.

The most exciting results of our *V. cholerae* screen was the identification of 6 positive ORFs lacking canonical cdiGMP-binding domains. These ORFs represent putative novel cdiGMP effectors and may regulate cdiGMP-dependent phenotypes in *V. cholerae.* For example, studies of the MSHA pilus demonstrate a positive role in attachment to chitinous surfaces and biofilm formation, but MSHA must be downregulated for mucus penetration during host infection (224,226,228). cdiGMP regulates *V. cholerae* colonization of an infant mouse model and multiple DGCs and PDEs are differentially-regulated during host infection and environmental persistence (173,221,222,259). Thus cdiGMP-binding by MshE may provide a mechanism for the differential regulation of the MSHA pilus as *Vibrio cholerae* transitions between host infection and aquatic reservoirs.

CdiGMP also regulates swimming motility in numerous organisms including *V. cholerae*. A second positive ORF encoding PstC was previously identified in a *V. cholerae* transposon mutagenesis screen where it was required for a decreased swimming motility phenotype observed in a *V. cholerae* PDE mutant with increased cellular cdiGMP concentrations (221). PstC is a component of a conserved phosphate transporter that regulates transcription by the two component response regulator PhoB. Loss of *phoB* or *pst* restored motility in the cdiGMP-high background, suggesting that cdiGMP may

bind PstC to regulate PhoB activity. A third positive ORF, VCA0593, encodes a hypothetical protein with weak homology to exopolyphosphatases. The low homology of VCA0593 with known exopolyphosphatases and the presence of a second *bona fide* exopolyphosphatase in the *V. cholerae* genome suggests that VCA0593 may not function as an exopolyphosphatase.

Finally, we identified 3 positive ORFs encoding transcriptional regulators. FliA and RpoN are sigma factors, while TyrR is an NtrC-type enhancer-binding protein similar to FleQ, VspR, and FlrA. A *V. cholerae* transcriptional microarray has revealed that cdiGMP regulates transcription of over 100 genes in *V. cholerae* including several operons for flagellar biosynthesis, which are regulated by FliA and RpoN (260). Expression of FliA and RpoN consistently resulted in elevated cdiGMP-binding in *E. coli* whole cell lysates, but the lack of cdiGMP-binding to purified FliA and RpoN suggests that cdiGMP-binding activity was lost during purification. This loss of activity could reflect loss of of FliA and RpoN activity during purification. Alternatively, these highly conserved sigma factors may be regulating transcription of endogenous *E. coli* cdiGMP-binding proteins or altering the affinity of *E. coli* cdiGMP-binding proteins which would be removed during purification. These possibilities were not investigated, and the role of FliA and RpoN in direct cdiGMP-binding remains inconclusive. TyrR has not been characterized in *V. cholerae,* but its homolog in *E. coli* has been well-studied as a transcriptional regulator of aromatic amino acid metabolism and transport (261). Genes involved in aromatic amino acid metabolism of *V. cholerae* were not differentially transcribed in response to elevated cdiGMP, but it is not clear if TyrR is expressed by *V. cholerae* in laboratory conditions (260). In total, the identification of positive ORFs

lacking conserved cdiGMP-binding domains has suggested new regulatory roles for cdiGMP signaling. Demonstration of direct cdiGMP-binding and cdiGMP-dependent regulation of protein activity is required to determine if these proteins are indeed cdiGMP effectors.

CdiGMP-dependent regulation of type IV pili have been demonstrated in *P. aeruginosa* and *Xanthomonas* species, and several GGDEF, HD-GYP, and PilZ proteins have been shown to interact with the extension ATPase PilB and retraction ATPases PilT and PilU in *Xanthomonas* (103,112,114,244,262,263). However, a precise mechanism for cdiGMP-dependent regulation of type IV pili has not been defined. The identification of MshE as a cdiGMP-binding protein prompted us to investigate homologous ATPases to determine whether they too might bind cdiGMP. MshE belongs to a broad family of T2SE ATPases required for extension and retraction of type IV pili and membrane translocation of type II secreted proteins (245,264). We tested several T2SE ATPases from *V. cholerae* and *P. aeruginosa* for cdiGMP-binding, but only detected cdiGMP-binding activity for PA14_29490. MshE and PA14_29490 form a monophyletic cluster of T2SE ATPases suggesting that a subset of T2SE ATPases may be regulated by cdiGMP. However, we were not able to observe cdiGMP-dependent regulation of ATPase activity in purified MshE (Figure 23). This suggests that cdiGMP binding may regulate other activities of MshE such as protein interactions within the MSHA biosynthetic complex. that phylogenetic clustering was correlated with the biological roles of T2SE ATPases (245). In the future, identification of a conserved cdiGMP-binding site in MshE and PA14_29490 may allow prediction of cdiGMP binding for other T2SE ATPases and reveal the regulatory effects of cdiGMP binding.

3.8 Materials and Methods

cdiGMP-binding Buffer

Whole cell lysate resuspensions, DRaCALA, and ATPase assays were carried out in cdiGMP-binding buffer containing 10 mM Tris pH = 8.0, 100 mM KCl, 5 mM $MgCl_2$.

Gateway Destination Vector Construction

pVL791 Cb GW and pVL847 Gn GW were constructed as destination vectors in LR reactions for cloning VC ORFs. pVL791 Cb and pVL847 Gn are pET-19 derivatives that are carbenecillin or gentamycin resistant and produce N-terminal His- and His-MBP fusions respectively. The gateway destination casette was amplified from pRFA and cloned in frame with the N-terminal fusions to produce the gateway adapted vectors.

ORFeome Library Construction

The *V. cholerae* N16961 ORF library was obtained from BEI. LR Clonase reactions were performed per NEB protocol using miniprepped pDONR vectors from the *V. cholerea* ORFeome in combination with pVL791 Cb GW and pVL847 Gn GW destination vectors. Gateway reactions were transformed into an *E. coli T7IQ* strain (NEB) and recombinants were selected on LB agar plates containing either carbenecillin or gentamycin. Multiple colonies from individual transformations were inoculated in LB M9 rich media in 96-well plate format and grown overnight with shaking at 30 ˚C. Overnight cultures were subcultured 1:50 into fresh media and grown for 4 hours at 30 ˚C with shaking. VC ORF expression was induced by addition of 1 mM IPTG and grown for an additional 4 hours. 1.5 mL of induced culture was centrifuged and cells were resuspended in 150 µL of cdiGMP-binding buffer supplemented with DNAse , Lysozyme

and the protease inhibitor PMSF. 20 µL aliquots were transferred to 96-well microtiter plates and stored at -80 ˚C.

DRaCALA

Whole cell lysates for DRaCALA screening were prepared by freeze-thawing resuspended cells in microtiter plates a total of 3 times. After the final thaw, 20 µL of cdiGMP-binding buffer supplemented with 16 pM ^{32}P-cdiGMP and 500 mM unlabeled GTP was added to whole cell lysate plates. 2 µL of this mixture was then spotted in duplicate on nitrocellulose using a 96-well pin tool. DRaCALA of purified proteins was performed with concentrations of protein and unlabeled competitor as indicated. Spots were allowed to dry completely (about 20 minutes) before exposing a phosphorimager screen and capturing with a Fujifilm FLA-7000. Photostimulated luminescence (PSL) from the inner spot and total PSL of the spot were quantitated with Fuji Image Gauge software. The fraction bound (F_b) (209) was calculated using measurements of the total area (A_{outer}), the area of the inner circle (A_{inner}), the total PSL intensity (I_{total}), and the inner intensity (I_{inner}) as follows:

$$F_B = \frac{I_{inner} - A_{inner} * \left(\frac{I_{total} - I_{inner}}{A_{total} - A_{inner}} \right)}{I_{total}}$$

Protein Purification

His-MBP-MshE, His-MBP-FliA, and His-MBP-RpoN were purified from strains constructed in the ORFeome library. *E. coli* strain NEB-T7IQ harboring recombined pVL847 Gn GW - ORF vectors expressing N-terminal His-MBP-ORFs were induced for 4 hours at 30 ˚C with 1 mM IPTG. Induced bacteria were collected by centrifugation and resuspended in His Buffer A (10 mM Tris, 100 mM NaCl and 25 mM imidazole, pH =

8.0) and frozen at -80 ˚C until purification. Thawed bacteria were lysed by sonication after addition of DNase I (Roche), lysozyme (Roche), and PMSF (1 mM final concentation). Insoluble material was removed by centrifugation and the His-fusion protein was purified from the clarified whole cell lysate by separation over an Ni-NTA column. Proteins were subsequently purified and concentrated using anion exchange to a concentration of at least 20 μM, supplemented with 25% glycerol, and frozen at -80°C until thawed for use.

ATPase Assay

24 nM ^{32}P-ATP was incubated with 4 μM His-MBP-MshE in the presence or absence of 50 μM cdiGMP in cdiGMP-binding buffer. ATP hydrolysis was monitored by thin layer chromatography using PEI cellulose plates and a buffer containing 15 mL 1.5 M KCl and 10 mL saturated $(NH_4)_2SO_4$. Aliquots of the ATPase reaction were spotted on the PEI cellulose plate at indicated time points and fraction of radiolabel associated with free phosphate was quantified by exposure to phosphorimager.

Copyright Notice

Chapter 4: DRaCALA For Affinity and Kinetic Determination of Protein-Oligonucleotide Interactions

4.1 Introduction

Previous studies have shown that DRaCALA can accurately measure protein–ligand interactions for purified proteins and whole-cell extracts expressing recombinant proteins. The simplicity of DRaCALA gives it potential for general applicability. Ligand mobility in DRaCALA is a necessity, but the possibility that ligands partition out of the mobile liquid phase during capillary action, and are therefore not mobile, has not yet been investigated.

Because mononucleotides and dinucleotides have been shown to be mobile, it is reasonable to expect that double stranded DNA would be mobile as well. This led us to apply the method to DNA–protein interactions using the well-characterized interaction between *E. coli* cyclic AMP receptor protein (CRP) and its DNA binding site ICAP. CRP

is a transcription factor that has regulatory function at approximately 200 sites on the *E. coli* genome (16,192,265). CRP binds cAMP and cGMP (266), but DNA binding and transcriptional activation by CRP is solely dependent on cAMP binding (14). A 28-bp symmetrical synthetic consensus sequence, called ICAP, binds CRP with the greatest affinity (15). Through filter-binding assays, the affinity of the CRP–ICAP interactions and the contributions of specific nucleotides (such as guanines at positions 8 and 10 and the cytosines at positions 19 and 21) have been defined (267).

In this study, DRaCALA is shown to allow quantification of CRP–ICAP interactions using ^{32}P-end-labeled oligonucleotides. Specificity of binding and competition studies were performed to establish this proof of principle. Furthermore, the method was used to obtain measurements of both affinity and kinetics. Much larger DNA probes derived from whole plasmids were tested in the same way. DNA could function as a carrier molecule for studying interactions between a protein and a molecule covalently linked to DNA. This also allows easy indirect ^{32}P-labelling of molecules that are more difficult to label than DNA. Finally, immobilization of nucleic acids with the biotin-streptavidin system is shown to allow study of small molecule interactions with RNA (riboswitches). We show here the different ways DRaCALA can be used to study molecular interactions with nucleic acids including protein–nucleic acid and riboswitch-small ligand interactions.

4.2 DNA Oligonucleotides are Mobile in DRaCALA and Sequestered by Protein Binding

Because radiolabeled mononucleotides and dinucleotides are mobile on nitrocellulose by capillary action (209), we reasoned this would be a property of double-

stranded DNA as well. If confirmed, this would allow study of DNA using the DRaCALA technique. Double-stranded mobility on nitrocellulose was tested using 5'-end-labeled duplex DNA formed by annealing a pair of 40-bp oligonucleotides that generate the CRP consensus binding site, ICAP (gd126 and gd127 in Table 6, Chapter 4.10 Materials and Methods). When the ^{32}P-labeled DNA was spotted on dry nitrocellulose, the ^{32}P radiolabel was mobilized by radial capillary action resulting in a homogenous signal across the total sample area (Figure 27A) similar to results previously obtained for cAMP and ATP (209). Addition of 100 nM CRP and 200 mM cAMP to the ICAP probe is known to promote DNA–protein complexes (267). Spotting of the CRP–ICAP mixture at equilibrium resulted in sequestration of the soluble probe by the immobilized protein. Maltose binding protein (MBP), which does not bind DNA, did not sequester the probe, resulting in a uniform distribution of the radiolabel as in the control without any protein. This shows that specific molecular interaction is required for probe sequestration. Quantification of the fraction bound revealed that probe alone and probe mixed with non-specific protein have no fraction bound (Figure 27B). These results demonstrate the ability of DRaCALA to detect interactions between proteins and double-stranded DNA.

4.3 Oligonucleotide–Protein Interactions Are Specific in DRaCALA

CRP interaction with ICAP requires sequence-specific inverted repeats (267). To test if DRaCALA can detect changes in DNA–protein interaction with single base pair changes, point mutants were generated in the ICAP site at positions that are known to abolish binding (267). Specifically, the guanosines at position 8 and position 10 were changed to cytosines. Because the site is symmetrical, the corresponding cytosines at

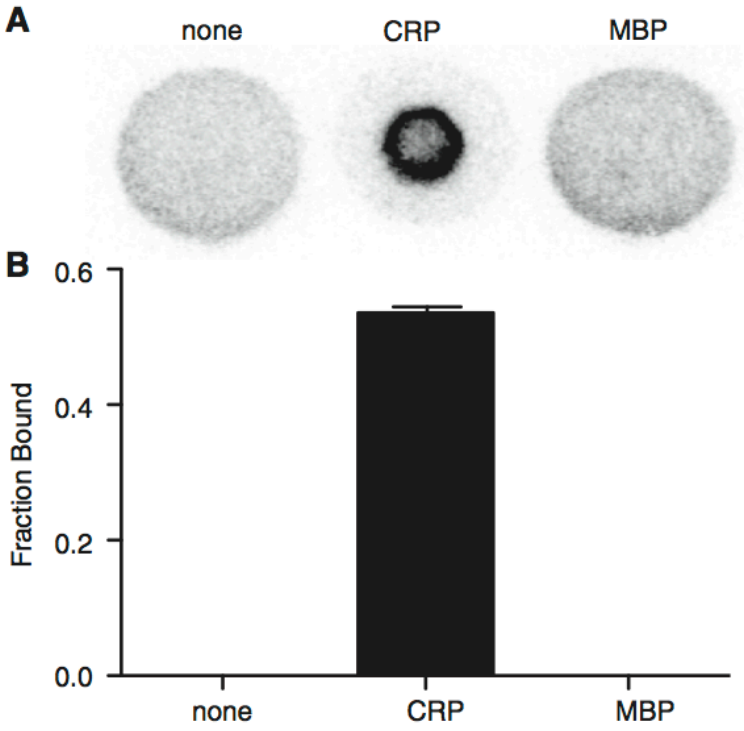

Figure 27. Detection of Protein–DNA Interaction by DRaCALA. (A) Phosphorimager visualization of DRaCALA spots of indicated proteins at 100 nM mixed with 4 nM ^{32}P-labeled ICAP fragments and 200 mM cAMP show distributions of the radioligand, which are diffused and homogenous (no protein, MBP) or sequestered (CRP). (B) The fraction bound was quantified using the formula in the 'Methods' section and error bars indicate the SD for three spots.

positions 19 and 21 were changed to guanosines (Figure 28A). These various probes were tested, at 4 nM, for binding to CRP by DRaCALA. The wild-type ICAP was sequestered by 100 nM CRP as before. The 8:GC mutant (G to C at position 8 and C to G at position 21) showed a very low level of binding to CRP while the10:GC mutant (G to C at 10 and C to G at 19) and the 8,10:GC double mutant exhibited no binding (Figure 28B). To confirm specificity, the binding between wild-type ICAP and 100 nM CRP was subjected to competition by wild-type and mutant-unlabeled DNA at 10, 100, or 1000 times the concentration of the labeled DNA. The wild-type competitor partially competed at 10-fold excess and competed more significantly with increased amount of competitor (Figure 28C). The 8:GC competitor showed no competition at 10- or 100-fold excess but did display some minor competition at 1000-fold. The 10:GC and 8,10:GC failed to compete regardless of their concentration. These results collectively show that DRaCALA measures sequence-specific DNA binding.

4.4 DNA-Binding Affinity and Kinetics Can Be Measured by DRaCALA

In order to accurately describe the activity of a transcription factor or other protein on a DNA binding site, it is desirable to determine the affinity and kinetics of the DNA–protein interaction. Because radionuclides can be detected with high sensitivity, DRaCALA can be used to make such measurements for high-affinity interactions. Serial 2-fold dilutions of CRP were mixed with limiting ^{32}P-labeled ICAP probe (5 pM) to find the affinity of CRP for ICAP. CRP bound ICAP with maximum affinity when it was saturated with 200 mM cAMP. Analysis of these results indicated a dissociation constant (K_d) of 3.6 ± 0.4 x10^{-11} M (SE) (Figure 29A). This is consistent with previously reported values for ICAP (266) (Table 5). In the absence of cAMP, the affinity of CRP for ICAP

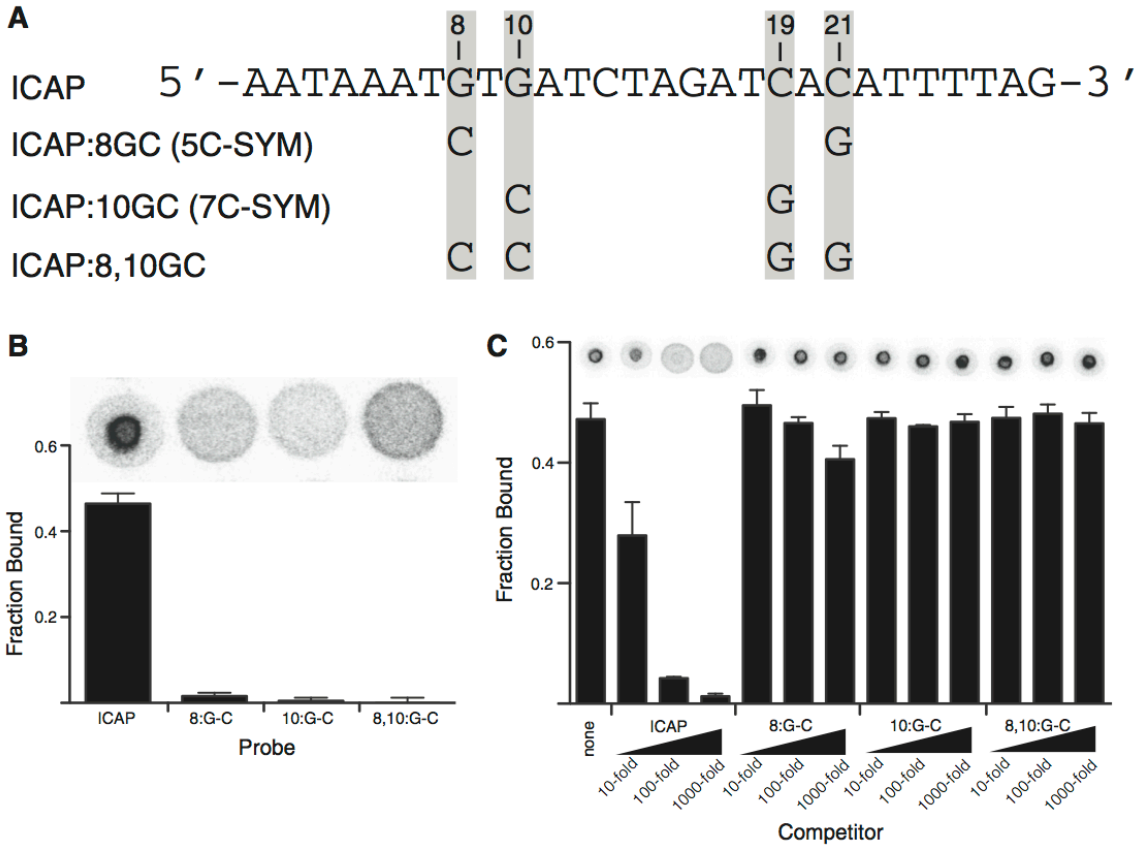

Figure 28. CRP binding to specific DNA sequences detected by DRaCALA. (A) The sequence of the 28-bp ICAP site. The positions perturbed in this study are marked in red. Names of mutant versions are listed next to the point mutations that define them. Equivalent nomenclature for mutants from Gunasekera et al. (267) is indicated in parentheses. (B) DRaCALA spots for direct binding of 100 nM CRP to 4 nM of ICAP, 8:G-C, 10:G-C and 8, 10:G-C probes with 200 mM cAMP are shown above the graphed quantification of fraction bound. (C) Binding of the ICAP probe to CRP was subjected to competition by unlabeled probes at 10, 100 or 1000 times the concentration of the radioligand. All error bars represent SD of three spots. DRaCALA spots shown above their respective conditions are separate images consolidated to fit the graph.

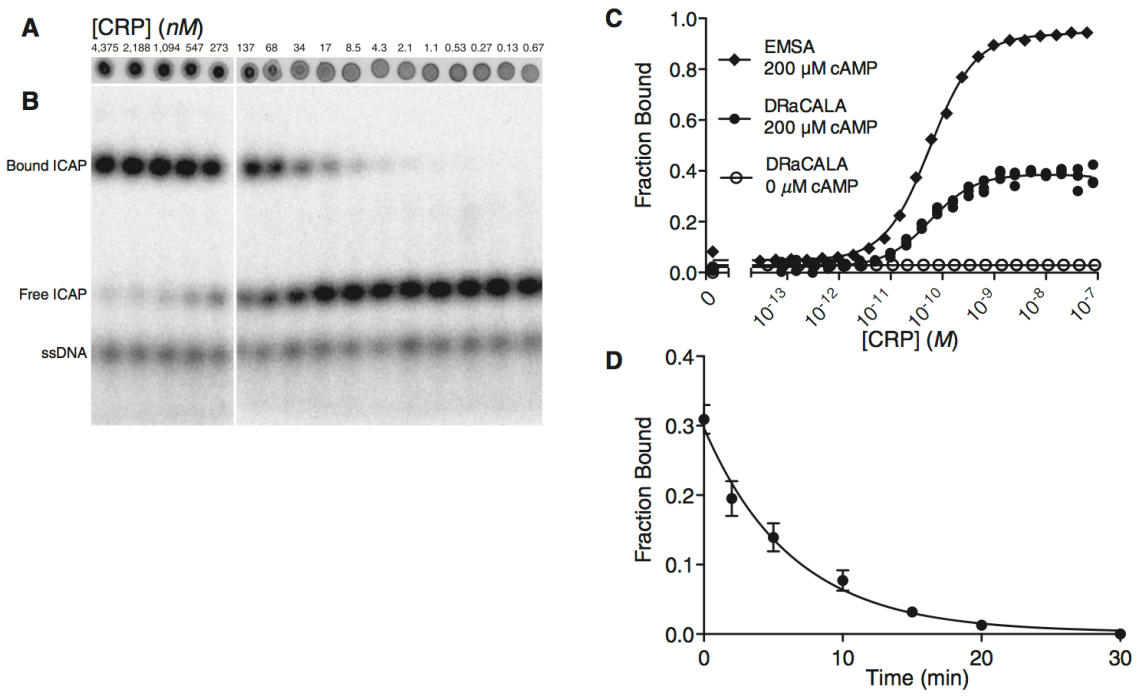

Figure 29. DRaCALA allows determination of affinity and kinetics of protein–DNA interaction. The affinity of CRP to the ICAP binding site reconstituted from annealed oligonucleotides (vl1427 and vl1428) was determined by the ability of serially diluted CRP to sequester 4 pM ^{32}P-labeled ICAP probe in the presence of 200 mM cAMP by (A) DRaCALA and (B) EMSA. (C) The fraction bound is plotted against each concentration of CRP as detected by EMSA in the presence of 200 mM cAMP or DRaCALA at 0 or 200 mM cAMP. Plot represents a single replicate for EMSA and three replicates for DRaCALA. All K_d values are reported in Table 5. (D) The observed off-rate, k_{off} = 2.6 ± 0.40 x 10^{-3} s^{-1} (SD), was measured by adding 1000-fold unlabeled competitor to 5 nM CRP with 5 pM ICAP oligonucleotide probe and spotting at different time points. All error bars represent the SD of three spots.

Table 5. Observed affinity of CRP to various ICAP probes from this and previous studies with indicated amounts of cAMP. All reported K_d values from this study were determined by DRaCALA and the standard error of three trials is reported.

Source	Method	Probe	[cAMP] (M)	K_d (M)(± SEM)
(267)	Filter binding	ICAP oligo ^{32}P	2×10^{-4}	$1.4 \pm 0.3 \times 10^{-11}$[a]
(267)	Filter binding	ICAP oligo ^{32}P	0	$> 1.0 \times 10^{-7}$[a]
This study	DRaCALA	ICAP oligo ^{32}P	2×10^{-4}	$3.6 \pm 0.4 \times 10^{-11}$
This study	DRaCALA	ICAP oligo ^{32}P	0	$> 1.0 \times 10^{-6}$
This study	DRaCALA	ICAP* plasmid ^{32}P	2×10^{-4}	$4.1 \pm 1.0 \times 10^{-11}$
This study	DRaCALA	ICAP* plasmid ^{32}P	0	$> 1.0 \times 10^{-6}$
This study	EMSA	ICAP oligo ^{32}P	2×10^{-4}	$8.1 \pm 0.8 \times 10^{-11}$

[a]The affinity reported in the Gunasekera *et al.* paper is the binding constant or association constant K_a. We have taken the inverse of those values to give the K_d reported in Table 5 to match our K_d measurements.

was at least 10,000-fold lower (K_d > 1.0 x 10^{-6} M) (Figure 29C). To confirm our DRaCALA results, we applied the same sample to an EMSA to determine the fraction bound (Figure 29B). The autoradiogram of the EMSA shows that the mobility of the free annealed oligonucleotide is retarded in the presence of CRP while the free the single-stranded oligonucleotide is not (Figure 29 and Figure 30). The results from the EMSA assay yielded a similar dissociation constant K_d of 8.1 ± 0.8 x 10^{-11} M (Figure 29C).

We also used the CRP–ICAP binding interaction to test whether DRaCALA can be used to easily monitor the dissociation kinetics for protein–DNA complexes. A limiting amount of ^{32}P-labeled ICAP (5 pM) was mixed with a protein concentration just above the K_d (5 nM). Then, unlabeled competitor ICAP was added in 1000-fold excess of radiolabeled ligand and spots were made over time, and these spots were analyzed to monitor the fraction of ICAP bound as a function of time. Our analysis indicated a dissociation rate (k_{off}) of 2.6 ± 0.40 x 10^{-3} s^{-1} (SD) for the CRP–cAMP complex, corresponding to a half-life of 4.42 min (Figure 29D). Using the DRaCALA-observed off-rate and affinity, the calculated on-rate is k_{on} = 7.2 x 107 M^{-1} s^{-1}. These results show that DRaCALA is a rapid method for determining affinity and kinetics of protein–DNA interactions.

4.5 Protein Binding of Whole-Plasmid Ligands is Detected Specifically by DRaCALA

The mobility of both nucleotides and double-stranded oligonucleotides on nitrocellulose suggests that molecular weight is not a critical limiting factor for what types of molecules can be used as the mobile, detectable ligand. The size limit of DNA ligands in DRaCALA was tested by cloning the same ICAP binding site and mutant sites

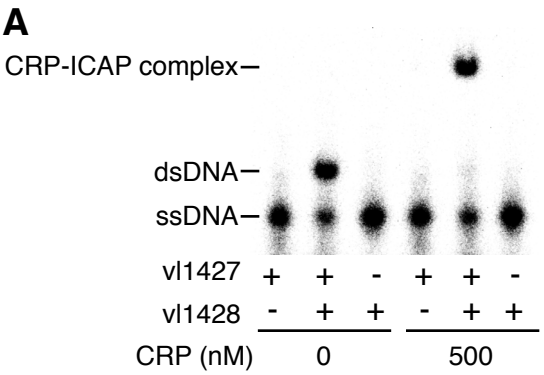

B Percent Intensity

CRP (nM)	0			500		
vl1427	+	+	-	+	+	-
vl1428	-	+	+	-	+	+
CRP-ICAP complex	2	2	1	3	58	2
dsDNA	7	64	5	7	6	5
ssDNA	91	35	93	90	36	93

Figure 30. **EMSA detection of single-stranded oligonucleotide and annealed ICAP site in the absence and presence of CRP**. The oligonucleotides (vl1427 and vl1428) are 5' end-labeled with ^{32}P by PNK. The labeled oligonucleotides are annealed individually or in combination as indicated. Labeled oligonucleotides are incubated with and without CRP and separated by PAGE. (A) Autoradiogram of EMSA. (B) Quantification of the percent of radiolabel at the indicated mobility for each sample.

onto a 3.5 kb pVL-Blunt plasmid, and using the entire linearized vector as a ligand. Each of the linearized plasmids was labeled with ^{32}P and shown to be mobile in DRaCALA (plasmids listed in Table 7, Chapter 4.10 Materials and Methods). Plasmids (50 pM) with ICAP sites bound 100 nM CRP. In contrast, plasmids with 8:GC bound weakly and 10:GC or 8,10:GC sites did not bind at all (Figure 31A).

Binding of a single ICAP insert on a plasmid probe (50 pM) to 100 nM CRP was next subjected to competition. Competitors in this case were made by PCR amplification of a 600-bp region of the plasmids containing wild-type and mutant ICAP sites. The wild-type PCR competitor partially inhibited radiolabeled plasmid binding to CRP at 10-fold excess of the radiolabeled ligand and fully competed at 1000-fold excess (Figure 31B). PCR products containing 8:GC, 10:GC, or 8,10:GC did not compete away binding even at 1000-fold excess concentration. Detected binding of CRP to whole-plasmid probes is therefore also site-specific in DRaCALA. These results show that the critical parameter for detection of protein–DNA interaction by DRaCALA is the mobility of the ligand on the solid support and not the molecular weight of the ligand.

4.6 Affinity and Kinetics Determined For Whole Plasmid Ligand

Whole plasmids can also be used in affinity and kinetic studies. With 200 mM cAMP, the observed K_d of CRP and a plasmid with a single ICAP site was $4.1 \pm 0.3 \times 10^{-11}$ M (SD) (Figure 32A). Without cAMP the K_d was $> 1.0 \times 10^{-6}$ M. These values are similar to those obtained for the labeled oligonucleotides and those from previous studies (Table 5). The off-rate for the plasmid was observed at $k_{off} = 4.8 \pm 0.17 \times 10^{-4}$ s^{-1}, corresponding to a half-life of 23.9 min (Figure 32B). The calculated on-rate for the plasmid was $k_{on} = 1.2 \times 10^{7}$ M^{-1} s^{-1}, which is 6-fold lower than that of the annealed

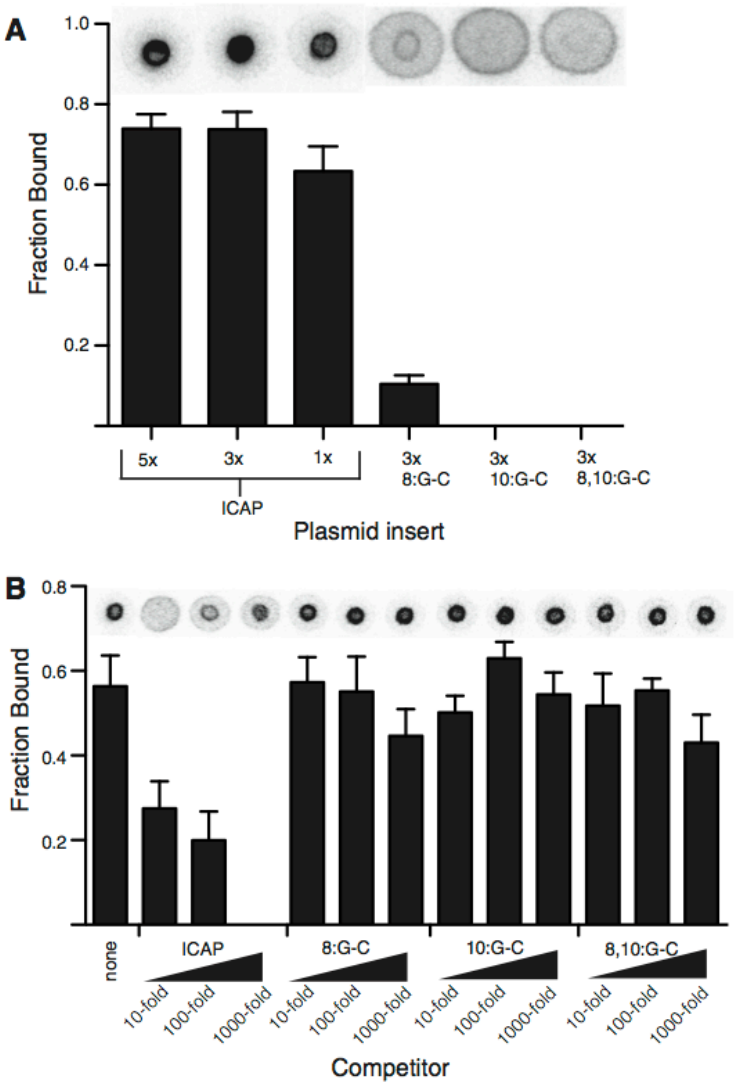

Figure 31. DRaCALA allows detection of specific interaction of CRP with plasmid carrying the ICAP site. (A) 50 pM individual plasmids with 1x, 3x or 5x wild-type binding sites or 3x mutant-binding sites cloned in series were tested for binding in the presence of 100 nM CRP and 200 mM cAMP. (B) Specificity was determined by competition of binding to ^{32}P-labeled 1x wild-type plasmid with unlabeled PCR products. Competitors used were 1x ICAP, 3x 8:G-C, 3x 10:G-C, 3x 8,10:G-C. All error bars represent SD of three spots with a representative spot (spot images consolidated to fit graph) shown above each column.

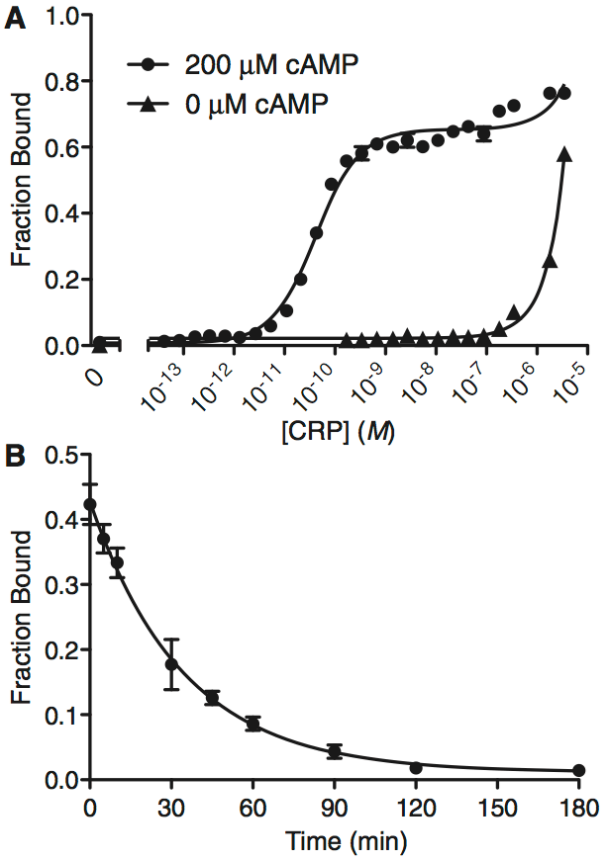

Figure 32. Affinity and kinetics of DNA-binding determined using 5 pM whole-plasmid probe with a single ICAP site. (A) Graphs of fraction of ICAP plasmid bound by various concentrations of CRP with indicated levels of cAMP (K_d reported in Table 5). (B) Graph of observed off-rate of k_{off} = 4.8 ± 0.17 x 10^{-4} s^{-1} (SD) for ICAP plasmid generated by adding 1000-fold unlabeled PCR product (1x ICAP) competitor to 5 nM CRP with plasmid probe and spotting at time points > 3 h. All error bars represent SDs of three spots.

oligonucleotides, likely due to the large excess of non-specific DNA in the plasmid probe. Affinity and kinetics can thus also be measured for sites contained on a plasmid.

4.7 Use of DNA As a Carrier/Label Molecule

Because such large pieces of DNA can be used in DRaCALA without altering specificity, we hypothesized that DNA could be used as a label and carrier for molecules that are not ordinarily mobile in DRaCALA and/or not easily labeled. Because ligand mobility and ligand detection are the only requirements for the mobile binding partner, DNA-conjugation could potentially make any molecule adaptable for use as a DRaCALA probe. A DNA component to the probe allows for easy labeling with ^{32}P. Many small, soluble molecules are not mobile in DRaCALA suggesting that fluorescently labeled low molecular weight ligands are not suitable for DRaCALA technique (Figure 33). However, addition of DNA to immobile ethidium bromide conferred mobility to the interacting dye (Figure 33) implying that conjugation to DNA can overcome the immobility of some dye molecules. DNA can also be covalently linked to molecules through bioconjugate PCR with modified primers. This technique was tested using the biotin–streptavidin system. PCR products including the binding sites of the 3x ICAP plasmid and 3x 8,10:GC plasmid were generated with a 5'-biotinylated primer and labeled with ^{32}P on the free 5'-end. These bioconjugate probes were tested with DRaCALA for binding to CRP, streptavidin and MBP. The wild-type probe without biotin-bound CRP but not streptavidin or MBP (Figure 34A). The biotinylated wild-type probe bound both CRP and streptavidin but not MBP. The 8,10:GC probe without biotin bound none of the proteins, whereas the biotinylated version bound only streptavidin.

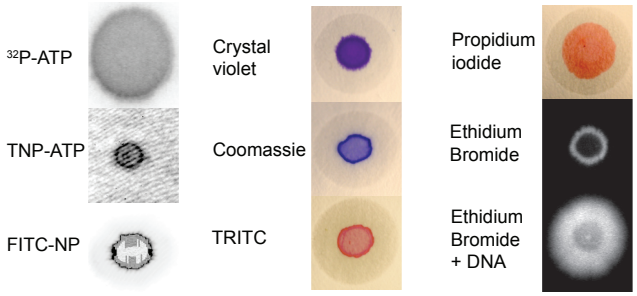

Figure 33. Small detectable molecules exhibit variable mobility by capillary action through nitrocellulose. 5 µl of given concentration of each molecule was spotted: 3 nM ^{32}P-ATP, 10 µM TNP-ATP, 200 µM FITC-NP, 250 µM crystal violet, 300 µM Coomassie, 200 µM TRITC, 500 µM propidium iodide, 250 µM EtBr, 250 µM EtBr with 1 µM DNA.

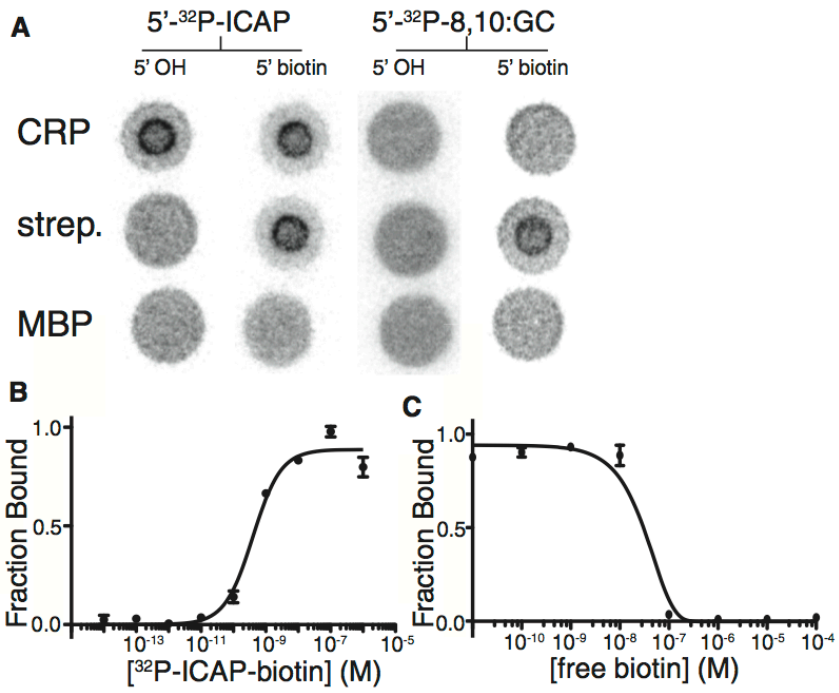

Figure 34. Bioconjugate DNA probes. Bioconjugate probes were generated by PCR with 5'-biotinylated primers. (A) Four probes (ICAP and 8,10:GC with and without biotin) were tested for binding to CRP, streptavidin and MBP. A mix of 50 pM ^{32}P-labeled probe, 100 nM protein and 200 mM cAMP was spotted on 0.8 m nitrocellulose and phosphor images of the spots are shown. (B) The ICAP–biotin probe affinity for streptavidin in PBS was determined by DRaCALA with 100 pM probe (K_d = 4.0 ± 0.6 x 10^{-10} M). (C) Binding of 10 nM streptavidin to the ICAP–biotin probe was competed with serial dilutions of free biotin (IC_{50} = 3.3 x 10^{-8} M).

The affinity of the biotinylated ICAP probe was determined using DRaCALA by diluting streptavidin (Figure 34B). The ability to assess affinity was limited by the concentration of the probe that could not be diluted below tens of pM without loss of signal. The limit of DRaCALA detecting binding seems to be therefore the limit of detection of the probe. The IC_{50} of free biotin was determined by competing against the probe with different concentrations of free biotin (Figure 34C). Here the IC_{50} of 33 nM is approximately enough to occupy the four sites of the 10 nM streptavidin. The observed affinity is lower than the previous published values for free biotin probably because the biotin molecule was conjugated to DNA (138). We were also able to measure the off-rate of the conjugated biotin by observing the exchange with excess free biotin (Figure 35). The exchange occurred in two steps, with an initial rapid off-rate and then a second slower rate corresponding to a half-life of 112 h and exchange-rate of $k_{off} = 1.7 \times 10^{-6}$ s^{-1}. The biphasic disscoation timecourse has been previously reported in a study of avidin and unconjugated biotin and is likely due to the tetramer protein having different affinites for biotin depending on the number of occupied sites (268). These results demonstrate that PCR conjugation can be used to link a molecule/ligand of interest to DNA, which allows facile ^{32}P-labeling and can confer mobility (in DRaCALA), allowing rapid determination of affinity and kinetics of the protein–ligand interaction.

4.8 Riboswitch-Binding cdiGMP

We have shown that protein interaction with DNA can be detected by DRaCALA. We wondered whether this technique could be applied to monitor RNA-ligand binding interactions. In particular, can the DRaCALA technology be used to detect the interaction of riboswitches with their small molecule ligands? One example of such an interaction

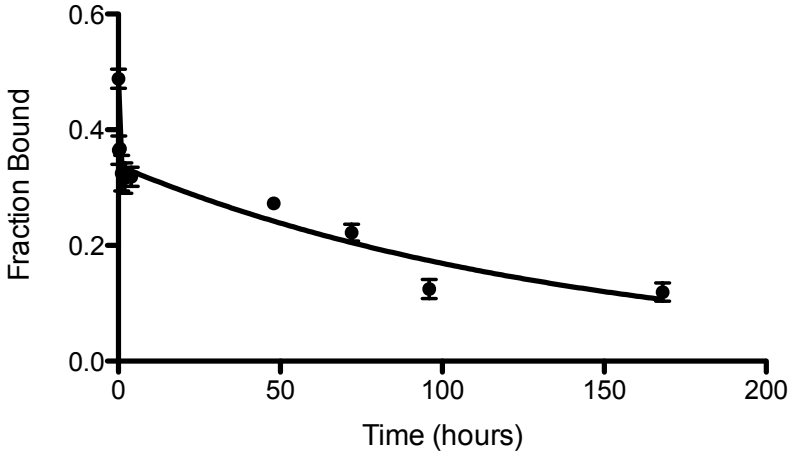

Figure 35: Off Rate of Streptavidin-Biotin Interaction. Binding of 10 nM streptavidin to 100 pM ^{32}P-ICAP-biotin probe measured over time after addition of 100 μM free biotin.

that has been of recent interest is the cdiGMP responsive Vc2 riboswitch identified in bacteria (138). To study such an interaction with DRaCALA, one of the binding partners must be immobilized. We achieved this through biotinylation of Vc2* riboswitch RNA (with a modified tetraloop and shortened 5'- and 3'-ends compared to the original Vc2) at the 3'-end by periodate cleavage of the terminal ribose and reductive amination to conjugate the biotin moiety. The biotinylated riboswitch was sequestered by streptavidin, allowing the nucleic acid to take the place of protein as the immobile partner in the binding assay (Figure X8). Vc2* was tested directly for sequestration of cdiGMP and also biotinylated and tested for binding to cdiGMP in the presence or absence of streptavidin. The 4 nM radiolabeled cdiGMP was mobile alone and in the presence of the Vc2* or biotinylated Vc2* RNA (Figure 36A, lanes 1–3). This suggests that RNA, like DNA, is mobile in this system, and therefore could be used as a labeled probe as well. Streptavidin did not sequester radiolabeled cdiGMP alone or with Vc2* RNA, so there is no detectable interaction between streptavidin and Vc2* RNA (lanes 4–5). Biotinylated Vc2* RNA and bound cdiGMP were immobilized by streptavidin as expected (lane 6). The affinity of Vc2* for cdiGMP was tested using both DRaCALA and an EMSA (or gel shift). These measurements were made in a Vc2 binding buffer (10 mM sodium cacodylate, 10 mM $MgCl_2$, 10 mM KCl) by heating the binding reaction to 70 ˚ C for 3 min, slowly cooling to room temperature, and then incubating at room temperature for 48 h (142). Remarkably similar results were obtained using DRaCALA and gel shift (Figure 36B). The affinity of the Vc2* RNA for cdiGMP was observed to be K_d = 7.8 ± 1.9 10^{-9} M with DRaCALA and K_d = 9.8 ± 1.6 x 10^{-9} M with EMSA. These results show that DRaCALA works as well as EMSA for studying the molecular interactions of

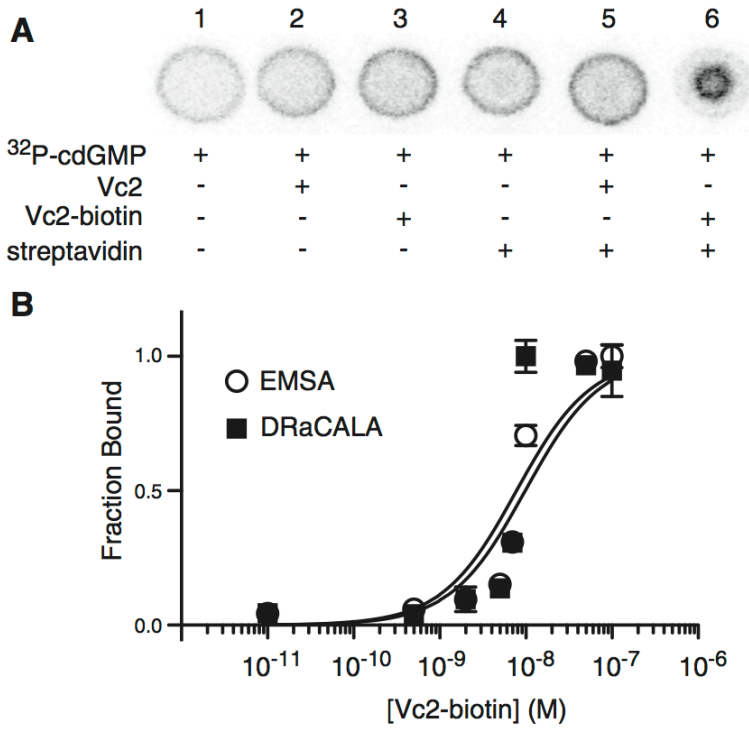

Figure 36. Vc2* RNA binding to ^{32}P-cdiGMP is detected by DRaCALA. (A) Spots visualized by phosphorimager with streptavidin used to immobilize biotinylated RNA. The binding reaction contained 4 nM ^{32}P-cdiGMP, 1 mM RNA and 200 nM streptavidin in buffer (10 mM KCl, 10 mM sodium cacodylate, 3 mM $MgCl_2$). (B) The affinity of Vc2*-biotin RNA for cdiGMP was determined with both EMSA and DRaCALA by diluting RNA in the binding reaction. The fraction bound is normalized such that 1.0 represents maximal binding. The DRaCALA-obtained affinity was K_d = 7.8 ± 1.9 x 10^{-9} M and the apparent affinity in EMSA was K_d = 9.8 ± 1.6 x 10^{-9} M

riboswitches. This strategy can be adapted to study interactions between the biotinylated nucleic acids and a mobile ligand (another nucleic acid or nucleotide).

4.9 Discussion

Nucleic acid interactions with proteins and low molecular weight ligands are fundamental for biological function. This has inspired the development of a number of assays to measure these interactions. We will compare and contrast the merits of DRaCALA with these various assay systems using CRP–cAMP as the classic example of a signal-responsive transcription factor and a model system for protein interaction with both a large nucleic acid and a mononucleotide. Study of the CRP system led to the establishment of some fundamental concepts related to transcription, such as regulation by second messengers (269), multiple promoter control of a single operon (270-272) and promoter control of RNA polymerase binding (273). Because of this foundational work, CRP and the lac repressor have been traditionally used to demonstrate proof of principal for various methods to detect DNA–protein interactions.

Nucleic acid–protein DRaCALA utilizes the differential mobility of nucleic acids through nitrocellulose to separate DNA that is bound to a protein from that which is unbound. The interactions measured in this way were specific to the nucleic acid sequences because point mutations at previously identified critical nucleic acids abolished specific binding of CRP to ICAP in both annealed oligonucleotides and plasmids (274). The affinity of the interaction was measured by diluting the protein before adding it to limiting amounts of probe and spotting on nitrocellulose. The K_d measured for the annealed oligonucleotide and plasmid closely matched what was reported in a previous study that used a filter-binding assay (267) as well as a study that

used gel shift (275) (Table 5). The off-rate determined with DRaCALA was slower for the plasmid than for the oligonucleotide probe, which is consistent with the finding that non-specific DNA concentration can affect the kinetics of specific DNA binding with protein (276). The off-rate for the plasmid (k_{off} = 4.84 ± 0.17 x 10^{-4} s^{-1}) was similar to that reported in a gel shift study (k_{off} = 1.2 x 10^{-4} s^{-1}) (276). This corresponds to an observed half lives of 23.9 min for DRaCALA and about an hour for gel shift. This difference may be explained by the amount of unlabeled competitor used to chase off the probe, which was at 25 times molar excess for the gel shift and 1000 times for DRaCALA. For DRaCALA with plasmid probes, another advantage is that high concentrations of competitor can easily be obtained by PCR amplification. The on-rate cannot be measured using DRaCALA, but it can be approximated by assuming a simple one-step binding mechanism with a calculation based on the affinity and off-rate. Using DRaCALA with plasmid probes allows for easy testing of direct binding and specific competition of any potential DNA-binding site simply by cloning into a plasmid that can be labeled for detection. One could make the case that studying kinetics in this system more accurately reflects DNA-binding activity in a cell compared to protein-oligo binding, because there is a great excess of DNA to which the protein can bind non-specifically.

Comparing DRaCALA to the traditional separation-based methods reveals the advantages of the new technique. The filter-binding assay was the first popular method that depended on separation of bound and unbound ligands based on differential mobility through a support (181). This technique was used for the first study of the interaction of CRP with DNA (274). One key difference between DRaCALA and filter-binding assays is that for DRaCALA, both the bound ligand and the total amount of ligand are always

measured. In contrast, the traditional filter-binding assay typically only measures the bound ligand. Thus, results of filter-binding assays are typically normalized to 1.0 fraction bound for the highest concentration of protein or ligand. In contrast, results for DRaCALA for the highest concentration of protein is often < 1.0. There are three potential reasons for the fraction bound detected by DRaCALA to be less than the theoretical 1.0. First, the off-rate of the protein–ligand interaction dictate that, during the assay time, a population of the bound ligand is dissociated, mobilized and cannot rebind the protein. Second, for all 5'-end-labeled nucleotide, a small fraction of labeled free phosphate can be hydrolyzed and appear as free ligand. Third, oligonucleotide probes can fold into non-native conformations. For example, the inverted repeat of the ICAP oligo can lead to the folding into hairpins that cannot be bound by CRP. Because DRaCALA measures both free and bound ligand, the determined fraction bound is far more accurate despite the detection of fraction bound of < 1.0. We do not think this is a concern as the K_d and k_{off} that we measured for CRP–ICAP interactions are similar to previously reported results. A similarity shared by DRaCALA and filter-binding assays is the interaction of proteins with nitrocellulose may alter the behavior of proteins. For DRaCALA, this effect is likely protein-specific since soluble and insoluble forms of Alg44 and PelD behave similarly when assayed for binding to cdiGMP by DRaCALA (209).

The EMSA (or gel shift), which detects interactions because they cause retardation in DNA mobility through a gel, was first introduced as an alternative to the filter-binding assay using the lac repressor as an example (277,278). Later it was used to study CRP in greater detail (275,276). The major strengths of the gel shift are that both bound and

unbound ligands are measured and supershifts provide information about binding structure. A potential issue is the length of time required to run the gel, during which time the protein and DNA can dissociate, which is a particular concern for lower affinity interactions (279). DRaCALA does not have a wash step and it measures total signal in every sample with a visual readout, making it preferable to the filter-binding assay. EMSA also measures total signal with a visual readout, but requires a much greater assay time than DRaCALA. Although DRaCALA is more rapid, EMSA still retains an advantage in the detection of supershifts that result from an antibody binding to a DNA-bound protein or multiple proteins binding to DNA. The ability of DRaCALA to detect interactions on plasmid DNA is a significant improvement over EMSA, which is most sensitive with probes <300-bp long (280).

More modern techniques include chromatin immunoprecipitation on a microarray chip (ChIP-chip) and sequencing of chromatin immunoprecipitated DNA (ChIP-Seq). These assays allow for a high-throughput approach to identify binding sites on the chromosome but provide no measure of affinity and cannot rule out indirect interactions (281,282). Because the readout of ChIP-chip is precipitation or a lack thereof, studies of transcription factors such as CRP often have false negatives and include a lot of background noise attributable to low-affinity binding sites (283). The most accurate analytical assays include isothermal titration calorimetry (ITC) and surface plasmon resonance (SPR). ITC uses a controlled chamber to assess heat changes as DNA binds protein, allowing for thermodynamic and kinetic measurements (284). SPR detects molecular weight changes on a metal surface in real time and can determine affinity and kinetics with remarkable sensitivity (285). The proof of principle for SPR studies of

DNA–protein interaction was first demonstrated using the lac repressor (286). ITC and SPR have the advantage over DRaCALA in that neither technique requires labeling of the ligand of interest. However, the common drawbacks of ChIP-chip, ITC and SPR are the relatively high associated costs and need for specialized equipment. DRaCALA uses small amounts of inexpensive materials and requires no special equipment, making biochemistry accessible to molecular biologists. DRaCALA is precise, with standard deviations (SDs) of measurements that are typically <5% of the mean. The value of DRaCALA lies in the simplicity of the technique. The only special tool required is a detector of the label on the probe. Only a small amount of sample and nitrocellulose are needed, making it inexpensive and easy to scale up. Capillary action of small volumes is fast, so separation of bound and unbound ligand takes only seconds. Together, these traits make DRaCALA especially cost and time efficient in comparison to established methods.

The simplicity of DRaCALA allows adaptation of the technique to study other molecular interactions. PCR conjugation of DNA to a variety of molecules can be achieved using commercially available modified primers that can have 5' reactive groups such as aldehydes, amines and thiols. This can serve the dual function of keeping the molecule mobile through nitrocellulose and providing a mechanism to label the probe in different ways. Radiolabelling small molecules directly is often impractical due to costs associated with chemical synthesis with radiolabeled chemicals, so DNA conjugation could be a good alternative. The free 5'-end of the DNA can be ^{32}P-labeled as in this study or occupied with a fluorescent dye from a second modified primer in the original PCR reaction. While fluorescence may be desirable for its ease of use, it cannot match the sensitivity of ^{32}P. Bioconjugate PCR was used in this study with the simple

streptavidin– biotin system. Biotinylated PCR products were mobile, detectable and showed specific interactions with CRP and streptavidin. This also allows selective immobilization of biotinylated nucleic acids so that they can take the role of the immobile binding partner in DRaCALA.

As shown in this study, immobilization of RNA allowed detection of RNA interaction with a small ligand. This area has been of great interest since the discovery of riboswitches, cis-acting RNA sequences on mRNAs that directly interact with small molecules and consequently self-regulate their transcriptional termination and/or translation (287,288). Such RNAs have been found to bind a variety of small molecules, including amino acid derivatives, coenzyme B12 and the bacterial second messenger cdiGMP (138,289,290). Studies of riboswitches have primarily used in-line probing and equilibrium dialysis to analyze direct RNA binding to its target molecule. These methods require long incubations that limit their accuracy in determining biochemical parameters. Others have used gel shift assays to measure the affinity and kinetics for riboswitches (142). By comparing DRaCALA to gel shift assays using a Vc2* RNA to establish a proof of principle, we have demonstrated that DRaCALA is a powerful alternative to these methods, which is much faster with at least equal accuracy and precision (Figure 36). In this study, RNA was immobilized using biotinylation, but RNA could also be immobilized by other means such as with a known binding protein or an additional sequence on the RNA that specifically binds a protein. Another alternative strategy is to use a biotinylated DNA oligonucleotide that can hybridize with the RNA molecule (3'-end of riboswitch) to provide a method for immobilization. The same technique could also be used to study RNA–RNA interactions in the context of regulatory RNAs, which

are ubiquitous in prokaryotes and eukaryotes and have therapeutic potential (291,292). As more research is done involving RNA interactions with a variety of other molecules, it is critical to have a rapid, quantitative and cost-effective method for directly testing these interactions.

DRaCALA requires one immobile binding partner and a ligand that is detectable and mobile by capillary action. This study provides a foundation for universal applicability of DRaCALA for studying any molecular interaction. There is evidence that DNA could serve as a label and carrier for any molecule that can be conjugated to it. Because bioconjugate PCR allows specific immobilization of biotinylated nucleic acids, the assay can be used with nucleic acids as the immobile and/or the mobile piece in binding studies. These manipulations of the mobility of molecules provide a window to the many potential uses of this assay. Additionally, the ease of running DRaCALA (little volume needed, no wash step, inexpensive materials and visual readout) makes it possibly amenable to usage as a portable rapid diagnostic tool in a 'lab-on-paper' design (293).

4.10 Chapter 4 Methods

Table 6. Primers used in Chapter 4. ICAP and mutant ICAP sites are indicated (RC = reverse complement).

Name	Content[a]	Use	Sequence (5'-3')	Reference
gd126	ICAP*	oligonucleotide probe	AGGAGGAATAAATGTGATCT AGATCACATTTTAGAGGAGG	This study
gd127	ICAP* RC	oligonucleotide probe	CCTCCTCTAAAATGTGATCT AGATCACATTTATTCCTCCT	This study
gd128	ICAP* 8:G-C	oligonucleotide probe	AGGAGGAATAAATCTGATCT AGATCAGATTTTAGAGGAGG	This study
gd129	ICAP* 8:G-C RC	oligonucleotide probe	CCTCCTCTAAAATCTGATCT AGATCAGATTTATTCCTCCT	This study
gd130	ICAP* 10:G-C	oligonucleotide probe	AGGAGGAATAAATGTCATCT AGATGACATTTTAGAGGAGG	This study
gd131	ICAP* 10:G-C RC	oligonucleotide probe	CCTCCTCTAAAATGTCATCT AGATGACATTTATTCCTCCT	This study
gd132	ICAP* 8,10:G-C	oligonucleotide probe	AGGAGGAATAAATCTCATCT AGATGAGATTTTAGAGGAG G	This study
gd133	ICAP* 8,10:G-C RC	oligonucleotide probe	CCTCCTCTAAAATCTCATCT AGATGAGATTTATTCCTCCT	This study
kr122	ICAP*	clone into plasmid	AATAAATGTGATCTAGATCA CATTTTAG	This study
kr123	ICAP* RC	clone into plasmid	CTAAAATGTGATCTAGATCA CATTTATT	This study
kr124	ICAP* 8:G-C	clone into plasmid	AATAAATCTGATCTAGATCA GATTTTAG	This study
kr125	ICAP* 8:G-C RC	clone into plasmid	CTAAAATCTGATCTAGATCA GATTTATT	This study
kr126	ICAP*10:G-C	clone into plasmid	AATAAATGTCATCTAGATGA CATTTTAG	This study
kr127	ICAP* 10:G-C RC	clone into plasmid	CTAAAATGTCATCTAGATGA CATTTATT	This study
kr128	ICAP* 8,10:G-C	clone into plasmid	AATAAATCTCATCTAGATGA GATTTTAG	This study
kr129	ICAP* 8,10:G-C RC	clone into plasmid	CTAAAATCTCATCTAGATGA GATTTATT	This study
vl1427	ICAP sequence	oligonucleotide probe	GCAACGCAATAAATGTGATC TAGATCACATTTTAGGCACC C	(267)[a]
vl1428	ICAP sequence	oligonucleotide probe	GGGGTGCCTAAAATGTGATC TAGATCACATTTATTGCGTT G	(267) [a]
vl880	-	PCR of insert	GACCATGATTACGCCAAGCT A	This study
vl881	-	PCR of insert	CAGCTTTCATCCCCGATATG	This study

[a] The original ICAP sequence described by Ebright, Ebright, and Gunasekara the same as vl1427 and vl1428. ICAP* sequences including gd126-133 and kr122-129 have the core 28bp of the ICAP sequence with the indicated sequences. gd126-133 have 6 bp flanking sequence that is different

Table 7. Plasmids used in Chapter 4. ICAP and mutant ICAP sites are indicated.

Name	Parent	Insert
pVL-Blunt	-	-
pGD7	pVL-Blunt	ICAP x5
pGD8	pVL-Blunt	ICAP x3
pGD9	pVL-Blunt	ICAP x1
pGD11	pVL-Blunt	ICAP 8:G-C x3
pGD12	pVL-Blunt	ICAP 10:G-C x3
pGD13	pVL-Blunt	ICAP 8,10:G-C x3

Proteins, nucleic acids, and chemicals

The Vc2* DNA template was ordered from Integrated DNA Technologies. Other DNA oligonucleotides, Nucaway size exclusion columns, and Turbo DNase were from Invitrogen. RNase was from Fermentas. RNase inhibitor and enzymes for restriction digests, PCR, and other nucleic acid manipulations were from New England Biolabs. Streptavidin MagneSphere Paramagnetic Particles, Wizard miniprep and PCR Purification kits for DNA purification were from Promega. Biotin hydrazide and streptavidin were from Sigma Aldrich.

CRP was purified according to (209). Briefly, His-CRP (CRP) was expressed from pBAD-CRP (a gift from Dr. Sankar Adhya) and purified using a Ni-NTA column. Proteins were dialyzed in 10 mM Tris, pH 8.0 and 100 mM NaCl. His-CRP was subsequently purified and concentrated using cation exchange to a concentration of 36 μM, frozen in liquid nitrogen, and stored at -80°C until thawing for use. The fraction of active CRP molecules in sequence-specific DNA binding (0.61) was determined by titration of DNA fragment ICAP under stoichiometric binding conditions. Specifically, serial dilutions of CRP were incubated with a concentration of ^{32}P ICAP dsDNA in excess of the K_d (200 nM) for 10 minutes at room temperature prior to determination of

binding by DRaCALA and EMSA. All data are reported in terms of molar concentrations of active CRP dimers.

Preparation and activity of DNA oligonucleotides and plasmid probes

Reverse complementary oligonucleotides gd126-133 and vl1427-1428 (Table 6) were used to generate probes by labeling 5 pmol of the forward primer with T4 Polynucleotide Kinase (PNK) and 15 pmol / 5 mCi of γ-^{32}P-labelled ATP. Five pmol of the reverse complementary primer were added and the PNK was heat-inactivated during primer annealing in a 80°C water bath for ten minutes, which was then allowed to cool to room temperature over 1 hour. The annealed product was separated from free ^{32}P-ATP using a Nucaway column and diluted 1:10 for binding and competitions studies and 1:1000 for affinity and kinetics studies. Plasmids with binding sites were generated by cloning annealed, PNK-treated primers pairs (kr122-129 of Table 6) into StuI-cut pVL-Blunt, and sequencing for verification (Table 7). Plasmids were 5' end-labeled by sequential digestion with the single cutter BamHI, dephosphorylation of the 5' overhang with Calf Intestinal Alkaline Phosphatase, separation from enzymes by a Wizard PCR Purification column, and treatment with PNK in the presence of γ-^{32}P-labelled ATP. The labeled product was purified by Wizard column and a Nucaway column and diluted 1:10 for affinity and kinetic study. The near 5' end of these labeled plasmids is about 40 bp from the cloned binding sites. Competitors for plasmid binding were PCR amplified from these plasmids using primers vl880-vl881, which amplify the cloned binding sites and 250 bp flanking on each side (Table 6). The concentration of the ICAP probes was determined by Nanodrop1000. The fraction of ICAP that is active for binding is determined by measuring the maximum fraction of ^{32}P-labeled ICAP in excess of K_d (200

nM) that could be specifically bound by excess CRP by both EMSA and DRaCALA. The fraction was multiplied by concentration of ICAP to yield the concentration of ICAP that is active.

Differential Radial Capillary Action of Ligand Assay (DRaCALA)

Protein, ^{32}P-labeled DNA, and 200 μM cAMP (unless otherwise noted) were mixed in CRP buffer (10 mM Tris, pH 7.9, 200 mM NaCl, 0.1 mM DTT, 50 μg/ml BSA) (15) and incubated at room temperature for ten minutes. Five microliter of the mix was spotted on nitrocellulose by first pipetting the liquid out onto the tip of the pipette and then touching the drop to the membrane. Spots were allowed to dry completely (about 20 minutes) before exposing a phosphorimager screen and capturing with a Fujifilm FLA-7000. Photostimulated luminescence (PSL) from the inner spot and total PSL of the spot were quantitated with Fuji Image Gauge software. The fraction bound (F_b) (209) was calculated using measurements of the total area (A_{outer}), the area of the inner circle (A_{inner}), the total PSL intensity (I_{total}), and the inner intensity (I_{inner}) as follows:

$$F_B = \frac{I_{inner} - A_{inner} * \left(\frac{I_{total} - I_{inner}}{A_{total} - A_{inner}} \right)}{I_{total}}$$

Electrophoretic Mobility Shift Assay (EMSA) for CRP binding to ICAP oligonucleotide

A fraction of the same mix described for the DRaCALA assay is supplemented with 10% glycerol and 0.001%Bromophenol Blue, and 5 μL was loaded onto an 8% 70:1 0.5x TBE (90 mM Tris pH = 8.0, 90 mM H_3BO_3, 2.5 mM Na_2EDTA) polyacrylamide gel (294). EMSA was preformed with 0.5x TBE Buffer at 4 ˚C. Gels were exposed to a phosphorimager screen and the image was captured with a Fujifilm FLA-7000. The

fraction bound was calculated as the intensity of the bound ICAP probe as a fraction of the total intensity of the bound and free ICAP probe.

Non-radioactive ligands and detection

Fluorescent dyes were imaged with a GE Typhoon Trio. TNP was detected with electrochemiluminescence excitation at 555 nm emission. FITC was detected with 488 nM excitation and 526 nM emission. Ethidium bromide was imaged under a UV light source. TRITC, Propidium iodide, crystal violet, and coomassie brilliant blue were imaged in visible light.

Bioconjugate PCR

Biotinylated probes were generated by PCR using 5'-biotinylated primer vl881 for amplification of a ~600 base pair region of plasmids pGD9 and pGD13 (Table 7). PCR products were extracted from an agarose gel and purified with a Wizard column. These were then γ-^{32}P-labelled as described for the whole plasmids.

Preparation and purification of Vc2* RNA

The Vc2* template sequence (138) including T7 promoter sequence and complimentary T7 promoter sequence 5′ - CTA ATA CGA CTC ACT ATA G - 3′ were purchased from Integrated DNA Technologies (IDT). Transcription was performed using 1.5 μg of template, 10 μL of 4 mg/ml T7 polymerase per 200 μL of transcription volume, 15 mM total NTP (A/C/G/UTPs), 15 mM $MgCl_2$ in a transcription buffer of 40 mM Tris-HCl (pH 8.1), 1 mM spermidine, 5 mM dithiothreitol (DTT), 0.01% Trixon X-100, 2 units of RNase inhibitor, 2 unit of inorganic pyrophosphatase. After 3 h, 0.4 units of Turbo DNase were added and incubated for another 15 min. The crude RNA was purified using a 12% denaturing PAGE with 1×TBE buffer. The product band was detected via

UV-shadowing the gel, excised and electro-eluted in a Schleicher and Schuell Elutrap eletro-separation system. The purified RNA was precipitated with three volumes of absolute ethanol and 10% volumes of 0.3 M sodium acetate. The RNA pellet was then resuspended in water and dialyzed in a Nestroup Biodialyzer with a 500 MWCO membrane for 24 h against 100 mM potassium phosphate buffer (pH 6.4), 0.5 M KCl, 10 mM EDTA, and then 1 and 0,1 mM EDTA, and finally against two changes of double distilled H_2O water before it was lyophilized.

Biotin labeling of RNA with biotin hydrazide at 3'-end

Seven μL of freshly prepared 0.5 M $NaIO_4$ was added to Vc2* RNA (210 μg) in 100 μL of water and the solution incubated at room temperature for 1 h. The excess $NaIO_4$ was removed by filtration, using an Amicon ultra 0.5 mL centrifugal filter with10K cut-off membrane. The RNA was washed with 3×0.5 mL of water and then recovered by reverse spin. After that, 5μL of 1M sodium acetate, pH 4.95, and 7 ml of 35 mM biotin hydrazide in DMSO were added to the RNA. Coupling was carried out at 37 ˚C for 1.5 hr, then 3 μL of 1 M $NaCNBH_3$ in acetonitrile was added and the reduction was carried out at room temperature for 1 hr. The unused biotin hydrazide and $NaCNBH_3$ were removed by centrifugal filter as above.

Testing the biotinylation efficiency with magnetic streptavidin beads

Four hundred μL of streptavidin MagneSphere Paramagnetic Particle solution (Promega; Binding capacity: greater than 0.75 nmol of biotinylated oligonucleotide (dT) bind per ml of particles) was taken and washed three times with 500 μL saline-sodium citrate (SSC) buffer (0.5X). The washing step was facilitated by applying a magnet to the side of the tube and the supernatant discarded during each wash. SSC buffer with 100 μl

of dissolved biotinylated RNA (2 μM) was added to streptavidin-coated magnetic particles and the tube was gently tapped to suspend the beads. The suspended beads were incubated at room temperature for 30 minutes, with occasional agitation by hand. A magnet was applied to the side of the tube and the supernatant was collected. The beads were washed with 100 μL SSC buffer (0.5X) two more times and the supernatant was collected and combined and UV_{260nm} measurement was made (OD_{260} = 0.123; 300μL of supernatant wash). Because the supernatant was diluted three times, the OD of the original supernatant must be 0.531. This OD value was compared to the OD of the biotinylated RNA before incubation with streptavidin-coated beads. The yield of the biotnylated RNA was calculated to be 76.8%.

To confirm that the biotinylated RNA was bound to the streptavidin magnetic beads, 0.5 μL of RNAse A/T1 Mix was added to the washed beads in 100 μL of SSC buffer (0.5X). The beads were incubated at 37 ˚C for 30 mins before the supernatant was collected by applying a magnet. The OD_{260} for the eluted nucleotides was 0.560. The slight increase in absorbance at 260 nm (compare OD of 0.531 for the RNA with an OD of 0.56 for the nucleotides generated from the RNA hydrolysis) is expected as free nucleotides have higher absorption than when in a polynucleotide (hypochromic effect).

Electrophoretic Mobility Shift Assay for RNA binding to cdiGMP

Gel shift assays were performed using 8% acrylamide gels with 100 mM Tris/HEPES, pH = 7.5, 10 mM $MgCl_2$, and 0.1 mM EDTA in the gel and running buffer. Gels were run at 4°C at 100V for 2 hours. Gels were imaged with a phosphorimager and fraction bound quantified with Fuji Image Guage software. The ^{32}P cdiGMP probe was synthesized from α-^{32}P-GTP by incubating overnight with purified diguanylate cyclase

WspR (PA3702 from *Pseudomonas aeruginosa*) in 10 mM Tris, pH = 8, 100 mM NaCl, and 5 mM $MgCl_2$ at 37°C.

Chapter 5: Conclusions and Perspective

5.1 Evaluation of DRaCALA ORFeome Screens for the Identification of cdiGMP-binding Proteins

The primary goal of my doctoral research has been to characterize the genetic basis of cdiGMP signaling in prokaryotes. Similar to eukaryotic cAMP signaling, prokaryotic cdiGMP signaling is complex with individual organisms containing dozens of DGCs and PDEs and multiple cdiGMP-dependent effectors (79). Genetic screens of cdiGMP-dependent phenotypes suffer from the intricate nature of cdiGMP regulated processes, which are diverse, multifactorial, and not necessarily observable under laboratory conditions. Despite these challenges, all cdiGMP-dependent processes rely on the allosteric regulation of effector proteins and RNAs by cdiGMP-binding. Therefore, to discover the molecular targets of cdiGMP signaling, I sought to systematically identify all proteins with cdiGMP-binding activity encoded within a bacterial genome. The identification of a complete set of cdiGMP effectors would reveal the potential regulatory activities of cdiGMP within a cell and provide a system level understanding of the cdiGMP regulatory network.

Several systematic methods for the identification of protein-ligand interactions have been applied to the identification cdiGMP-binding proteins. Most notably, the identification of conserved cdiGMP-binding domains (PilZ, GGDEF, EAL, HD-GYP) has allowed bioinformatic prediction of cdiGMP-binding proteins from sequenced genomes (109,112,126). However, several cdiGMP-binding proteins have been described that lack these domains (148,157,160,165,166). In the absence of conserved binding domains, cdiGMP-binding proteins have been identified based on their affinity for

cdiGMP. Several studies have attempted to identify cdiGMP effectors by affinity pulldown coupled with LC-MS for protein identification (208,295). However, affinity pull downs are limited by the requirement for expression of cdiGMP-binding proteins under laboratory conditions. Additionally, chemically derivatized cdiGMP probes may not interact with all cdiGMP-binding proteins (296-298). These limitations are overcome by DRaCALA through the use of radiolabeled cdiGMP probes and heterologous expression of fusion proteins in whole cell lysate. Thus, DRaCALA provides an alternative method for cdiGMP-binding protein identification that can be applied on a genomic scale. By systematically testing every individual open reading frame present within a genome for the expression of a cdiGMP-binding protein, DRaCALA may allow identification of a complete set of genomically-encoded cdiGMP effectors.

The DRaCALA ORFeome screen of the *Vibrio cholearae* open reading frame library had considerable success in identifying predicted, empirically characterized, and novel cdiGMP effector proteins. However, several proteins with demonstrated cdiGMP-binding proteins were not identified (Chapter 3.3). While positive ORFs generally encode cdiGMP-binding proteins, negative ORFs may not be active as fusion proteins, improperly folded during heterologous expression, have low affinity for cdiGMP, require multi-protein complexes for binding, or not be expressed at sufficiently high levels for detection. Furthermore, DGC activity may affect the ability to detect binding to cdiGMP. Overexpression of GGDEF-domain proteins with DGC activity produces excess unlabeled cdiGMP thereby lowering fraction bound ^{32}P-cdiGMP (Figure 16). In total, we identified 28 ORFs encoding putative cdiGMP-binding proteins, including 5 of 10 ORFs encoding proteins with empirically demonstrated cdiGMP-binding activity (Chapter 4.9).

A DRaCALA ORFeome screen to identify cdiAMP binding proteins from a *Staphylococcus aureus* open reading frame library obtained similar results. In collaboration with our lab, a report by Corrigan *et al.* identified 4 novel cdiAMP binding proteins and 3 of these proteins were identified in the DRaCALA screen (254). The fourth protein CpaA was not present in the *S. aureus* ORFeome. Together, these studies show that DRaCALA ORFeome screens are a systematic method for the identification of cyclic di-nucleotide binding proteins. However, DRaCALA alone is not sufficient to determine a complete set of binding proteins within a given genome. Nonetheless, the characterization of new binding proteins will allow identification of evolutionarily conserved cdiGMP-binding motifs, thereby enabling prediction of new cdiGMP-binding proteins in sequenced organisms. Subsequent genetic and biochemical characterization can determine if these cdiGMP-binding proteins are sufficient to mediate cdiGMP-dependent phenotypes. A combination of these approaches may enable identification of a complete set of genomically-encoded cdiGMP-binding proteins.

5.2 Linking cdiGMP-binding Proteins to cdiGMP Regulated Phenotypes

Previous identification of cdiGMP-binding proteins has provided insight into the cellular targets and molecular mechanisms of cdiGMP-dependent regulation. For example, YcgR is a regulator of flagellar motility that interacts with the flagellar motor complex. Identification of a PilZ domain in YcgR suggested that cdiGMP regulates flagellar motility by binding to YcgR (122). Subsequent studies on the molecular mechanism of cdiGMP regulation by YcgR have revealed that cdiGMP-binding to YcgR alters protein-protein interactions between YcgR and the flagellar motor complex (195,299,300). This causes a decrease in flagellar velocity and induces a counter-

clockwise bias in flagellar rotation. Counterclock-wise rotation produces long runs and decreased tumbling, preventing bacteria from changing direction upon encountering microscopic obstructions (301). In a second example, the Alg44 protein was identified as a unique regulator of alginate biosynthesis in *P. aeruginosa* (125). Subsequent identification of a PilZ domain in the Alg44 protein led to the discovery that cdiGMP-binding to Alg44 regulates alginate biosynthesis (121,126).Thus, the discovery of cdiGMP-binding to proteins with previously characterized regulatory activity has provided valuable insight into the specific cellular processes regulated by cdiGMP.

In the absence of known phenotypes and biochemical activities, identification of specific regulatory targets and mechanisms for individual cdiGMP-binding proteins can be challenging. For example, *V. cholerae* encodes 3 PilZ domain proteins that bind cdiGMP and contain no other identifiable domain (127). Genetic analysis of their requirement for cdiGMP-dependent phenotypes revealed pleiotropic effects on motility, biofilm formation and intestinal colonization (127). The specific molecular activities of these proteins have yet to be described. Similarly, *P. aeruginosa* contains 7 PilZ domain proteins that bind cdiGMP, but the biological effects of cdiGMP-binding to these proteins have only been described for Alg44 (126). Thus, connecting cdiGMP-binding proteins to specific cdiGMP regulated processes remains a challenge. To determine the specific activities of cdiGMP-binding proteins, genetic and biochemical dissection of the specific cellular processes that underlie complex cdiGMP-dependent phenotypes must be identified.

5.3 MshE and cdiGMP-dependent Regulation of Type IV Pili

The identification of cdiGMP-binding to MshE has suggested a new mechanism for cdiGMP-dependent regulation of MSHA type IV pili in *Vibrio cholerae*. MshE is a member of a family of hexameric ATPases (here referred to as T2SE ATPases) that are required for both biosynthesis and retraction of type IV pili (245). Previous work has demonstrated that cdiGMP regulates type IV pili-dependent motility in *Pseudomonas aeruginosa* and pathogenesis in *Xanthomonas campestris*. Some genetic requirements have been identified for this cdiGMP dependent regulation, but the precise mechanism by which cdiGMP regulates pili function is unknown.

Regulation in *Pseudomonas aeruginosa*

In *P. aeruginosa,* the PilZ protein is required for type IV pili biogenesis but does not bind cdiGMP directly (126,302). Instead, a cdiGMP-binding protein FimX was shown to regulate type IV pili formation (112,114,116). However, FimX and PilZ do not interact in *P. aeruginosa,* and the mechanism of FimX regulation of type IV pili is not known. Furthermore, a recent screen of type IV pili formation in a *fimX* mutant revealed that high cdiGMP levels allow pilus formation in the a *fimX* independent manner, suggesting that other cdiGMP-binding proteins may be involved in type IV pili regulation (263).

Regulation in *Xanthomonas campestris sp.*

cdiGMP-dependent regulation of type IV pili has been studied in two *Xanthomonas* species, *X. campestris citri,* and *X. campestris campestris.* In both organisms, cdiGMP signaling components interact with either the PilB extension ATPase or PilT/PilU retraction ATPases of type IV pili. In *X. campestris citri,* a FimX homolog

has been shown to directly interact with a PilZ protein deficient in cdiGMP-binding to regulate type IV pili (244). The FimX and PilZ protein of *X. campestris citri* have been crystallized in complex with a MshE homolog, PilB, suggesting that cdiGMP may regulate type IV pili via protein-protein interactions with PilB (262). In the related organism *X. campestris campestris*, studies have shown that an HD-GYP domain protein, RpfG, interacts with a GGDEF-domain protein to recruit a PilZ domain protein that has cdiGMP-binding activity (103,242). This RpfG/GGDEF/PilZ protein complex interacts with a different set of conserved MshE homologs, PilT and PilU which function in type IV pili retraction (242).

In this work, purified MshE was shown to bind cdiGMP and have ATPase activity (Chapter 3.4). However, cdiGMP-binding did not alter the rate of ATP hydrolysis, suggesting that cdiGMP binding may alter other activties of MshE such as protein-protein interactions. Thus, cdiGMP-dependent regulation of type IV pili appears to converge on the regulatory ATPases, but the molecular mechanisms of this regulation appear to have diverged. Studies in *X. campestris* demonstrate multiple cdiGMP effector interactions with MshE homologs and direct cdiGMP-binding to MshE may represent a *V. cholerae* specific mechanism for cdiGMP-dependent regulation of type IV pili.

Alternatively, the identification of cdiGMP-binding activity for the *P aeruginosa* MshE homolog PA14_29490 indicates that direct cdiGMP-binding may be a conserved regulatory feature. MshE and PA14_29490 represent a monophyletic cluster among the T2SE ATPases that that regulate type IV pili and type II secretion systems (245). Type II secretion systems and type IV pili assembly apparatus are evolved from a common ancestor and composed of proteins with similar structure and function, suggesting a

conserved mechanism for type IV pilus assembly and type II secretion (303). For example, both systems contain pilin-like proteins that are assembled by T2SE ATPases to form the type IV pili or a piston like pseudopilus required for secretion of type II secretion substrates (304). Several T2SE ATPases have been structurally and genetically characterized including PilB homologs required for type IV pili polymerization, PilT/PilU homologs required for type IV pili retraction, and EspE and XcpR required for type II secretion in *V. cholerae* and *P. aeruginosa* respectively (246-249,305-309). cdiGMP-binding was not detected for these and other T2SE ATPase homologs, suggesting that MshE and PA14_29490 represent a subset of T2SE ATPases that evolved cdiGMP-binding (Figure 24). The identification of conserved residues for cdiGMP-binding in MshE and PA14_29490 will allow prediction of cdiGMP-binding for a subset of T2SE ATPases and reveal if this subset of type II secretion is a target of cdiGMP regulation.

5.4 Future Applications for DRaCALA

DRaCALA has proven to be a valuable tool for identifying cdiGMP and cdiAMP binding proteins. Identification has relied on the use of large open reading frame libraries that were cloned to represent the majority of ORFs within a genome. DRaCALA ORFeome screens are useful for the identification of novel cyclic di-nucloeitde binding proteins, and targeted screens of positive ORF homologs can allow rapid identification of conserved cyclic di-nucleotide binding sites. For example, the identification of MshE prompted the cloning and testing of a set of homologous ATPases from *P. aeruginosa* leading to the discovery of PA14_29490 as a cdiGMP-binding protein. Similarly, the identification of cdiAMP binding to the RCK_C domain of KtrA prompted the testing

and discovery of CpaA, which also contains an RCK_C domain (254). While a lack of binding in the DRaCALA ORFeome screens is not definitive, verification of fusion protein expression is useful for discriminating between non-binding and lack of protein production. However, false positives may be produced if heterologous protein expression alters levels of the endogenous signaling system. Thus, cdiGMP binding should be verified for the positive ORFs that lack non-canonical cdiGMP binding sites including PstC, VCA0593, and TyrR. If verified, targeted DRaCALA screens of homologous proteins in other organisms with cdiGMP signaling systems could be performed. Several cdiGMP-binding homologs of the NtrC-class enhancer binding protein TyrR have already been identified including FleQ in *P. aeruginosa* and VpsR and FlrA in *V. cholerae* (148,160,165). Other NtrC class enhancer-binding proteins, such as AlgB of *P. aeruginosa* which regulates transcription of the cdiGMP-regulated alginate biosynthetic operon, should be tested for cdiGMP-binding (310,311). The results of these screens will rapidly determine if cdiGMP-binding activity is conserved among homologous groups of proteins. The identification of cdiGMP-binding for only a subset of homologs may reveal specific features that are required for cdiGMP-binding.

In addition to measuring protein-nucleotide interactions, DRaCALA has been adapted for quantification of RNA-ligand interactions using purified RNA aptamers (Figure 36). To date, two classes of cdiGMP-binding RNAs have been identified by computationally prediction of structured RNA aptamers (138,139). Potentially, DRaCALA could be used to systematically identify cdiGMP-binding RNAs. One of the first challenges of such a screen would be the construction of a library of candidate RNA molecules. Such a library could be constructed from cDNA clones of endogenously

produced RNA. Alternatively, intergenic regions and 5' UTRs above a certain length could be systematically cloned for screening. An RNA library would also require a general method for RNA immobilization to detect binding of radiolabeled cdiGMP. For purified RNAs, immobilization in DRaCALA has been accomplished by the use of streptavidin and conjugation of biotin to purified RNA aptamers. The high affinity of streptavidin and biotin allows the majority of RNA to be immobilized during DRaCALA, but biotin conjugation to a library of RNAs expressed in whole cell lysates is not practical (298). However, the coat protein of the MS2 bacteriophage has been used to bind RNAs containing a series of stem loop structures that are specifically recognized by the coat protein (312,313). The MS2 RNA binding motif is not common in *E. coli* and would thus allow specific immobilization of RNAs transcripts that include the MS2-binding motifs in whole cell lysates (314). A library of whole cell lysates expressing MS2 labeled RNA transcripts could be screened by DRaCALA for binding to radiolabeled molecules. Binding specifically in the presence of the MS2 coat protein would reveal the presence of specific activity for putative RNA aptamers. Currently, the regulatory activities of RNA binding to cdiGMP are not well understood in comparison to regulation by cdiGMP-binding proteins. The systematic identification of cdiGMP-binding RNA aptamers would provide valuable insight into the role of RNA effectors in the regulation of cyclic di-nucleotide dependent phenotypes.

Finally, the simplicity and versatility of DRaCALA suggests that it may be useful for studying a variety of nucleotide signaling molecules. In addition to cdiGMP and cdiAMP, several other small nucleotide signaling molecules are known to participate in biological signaling including cAMP, cGMP and (p)ppGpp (315,316). Furthermore, a

novel class of cGMP/AMP hybrid molecules has been identified in both *V. cholerae* and eukaryotic innate immune signaling (317-321). These nucleotide signaling molecules have similar physical properties, indicating that they are suitable for DRaCALA ORFeome screens. Systematic identification of the binding proteins for these nucleotides could reveal their regulatory targets and provide insight into the molecular mechanisms of biological regulation by low molecular weight signaling molecules.

Appendix A

Table 9. PSL Quantification for Figure 3A. Average and standard deviation of total signal intensity for the triplicate DRaCALA spots depicted in Figure 3A.

	Total Signal Intensity	cAMP	ATP	cdiGMP
MBP	Average	1533	40980	110179
	Standard Deviation	132	1159	2138
CRP	Average	2479	38352	112918
	Standard Deviation	177	5277	4038
NtrB	Average	2143	23465	99336
	Standard Deviation	73	1836	3145
Alg44	Average	2291	40277	116184
	Standard Deviation	217	2307	1458

Table 10. PSL Quantification for Figure 3B. Average and standard deviation of total signal intensity for the triplicate DRaCALA spots depicted in Figure 3B.

	Total Signal Intensity		
1 mM Competitor	**1st Triplicate**	**2nd Triplicate**	**3rd Triplicate**
NC	47293	46379	43335
cdiGMP	30609	31213	34001
GTP	42359	45655	41391
GDP	42526	40561	42042
GMP	40367	48893	46280
cGMP	39354	40539	43532
ATP	39782	49712	37376
CTP	42686	42958	33382
UTP	41575	43598	35762
Average	40728	43279	39678
Standard Deviation	4456	5577	4648

Table 11. PSL Quantification for Figure 10A. Average and standard deviation of total signal intensity for the triplicate DRaCALA spots depicted in Figure 10A.

[$Alg44_{PilZ}$] (μM)	Total Signal Intensity
100.000	77021
50.000	82563
25.000	86246
12.500	86809
6.250	94695
3.125	87742
1.563	96559
0.781	86216
0.391	93135
0.195	83710
0.098	93767
0.049	87169
0.024	85644
0.012	80883
0.006	77804
Average	86664
Standard Deviation	5704

Table 12. PSL Quantification for Figure 10C. Average and standard deviation of total signal intensity for the triplicate DRaCALA spots depicted in Figure 10C.

Time (s)	1st Triplicate	2nd Triplicate	3rd Triplicate
0	109607	82354	83547
10	83366	72748	70773
15	84462	70645	73335
20	82922	69334	70831
30	80647	68939	68335
45	81803	68864	67199
60	81468	66620	66282
90	83626	69013	66519
120	77729	66088	65528
180	78442	65317	63472
Average	84407	69992	69582
Standard Deviation	9121	4866	5709

Table 13. PSL Quantification for Figure 13A. Average and standard deviation of total signal intensity for the triplicate DRaCALA spots of whole cell lysates depicted in Figure 13A.

BL21(DE3) Whole Cell Lysates				
		Total Signal Intensity		
$Alg44_{PilZ}$	Competitor (1 mM)	1st Triplicate	2nd Triplicate	3rd Triplicate
WT	cdiGMP	15895	18914	16999
	GTP	17215	25180	20686
R21A	cdiGMP	18611	22763	19111
	GTP	23957	25116	23905
S46A	cdiGMP	17251	23318	20944
	GTP	15022	24176	21991
D44A	cdiGMP	14558	20624	19909
	GTP	16684	22550	19379
R17A,R21A	cdiGMP	20636	22338	21226
	GTP	21244	23423	18439
	Average	18107	22840	20259
	Standard Deviation	3005	1934	1945

Table 14. PSL Quantification for Figure 13A. Average and standard deviation of total signal intensity for the triplicate DRaCALA spots of purified proteins depicted in Figure 13A.

Purified Proteins		
$Alg44_{PilZ}$	Competitor (1 mM)	Total Signal Intensity
WT	cdiGMP	14315
	GTP	16387
R21A	cdiGMP	13676
	GTP	14499
S46A	cdiGMP	13636
	GTP	13921
D44A	cdiGMP	15080
	GTP	15897
R17A,R21A	cdiGMP	14553
	GTP	14840
	Average	14680
	Standard Deviation	909

Table 15. DRaCALA analysis of cdiGMP-binding by whole cell lysates of *P. aeruginosa* strains.

Plate Well	Strain Name	Source [a]	B_G [b]	B_C [c]	B_{Sp} [d]	A_{280} [e]
1_A1	PA15	UTI	0.213	0.169	1.26	51.3
1_B1	PA14	UTI	0.151	0.148	1.02	19.4
1_C1	PA13	UTI	0.241	0.166	1.45	52.8
1_D1	PA8	UTI	0.232	0.183	1.27	54.2
1_E1	CPs 433	CF	0.175	0.165	1.06	45.3
1_F1	CPs 433	CF	0.228	0.162	1.41	38.8
1_G1	CPs 231	CF	0.285	0.176	1.62	53.1
1_H1	CPs 204	CF	0.259	0.160	1.62	50.0
1_A2	PAK	Hospital/laboratory	0.295	0.182	1.62	55.4
1_B2	IT-01	ATCC type strain	0.248	0.198	1.25	59.2
1_C2	IT-02	ATCC type strain	0.193	0.163	1.18	43.3
1_D2	IT-03	ATCC type strain	0.310	0.185	1.68	60.6
1_E2	IT-04	ATCC type strain	0.289	0.171	1.69	50.1
1_F2	IT-05	ATCC type strain	0.271	0.184	1.47	53.7
1_G2	IT-06	ATCC type strain	0.273	0.171	1.60	41.3
1_H2	IT-07	ATCC type strain	0.288	0.169	1.70	43.6
1_A3	IT-08	ATCC type strain	0.273	0.171	1.60	54.1
1_B3	IT-09	ATCC type strain	0.208	0.161	1.30	38.1
1_C3	IT-010	ATCC type strain	0.263	0.172	1.53	51.4
1_D3	IT-011	ATCC type strain	0.246	0.165	1.49	47.1
1_E3	IT-013	ATCC type strain	0.267	0.164	1.63	44.4
1_F3	IT-015	ATCC type strain	0.280	0.169	1.65	50.4
1_G3	IT-016	ATCC type strain	0.257	0.167	1.54	54.1
1_H3	IT-017	ATCC type strain	0.246	0.180	1.37	59.0
1_A4	IT-018	ATCC type strain	0.256	0.174	1.47	40.3
1_B4	IT-019	ATCC type strain	0.188	0.174	1.08	35.5
1_C4	IT-020	ATCC type strain	0.250	0.177	1.41	49.2
1_D4	A 2 A	CF	0.242	0.165	1.46	50.0
1_E4	A 2 B	CF	0.206	0.157	1.31	37.4
1_F4	A 3	CF	0.214	0.155	1.38	42.6
1_G4	A 7	CF	0.266	0.171	1.55	53.5
1_H4	A 8	CF	0.207	0.156	1.33	35.9
1_A5	A 9B	CF	0.193	0.161	1.20	28.3
1_B5	A 10A	CF	0.235	0.174	1.35	34.1
1_C5	A 15A	CF	0.275	0.173	1.59	46.9
1_D5	A 15B	CF	0.251	0.173	1.45	44.5
1_E5	SE1	CF	0.218	0.162	1.34	55.2
1_F5	SE4	CF	0.253	0.173	1.47	45.6
1_G5	SE5	CF	0.215	0.178	1.21	39.9
1_H5	SE8	CF	0.198	0.159	1.25	37.4
1_A6	SE9A	CF	0.215	0.201	1.07	38.9

1_B6	SE10A	CF	0.226	0.182	1.24	42.9
1_C6	SE11	CF	0.226	0.169	1.34	44.9
1_D6	SE12B	CF	0.200	0.157	1.27	51.4
1_E6	SE13	CF	0.217	0.174	1.25	37.5
1_F6	SE14	CF	0.220	0.174	1.26	44.3
1_G6	SE16	CF	0.193	0.170	1.14	36.3
1_H6	SE17	CF	0.201	0.164	1.23	40.3
1_A7	SE19	CF	0.202	0.172	1.17	19.9
1_B7	SE21A	CF	0.204	0.168	1.21	16.5
1_C7	SE21C	CF	0.202	0.172	1.17	18.1
1_D7	SE22B	CF	0.205	0.178	1.15	14.4
1_E7	MI3A	CF	0.240	0.171	1.41	22.2
1_F7	MI3B	CF	0.246	0.180	1.36	20.2
1_G7	MI4A	CF	0.277	0.180	1.54	21.9
1_H7	MI4B	CF	0.272	0.184	1.48	22.7
1_A8	MI5A	CF	0.249	0.177	1.41	58.6
1_B8	MI5B	CF	0.270	0.175	1.54	51.7
1_C8	MI6	CF	0.269	0.181	1.49	59.7
1_D8	MI8	CF	0.242	0.166	1.46	48.3
1_E8	MI9A	CF	0.215	0.158	1.36	40.8
1_F8	MI9B	CF	0.218	0.171	1.27	37.5
1_G8	MI9C	CF	0.231	0.173	1.34	37.7
1_H8	MI11A	CF	0.277	0.172	1.61	30.2
1_A9	MI11C	CF	0.225	0.176	1.28	42.1
1_B9	6073	Corneal	0.267	0.184	1.45	54.9
1_C9	6206	Corneal	0.310	0.182	1.70	56.2
1_D9	6382	Corneal	0.301	0.183	1.64	57.0
1_E9	6389	Corneal	0.272	0.175	1.56	48.7
1_F9	6452	Corneal	0.238	0.178	1.34	42.9
1_G9	PAO1	Wound/laboratory	0.281	0.187	1.51	53.4
1_H9	696	ATCC	0.204	0.167	1.22	32.8
1_A10	762	ATCC	0.293	0.172	1.70	60.0
1_B10	769	ATCC	0.233	0.170	1.37	53.0
1_C10	27853	ATCC	0.257	0.169	1.52	57.4
1_D10	6354	Corneal	0.331	0.173	1.92	57.2
1_E10	6487	Corneal	0.256	0.170	1.50	42.8
1_F10	PAO381	CF	0.304	0.173	1.76	45.8
1_G10	PAO578I	Mucoid	0.322	0.167	1.93	48.8
1_H10	PAO578II	Mucoid	0.320	0.165	1.94	52.2
1_A11	PAO579	Mucoid	0.292	0.166	1.77	43.0
1_B11	PA27853	ATCC	0.295	0.180	1.63	55.1
1_C11	MCW0001	CF	0.281	0.176	1.60	49.8
1_D11	725	CF	0.294	0.172	1.71	45.8
1_E11	1328	CF	0.294	0.167	1.76	42.0
1_F11	1641	CF	0.312	0.173	1.81	51.8
1_G11	381	CF	0.382	0.164	2.32	37.5

1_H11	578I	CF	0.280	0.167	1.68	47.8
1_A12	PA14 pMMB-RocR		0.605	0.173	3.51	30.5
1_B12	PA14 ΔpelD pmmB:RocR		0.501	0.186	2.70	34.9
1_C12	CF27		0.211	0.164	1.29	32.6
1_D12	PA14 pmmB-WspR		0.205	0.172	1.19	29.6
1_E12	PA14 ΔretS		0.219	0.171	1.28	27.0
1_F12	PA14	Hospital/laboratory	0.228	0.180	1.27	37.9
1_G12	PAO1	Wound/ laboratory	0.256	0.180	1.42	44.0
1_H12	PAK	Hospital/laboratory	0.295	0.185	1.59	50.9
2_A1	MSH18	Environmental	0.341	0.200	1.71	16.5
2_B1	MSH12	Environmental	0.310	0.197	1.57	20.8
2_C1	MSH13	Environmental	0.259	0.195	1.33	18.1
2_D1	MSH	Environmental	0.328	0.200	1.64	26.4
2_E1	H14	Hospital	0.369	0.200	1.85	26.1
2_F1	H12	Hospital	0.392	0.209	1.87	17.7
2_G1	H19	Hospital	0.377	0.200	1.89	14.5
2_H1	H25	Hospital	0.214	0.112	1.90	23.9
2_A2	H26	Hospital	0.379	0.203	1.87	20.2
2_B2	MSH3	Environmental	0.349	0.189	1.85	29.0
2_C2	H28	Hospital	0.307	0.194	1.59	16.0
2_D2	H17	Hospital	0.292	0.191	1.53	30.3
2_E2	H27	Hospital	0.329	0.195	1.69	27.9
2_F2	MSH1	Environmental	0.373	0.193	1.93	28.0
2_G2	H15	Hospital	0.345	0.198	1.74	30.0
2_H2	H21	Hospital	0.327	0.186	1.76	22.0
2_A3	MSH5	Environmental	0.377	0.182	2.07	16.9
2_B3	H24	Hospital	0.235	0.175	1.34	6.0
2_C3	H22	Hospital	0.374	0.192	1.95	24.3
2_D3	H29	Hospital	0.312	0.205	1.53	24.8
2_E3	H2	Hospital	0.394	0.199	1.98	22.5
2_F3	Pa	Hospital	0.409	0.208	1.97	21.5
2_G3	MSH17	Environmental	0.353	0.200	1.76	21.3
2_H3	MSH12	Environmental	0.371	0.196	1.89	19.9
2_A4	H1	Hospital	0.376	0.194	1.93	21.2
2_B4	PB2036		0.411	0.200	2.06	20.9
2_C4	WR5	Hospital	0.294	0.195	1.50	13.1
2_D4	PA103		0.368	0.213	1.72	28.0
2_E4	MSH11	Environmental	0.281	0.181	1.56	26.9
2_F4	MSH16	Environmental	0.345	0.192	1.80	15.8
2_G4	MSH10	Environmental	0.315	0.188	1.67	13.4
2_H4	H30	Hospital	0.309	0.187	1.65	12.9
2_A5	H23	Hospital	0.290	0.205	1.41	11.6
2_B5	H16	Hospital	0.306	0.185	1.65	16.9
2_C5	S11	Soil	0.310	0.208	1.49	22.4
2_D5	Nathan II		0.344	0.192	1.79	20.0
2_E5	PAK	Hospital/laboratory	0.397	0.192	2.06	22.1

2_F5	S11	Soil	0.298	0.205	1.45	20.4
2_G5	Pa		0.413	0.203	2.04	24.6
2_H5	Pa		0.333	0.198	1.68	21.8
2_A6	PAK*	EMS mutant	0.378	0.201	1.88	19.8
2_B6	PAO2003		0.230	0.192	1.20	14.5
2_C6	PA103	CF	0.337	0.199	1.69	21.4
2_D6	8823	CF	0.300	0.192	1.56	16.6
2_E6	BHE08	Brazil	0.282	0.188	1.50	17.9
2_F6	BHE07	Brazil	0.265	0.186	1.42	19.0
2_G6	BHE06	Brazil	0.326	0.197	1.66	22.8
2_H6	BHE05	Brazil	0.342	0.203	1.69	18.9
2_A7	BHE04	Brazil	0.192	0.186	1.03	17.3
2_B7	BHE03	Brazil	0.268	0.190	1.41	14.7
2_C7	B27	Brazil	0.308	0.205	1.51	27.5
2_D7	V209 (Alg +)	CF	0.278	0.196	1.42	22.6
2_E7	V209 (Alg -)	CF	0.304	0.194	1.57	22.9
2_F7	isolate	CF	0.373	0.192	1.94	20.5
2_G7	isolate	CF	0.383	0.188	2.03	19.0
2_H7	CF1	CF	0.309	0.201	1.54	18.8
2_A8	CF2	CF	0.310	0.191	1.62	21.8
2_B8	CF3	CF	0.231	0.188	1.23	13.9
2_C8	CF4	CF	0.243	0.186	1.31	19.7
2_D8	CF5	CF	0.295	0.194	1.52	28.0
2_E8	CF6	CF	0.327	0.197	1.66	29.5
2_F8	CF26	CF	0.281	0.184	1.53	6.6
2_G8	CF27	CF	0.318	0.181	1.75	18.0
2_H8	CF28	CF	0.503	0.188	2.68	19.5
2_A9	CF29	CF	0.298	0.189	1.57	20.2
2_B9	R37	CF	0.376	0.183	2.06	8.0
2_C9	R71	CF	0.276	0.193	1.43	11.6
2_D9	6077	Corneal	0.357	0.206	1.74	18.7
2_E9	6294	Corneal	0.368	0.199	1.86	11.1
2_F9	19660	Corneal	0.327	0.199	1.65	24.6
2_G9	F34842	UTI	0.362	0.206	1.75	18.6
2_H9	F35896	UTI	0.356	0.209	1.71	24.5
2_A10	H38036	UTI	0.282	0.197	1.43	20.6
2_B10	M28497	UTI	0.263	0.205	1.29	19.2
2_C10	W57761	UTI	0.300	0.214	1.40	25.1
2_D10	X24509	UTI	0.402	0.215	1.87	25.0
2_E10	UTI121	UTI	0.331	0.204	1.62	19.7
2_F10	UTI122	UTI	0.339	0.200	1.69	15.5
2_G10	UTI123	UTI	0.277	0.200	1.38	14.5
2_H10	UTI124	UTI	0.366	0.203	1.80	25.4
2_A11	UTI125	UTI	0.307	0.193	1.59	10.8
2_B11	UTI126	UTI	0.267	0.201	1.33	12.2
2_C11	UTI127	UTI	0.287	0.200	1.44	19.3

2_D11	B312	Blood	0.313	0.204	1.53	17.1
2_E11	B1460A	Blood	0.321	0.203	1.58	21.4
2_F11	B1874-2	Blood	0.335	0.203	1.65	19.9
2_G11	CF32	CF	0.328	0.215	1.53	21.6
2_H11	U130	UTI	0.365	0.210	1.74	15.3
2_A12	U169	UTI	0.255	0.190	1.34	25.5
2_B12	U779	UTI	0.340	0.218	1.56	36.0
2_C12	U2504	UTI	0.303	0.206	1.47	35.5
2_D12	H21651	Blood	0.323	0.212	1.53	33.6
2_E12	X13397	Blood	0.310	0.207	1.50	39.4
2_F12	X16259	Blood	0.276	0.202	1.37	26.6
2_G12	S29712	Blood	0.331	0.208	1.59	24.0
2_H12	S35004	Blood	0.347	0.225	1.54	35.6

Average B_C =	**0.185**
Standard Deviation B_C =	**0.016**
2 *Standard Deviation B_C =	**0.031**
B_{Sp} Positive-Cutoff =	**1.17**

[a] Strains are classified as indicated. "CF" denotes cystic fibrosis isolate and "UTI" denotes urinary tract infection isolate.
[b] ^{32}P-cdiGMP bound during 1 mM GTP competition.
[c] ^{32}P-cdiGMP bound during 1 mM cdiGMP competition.
[d] Specific binding of whole cell lysate (B_G / B_C).
[e] Total protein concentration of whole cell lysate measured by absorbance at 280 nM by Thermo Fischer Nanodrop 8000 using 0.2 μM path length. Absorbance units are reported as if measured with 10 mm path length (actual path length of 0.2 mm).

Table 16. DRaCALA analysis of cdiGMP-binding by lysates from various organisms or tissues.

Plate Well	Genus	Species	Strain / tissue / cell type	B_G [a]	B_C [b]	B_{Sp} [c]	Predicted DGC [d]	Reference for cdiGMP signaling [e]
3_A1	*Aeromonas*	*hydrophila*	SJ11R	0.248	0.162	1.53 *	Yes	None
3_B1	*Salmonella*	*typhimurium*	SL1334	0.164	0.153	1.07	Yes	(124)
3_C1	*Escherichia*	*coli*	ZK57	0.149	0.141	1.06	Yes	(124)
3_D1	*Yersinia*	*enterocolitica*	W22703	0.161	0.147	1.10	Yes	None
3_E1	*Yersinia*	*enterocolitica*	8081	0.181	0.155	1.17 *	Yes	None
3_F1	*Yersinia*	*pseudotuberculosis*	pIB1	0.155	0.158	0.99	Yes	None
3_G1	*Yersinia*	*pseudotuberculosis*	pYPIII	0.152	0.150	1.01	Yes	None
3_H1	*Escherichia*	*coli*	JM109	0.171	0.165	1.03	Yes	(124)
3_A2	*Vibrio*	*cholerae*	N16961	0.354	0.179	1.98 *	Yes	(94)
3_B2	*Burkholderia*	*dolosa*	HI2914	0.301	0.166	1.82 *	Yes	None
3_C2	*Burkholderia*	*dolosa*	AU3960	0.278	0.178	1.56 *	Yes	None
3_D2	*Bacillus*	*subtilus*	3160	0.185	0.162	1.14	Yes	(118)
3_E2	*Bacillus*	*subtilus*	168	0.189	0.157	1.20 *	Yes	(118)
3_F2	*Bacillus*	*subtilus*	PY79	0.206	0.152	1.36 *	Yes	(118)
3_G2	*Actinomyces*	*naeslundii*	MG1	0.162	0.159	1.02	No sequence	None
3_H2	*Staphylococcus*	*aureus*	Newman	0.148	0.141	1.05	Yes	cdiGMP-independent (322,323)
3_A3	*Streptococcus*	*agalactiae*	2603	0.156	0.152	1.03	No	None
3_B3	*Pseudomonas*	*putida*	pB2440	0.143	0.133	1.07	Yes	(324)
3_C3	*Proteus*	*mirabilis*	SC81c M1061	0.158	0.165	0.96	Yes	None
3_D3	*Caenorhabditis*	*elegans*		0.151	0.157	0.96	No	None
3_E3	*Pseudomonas*	*stutzeri*	K2186	0.244	0.150	1.62 *	Yes	None
3_F3	*Pseudomonas*	*stutzeri*	K1412 M1035	0.224	0.158	1.42 *	Yes	None
3_G3	*Pseudomonas*	*stutzeri*	K79	0.287	0.155	1.85 *	Yes	None
3_H3	*Pseudomonas*	*fluorescens*	K2122	0.277	0.159	1.74 *	Yes	(324)
3_A4	*Stenotrophomonas*	*maltophilia*	K2227	0.279	0.167	1.67 *	Yes	None
3_B4	*Brevundimonas*	*vesicularis*	K136	0.298	0.175	1.71 *	No sequence	None
3_C4	*Providencia*	*stuartii*	SC145 M1062	0.156	0.170	0.92	Yes	None
3_D4	*Pseudomonas*	*fluorescens*	K2017 M1088	0.207	0.169	1.23 *	Yes	(324)
3_E4	*Burkholderia*	*cenocepacia*	K2313	0.152	0.163	0.93	Yes	None
3_F4	*Moraxella*	*osloensis*	K1980	0.144	0.145	0.99	No sequence	None
3_G4	*Pseudomonas*	*fluorescens*	E-38	0.185	0.144	1.29 *	Yes	(324)
3_H4	*Proteus*	*mirabilis*	H-62	0.156	0.163	0.95	Yes	None
3_A5	*Proteus*	*vulgaris*		0.158	0.168	0.94	No sequence	None
3_B5	*Pseudomonas*	*alcaligenes*	D13	0.313	0.174	1.80 *	No sequence	None
3_C5	*Delftia*	*acidovorans*	D12	0.324	0.177	1.83 *	Yes	None
3_D5	*Comamonas*	*testosteroni*	D14	0.279	0.164	1.70 *	Yes	None
3_E5	*Pseudomonas*	*mendocina*	D57	0.134	0.141	0.95	Yes	None
3_F5	*Stenotrophomonas*	*maltophilia*	C40	0.277	0.199	1.39 *	Yes	None
3_G5	*Pseudomonas*	*putida*	C14	0.192	0.171	1.12	Yes	(324)
3_H5	*Shewanella*	*putrefaciens*	F17	0.300	0.165	1.82 *	Yes	None
3_A6	*Pseudomonas*	*stutzeri*	H24	0.192	0.157	1.22 *	Yes	None

3_B6	*Nicotiana*	*benthamiana*		0.199	0.170	1.17 *	No sequence	None
3_C6	*Burkholderia*	*cenocepacia*	F2	0.218	0.174	1.25 *	Yes	None
3_D6	*Burkholderia*	*cenocepacia*	F27	0.188	0.158	1.19 *	Yes	None
3_E6	*Pseudomonas*	*diminuta*		0.211	0.162	1.30 *	No sequence	None
3_F6	*Mus*	*musculus*	Brain	0.315	0.243	1.29 *	No	(325)
3_G6	*Vibrio*	*cholerae*	IRA J13	0.328	0.169	1.94 *	Yes	(94)
3_H6	*Klebsiella*	*pneumoniae*	W63917	0.160	0.155	1.03	Yes	(326)
3_A7	*Sinorhizobium*	*meliloti*	Rm1021	0.164	0.162	1.02	Yes	None
3_B7	*Mus*	*musculus*	RAW Cells	0.151	0.169	0.89	No	(325)
3_C7	*Vibrio*	*harveyi*	MM32	0.207	0.162	1.28 *	Yes	None
3_D7	*Salmonella*	*typhimurium*		0.160	0.163	0.98	Yes	(124)
3_E7	*Escherichia*	*coli*		0.256	0.173	1.48 *	Yes	(124)
3_F7	*Citrobacter*	*freundii*		0.154	0.156	0.99	No sequence	None
3_G7	*Serratia*	*marcescens*		0.204	0.170	1.20 *	No sequence	None
3_H7	*Hafnia*	*alvei*		0.172	0.152	1.13	No sequence	None
3_A8	*Micrococcus*	*luteus*		0.136	0.140	0.98	No	None
3_B8	*Staphylococcus*	*epidermidis*		0.145	0.155	0.94	Yes	cdiGMP-independent (322,323)
3_C8	*Enterobacter*	*aerogenes*		0.169	0.152	1.11	No sequence	None
3_D8	*Bacillus*	*megaterium*		0.164	0.147	1.12	Yes	None
3_E8	*Pseudomonas*	*putida*	NCIMB	0.155	0.157	0.99	Yes	(324)
3_F8	*Ochrobactrum*	*anthropi*	NCIMB 8686	0.222	0.168	1.32 *	Yes	None
3_G8	*Moraxella*	*catarrhalis*		0.155	0.161	0.96	No	None
3_H8	*Acinetobacter*	*spp*	MD4	0.157	0.158	0.99	Yes	None
3_A9	*Moraxella*	*spp*	B88	0.154	0.149	1.03	No	None
3_B9	*Lactococcus*	*lactis*		0.243	0.166	1.46 *	Yes	None
3_C9	*Staphylococcus*	*aureus*		0.197	0.162	1.21 *	Yes	cdiGMP-independent (322,323)
3_D9	*Alcaligenes*	*faecalis*		0.172	0.164	1.05	No sequence	None
3_E9	*Corynebacterium*	*xerosis*		0.145	0.152	0.95	No sequence	None
3_F9	*Staphylococcus*	*sciuri*		0.148	0.154	0.96	No sequence	None
3_G9	*Proteus*	*mirabilis*		0.168	0.176	0.96	Yes	None
3_H9	*Enterococcus*	*durans*		0.155	0.154	1.01	No sequence	None
3_A10	*Marinococcus*	*halophilus*		0.169	0.147	1.14	No sequence	None
3_B10	*Clostridium*	*sporogenes*		0.171	0.195	0.87	Yes	None
3_C10	*Saccharomyces*	*cerevisiae*		0.160	0.159	1.01	No	None
3_D10	*Providencia*	*stuartii*		0.157	0.166	0.95	Yes	None
3_E10	*Bacillus*	*cereus*		0.161	0.152	1.06	Yes	(138)
3_F10	*Enterococcus*	*faecalis*		0.175	0.160	1.10	No	None
3_G10	*Staphylococcus*	*aureus*	MRSA	0.152	0.156	0.97	Yes	cdiGMP-independent (322,323)
3_H10	*Neisseria*	*gonorrhoeae*	MS11	0.151	0.150	1.01	No	None
3_A11	*Neisseria*	*gonorrhoeae*	F11090	0.149	0.155	0.96	No	None
3_B11	*Neisseria*	*sicca*		0.173	0.158	1.09	No	None
3_C11	*Streptococcus*	*pyogenes*	GA40634	0.145	0.146	1.00	Yes	None
3_D11	*Streptococcus*	*pyogenes*	NZ131	0.160	0.144	1.12	Yes	None
3_E11	*Streptococcus*	*pyogenes*	5448-AN	0.151	0.152	0.99	Yes	None
3_F11	*Streptococcus*	*pyogenes*	GA19681	0.153	0.149	1.03	Yes	None
3_G11	*Mycobacterium*	*smegmatis*		0.156	0.156	1.00	Yes	None

3_H11	*Aspergillus*	*niger*		0.156	0.157	0.99	No	None
3_A12	*Mus*	*musculus*	Heart	0.213	0.196	1.09	No	(325)
3_B12	*Saccharomyces*	*cerevisiae*	cry1-2	0.168	0.170	0.99	No	None
3_C12	*Saccharomyces*	*cerevisiae*	AH109	0.161	0.158	1.02	No	None
3_D12	*Leishmania*	*major*		0.154	0.170	0.91	No	None
3_E12	*Homo*	*sapiens*	U397 cells	0.181	0.271	0.67	No	(327)
3_F12	*Homo*	*sapiens*	HuH7 cells	0.149	0.151	0.99	No	(327)
3_G12	*Cricetulus*	*griseus*	CHO cells	0.179	0.273	0.66	No sequence	None
3_H12	*Mus*	*musculus*	Spleen	0.227	0.299	0.76	No	(325)

[a] B_G indicates ^{32}P-cdiGMP bound in the presence of the non-specific competitor GTP at 1 mM.
[b] B_C indicates ^{32}P-cdiGMP bound in the presence of the specific competitor cdiGMP at 1 mM.
[c] Specific binding of whole cell lysate (B_G / B_C). Organisms with values above the 1.17 cut-off are indicated by asterisks (*).
[d] Genomes that encode DGC were identified on October 7th, 2010 by a search at http://www.ncbi.nlm.nih.gov/protein using a search term consisting of the genus and species of each organism along with "DGC", "GGDEF" or "diguanylate". Organisms positive for DGC are indicated by "Yes". Organisms negative for DGC are indicated by "No". Those without a sequenced genome are indicated by "No sequence".
[e] References for organisms using cdiGMP signaling were identified by a PubMed search using a search term consisting of the genus and species of each organism and "cyclic-di-GMP" on October 7th, 2010. Earliest reference reporting cdiGMP signaling in each species is shown. Organisms for which no citations were available are indicated by "None". "cdiGMP independent" is noted for those strains that have a protein with a DGC domain and observed regulation that is independent of cdiGMP.

Table 17: Fraction bound ^{32}P-cdiGMP in primary DRaCALA screen of *V. cholerae* ORFs

VC Gene #	His-ORF Fraction Bound		His-MBP-ORF Fraction Bound	
	Replicate 1	Replicate 2	Replicate 1	Replicate 2
VC0001	0.09	0.07	0.02	0.00
VC0002	0.04	0.05	0.06	0.06
VC0003	0.04	0.03	0.07	0.08
VC0004	0.04	0.06	0.06	0.08
VC0005	0.09	0.05	0.05	0.07
VC0006	0.03	0.04	0.06	0.05
VC0007	0.00	0.04	0.05	0.06
VC0008	0.03	0.04	0.06	0.04
VC0009	0.05	0.06	0.06	0.07
VC0010	0.05	0.05	0.05	0.06
VC0011	0.05	0.05	0.03	0.03
VC0012	0.01	0.02	0.01	0.02
VC0013	0.01	0.01	0.02	0.00
VC0014	0.03	0.04	0.04	0.03
VC0015	0.05	0.08	0.05	0.05
VC0016	0.04	0.06	0.05	0.04
VC0017	0.09	0.09	0.03	0.05
VC0018	0.02	0.02	0.06	0.09
VC0019	0.06	0.06	0.05	0.06
VC0020	0.09	0.10	0.02	0.02
VC0021	0.04	0.03	0.09	0.13
VC0022	0.04	0.04	0.04	0.02
VC0023	0.10	0.10	0.01	0.03
VC0024	0.04	0.05	0.08	0.06
VC0025	0.10	0.10	0.03	0.05
VC0026	0.04	0.05	0.08	0.06
VC0027	0.03	0.05	0.07	0.04
VC0028	0.03	0.03	0.10	0.06
VC0029	0.03	0.02	0.06	0.08
VC0030	0.06	0.06	0.06	0.08
VC0031	0.05	0.06	0.04	0.04
VC0032	0.08	0.08	0.03	0.03
VC0033	0.08	0.08	0.04	0.09
VC0034	0.05	0.04	0.04	0.05
VC0035	0.05	0.05	0.05	0.04
VC0036	0.03	0.04	0.04	0.05
VC0037	0.07	0.10	0.06	0.07

VC0038	0.09	0.06	0.06	0.05
VC0039	0.04	0.04	0.04	0.05
VC0040	0.04	0.07	0.06	0.06
VC0041	0.03	0.05	0.06	0.06
VC0042	-0.01	0.00	0.06	0.06
VC0043	0.01	0.03	0.05	0.04
VC0044	0.04	0.06	0.04	0.05
VC0045	0.04	0.06	0.04	0.06
VC0046	0.03	0.03	0.00	0.00
VC0047	0.02	0.01	0.01	0.02
VC0048	0.03	0.03	0.04	0.04
VC0049	0.04	0.05	0.05	0.05
VC0050	0.04	0.06	0.06	0.07
VC0051	0.05	0.04	0.07	0.05
VC0052	0.06	0.06	0.07	0.07
VC0053	0.05	0.06	0.07	0.05
VC0054	0.03	0.05	0.07	0.07
VC0055	0.04	0.06	0.06	0.05
VC0056	0.02	0.05	0.04	0.04
VC0057	0.05	0.05	0.05	0.06
VC0058	0.06	0.07	0.09	0.07
VC0060	0.05	0.06	0.05	0.05
VC0061	0.05	0.05	0.04	0.06
VC0062	0.06	0.09	0.06	0.05
VC0063	0.10	0.13	0.08	0.07
VC0064	0.06	0.08	0.04	0.06
VC0065	0.05	0.05	0.05	0.06
VC0066	0.01	0.03	0.05	0.06
VC0067	0.05	0.05	0.06	0.06
VC0068	0.04	0.05	0.03	0.03
VC0069	0.04	0.05	0.05	0.05
VC0070	0.09	0.10	0.03	0.04
VC0071	0.02	0.03	0.10	0.12
VC0072	0.55	0.53	0.48	0.53
VC0072	0.01	0.04	0.05	0.06
VC0073	0.05	0.04	0.13	0.17
VC0074	0.06	0.06	0.02	0.04
VC0075	0.05	0.06	0.08	0.09
VC0076	0.06	0.06	0.05	0.05
VC0077	0.07	0.10	0.02	0.03
VC0078	0.00	0.00	0.05	0.09
VC0079	0.08	0.08	0.10	0.03
VC0080	0.03	0.03	0.03	0.04

VC0081	0.05	0.06	0.07	0.05
VC0082	0.00	0.02	0.01	0.02
VC0083	0.07	0.07	0.04	0.03
VC0084	0.04	0.03	0.06	-0.01
VC0085	0.04	0.04	0.04	0.04
VC0086	0.05	0.06	0.01	0.02
VC0087	0.04	0.02	0.05	0.06
VC0088	-0.02	0.01	0.05	0.04
VC0089	0.03	0.02	0.04	0.05
VC0090	0.04	0.03	0.05	0.05
VC0091	0.02	0.02	0.06	0.08
VC0092	0.07	0.08	0.03	0.03
VC0093	0.05	0.06	0.06	0.06
VC0094	0.06	0.06	0.05	0.04
VC0095	0.04	0.04	0.05	0.04
VC0096	0.09	0.06	0.06	0.07
VC0097	0.04	0.03	0.13	0.10
VC0098	0.13	0.14	0.05	0.05
VC0099	0.05	0.05	0.02	0.02
VC0100	0.10	0.11	0.06	0.06
VC0101	0.09	0.07	0.04	0.04
VC0102	0.04	0.07	0.06	0.07
VC0103	0.07	0.08	0.06	0.04
VC0104	0.05	0.05	0.04	0.03
VC0105	0.05	0.04	0.05	0.02
VC0106	0.06	0.07	0.09	0.08
VC0107	0.04	0.05	0.05	0.05
VC0108	0.02	0.03	0.03	0.02
VC0109	0.02	0.06	0.04	0.05
VC0110	0.05	0.08	0.04	0.04
VC0111	0.09	0.10	0.06	0.06
VC0112	0.09	0.11	0.07	0.07
VC0113	0.12	0.10	0.09	0.09
VC0114	0.09	0.08	0.07	0.06
VC0115	0.12	0.12	0.07	0.08
VC0116	0.04	0.05	0.02	0.03
VC0117	0.13	0.14	0.06	0.06
VC0118	0.05	0.05	0.03	0.04
VC0119	0.09	0.09	0.02	0.03
VC0120	0.06	0.08	0.00	0.04
VC0121	0.08	0.07	0.04	0.04
VC0123	0.07	0.07	0.04	0.03
VC0124	0.09	0.11	0.05	0.04

VC0125	0.07	0.08	0.05	0.06
VC0126	0.09	0.08	0.03	0.03
VC0127	0.09	0.10	0.04	0.04
VC0128	0.09	0.09	0.04	0.04
VC0129	0.07	0.07	0.06	0.04
VC0130	0.00	0.01	0.01	0.02
VC0131	0.11	0.12	0.07	0.06
VC0132	0.09	0.08	0.06	0.06
VC0133	0.05	0.05	0.04	0.04
VC0133	0.06	0.06	0.04	0.05
VC0134	0.06	0.05	0.04	0.04
VC0135	0.05	0.06	0.07	0.06
VC0136	0.06	0.06	0.03	0.04
VC0137	0.01	0.03	0.00	-0.01
VC0138	0.05	0.06	0.06	0.07
VC0139	0.11	0.11	0.07	0.07
VC0140	0.11	0.12	0.06	0.06
VC0141	0.03	0.06	0.04	0.08
VC0142	0.07	0.05	0.03	0.03
VC0143	0.01	0.02	0.00	0.01
VC0144	0.08	0.08	0.07	0.07
VC0145	0.02	0.04	0.05	0.05
VC0146	0.03	0.03	0.02	0.03
VC0147	0.05	0.06	0.03	0.04
VC0148	0.01	0.02	0.00	0.00
VC0149	0.02	0.03	0.01	0.01
VC0150	0.08	0.06	0.05	0.07
VC0151	0.02	0.02	0.01	0.01
VC0152	0.07	0.06	0.04	0.04
VC0153	0.02	0.02	0.01	0.01
VC0154	0.02	0.00	0.00	0.00
VC0156	0.04	0.05	-0.02	-0.02
VC0157	0.03	0.04	0.05	0.03
VC0158	0.06	0.10	0.06	0.06
VC0159	0.02	0.03	0.01	0.02
VC0160	0.07	0.07	0.04	0.05
VC0161	0.03	0.03	0.04	0.03
VC0162	0.09	0.09	0.05	0.08
VC0163	0.05	0.13	0.06	0.06
VC0164	0.05	0.06	0.04	0.03
VC0165	0.02	0.03	0.00	0.00
VC0166	0.02	0.02	0.01	0.02
VC0167	0.03	0.05	0.03	0.03

VC0168	0.05	0.04	0.07	0.07
VC0169	0.07	0.07	0.02	0.03
VC0170	0.08	0.10	0.04	0.08
VC0171	0.03	0.05	0.03	0.03
VC0172	0.09	0.08	0.02	0.03
VC0173	0.04	0.04	0.00	0.02
VC0174	0.02	0.02	0.01	0.02
VC0175	0.04	0.05	0.04	0.04
VC0176	0.11	0.08	0.03	0.05
VC0177	0.03	0.04	0.02	0.02
VC0178	0.03	0.03	0.01	0.02
VC0179	0.04	0.03	0.04	0.04
VC0180	0.07	0.08	0.07	0.05
VC0181	0.01	0.02	0.01	0.02
VC0182	0.01	0.02	0.02	0.03
VC0183	0.03	0.03	0.05	0.05
VC0184	0.08	0.09	0.05	0.05
VC0185	0.02	0.02	0.01	0.01
VC0186	0.07	0.07	0.05	0.06
VC0187	0.01	0.02	0.01	0.02
VC0188	0.06	0.07	0.03	0.03
VC0189	0.05	0.05	0.03	0.03
VC0189	0.04	0.05	0.03	0.04
VC0190	0.01	0.02	0.08	0.08
VC0191	0.06	0.06	0.04	0.04
VC0192	0.01	0.02	0.01	0.01
VC0193	0.08	0.09	0.05	0.08
VC0194	0.09	0.08	0.08	0.12
VC0195	0.04	0.05	0.01	0.01
VC0196	0.08	0.06	0.08	0.07
VC0197	0.05	0.05	0.01	0.01
VC0198	0.01	0.02	-0.01	0.00
VC0199	0.09	0.09	0.14	0.10
VC0200	0.01	0.01	0.02	0.02
VC0201	0.02	0.06	0.06	0.05
VC0202	0.08	0.10	0.04	0.03
VC0203	0.01	0.03	0.04	0.04
VC0204	0.00	0.00	0.10	0.06
VC0205	0.08	0.07	0.06	0.03
VC0206	0.01	0.02	0.16	0.13
VC0207	0.02	0.04	0.03	0.03
VC0208	0.01	0.03	0.03	0.02
VC0209	0.05	0.05	0.06	0.04

VC0210	0.00	0.02	0.11	0.10
VC0211	0.06	0.06	0.04	0.04
VC0212	0.01	0.00	0.12	0.09
VC0213	0.00	0.00	0.12	0.08
VC0214	0.06	0.05	0.07	0.02
VC0215	0.03	0.03	0.03	0.03
VC0216	0.04	0.06	0.04	0.02
VC0217	0.03	0.06	0.04	0.04
VC0218	0.06	0.04	0.04	0.03
VC0219	0.04	0.05	0.06	0.04
VC0220	0.05	0.05	0.02	0.02
VC0221	0.00	0.00	0.07	0.05
VC0222	0.06	0.06	0.06	0.04
VC0223	0.02	0.03	0.08	0.07
VC0224	0.01	0.02	0.09	0.06
VC0225	0.04	0.07	0.04	0.04
VC0226	0.07	0.10	0.04	0.04
VC0227	0.01	0.00	0.04	0.04
VC0228	0.06	0.06	0.07	0.05
VC0229	-0.01	0.00	0.08	0.06
VC0230	0.02	0.01	0.02	0.03
VC0231	0.06	0.06	0.06	0.06
VC0232	0.04	0.05	0.06	0.02
VC0233	0.00	0.03	0.07	0.06
VC0234	0.00	0.01	0.05	0.04
VC0235	0.05	0.10	0.04	0.04
VC0236	0.00	0.00	0.08	0.05
VC0237	-0.01	0.01	0.12	0.11
VC0238	0.01	0.01	0.09	0.06
VC0239	0.01	0.04	0.06	0.05
VC0240	0.10	0.08	0.02	0.02
VC0241	-0.01	0.00	0.12	0.11
VC0242	0.00	0.01	0.15	0.13
VC0243	0.02	0.04	0.03	0.03
VC0244	0.00	0.02	0.09	0.05
VC0245	0.01	0.03	0.04	0.04
VC0246	0.04	0.05	0.03	0.03
VC0247	0.02	0.02	0.07	0.06
VC0248	0.06	0.06	0.06	0.02
VC0249	0.01	0.02	0.05	0.04
VC0250	0.00	0.03	0.02	0.01
VC0251	0.03	0.04	0.05	0.05
VC0252	0.01	0.01	0.17	0.17

VC0253	0.06	0.06	0.03	0.04
VC0254	0.02	0.02	0.08	0.08
VC0254	0.01	0.02	0.05	0.05
VC0255	0.04	0.04	0.03	0.03
VC0256	0.01	0.01	0.09	0.07
VC0257	0.02	0.02	0.05	0.05
VC0258	0.01	0.00	0.02	0.03
VC0259	0.00	0.01	0.05	0.04
VC0260	0.04	0.06	0.07	0.06
VC0261	0.04	0.03	0.06	0.05
VC0262	0.00	0.02	0.03	0.02
VC0263	0.05	0.07	0.02	0.05
VC0264	0.09	0.08	0.05	0.07
VC0265	0.04	0.03	0.05	0.04
VC0266	0.03	0.06	0.04	0.07
VC0267	0.03	0.05	0.11	0.09
VC0268	0.07	0.04	0.02	0.07
VC0269	0.03	0.03	0.08	0.06
VC0270	0.08	0.04	0.08	0.09
VC0271	0.01	0.04	0.08	0.07
VC0272	0.09	0.07	0.07	0.03
VC0273	0.04	0.04	0.06	0.06
VC0274	0.05	0.04	0.07	0.09
VC0275	0.03	0.03	0.06	0.06
VC0276	0.08	0.09	0.06	0.06
VC0277	0.11	0.11	0.07	0.06
VC0278	0.07	0.04	0.04	0.03
VC0279	0.05	0.04	0.04	0.05
VC0280	0.03	0.03	0.05	0.04
VC0281	0.05	0.02	0.03	0.03
VC0282	0.06	0.06	0.08	0.06
VC0283	0.06	0.07	0.06	0.06
VC0284	0.05	0.04	0.05	0.06
VC0285	0.06	0.06	0.06	0.09
VC0286	0.03	0.03	0.01	0.03
VC0286	0.00	0.00	0.04	0.05
VC0287	0.02	0.02	0.04	0.04
VC0287	0.01	0.05	0.05	0.05
VC0288	0.06	0.07	0.04	0.07
VC0289	0.07	0.07	0.10	0.09
VC0290	0.07	0.07	0.08	0.13
VC0291	0.07	0.05	0.09	0.07
VC0292	0.07	0.06	0.02	0.03

VC0293	0.06	0.06	0.03	0.04
VC0294	0.08	0.10	0.10	0.11
VC0295	0.11	0.09	0.08	0.07
VC0297	0.10	0.08	0.07	0.04
VC0298	-0.01	0.03	0.07	0.06
VC0299	0.05	0.08	0.03	0.04
VC0300	0.07	0.07	0.04	0.04
VC0301	0.06	0.06	0.07	0.05
VC0302	0.06	0.06	0.03	0.05
VC0303	0.05	0.08	0.06	0.08
VC0304	0.03	0.02	0.11	0.07
VC0305	0.03	0.06	0.12	0.12
VC0306	0.05	0.05	0.04	0.06
VC0307	0.08	0.10	0.07	0.07
VC0308	0.02	0.06	0.04	0.03
VC0309	0.01	0.02	0.04	0.04
VC0311	0.03	0.04	0.04	0.05
VC0312	0.05	0.08	0.03	0.03
VC0313	0.05	0.05	0.06	0.06
VC0314	0.06	0.06	0.07	0.06
VC0316	0.05	0.06	0.02	0.03
VC0317	0.06	0.08	0.05	0.11
VC0318	0.03	0.04	0.07	0.07
VC0319	0.07	0.08	0.07	0.05
VC0320	0.04	0.03	0.04	0.04
VC0321	0.02	0.02	0.00	0.00
VC0322	0.05	0.07	0.05	0.04
VC0323	0.11	0.10	0.06	0.06
VC0324	0.03	0.03	0.01	0.02
VC0326	0.01	0.03	0.01	0.01
VC0327	0.10	0.06	0.05	0.07
VC0328	0.03	0.03	0.05	0.06
VC0329	0.06	0.07	0.06	0.04
VC0330	0.02	0.03	0.06	0.07
VC0331	0.04	0.04	0.09	0.08
VC0332	0.03	0.03	0.00	0.01
VC0333	0.04	0.04	0.08	0.07
VC0334	0.04	0.04	0.03	0.03
VC0335	0.08	0.08	0.05	0.05
VC0336	0.06	0.07	0.06	0.05
VC0337	0.05	0.04	0.03	0.01
VC0338	0.06	0.06	0.06	0.06
VC0339	0.02	0.03	0.04	0.04

VC0341	0.08	0.08	0.07	0.07
VC0342	0.06	0.06	0.03	0.04
VC0343	0.06	0.07	0.03	0.02
VC0344	0.06	0.05	0.01	0.02
VC0345	0.08	0.10	0.06	0.05
VC0346	0.04	0.06	0.05	0.05
VC0347	0.12	0.10	0.10	0.09
VC0348	0.02	0.02	0.06	0.07
VC0349	0.04	0.03	0.09	0.08
VC0350	0.05	0.05	0.03	0.03
VC0351	0.02	0.03	0.05	0.05
VC0352	0.06	0.04	0.03	0.03
VC0353	0.03	0.02	0.05	0.06
VC0354	0.01	0.01	0.02	0.02
VC0355	0.06	0.07	0.06	0.06
VC0356	0.07	0.07	0.06	0.05
VC0357	0.05	0.05	0.09	0.07
VC0358	0.04	0.05	0.04	0.07
VC0359	0.07	0.08	0.06	0.07
VC0360	0.06	0.06	0.10	0.10
VC0361	0.06	0.07	0.04	0.05
VC0362	0.01	0.02	0.00	0.00
VC0363	0.07	0.07	0.03	0.04
VC0364	0.07	0.06	0.03	0.03
VC0365	0.06	0.05	0.06	0.05
VC0366	0.07	0.10	0.03	0.04
VC0367	0.03	0.04	0.08	0.05
VC0368	0.06	0.07	0.03	0.03
VC0369	0.04	0.04	0.05	0.04
VC0370	0.03	0.04	0.04	0.04
VC0371	0.03	0.04	0.01	0.01
VC0372	0.03	0.02	0.04	0.04
VC0373	0.06	0.07	0.04	0.03
VC0374	0.05	0.06	0.11	0.10
VC0375	0.05	0.05	0.07	0.06
VC0376	0.07	0.07	0.03	0.04
VC0377	0.02	0.02	0.04	0.04
VC0378	0.06	0.07	0.06	0.04
VC0379	0.04	0.03	0.03	0.03
VC0380	0.09	0.09	0.05	0.03
VC0381	0.02	0.02	0.04	0.04
VC0382	0.05	0.06	0.06	0.06
VC0383	0.08	0.06	0.10	0.04

VC0384	0.04	0.04	0.07	0.03
VC0385	0.01	0.03	0.05	0.05
VC0386	0.07	0.08	0.07	0.05
VC0387	0.07	0.08	0.08	0.07
VC0388	0.07	0.06	0.06	0.08
VC0389	0.02	0.02	0.03	0.05
VC0390	0.04	0.06	0.02	0.02
VC0391	0.03	0.03	0.04	0.07
VC0392	0.03	0.05	0.06	0.07
VC0393	0.05	0.05	0.08	0.07
VC0394	0.08	0.06	0.12	0.09
VC0395	0.03	0.04	0.05	0.08
VC0396	0.06	0.09	0.08	0.08
VC0397	0.03	0.04	0.06	0.06
VC0399	0.00	0.01	0.04	0.03
VC0400	0.05	0.06	0.07	0.06
VC0401	0.01	0.02	0.07	0.06
VC0402	0.01	0.00	0.01	0.02
VC0403	0.03	0.01	0.03	0.02
VC0404	0.02	0.02	0.10	0.08
VC0405	0.17	0.19	0.23	0.24
VC0406	0.00	0.02	0.05	0.04
VC0407	0.03	0.02	0.05	0.05
VC0408	0.00	0.00	0.05	0.05
VC0409	0.05	0.05	0.01	0.03
VC0410	0.01	0.01	0.04	0.04
VC0411	0.01	0.01	0.01	0.03
VC0412	0.00	0.00	0.03	0.03
VC0413	0.05	0.04	0.04	0.04
VC0414	0.24	0.23	0.04	0.04
VC0415	0.01	0.02	0.01	0.01
VC0416	0.00	0.02	0.07	0.08
VC0417	0.06	0.05	0.03	0.02
VC0418	0.02	0.01	0.03	0.04
VC0419	-0.01	0.00	0.06	0.07
VC0420	0.04	0.03	0.01	0.04
VC0420	0.01	0.02	0.04	0.05
VC0421	0.02	0.04	0.05	0.07
VC0422	0.00	0.00	0.05	0.04
VC0423	0.02	0.03	0.06	0.03
VC0424	0.04	0.04	0.08	0.06
VC0425	0.01	0.01	0.04	0.05
VC0426	0.01	0.03	0.04	0.04

VC0427	0.05	0.06	0.03	0.03
VC0428	0.01	0.01	0.07	0.06
VC0429	0.04	0.04	0.05	0.06
VC0430	0.04	0.02	0.04	0.04
VC0431	0.03	0.02	0.05	0.07
VC0432	0.03	0.03	0.05	0.08
VC0433	0.00	0.02	0.10	0.12
VC0435	0.14	0.13	0.01	0.01
VC0436	0.04	0.05	0.03	0.04
VC0437	0.06	0.05	0.05	0.05
VC0439	0.04	0.05	0.07	0.08
VC0440	0.07	0.07	0.08	0.09
VC0441	0.03	0.04	0.05	0.04
VC0442	0.06	0.07	0.04	0.03
VC0443	0.03	0.04	0.07	0.06
VC0444	0.03	0.03	0.05	0.05
VC0445	0.03	0.03	0.07	0.07
VC0446	0.03	0.04	0.04	0.04
VC0447	0.03	0.02	0.02	0.02
VC0448	0.02	0.03	0.04	0.06
VC0449	0.04	0.04	0.06	0.05
VC0450	0.06	0.06	0.07	0.06
VC0451	0.07	0.08	0.06	0.04
VC0452	0.03	0.04	0.11	0.07
VC0453	0.02	0.02	0.12	0.10
VC0454	0.03	0.03	0.04	0.04
VC0455	0.05	0.05	0.06	0.05
VC0456	0.03	0.04	0.13	0.12
VC0457	0.03	0.03	0.09	0.07
VC0458	0.02	0.02	0.05	0.05
VC0458	0.00	0.05	0.04	0.03
VC0459	0.03	0.02	0.14	0.13
VC0460	0.04	0.04	0.05	0.05
VC0461	0.05	0.06	0.07	0.06
VC0462	0.03	0.04	0.08	0.08
VC0463	0.02	0.02	0.05	0.04
VC0464	0.07	0.06	0.06	0.07
VC0465	0.02	0.05	0.07	0.07
VC0466	0.03	0.04	0.07	0.08
VC0467	0.02	0.02	0.03	0.03
VC0468	0.00	0.00	0.07	0.05
VC0469	0.06	0.06	0.08	0.07
VC0470	0.02	0.02	0.03	0.02

VC0471	0.02	0.02	0.07	0.09
VC0472	0.02	0.02	0.01	0.01
VC0473	0.04	0.05	0.03	0.04
VC0474	0.02	0.02	0.06	0.06
VC0475	0.01	0.00	0.02	0.02
VC0476	0.01	0.03	0.03	0.08
VC0477	0.02	0.03	0.04	0.03
VC0477	0.01	0.02	0.03	0.04
VC0478	0.02	0.04	0.05	0.06
VC0479	0.03	0.04	0.04	0.03
VC0480	0.00	0.01	0.01	0.02
VC0481	0.04	0.04	0.03	0.02
VC0482	0.05	0.05	0.05	0.05
VC0483	0.02	0.02	0.04	0.09
VC0484	0.04	0.03	0.05	0.05
VC0485	0.02	0.01	0.05	0.06
VC0486	0.05	0.07	0.07	0.06
VC0487	0.09	0.12	0.03	0.05
VC0488	0.01	0.03	0.05	0.07
VC0489	0.06	0.07	0.02	0.03
VC0490	0.03	0.02	0.05	0.05
VC0491	0.05	0.05	0.03	0.03
VC0492	0.02	0.02	0.04	0.05
VC0492	0.01	0.01	0.04	0.04
VC0493	0.04	0.05	0.04	0.05
VC0494	0.02	0.02	0.08	0.08
VC0495	0.02	0.02	0.06	0.05
VC0496	0.02	0.03	0.05	0.05
VC0497	0.04	0.05	0.04	0.05
VC0498	0.07	0.06	0.05	0.05
VC0499	0.03	0.04	0.07	0.09
VC0500	0.04	0.06	0.04	0.05
VC0501	0.03	0.04	0.06	0.06
VC0502	0.03	0.03	0.09	0.04
VC0503	0.02	0.02	0.02	0.02
VC0504	0.02	0.06	0.03	0.05
VC0505	0.06	0.06	0.06	0.06
VC0506	0.08	0.08	0.06	0.04
VC0507	0.07	0.08	0.01	0.03
VC0508	0.05	0.06	0.09	0.08
VC0509	0.05	0.06	0.08	0.07
VC0510	0.00	0.01	0.07	0.04
VC0511	0.05	0.05	0.05	0.04

VC0512	0.04	0.05	0.08	0.05
VC0513	0.01	0.01	0.09	0.08
VC0514	0.04	0.03	0.05	0.07
VC0515	0.01	0.01	0.02	0.02
VC0516	0.01	0.03	0.06	0.06
VC0517	0.07	0.05	0.04	0.06
VC0518	0.02	0.04	0.04	0.05
VC0519	0.05	0.06	0.08	0.09
VC0520	0.05	0.06	0.04	0.05
VC0521	0.09	0.07	0.06	0.06
VC0522	0.05	0.07	0.04	0.03
VC0523	-0.01	0.00	0.07	0.06
VC0524	0.05	0.06	0.09	0.10
VC0525	0.00	0.01	0.10	0.08
VC0526	0.03	0.03	0.04	0.05
VC0527	0.06	0.05	0.01	0.02
VC0528	-0.01	-0.01	0.12	0.13
VC0529	0.02	0.02	0.06	0.05
VC0530	0.06	0.07	0.06	0.04
VC0531	0.06	0.05	0.04	0.03
VC0532	0.00	0.00	0.09	0.10
VC0533	0.02	0.03	0.02	0.01
VC0534	0.00	0.00	0.08	0.07
VC0535	0.05	0.05	0.07	0.05
VC0536	0.05	0.05	0.06	0.07
VC0537	-0.01	-0.01	0.07	0.06
VC0538	0.06	0.05	0.06	0.05
VC0539	-0.01	0.03	0.04	0.04
VC0540	0.03	0.03	0.03	0.03
VC0541	0.02	0.02	0.03	0.06
VC0542	0.06	0.05	0.07	0.06
VC0543	0.04	0.03	0.07	0.07
VC0544	0.04	0.04	0.06	0.05
VC0545	0.10	0.10	0.06	0.06
VC0546	0.05	0.06	0.03	0.02
VC0547	0.03	0.04	0.05	0.05
VC0548	0.11	0.06	0.06	0.03
VC0549	0.06	0.06	0.02	0.02
VC0550	0.02	0.01	0.06	0.05
VC0551	0.01	0.03	0.02	0.02
VC0552	0.02	0.06	0.03	0.04
VC0553	0.04	0.04	0.07	0.06
VC0554	0.07	0.05	0.08	0.10

VC0555	0.03	0.03	0.02	0.02
VC0556	0.04	0.05	0.07	0.05
VC0557	0.04	0.04	0.06	0.08
VC0558	0.03	0.02	0.04	0.18
VC0559	0.00	0.01	0.03	0.03
VC0560	0.07	0.05	0.07	0.07
VC0561	0.03	0.03	0.02	0.03
VC0562	0.04	0.03	0.06	0.07
VC0563	0.03	0.04	0.07	0.07
VC0564	0.04	0.10	0.04	0.05
VC0565	0.02	0.05	0.04	0.04
VC0567	0.05	0.04	0.05	0.22
VC0568	0.05	0.05	0.05	0.04
VC0569	0.07	0.07	0.04	0.03
VC0570	0.06	0.07	0.07	0.03
VC0571	0.10	0.10	0.05	0.04
VC0572	0.08	0.08	0.01	0.02
VC0573	0.02	0.02	0.03	0.04
VC0574	0.08	0.07	0.03	0.03
VC0575	0.00	0.02	0.05	0.16
VC0576	0.08	0.06	0.04	0.02
VC0577	0.00	0.01	0.01	0.05
VC0578	0.03	0.03	0.01	0.01
VC0579	0.05	0.06	0.03	0.04
VC0580	0.07	0.07	0.08	0.05
VC0581	0.04	0.04	0.05	0.04
VC0582	0.02	0.03	0.03	0.04
VC0583	0.09	0.07	0.02	0.03
VC0584	0.05	0.06	0.05	0.04
VC0585	0.07	0.06	0.05	0.06
VC0586	0.07	0.06	0.01	0.02
VC0587	0.04	0.04	0.03	0.07
VC0588	0.07	0.06	0.04	0.05
VC0589	0.04	0.04	0.04	0.07
VC0590	0.04	0.05	0.03	0.04
VC0591	0.03	0.04	0.03	0.07
VC0592	0.01	0.01	0.08	0.05
VC0593	0.03	0.05	0.08	0.08
VC0596	0.07	0.07	0.08	0.06
VC0597	0.03	0.04	0.05	0.06
VC0598	0.04	0.04	0.03	0.04
VC0599	0.07	0.06	0.04	0.05
VC0600	0.06	0.08	0.03	0.03

VC0601	0.01	0.01	0.05	0.04
VC0602	0.01	0.02	0.04	0.04
VC0603	0.02	0.02	0.04	0.02
VC0604	0.03	0.04	0.05	0.06
VC0605	0.09	0.08	0.05	0.07
VC0606	0.07	0.07	0.05	0.04
VC0607	0.03	0.04	0.00	0.04
VC0607	0.01	0.00	0.07	0.07
VC0609	0.02	0.04	0.02	0.02
VC0610	0.02	0.02	0.04	0.04
VC0611	0.02	0.03	0.02	0.05
VC0611	0.01	0.02	0.05	0.05
VC0612	0.00	0.01	0.03	0.04
VC0613	0.05	0.07	0.03	0.06
VC0614	0.04	0.03	0.12	0.12
VC0615	0.02	0.02	0.04	0.06
VC0615	-0.01	0.07	0.06	0.05
VC0616	0.02	0.01	0.04	0.06
VC0617	0.00	0.03	0.04	0.05
VC0619	0.03	0.04	0.06	0.04
VC0620	0.02	0.03	0.02	0.04
VC0620	0.01	0.04	0.03	0.04
VC0621	0.07	0.08	0.06	0.05
VC0622	0.02	0.03	0.04	0.04
VC0623	0.03	0.03	0.05	0.04
VC0624	0.06	0.05	0.10	0.10
VC0625	0.04	0.07	0.05	0.05
VC0626	0.08	0.06	0.07	0.06
VC0627	0.05	0.06	0.05	0.05
VC0628	0.05	0.09	0.05	0.05
VC0629	0.02	0.04	0.04	0.04
VC0630	0.08	0.06	0.07	0.06
VC0631	0.07	0.05	0.11	0.08
VC0632	0.03	0.03	0.05	0.05
VC0633	0.06	0.05	0.09	0.06
VC0634	0.07	0.16	0.08	0.10
VC0635	0.06	0.05	0.12	0.11
VC0636	0.06	0.07	0.09	0.08
VC0637	0.10	0.08	0.06	0.09
VC0638	0.03	0.04	0.08	0.04
VC0639	0.06	0.06	0.08	0.09
VC0640	0.06	0.05	0.09	0.06
VC0641	0.08	0.09	0.05	0.05

VC0642	0.04	0.05	0.01	0.01
VC0643	0.10	0.10	0.04	0.06
VC0644	0.01	0.02	0.01	0.02
VC0645	0.08	0.06	0.16	0.20
VC0646	0.08	0.06	0.03	0.04
VC0647	0.08	0.08	0.05	0.06
VC0648	0.04	0.04	0.08	0.07
VC0649	0.05	0.04	0.06	0.05
VC0650	0.04	0.05	0.06	0.06
VC0651	0.05	0.04	0.08	0.07
VC0652	0.07	0.06	0.07	0.07
VC0653	-0.02	-0.01	-0.01	-0.01
VC0654	0.04	0.06	0.07	0.06
VC0655	0.03	0.03	0.01	0.02
VC0656	0.03	0.03	0.07	0.05
VC0657	0.06	0.06	0.06	0.05
VC0658	0.60	0.64	0.58	0.54
VC0659	0.06	0.05	0.05	0.06
VC0660	0.04	0.05	0.03	0.03
VC0661	0.07	0.07	0.14	0.13
VC0662	0.04	0.05	0.12	0.15
VC0663	0.07	0.06	0.09	0.10
VC0664	0.04	0.03	0.06	0.06
VC0665	0.12	0.13	0.15	0.13
VC0666	0.04	0.04	0.07	0.09
VC0667	0.03	0.03	0.03	0.04
VC0668	0.06	0.06	0.08	0.08
VC0669	0.06	0.06	0.05	0.04
VC0670	0.08	0.08	0.01	0.03
VC0671	0.04	0.05	0.05	0.05
VC0672	0.02	0.02	0.03	0.04
VC0673	0.04	0.04	0.06	0.07
VC0674	0.05	0.05	0.09	0.09
VC0675	0.01	0.01	0.00	0.01
VC0676	0.08	0.09	0.05	0.08
VC0677	0.06	0.06	0.09	0.08
VC0678	0.02	0.04	0.07	0.07
VC0679	0.03	0.06	0.05	0.04
VC0680	0.04	0.03	0.06	0.05
VC0681	0.01	0.01	0.00	0.01
VC0682	0.11	0.14	0.03	0.08
VC0683	0.05	0.04	0.08	0.07
VC0684	0.04	0.04	0.10	0.09

VC0685	0.04	0.05	0.09	0.07
VC0686	0.07	0.09	0.05	0.06
VC0687	0.04	0.05	0.05	0.06
VC0688	0.05	0.04	0.06	0.06
VC0689	0.08	0.07	0.04	0.03
VC0690	0.08	0.07	0.13	0.08
VC0691	0.05	0.06	0.08	0.07
VC0692	0.03	0.07	0.13	0.09
VC0693	0.09	0.08	0.04	0.04
VC0694	0.05	0.09	0.03	0.05
VC0695	0.06	0.06	0.12	0.09
VC0696	0.07	0.05	0.16	0.14
VC0697	0.04	0.04	0.07	0.06
VC0698	0.07	0.09	0.03	0.09
VC0699	0.09	0.14	0.09	0.07
VC0700	0.06	0.05	0.03	0.05
VC0701	0.08	0.07	0.10	0.11
VC0702	0.03	0.04	0.02	0.03
VC0703	0.07	0.07	0.15	0.14
VC0703	0.00	0.04	0.04	0.03
VC0704	0.02	0.02	0.05	0.05
VC0705	0.04	0.04	0.05	0.05
VC0706	0.03	0.04	0.04	0.04
VC0707	0.06	0.07	0.03	0.03
VC0708	0.04	0.03	0.07	0.05
VC0709	0.07	0.06	0.05	0.06
VC0710	0.05	0.04	0.08	0.06
VC0711	0.05	0.07	0.03	0.03
VC0712	0.05	0.06	0.06	0.06
VC0713	0.03	0.03	0.07	0.05
VC0714	0.02	0.00	0.00	0.02
VC0715	0.06	0.07	0.04	0.06
VC0716	0.02	0.02	0.00	0.01
VC0717	0.04	0.04	0.02	0.02
VC0718	0.04	0.05	0.06	0.06
VC0719	0.09	0.08	0.03	0.05
VC0720	0.02	0.02	0.01	0.02
VC0721	0.02	0.02	0.04	0.01
VC0722	0.07	0.05	0.05	0.04
VC0723	0.03	0.02	0.06	0.06
VC0724	0.01	0.01	0.07	0.07
VC0725	-0.03	0.01	0.09	0.07
VC0726	0.08	0.08	0.06	0.06

VC0727	0.05	0.07	0.06	0.06
VC0728	0.02	0.03	0.04	0.04
VC0729	0.07	0.07	0.04	0.04
VC0729	0.06	0.06	0.04	0.04
VC0730	0.13	0.10	0.06	0.06
VC0731	0.17	0.14	0.02	0.04
VC0732	0.09	0.08	0.04	0.05
VC0733	0.05	0.05	0.03	0.03
VC0734	0.00	0.02	0.06	0.04
VC0735	0.06	0.08	0.07	0.08
VC0736	0.17	0.17	0.04	0.02
VC0737	0.08	0.09	0.05	0.06
VC0738	0.06	0.08	0.08	0.08
VC0738	0.07	0.09	0.06	0.06
VC0739	0.15	0.13	0.03	0.03
VC0740	0.05	0.05	0.06	0.06
VC0741	0.03	0.05	0.05	0.05
VC0742	0.11	0.10	0.07	0.06
VC0743	0.04	0.06	0.03	0.04
VC0744	0.03	0.03	0.01	0.02
VC0745	0.15	0.11	0.01	0.00
VC0746	0.13	0.12	0.02	0.01
VC0747	0.09	0.08	0.01	0.02
VC0748	0.15	0.14	0.02	0.01
VC0749	0.10	0.09	0.00	0.01
VC0750	0.08	0.05	0.06	0.06
VC0751	0.07	0.07	0.03	0.04
VC0752	0.07	0.08	0.05	0.05
VC0753	0.10	0.10	0.01	0.04
VC0754	0.09	0.08	0.05	0.05
VC0755	0.11	0.09	0.04	0.04
VC0756	0.05	0.05	0.02	0.03
VC0757	0.14	0.15	0.03	0.03
VC0758	0.07	0.04	0.03	0.02
VC0759	0.09	0.07	0.00	0.00
VC0760	0.04	0.05	0.09	0.09
VC0761	0.12	0.09	0.01	0.00
VC0762	0.10	0.07	0.05	0.05
VC0763	0.00	0.02	0.01	0.01
VC0764	0.02	0.03	0.04	0.05
VC0765	0.13	0.11	0.03	0.01
VC0766	0.05	0.06	0.08	0.06
VC0767	-0.01	0.02	0.05	0.05

VC0768	0.01	0.01	0.07	0.05
VC0769	0.01	0.02	0.04	0.04
VC0770	0.07	0.10	0.01	0.00
VC0771	0.02	0.02	0.06	0.01
VC0772	-0.03	-0.03	0.07	0.06
VC0773	0.06	0.06	0.07	0.06
VC0774	0.06	0.08	0.03	0.04
VC0775	0.13	0.14	0.00	0.01
VC0776	0.02	0.03	0.07	0.02
VC0777	0.11	0.10	0.01	0.02
VC0778	0.12	0.11	0.02	-0.01
VC0779	0.03	0.04	0.05	0.05
VC0780	0.13	0.11	0.00	0.01
VC0781	0.12	0.11	0.00	0.01
VC0782	0.05	0.05	0.10	0.07
VC0783	0.06	0.05	0.07	0.06
VC0784	0.10	0.11	0.03	0.03
VC0785	0.05	0.05	0.04	0.05
VC0786	0.06	0.06	0.06	0.09
VC0787	0.03	0.04	0.06	0.06
VC0788	0.05	0.04	0.04	0.04
VC0788	0.02	0.01	0.03	0.04
VC0789	0.06	0.05	0.08	0.05
VC0790	0.05	0.03	0.09	0.07
VC0791	0.08	0.09	0.04	0.04
VC0792	0.02	0.03	0.08	0.08
VC0793	0.01	0.14	0.02	0.03
VC0793m	0.04	0.04	0.06	0.06
VC0794	0.10	0.11	0.01	0.02
VC0795	0.03	0.05	0.04	0.05
VC0796	0.05	0.06	0.06	0.07
VC0797	0.07	0.06	0.07	0.06
VC0798	0.05	0.04	0.03	0.04
VC0799	0.02	0.02	0.04	0.04
VC0800	0.08	0.07	0.12	0.12
VC0801	0.05	0.04	0.08	0.06
VC0802	0.05	0.05	0.07	0.06
VC0803	0.03	0.02	0.03	0.04
VC0805	0.02	0.02	0.04	0.05
VC0806	0.06	0.04	0.05	0.04
VC0807	0.02	0.02	0.10	0.06
VC0808	0.03	0.03	0.05	0.06
VC0809	0.04	0.05	0.06	0.04

VC0810	0.05	0.03	0.10	0.08
VC0811	0.05	0.05	0.07	0.07
VC0812	0.03	0.04	0.08	0.08
VC0813	0.06	0.07	0.06	0.06
VC0814	0.02	0.02	0.15	0.11
VC0815	0.22	0.24	0.01	0.01
VC0816	0.09	0.08	0.04	0.03
VC0817	0.03	0.06	0.08	0.07
VC0818	0.07	0.06	0.05	0.05
VC0819	0.02	0.02	0.07	0.06
VC0820	0.03	0.03	0.01	0.01
VC0821	0.02	0.04	0.05	0.04
VC0822	0.01	0.02	0.06	0.07
VC0823	0.02	0.02	0.05	0.05
VC0824	0.02	0.02	0.03	0.04
VC0824	0.01	0.02	0.06	0.05
VC0825	0.05	0.05	0.06	0.06
VC0826	0.04	0.05	0.06	0.05
VC0827	0.02	0.02	0.07	0.07
VC0827	0.01	-0.02	0.05	0.07
VC0828	0.01	0.01	0.04	0.03
VC0829	0.08	0.06	0.03	0.04
VC0830	0.06	0.07	0.07	-0.07
VC0831	0.05	0.05	0.06	0.04
VC0832	0.01	0.02	0.04	0.04
VC0833	0.04	0.05	0.07	0.07
VC0834	0.01	0.02	0.06	0.08
VC0835	0.06	0.06	0.07	0.06
VC0836	0.03	0.04	0.03	0.05
VC0837	0.04	0.06	0.11	0.12
VC0838	0.03	0.04	0.03	0.03
VC0839	0.03	0.04	0.05	0.04
VC0840	0.01	0.04	0.06	0.04
VC0841	0.01	0.01	0.01	0.02
VC0842	0.01	0.02	0.05	0.08
VC0843	0.02	0.03	0.04	0.04
VC0846	0.01	0.02	0.07	0.09
VC0847	0.05	0.05	0.05	0.04
VC0848	0.01	0.01	0.08	0.09
VC0849	-0.01	0.01	0.02	0.04
VC0850	0.07	0.06	0.06	0.10
VC0851	0.02	0.05	0.04	0.06
VC0852	0.06	0.07	0.11	0.13

VC0853	0.05	0.06	0.07	0.07
VC0854	0.08	0.07	0.04	0.05
VC0855	0.04	0.04	0.10	0.08
VC0856	0.03	0.06	0.04	0.04
VC0857	0.06	0.07	0.05	0.04
VC0858	0.03	0.02	0.05	0.04
VC0859	0.03	0.04	0.06	0.05
VC0860	0.04	0.04	0.04	0.04
VC0861	0.04	0.10	0.08	0.07
VC0862	0.05	0.05	0.10	0.06
VC0863	0.03	0.03	0.08	0.05
VC0864	0.05	0.07	0.07	0.08
VC0865	0.06	0.07	0.03	0.03
VC0866	0.00	0.00	0.03	0.02
VC0867	0.05	0.05	0.02	0.02
VC0868	0.04	0.03	0.06	0.06
VC0869	0.07	0.08	0.09	0.07
VC0870	0.01	0.03	0.05	0.04
VC0871	0.10	0.09	0.04	0.03
VC0872	0.08	0.08	0.03	0.03
VC0873	0.02	0.03	0.06	0.08
VC0874	0.03	0.03	0.07	0.04
VC0875	0.06	0.06	0.01	0.03
VC0876	0.02	0.02	0.07	0.10
VC0877	0.10	0.09	0.04	0.05
VC0878	0.07	0.08	0.06	0.08
VC0879	0.07	0.07	0.03	0.03
VC0880	0.04	0.03	0.04	0.05
VC0881	0.03	0.03	0.08	0.06
VC0882	0.06	0.06	0.02	0.03
VC0883	0.04	0.04	0.04	0.04
VC0884	0.01	0.02	0.02	0.04
VC0885	0.05	0.05	0.02	0.02
VC0886	0.04	0.01	0.03	0.05
VC0887	0.04	0.02	0.03	0.04
VC0888	0.09	0.06	0.05	0.07
VC0889	0.03	0.04	0.05	0.04
VC0890	0.03	0.04	0.01	0.01
VC0891	0.05	0.06	0.04	0.05
VC0892	0.03	0.03	0.05	0.03
VC0893	0.04	0.04	0.03	0.04
VC0894	0.01	0.02	0.07	0.06
VC0895	0.02	0.04	0.05	0.05

VC0897	0.03	0.03	0.12	0.09
VC0898	0.07	0.08	0.06	0.07
VC0899	0.00	0.02	0.11	0.08
VC0900	0.04	0.04	0.04	0.04
VC0901	0.06	0.06	0.06	0.08
VC0902	0.05	0.04	0.07	0.05
VC0903	0.14	0.06	0.01	0.03
VC0904	0.02	0.01	0.10	0.08
VC0905	0.04	0.04	0.09	0.09
VC0906	0.02	0.02	0.15	0.14
VC0907	0.06	0.07	0.05	0.05
VC0908	0.04	0.06	0.05	0.03
VC0909	0.03	0.02	0.04	0.06
VC0910	0.02	0.02	0.11	0.16
VC0911	0.08	0.09	0.05	0.04
VC0912	0.02	0.04	0.04	0.05
VC0914	0.04	0.05	0.06	0.05
VC0915	0.05	0.05	0.06	0.04
VC0916	0.05	0.05	0.05	0.05
VC0917	0.04	0.04	0.06	0.06
VC0918	0.05	0.06	0.11	0.12
VC0919	0.07	0.08	0.04	0.03
VC0920	0.03	0.03	0.14	0.12
VC0921	0.04	0.05	0.18	0.16
VC0922	0.02	0.01	0.03	0.08
VC0923	0.04	0.05	0.00	0.04
VC0924	0.04	0.01	0.03	0.04
VC0925	0.05	0.06	0.04	0.04
VC0926	0.01	0.03	0.04	0.03
VC0927	0.02	0.01	0.04	0.03
VC0928	0.03	0.05	0.05	0.03
VC0929	0.04	0.02	0.03	0.03
VC0930	0.06	0.05	0.06	0.06
VC0931	0.01	0.02	0.04	0.04
VC0932	0.01	0.01	0.03	0.04
VC0932	0.01	0.02	0.03	0.02
VC0934	0.03	0.01	0.05	0.05
VC0935	0.02	0.03	0.03	0.05
VC0936	0.03	0.04	0.02	0.03
VC0937	0.02	0.04	0.07	0.06
VC0938	0.01	0.00	0.07	0.05
VC0939	0.06	0.05	0.01	0.02
VC0940	0.06	0.06	0.01	0.01

VC0941	0.05	0.06	0.03	0.03
VC0943	0.02	0.01	0.03	0.02
VC0944	0.04	0.05	0.09	0.09
VC0945	0.04	0.06	0.05	0.05
VC0946	0.05	0.05	0.05	0.05
VC0947	0.00	0.00	0.10	0.08
VC0948	0.03	0.03	0.10	0.09
VC0949	0.02	0.05	0.03	0.03
VC0950	0.03	0.03	0.03	0.03
VC0951	0.04	0.04	0.08	0.07
VC0952	0.03	0.01	0.11	0.10
VC0953	0.00	0.01	0.00	0.01
VC0954	0.03	0.04	0.03	0.03
VC0955	0.02	0.02	0.04	0.06
VC0957	0.07	0.06	0.04	0.07
VC0958	0.00	0.04	0.02	0.02
VC0959	0.03	0.02	0.08	0.06
VC0960	0.04	0.05	0.06	0.07
VC0961	0.05	0.06	0.05	0.05
VC0962	0.04	0.04	0.07	0.06
VC0963	0.04	0.05	0.06	0.06
VC0964	0.07	0.05	0.08	0.06
VC0965	0.07	0.07	0.06	0.05
VC0966	0.04	0.05	0.07	0.05
VC0967	-0.01	0.00	0.09	0.06
VC0968	0.00	0.02	0.06	0.05
VC0969	0.01	0.01	0.08	0.07
VC0970	-0.01	0.04	0.05	0.04
VC0972	-0.01	-0.01	0.09	0.03
VC0973	0.04	0.03	0.05	0.05
VC0974	0.07	0.05	0.05	0.05
VC0975	0.05	0.11	0.05	0.08
VC0976	-0.01	-0.01	0.07	0.04
VC0977	0.00	0.01	0.04	0.04
VC0978	0.05	0.06	0.05	0.04
VC0979	0.04	0.03	0.04	0.04
VC0980	0.00	0.00	0.07	0.07
VC0981	0.00	0.01	0.09	0.09
VC0982	0.05	0.04	0.08	0.06
VC0983	-0.01	-0.01	0.04	0.04
VC0984	0.01	0.03	0.05	0.05
VC0985	0.03	0.04	0.10	0.09
VC0986	0.05	0.07	0.06	0.08

VC0987	0.04	0.04	0.06	0.04
VC0988	0.00	0.00	0.06	0.05
VC0989	0.04	0.05	0.03	0.03
VC0990	0.00	-0.01	0.09	0.06
VC0991	0.01	0.00	0.08	0.08
VC0992	0.00	0.01	0.07	0.07
VC0993	-0.01	-0.01	0.06	0.06
VC0994	-0.02	-0.01	0.07	0.06
VC0995	0.13	0.10	0.05	0.07
VC0996	0.05	0.02	0.02	0.01
VC0997	0.06	0.09	0.04	0.05
VC0998	0.00	0.04	0.03	0.04
VC0999	0.05	0.04	0.06	0.05
VC1000	0.05	0.06	0.04	0.06
VC1001	0.04	0.04	0.06	0.07
VC1002	0.03	0.04	0.04	0.04
VC1003	0.02	0.03	0.06	0.05
VC1004	0.02	0.04	0.04	0.05
VC1005	0.03	0.03	0.05	0.05
VC1006	0.00	0.01	0.00	0.00
VC1007	0.03	0.05	0.06	0.05
VC1008	0.02	0.13	0.05	0.05
VC1009	0.04	0.05	0.05	0.04
VC1010	0.03	0.03	0.05	0.10
VC1011	0.00	0.03	0.06	0.05
VC1012	0.04	0.03	0.05	0.05
VC1013	0.08	0.02	0.02	0.04
VC1014	0.02	0.01	-0.01	-0.01
VC1015	0.05	0.07	-0.03	-0.01
VC1016	0.02	0.02	0.04	0.03
VC1017	0.04	0.03	0.04	0.05
VC1018	0.04	0.04	0.02	0.02
VC1020	0.10	0.07	0.05	0.07
VC1021	0.03	0.02	0.05	0.05
VC1022	-0.02	-0.02	0.06	0.01
VC1023	0.03	0.04	0.09	0.08
VC1024	0.01	0.03	0.02	0.02
VC1025	0.04	0.05	0.02	0.03
VC1026	0.09	0.09	0.02	0.05
VC1027	0.06	0.06	0.04	0.06
VC1028	0.02	0.03	0.04	0.04
VC1029	0.00	-0.01	-0.02	-0.01
VC1030	0.07	0.06	0.04	0.03

VC1031	0.04	0.06	0.03	0.03
VC1032	0.06	0.08	0.05	0.02
VC1033	0.03	0.04	0.03	0.01
VC1034	0.03	0.03	0.04	0.06
VC1035	0.07	0.05	0.04	0.04
VC1037	0.05	0.06	0.06	0.05
VC1038	0.09	0.07	0.07	0.09
VC1039	0.02	0.04	0.01	0.01
VC1040	0.04	0.04	0.06	0.05
VC1041	0.03	0.04	0.02	0.03
VC1043	0.04	0.03	0.04	0.04
VC1044	0.03	0.04	0.04	0.02
VC1045	0.03	0.03	-0.01	-0.01
VC1046	0.07	0.06	0.04	0.05
VC1047	0.03	0.03	0.06	0.04
VC1048	0.04	0.05	0.04	0.03
VC1049	0.06	0.06	0.07	0.07
VC1050	0.02	0.03	0.04	0.06
VC1051	0.08	0.07	0.03	0.05
VC1052	0.05	0.06	0.03	0.03
VC1053	0.09	0.08	0.03	0.05
VC1054	0.08	0.08	0.03	0.06
VC1055	0.13	0.14	0.07	0.09
VC1056	0.04	0.05	0.04	0.03
VC1057	0.05	0.05	0.04	0.05
VC1058	0.06	0.07	0.04	0.07
VC1059	0.05	0.05	0.04	0.03
VC1060	0.02	0.02	0.05	0.06
VC1061	0.01	0.01	0.06	0.06
VC1062	0.05	0.06	0.08	0.04
VC1063	0.08	0.11	0.08	0.07
VC1064	0.08	0.08	0.04	0.04
VC1065	0.10	0.09	0.03	0.02
VC1066	0.08	0.07	0.04	0.04
VC1067	0.02	0.01	-0.02	-0.02
VC1068	0.08	0.07	0.06	0.04
VC1069	0.02	0.04	0.05	0.05
VC1070	0.13	0.09	0.03	0.10
VC1071	0.06	0.08	0.04	0.06
VC1072	0.06	0.06	0.11	0.14
VC1074	0.07	0.05	0.07	0.06
VC1075	0.09	0.08	0.07	0.06
VC1077	0.06	0.09	0.02	0.02

VC1078	0.06	0.06	0.06	0.07
VC1079	0.02	0.02	0.04	0.05
VC1080	0.08	0.08	0.06	0.04
VC1081	0.08	0.09	0.06	0.05
VC1082	0.06	0.06	0.07	0.05
VC1083	0.04	0.06	0.07	0.09
VC1084	0.08	0.09	0.06	0.05
VC1085	0.07	0.07	0.08	0.07
VC1086	0.00	0.00	0.02	0.02
VC1087	0.05	0.05	0.04	0.06
VC1088	0.05	0.05	0.04	0.05
VC1089	0.07	0.07	0.05	0.05
VC1090	0.08	0.08	0.02	0.03
VC1091	0.04	0.05	0.05	0.06
VC1092	0.04	0.05	0.07	0.08
VC1093	0.05	0.07	0.04	0.06
VC1094	0.04	0.05	0.07	0.05
VC1095	0.05	0.04	0.06	0.06
VC1096	0.07	0.06	0.10	0.08
VC1097	0.02	0.02	0.06	0.06
VC1098	0.07	0.08	0.08	0.08
VC1099	0.05	0.04	0.12	0.07
VC1100	0.07	0.06	0.16	0.12
VC1101	0.06	0.05	0.09	0.08
VC1102	0.04	0.04	0.03	0.02
VC1103	0.04	0.05	0.03	0.03
VC1104	0.04	0.04	0.00	0.00
VC1105	0.02	0.03	0.03	0.05
VC1106	0.08	0.07	0.08	0.08
VC1107	0.03	0.04	0.05	0.04
VC1108	0.07	0.05	0.04	0.05
VC1109	0.04	0.06	0.06	0.03
VC1109	0.05	0.07	0.05	0.06
VC1110	0.03	0.05	0.05	0.04
VC1111	0.08	0.09	0.04	0.06
VC1112	0.10	0.07	0.05	0.05
VC1113	0.06	0.05	0.07	0.08
VC1114	0.06	0.05	0.06	0.08
VC1115	0.07	0.06	0.11	0.11
VC1116	0.04	0.04	0.04	0.04
VC1117	0.04	0.05	0.11	0.10
VC1118	0.04	0.04	0.04	0.05
VC1119	0.04	0.06	0.10	0.09

VC1120	0.05	0.04	0.03	0.05
VC1121	0.04	0.04	0.03	0.03
VC1122	0.06	0.06	0.05	0.06
VC1123	0.04	0.04	0.07	0.06
VC1124	0.00	0.04	0.07	0.08
VC1125	0.05	0.05	0.06	0.06
VC1126	0.05	0.08	0.08	0.09
VC1127	0.06	0.06	0.07	0.14
VC1128	0.02	0.02	0.01	0.02
VC1129	0.06	0.07	0.08	0.06
VC1130	0.07	0.07	0.08	0.07
VC1131	0.06	0.07	0.09	0.09
VC1132	0.03	0.04	0.10	0.11
VC1133	0.04	0.04	0.07	0.06
VC1134	0.03	0.03	0.05	0.06
VC1135	0.03	0.03	0.08	0.09
VC1136	0.04	0.03	0.05	0.05
VC1137	0.04	0.05	0.06	0.08
VC1138	0.06	0.05	0.08	0.09
VC1139	0.04	0.03	0.07	0.06
VC1140	0.06	0.06	0.12	0.07
VC1141	0.02	0.02	0.06	0.05
VC1142	0.05	0.05	0.05	0.09
VC1143	0.05	0.05	0.15	0.08
VC1144	0.02	0.04	0.04	0.04
VC1145	0.03	0.06	0.03	0.03
VC1146	0.06	0.05	0.09	0.11
VC1147	0.07	0.07	0.10	0.15
VC1148	0.05	0.06	0.02	0.04
VC1149	0.08	0.07	0.03	0.05
VC1150	0.03	0.03	0.09	0.08
VC1151	0.07	0.06	0.10	0.06
VC1152	0.07	0.06	0.11	0.06
VC1153	0.01	0.01	0.20	0.18
VC1154	0.05	0.05	0.06	0.05
VC1155	0.05	0.05	0.09	0.10
VC1156	0.03	0.03	0.03	0.03
VC1156	0.00	0.05	0.06	0.06
VC1158	0.00	0.00	0.07	0.07
VC1159	0.03	0.02	0.06	0.04
VC1160	0.07	0.05	0.05	0.04
VC1161	0.04	0.05	0.08	0.07
VC1162	0.07	0.07	0.06	0.07

VC1163	0.04	0.04	0.06	0.01
VC1164	0.08	0.09	0.05	0.05
VC1165	0.05	0.06	0.03	0.03
VC1165	0.05	0.04	0.01	0.05
VC1166	0.01	0.04	0.05	0.05
VC1167	0.04	0.04	0.04	0.04
VC1169	0.03	0.03	0.01	0.02
VC1170	0.07	0.07	0.08	0.06
VC1171	0.09	0.08	0.04	0.05
VC1172	0.02	0.02	0.01	0.02
VC1173	0.02	0.03	0.01	0.02
VC1174	0.07	0.07	0.09	0.08
VC1175	0.07	0.05	0.13	0.06
VC1176	0.04	0.04	0.04	0.07
VC1177	0.03	0.03	0.07	0.06
VC1178	0.02	0.03	0.00	0.01
VC1179	0.06	0.06	0.08	0.07
VC1180	0.07	0.07	0.04	0.04
VC1181	0.06	0.07	0.11	0.14
VC1182	0.03	0.03	0.02	0.03
VC1183	0.16	0.15	0.03	0.02
VC1184	0.13	0.11	0.03	0.04
VC1185	0.07	0.06	0.00	0.00
VC1186	0.09	0.10	0.02	0.02
VC1187	0.08	0.07	0.06	0.05
VC1188	0.04	0.03	0.05	0.07
VC1189	0.03	0.03	0.02	0.05
VC1189	0.01	0.01	0.05	0.06
VC1190	0.15	0.12	0.04	0.03
VC1191	0.10	0.10	0.02	0.04
VC1192	0.06	0.06	0.06	0.03
VC1193	0.05	0.10	0.06	0.05
VC1194	0.12	0.11	0.02	0.04
VC1195	0.10	0.11	0.07	0.10
VC1196	0.04	0.05	0.06	0.06
VC1197	0.04	0.05	0.07	0.08
VC1198	0.02	0.01	0.03	0.03
VC1199	0.12	0.11	0.02	0.01
VC1200	0.12	0.09	0.02	0.01
VC1201	0.07	0.07	0.02	0.04
VC1202	0.14	0.17	0.04	0.05
VC1203	0.09	0.06	-0.02	-0.02
VC1204	0.08	0.06	-0.02	-0.02

VC1205	0.09	0.08	0.00	0.00
VC1206	0.15	0.17	0.07	0.06
VC1207	0.07	0.05	0.01	0.00
VC1208	0.08	0.08	0.00	0.00
VC1209	0.12	0.09	0.03	0.02
VC1210	0.15	0.19	0.07	0.06
VC1211	-0.01	-0.01	-0.01	0.15
VC1212	0.05	0.05	0.04	0.05
VC1213	0.11	0.12	0.01	0.01
VC1214	0.05	0.03	0.03	0.05
VC1215	0.06	0.07	0.07	0.08
VC1216	0.13	0.15	0.02	0.03
VC1217	0.16	0.16	0.04	0.05
VC1218	0.06	0.06	0.04	0.04
VC1219	0.13	0.11	0.02	0.01
VC1220	0.07	0.07	0.04	0.04
VC1221	0.14	0.11	0.03	0.04
VC1222	0.11	0.10	0.03	0.05
VC1223	0.02	0.02	0.06	0.04
VC1223	0.04	0.05	0.06	0.06
VC1224	0.04	0.03	0.08	0.08
VC1225	0.08	0.08	0.05	0.06
VC1226	0.13	0.13	0.03	0.04
VC1227	0.10	0.09	0.07	0.07
VC1228	0.10	0.10	0.07	0.09
VC1229	0.07	0.07	0.04	0.05
VC1230	0.05	0.05	0.10	0.10
VC1230	0.07	0.09	0.06	0.04
VC1231	0.09	0.07	0.03	0.04
VC1232	0.03	0.05	0.06	0.06
VC1233	0.05	0.04	0.07	0.07
VC1234	0.04	0.04	0.06	0.05
VC1235	0.04	0.04	0.03	0.04
VC1236	0.06	0.08	0.09	0.10
VC1237	0.04	0.05	0.11	0.08
VC1238	0.08	0.07	0.09	0.08
VC1239	0.10	0.09	0.06	0.06
VC1240	0.10	0.06	0.08	0.06
VC1241	0.05	0.04	0.08	0.05
VC1242	0.08	0.06	0.06	0.08
VC1243	0.05	0.06	0.04	0.07
VC1244	0.03	0.03	0.05	0.05
VC1245	0.14	0.14	0.05	0.04

VC1246	0.11	0.08	0.04	0.05
VC1247	0.06	0.04	0.09	0.08
VC1248	0.05	0.05	0.05	0.04
VC1249	0.06	0.06	0.05	0.05
VC1250	0.12	0.12	0.18	0.06
VC1251	0.06	0.08	0.03	0.04
VC1252	0.08	0.06	0.08	0.09
VC1253	0.05	0.05	0.07	0.06
VC1254	0.05	0.05	0.06	0.05
VC1255	0.02	0.02	0.01	0.01
VC1256	0.09	0.09	0.04	0.04
VC1257	0.07	0.07	0.09	0.08
VC1258	0.02	0.02	0.05	0.05
VC1259	0.06	0.05	0.06	0.05
VC1260	0.03	0.03	0.08	0.07
VC1261	0.05	0.07	0.09	0.06
VC1262	0.06	0.04	0.07	0.06
VC1263	0.03	0.03	0.06	0.06
VC1265	0.06	0.07	0.03	0.06
VC1266	0.01	0.01	0.05	0.03
VC1267	0.00	0.01	0.06	0.05
VC1268	0.01	0.02	0.04	0.03
VC1269	0.04	0.04	0.06	0.05
VC1270	0.00	0.03	0.04	0.03
VC1271	0.01	0.02	0.05	0.04
VC1272	0.02	0.02	0.06	0.06
VC1273	0.04	0.04	0.06	0.09
VC1274	0.04	0.04	0.05	0.04
VC1275	0.02	0.02	0.04	0.03
VC1276	0.03	0.03	0.04	0.03
VC1277	0.04	0.03	0.07	0.06
VC1278	0.02	0.03	0.11	0.10
VC1279	0.04	0.05	0.03	0.03
VC1280	0.02	0.02	0.06	0.05
VC1281	0.06	0.05	0.04	0.03
VC1282	0.01	0.02	0.03	0.03
VC1283	0.09	0.09	0.03	0.03
VC1284	0.03	0.03	0.04	0.03
VC1285	0.03	0.03	0.06	0.05
VC1286	0.01	0.02	0.06	0.04
VC1287	0.02	0.02	0.05	0.05
VC1288	0.03	0.04	0.05	0.05
VC1289	0.01	0.02	0.05	0.05

VC1290	0.03	0.03	0.08	0.07
VC1291	0.03	0.03	0.06	0.05
VC1292	0.07	0.08	0.07	0.07
VC1293	0.05	0.05	0.06	0.06
VC1294	0.05	0.06	0.04	0.06
VC1295	0.46	0.47	0.48	0.54
VC1296	0.04	0.05	0.05	0.06
VC1297	0.01	0.02	0.00	0.01
VC1298	0.09	0.08	0.03	0.03
VC1299	0.05	0.04	0.07	0.07
VC1300	0.03	0.03	0.05	0.06
VC1301	0.13	0.12	0.08	0.08
VC1302	0.07	0.07	0.07	0.06
VC1303	0.04	0.05	0.05	0.08
VC1304	0.08	0.07	0.06	0.06
VC1305	0.03	0.03	0.03	0.04
VC1306	0.01	0.02	0.04	0.07
VC1307	0.02	0.06	0.02	0.03
VC1308	0.18	0.17	0.09	0.09
VC1309	0.10	0.07	0.05	0.08
VC1310	0.06	0.04	0.06	0.07
VC1311	0.03	0.03	0.06	0.05
VC1312	0.04	0.05	0.06	0.10
VC1313	0.09	0.05	0.05	0.05
VC1314	0.05	0.05	0.06	0.05
VC1315	0.04	0.05	0.07	0.05
VC1316	0.09	0.06	0.07	0.08
VC1317	0.05	0.05	0.07	0.06
VC1319	0.00	0.04	0.05	0.06
VC1320	0.03	0.03	0.03	0.03
VC1321	0.02	0.02	0.03	0.05
VC1322	0.07	0.06	0.04	0.03
VC1323	0.04	0.04	0.07	0.06
VC1324	0.07	0.06	0.03	0.03
VC1325	0.05	0.05	0.09	0.08
VC1326	0.12	0.14	0.03	0.03
VC1327	0.02	0.03	0.04	0.04
VC1329	0.03	0.04	0.05	0.04
VC1330	0.10	0.08	0.05	0.04
VC1331	0.01	0.03	0.05	0.04
VC1332	0.02	0.02	0.02	0.05
VC1332	0.01	0.02	0.04	0.04
VC1333	0.03	0.02	0.07	0.11

VC1334	0.03	0.02	0.04	0.05
VC1335	0.02	0.03	0.06	0.07
VC1336	0.07	0.07	0.04	0.05
VC1337	0.06	0.06	0.04	0.04
VC1338	0.04	0.04	0.08	0.04
VC1339	0.04	0.04	0.06	0.05
VC1340	0.05	0.03	0.04	0.03
VC1341	0.05	0.05	0.10	0.08
VC1341	0.01	0.01	0.05	0.05
VC1342	0.02	0.01	0.04	0.04
VC1343	0.03	0.05	0.05	0.05
VC1344	0.08	0.07	0.07	0.07
VC1345	0.08	0.08	0.11	0.15
VC1346	0.05	0.03	0.06	0.06
VC1348	0.45	0.44	0.43	0.41
VC1349	0.10	0.12	0.03	0.03
VC1350	0.06	0.06	0.09	0.08
VC1351	0.04	0.04	0.06	0.05
VC1352	0.03	0.05	0.04	0.05
VC1353	0.01	0.01	0.01	0.00
VC1354	0.05	0.05	0.06	0.05
VC1355	0.06	0.06	0.04	0.05
VC1356	0.05	0.06	0.09	0.12
VC1357	0.07	0.08	0.06	0.02
VC1358	0.07	0.07	0.05	0.04
VC1359	0.04	0.05	0.10	0.07
VC1360	0.05	0.04	0.07	0.08
VC1361	0.04	0.05	0.07	0.07
VC1362	0.07	0.04	0.06	0.07
VC1363	0.02	0.06	0.06	0.07
VC1364	0.06	0.07	0.05	0.04
VC1365	0.07	0.08	0.04	0.06
VC1366	0.08	0.04	0.05	0.05
VC1367	0.02	0.05	0.06	0.07
VC1368	0.04	0.05	0.06	0.06
VC1369	0.03	0.03	0.06	0.04
VC1370	0.40	0.43	0.40	0.39
VC1371	0.05	0.04	0.04	0.05
VC1372	0.04	0.02	0.03	0.04
VC1373	0.07	0.07	0.07	0.06
VC1374	0.08	0.05	0.05	0.04
VC1375	0.06	0.05	0.05	0.07
VC1377	0.04	0.05	0.04	0.04

VC1378	0.04	0.05	0.07	0.07
VC1379	0.07	0.08	0.08	0.07
VC1380	0.05	0.05	0.05	0.05
VC1381	0.08	0.07	0.05	0.05
VC1382	-0.01	0.02	0.03	0.05
VC1382	0.02	0.04	0.05	0.04
VC1383	0.03	0.04	0.08	0.07
VC1384	0.02	0.03	0.03	0.03
VC1385	0.09	0.06	0.10	0.06
VC1386	0.07	0.04	0.06	0.05
VC1387	0.06	0.05	0.04	0.04
VC1388	0.06	0.05	0.08	0.07
VC1389	0.04	0.05	0.07	0.06
VC1390	0.06	0.06	0.05	0.04
VC1391	0.02	0.03	0.08	0.06
VC1392	0.05	0.06	0.04	0.06
VC1393	0.02	0.02	0.04	0.03
VC1394	0.08	0.13	0.06	0.05
VC1395	0.04	0.04	0.07	0.04
VC1396	0.07	0.06	0.04	0.04
VC1397	0.08	0.07	0.06	0.06
VC1398	0.07	0.07	0.03	0.04
VC1399	0.04	0.05	0.04	0.03
VC1400	0.05	0.06	0.05	0.05
VC1401	0.01	0.03	0.05	0.05
VC1402	0.02	0.02	0.04	0.04
VC1403	0.07	0.08	0.06	0.06
VC1404	0.09	0.08	0.02	0.03
VC1405	0.02	0.02	0.13	0.10
VC1406	0.07	0.06	0.14	0.14
VC1407	0.05	0.05	0.02	0.04
VC1408	0.01	0.02	0.04	0.04
VC1409	0.06	0.04	0.03	0.02
VC1410	0.06	0.05	0.05	0.05
VC1411	0.03	0.03	0.03	0.03
VC1412	0.09	0.07	0.06	0.08
VC1413	0.10	0.10	0.00	0.02
VC1414	0.02	0.02	0.05	0.03
VC1415	0.09	0.09	0.06	0.06
VC1416	0.04	0.06	0.04	0.05
VC1417	0.03	0.03	0.07	0.07
VC1418	0.01	0.02	0.01	0.01
VC1419	0.02	0.03	0.05	0.03

VC1420	0.02	0.02	0.02	0.03
VC1421	0.01	0.02	0.00	0.03
VC1422	0.08	0.05	0.06	0.06
VC1423	0.06	0.05	0.05	0.05
VC1424	0.03	0.04	0.05	0.04
VC1425	0.05	0.06	0.05	0.04
VC1426	0.06	0.06	0.06	0.05
VC1427	0.07	0.03	0.04	0.04
VC1428	0.02	0.02	0.04	0.08
VC1429	0.04	0.03	0.05	0.04
VC1430	0.02	0.04	0.03	0.00
VC1431	0.06	0.06	0.06	0.04
VC1432	0.01	0.03	0.06	0.05
VC1433	0.01	0.01	0.03	0.03
VC1434	0.04	0.07	0.05	0.06
VC1435	0.05	0.04	0.03	0.03
VC1436	0.04	0.04	0.04	0.03
VC1437	0.02	0.03	0.06	0.06
VC1438	0.06	0.05	0.06	0.05
VC1439	0.01	0.02	0.04	0.04
VC1440	0.06	0.05	0.06	0.04
VC1441	0.02	0.01	0.06	0.09
VC1442	-0.01	-0.01	0.07	0.05
VC1443	0.02	0.03	0.03	0.04
VC1444	0.03	0.03	0.02	0.04
VC1445	0.03	0.02	0.04	0.05
VC1446	0.09	0.06	0.04	0.05
VC1447	0.01	0.02	0.09	0.07
VC1448	0.03	0.05	0.03	0.05
VC1449	0.03	0.04	0.07	0.06
VC1450	0.03	0.04	0.04	0.03
VC1452	0.07	0.05	0.07	0.08
VC1453	0.03	0.05	0.06	0.05
VC1454	0.05	0.07	0.06	0.04
VC1455	0.04	0.04	0.07	0.06
VC1456	0.04	0.04	0.05	0.04
VC1457	0.07	0.08	0.05	0.05
VC1458	0.03	0.04	0.07	0.04
VC1459	0.06	0.07	0.04	0.03
VC1460	0.06	0.06	0.10	0.08
VC1461	0.09	0.10	0.04	0.04
VC1462	0.05	0.08	0.06	0.05
VC1463	0.07	0.07	0.05	0.05

VC1464	0.06	0.05	0.04	0.05
VC1465	0.03	0.01	0.08	0.08
VC1466	0.03	0.02	0.07	0.07
VC1467	0.04	0.05	0.02	0.02
VC1468	0.10	0.10	0.05	0.04
VC1469	-0.01	0.00	0.04	0.07
VC1470	0.07	0.08	0.09	0.08
VC1471	0.06	0.07	0.06	0.03
VC1472	0.04	0.04	0.07	0.06
VC1473	0.06	0.05	0.07	0.07
VC1474	0.09	0.10	0.00	0.05
VC1475	0.05	0.06	0.04	0.04
VC1476	0.00	0.01	0.03	0.05
VC1477	0.00	0.02	0.04	0.06
VC1478	0.06	0.08	0.05	0.05
VC1479	-0.01	0.00	0.04	0.07
VC1480	0.07	0.07	0.03	0.02
VC1481	0.04	0.02	0.04	0.06
VC1482	0.02	0.02	0.04	0.04
VC1483	0.03	0.03	0.07	0.06
VC1484	0.03	0.06	0.06	0.07
VC1485	0.03	0.05	0.05	0.04
VC1486	0.02	0.01	0.05	0.08
VC1487	0.00	0.02	0.04	0.04
VC1488	0.07	0.07	0.04	0.06
VC1489	0.09	0.09	0.03	0.04
VC1490	0.08	0.09	0.03	0.04
VC1491	0.00	0.04	0.09	0.10
VC1492	0.03	0.03	0.05	0.06
VC1492	0.01	0.03	0.04	0.04
VC1493	0.08	0.07	0.04	0.05
VC1494	0.04	0.06	0.07	0.06
VC1495	0.01	0.01	0.08	0.08
VC1496	0.05	0.04	0.04	0.04
VC1497	0.05	0.06	0.05	0.05
VC1498	0.05	0.04	0.02	0.02
VC1499	0.05	0.07	0.04	0.05
VC1500	0.04	0.06	0.05	0.05
VC1500	0.05	0.04	0.02	0.02
VC1501	0.07	0.06	0.03	0.08
VC1502	0.11	0.15	0.02	0.05
VC1503	0.06	0.04	0.05	0.07
VC1505	0.03	0.03	0.05	0.05

VC1506	0.05	0.07	0.06	0.07
VC1507	0.03	0.04	0.08	0.07
VC1508	0.05	0.06	0.02	0.05
VC1509	0.05	0.04	0.07	0.07
VC1510	0.03	0.05	0.07	0.06
VC1511	0.09	0.09	0.08	0.10
VC1512	0.05	0.05	0.08	0.09
VC1513	0.08	0.05	0.07	0.06
VC1514	0.04	0.04	0.05	0.07
VC1515	0.09	0.08	0.07	0.06
VC1516	0.06	0.05	0.07	0.04
VC1517	0.04	0.05	0.05	0.04
VC1518	0.05	0.12	0.07	0.10
VC1519	0.08	0.06	0.05	0.06
VC1520	0.05	0.05	0.04	0.05
VC1521	0.04	0.04	0.07	0.08
VC1523	0.12	0.08	0.04	0.04
VC1524	0.03	0.06	0.05	0.05
VC1525	0.07	0.07	0.03	0.06
VC1526	0.06	0.05	0.06	0.06
VC1527	0.12	0.12	0.05	0.06
VC1528	0.02	0.02	0.03	0.03
VC1529	0.03	0.03	0.06	0.04
VC1530	0.04	0.04	0.08	0.06
VC1531	0.04	0.06	0.08	0.08
VC1532	0.05	0.06	0.04	0.06
VC1533	0.04	0.05	0.03	0.03
VC1534	0.03	0.02	0.09	0.10
VC1535	0.02	0.01	0.04	0.03
VC1537	0.03	0.03	0.04	0.03
VC1538	0.04	0.06	0.05	0.06
VC1539	0.05	0.04	0.06	0.06
VC1540	0.00	0.04	0.04	0.04
VC1541	0.02	0.04	0.05	0.07
VC1542	0.03	0.02	0.05	0.04
VC1543	0.03	0.04	0.07	0.06
VC1544	0.03	0.03	0.03	0.03
VC1545	0.05	0.06	0.06	0.06
VC1546	0.02	0.04	0.02	0.03
VC1547	0.03	0.03	0.06	0.05
VC1548	0.02	0.02	0.05	0.04
VC1549	0.05	0.05	0.03	0.05
VC1550	0.02	0.03	0.07	0.06

VC1551	0.06	0.06	0.05	0.07
VC1552	0.03	0.05	0.09	0.11
VC1553	0.05	0.05	0.05	0.06
VC1554	0.09	0.09	0.07	0.05
VC1555	0.06	0.04	0.09	0.08
VC1556	0.04	0.03	0.06	0.06
VC1557	0.02	0.03	0.06	0.05
VC1558	0.04	0.05	0.05	0.05
VC1559	0.05	0.05	0.03	0.08
VC1560	0.08	0.06	0.08	0.11
VC1561	0.05	0.07	0.04	0.07
VC1562	0.03	0.04	0.05	0.05
VC1563	0.02	0.08	0.04	0.04
VC1565	0.08	0.11	0.07	0.07
VC1566	0.07	0.07	0.06	0.05
VC1567	0.13	0.14	0.07	0.08
VC1568	0.05	0.08	0.05	0.06
VC1569	0.06	0.06	0.04	0.05
VC1570	0.03	0.08	0.06	0.06
VC1571	0.05	0.05	0.04	0.03
VC1572	0.00	0.03	0.04	0.04
VC1573	0.06	0.08	0.06	0.06
VC1574	0.04	0.07	0.05	0.04
VC1575	0.08	0.11	0.05	0.05
VC1576	0.05	0.08	0.04	0.06
VC1577	0.04	0.06	0.07	0.06
VC1578	0.04	0.04	0.10	0.10
VC1579	0.00	0.02	0.04	0.04
VC1580	0.04	0.07	0.03	0.05
VC1581	0.08	0.07	0.03	0.03
VC1582	0.06	0.05	0.05	0.05
VC1583	0.08	0.09	0.04	0.04
VC1584	0.03	0.04	0.03	0.05
VC1585	0.12	0.12	0.04	0.06
VC1586	0.07	0.08	0.05	0.04
VC1586	0.06	0.07	0.04	0.05
VC1587	0.03	0.07	0.06	0.06
VC1588	0.07	0.08	0.09	0.07
VC1589	0.05	0.07	0.07	0.07
VC1590	0.06	0.08	0.04	0.03
VC1591	0.06	0.07	0.07	0.07
VC1592	0.00	0.01	0.00	0.00
VC1593	0.05	0.06	0.05	0.05

VC1595	0.07	0.07	0.06	0.06
VC1596	0.09	0.09	0.06	0.07
VC1597	0.05	0.04	0.07	0.05
VC1598	0.04	0.06	0.06	0.06
VC1599	-0.03	0.02	-0.01	-0.01
VC1600	0.02	0.08	0.10	0.10
VC1601	0.13	0.11	0.03	0.04
VC1602	0.04	0.05	0.07	0.07
VC1603	0.04	0.07	0.04	0.04
VC1604	0.07	0.06	0.05	0.07
VC1605	0.01	0.01	0.03	0.03
VC1606	0.04	0.05	0.07	0.08
VC1607	0.02	0.03	0.05	0.04
VC1608	0.05	0.04	0.06	0.05
VC1609	0.01	0.01	0.06	0.06
VC1610	0.04	0.05	0.07	0.07
VC1611	0.05	0.04	0.05	0.05
VC1612	0.02	0.02	0.07	0.06
VC1613	0.07	0.07	0.01	0.02
VC1614	0.03	0.03	0.07	0.05
VC1615	0.06	0.07	0.07	0.07
VC1616	0.07	0.08	0.05	0.06
VC1617	0.05	0.07	0.07	0.06
VC1618	0.05	0.04	0.05	0.08
VC1619	0.03	0.03	0.05	0.04
VC1621	0.03	0.01	0.05	0.08
VC1622	0.09	0.09	0.07	0.06
VC1623	0.06	0.05	0.05	0.04
VC1624	0.09	0.07	0.05	0.05
VC1625	0.03	0.06	0.05	0.05
VC1627	0.03	0.02	0.03	0.05
VC1628	0.05	0.04	0.03	0.02
VC1629	0.01	0.01	0.07	0.06
VC1630	0.04	0.04	0.05	0.04
VC1631	0.03	0.06	0.05	0.07
VC1632	0.10	0.09	0.06	0.06
VC1633	0.04	0.06	0.06	0.07
VC1634	0.05	0.05	0.05	0.05
VC1635	0.15	0.05	0.10	0.11
VC1636	0.07	0.09	0.04	0.07
VC1637	0.05	0.03	0.02	0.05
VC1638	0.02	0.03	0.06	0.08
VC1639	0.01	0.03	0.05	0.08

VC1640	0.05	0.06	0.06	0.05
VC1641	0.56	0.56	0.58	0.60
VC1642	0.07	0.05	0.09	0.11
VC1643	0.01	0.01	0.05	0.03
VC1644	0.01	0.02	0.04	0.07
VC1646	0.07	0.08	0.05	0.05
VC1647	0.02	0.01	0.04	0.03
VC1648	0.05	0.09	0.05	0.06
VC1648	0.06	0.06	0.01	0.04
VC1649	0.01	0.03	0.02	0.02
VC1651	0.01	0.01	0.04	0.04
VC1652	0.29	0.28	0.04	0.03
VC1653	0.06	0.06	0.05	0.06
VC1654	0.06	0.06	0.04	0.04
VC1656	0.05	0.06	0.04	0.04
VC1657	0.07	0.09	0.04	0.04
VC1658	0.07	0.11	0.06	0.05
VC1659	0.05	0.08	0.13	0.06
VC1660	0.05	0.06	0.07	0.05
VC1661	0.05	0.06	0.04	0.04
VC1662	0.05	0.06	0.06	0.07
VC1663	0.09	0.11	0.06	0.06
VC1664	0.04	0.12	0.07	0.07
VC1665	0.08	0.08	0.05	0.05
VC1666	0.04	0.05	0.04	0.05
VC1667	0.03	0.02	0.05	0.05
VC1668	0.03	0.04	0.06	0.06
VC1669	0.02	0.02	0.01	0.04
VC1670	0.06	0.06	0.05	0.06
VC1671	0.07	0.06	0.15	0.12
VC1672	0.06	0.05	0.12	0.09
VC1673	0.04	0.05	0.08	0.11
VC1674	0.06	0.06	0.12	0.09
VC1675	0.03	0.03	0.10	0.09
VC1676	0.06	0.07	0.09	0.10
VC1677	0.03	0.04	0.06	0.06
VC1678	0.08	0.07	0.15	0.15
VC1679	0.05	0.05	0.09	0.08
VC1680	0.05	0.04	0.05	0.03
VC1681	0.05	0.06	0.09	0.09
VC1682	0.06	0.06	0.12	0.10
VC1683	0.04	0.05	0.02	0.02
VC1684	0.05	0.06	0.09	0.09

VC1685	0.05	0.05	0.10	0.08
VC1686	0.11	0.12	0.09	0.05
VC1687	0.07	0.08	0.16	0.10
VC1688	0.09	0.05	0.05	0.06
VC1689	0.07	0.06	0.08	0.04
VC1690	0.04	0.04	0.06	0.05
VC1691	0.10	0.05	0.01	0.05
VC1692	0.03	0.04	0.06	0.04
VC1693	0.06	0.03	0.03	0.04
VC1695	0.07	0.06	0.13	0.09
VC1696	0.08	0.08	0.10	0.09
VC1697	0.07	0.08	0.15	0.11
VC1698	0.06	0.05	0.05	0.04
VC1699	0.04	0.05	0.02	0.06
VC1700	0.06	0.05	0.03	0.03
VC1701	0.04	0.05	0.05	0.05
VC1702	0.05	0.05	0.08	0.08
VC1703	0.03	0.03	0.09	0.06
VC1704	0.04	0.05	0.05	0.06
VC1705	0.03	0.03	0.04	0.03
VC1706	0.06	0.07	0.10	0.08
VC1707	0.07	0.07	0.12	0.12
VC1708	0.04	0.06	0.07	-0.05
VC1709	0.02	0.02	0.02	0.07
VC1710	0.34	0.30	0.30	0.26
VC1711	0.04	0.05	0.04	0.05
VC1712	0.02	0.02	0.06	0.04
VC1713	0.10	0.10	0.10	0.08
VC1714	0.01	0.02	0.06	0.05
VC1714	0.02	0.03	0.04	0.04
VC1715	0.07	0.06	0.05	0.03
VC1716	0.09	0.11	0.05	0.05
VC1717	0.06	0.07	0.07	0.13
VC1718	0.08	0.09	0.10	0.08
VC1719	0.01	0.03	0.05	0.04
VC1720	0.04	0.06	0.05	0.04
VC1721	0.05	0.06	0.07	0.07
VC1722	0.05	0.05	0.04	0.04
VC1724	0.06	0.06	0.06	0.05
VC1725	0.07	0.08	0.10	0.10
VC1726	0.02	0.02	0.02	0.02
VC1727	0.01	0.01	0.05	0.04
VC1728	0.04	0.06	0.02	0.04

VC1729	0.07	0.07	0.05	0.08
VC1730	0.02	0.02	0.03	0.04
VC1730	0.00	0.04	0.05	0.05
VC1731	0.03	0.04	0.06	0.05
VC1732	0.06	0.07	0.07	0.09
VC1733	0.05	0.08	0.07	0.06
VC1734	0.06	0.06	0.04	0.03
VC1735	0.07	0.08	0.05	0.04
VC1736	0.04	0.06	0.05	0.04
VC1737	0.05	0.06	0.07	0.07
VC1738	0.02	0.02	0.05	0.07
VC1740	0.05	0.04	0.04	0.03
VC1741	0.08	0.07	0.06	0.06
VC1742	0.04	0.05	0.09	0.06
VC1743	0.06	0.06	0.06	0.05
VC1744	0.06	0.09	0.07	0.06
VC1745	0.04	0.05	0.04	0.04
VC1746	0.05	0.07	0.05	0.08
VC1747	0.04	0.07	0.05	0.05
VC1748	0.06	0.07	0.05	0.04
VC1749	0.11	0.08	0.06	0.06
VC1750	0.15	0.05	0.02	0.02
VC1751	0.06	0.07	0.07	0.06
VC1752	0.06	0.07	0.04	0.03
VC1753	0.03	0.04	0.05	0.05
VC1754	0.06	0.07	0.06	0.06
VC1755	0.07	0.07	0.06	0.06
VC1756	0.04	0.04	0.07	0.05
VC1757	0.02	0.03	0.05	0.04
VC1758	0.05	0.08	0.06	0.06
VC1759	0.07	0.06	0.05	0.06
VC1760	0.02	0.04	0.04	0.04
VC1761	0.03	0.05	0.04	0.03
VC1762	0.06	0.09	0.06	0.05
VC1763	0.02	0.03	0.03	0.03
VC1764	0.02	0.03	0.02	0.03
VC1765	0.04	0.04	0.02	0.02
VC1766	0.08	0.10	0.04	0.05
VC1767	0.04	0.05	0.06	0.03
VC1768	0.06	0.07	0.07	0.08
VC1769	0.02	0.02	0.05	0.05
VC1770	0.03	0.03	0.05	0.04
VC1771	0.02	0.03	0.06	0.07

VC1772	0.05	0.06	0.07	0.07
VC1773	0.09	0.07	0.04	0.06
VC1774	0.06	0.07	0.09	0.10
VC1775	0.06	0.06	0.05	0.07
VC1776	0.04	0.05	0.06	0.06
VC1777	0.06	0.08	0.07	0.06
VC1778	0.05	0.05	0.06	0.06
VC1779	0.06	0.07	0.06	0.04
VC1780	0.04	0.06	0.08	0.08
VC1781	0.08	0.09	0.08	0.06
VC1782	0.06	0.08	0.07	0.07
VC1783	0.05	0.06	0.07	0.06
VC1784	0.04	0.06	0.05	0.03
VC1785	0.05	0.06	0.06	0.08
VC1786	0.06	0.08	0.06	0.07
VC1787	0.06	0.07	0.07	0.07
VC1788	0.07	0.07	0.04	0.05
VC1789	0.05	0.05	0.03	0.04
VC1790	0.11	0.08	0.04	0.06
VC1791	0.06	0.07	0.04	0.05
VC1792	0.09	0.08	0.07	0.05
VC1793	0.10	0.08	0.04	0.05
VC1794	0.08	0.08	0.10	0.11
VC1795	0.10	0.08	0.06	0.07
VC1796	0.08	0.06	0.04	0.06
VC1797	0.08	0.07	0.04	0.04
VC1798	0.01	0.01	-0.01	0.01
VC1799	0.10	0.12	0.05	0.09
VC1800	0.02	0.02	0.04	0.04
VC1801	0.01	0.01	0.09	0.08
VC1802	0.13	0.11	0.07	0.09
VC1803	0.10	0.09	0.04	0.05
VC1804	0.10	0.09	0.05	0.04
VC1805	0.09	0.07	0.05	0.07
VC1806	0.07	0.07	0.05	0.05
VC1807	0.01	0.04	0.05	0.03
VC1807	0.00	0.03	0.05	0.04
VC1808	0.09	0.08	0.05	0.06
VC1809	0.06	0.07	0.04	0.05
VC1810	0.08	0.07	0.05	0.05
VC1811	0.04	0.07	0.04	0.04
VC1812	0.06	0.08	0.06	0.07
VC1813	0.04	0.05	0.06	0.09

VC1814	0.06	0.07	0.09	0.07
VC1815	0.07	0.06	0.07	0.06
VC1816	0.03	0.05	0.07	0.08
VC1817	0.06	0.06	0.05	0.06
VC1818	0.02	0.04	0.06	0.05
VC1819	0.05	0.06	0.03	0.05
VC1820	0.11	0.08	0.08	0.10
VC1821	0.05	0.06	0.02	0.04
VC1822	0.08	0.06	0.08	0.05
VC1823	0.11	0.12	0.04	0.06
VC1824	0.10	0.11	0.07	0.05
VC1825	0.14	0.15	0.05	0.06
VC1826	0.04	0.04	0.04	0.06
VC1827	0.06	0.04	0.07	0.07
VC1828	0.09	0.09	0.07	0.05
VC1829	0.04	0.06	0.09	0.10
VC1830	0.05	0.05	0.06	0.04
VC1830	0.06	0.07	0.09	0.07
VC1831	0.03	0.04	0.05	0.06
VC1831	0.02	0.01	0.03	0.02
VC1832	0.03	0.02	0.08	0.05
VC1833	0.10	0.11	0.04	0.04
VC1834	0.08	0.07	0.05	0.04
VC1835	0.03	0.02	0.06	0.06
VC1836	0.06	0.06	0.06	0.06
VC1837	0.03	0.06	0.09	0.09
VC1838	0.09	0.08	0.07	0.07
VC1839	0.06	0.06	0.07	0.08
VC1840	0.06	0.04	0.05	0.05
VC1841	0.05	0.07	0.05	0.06
VC1842	0.04	0.05	0.04	0.03
VC1842	0.05	0.06	0.06	0.07
VC1843	0.01	0.01	0.00	0.00
VC1844	0.09	0.09	0.04	0.06
VC1845	0.09	0.08	0.08	0.07
VC1846	0.18	0.14	0.08	0.05
VC1847	0.04	0.03	0.06	0.06
VC1848	0.03	0.05	0.08	0.06
VC1849	0.05	0.05	0.10	0.09
VC1851	0.00	-0.02	0.00	-0.01
VC1852	0.10	0.09	0.11	0.09
VC1853	0.07	0.16	0.04	0.04
VC1854	0.15	0.13	0.08	0.09

VC1855	0.01	0.03	0.04	0.04
VC1856	0.11	0.12	0.06	0.04
VC1857	0.05	0.04	0.09	0.07
VC1858	0.05	0.05	0.05	0.06
VC1859	0.03	0.04	0.05	0.04
VC1860	0.12	0.12	0.05	0.06
VC1861	0.04	0.04	0.06	0.05
VC1862	0.09	0.10	0.05	0.06
VC1863	0.12	0.11	0.04	0.05
VC1864	0.05	0.06	0.05	0.06
VC1865	0.10	0.11	0.05	0.04
VC1866	0.04	0.04	0.04	0.05
VC1868	0.07	0.08	0.03	0.07
VC1869	0.03	0.05	0.05	0.06
VC1870	0.03	0.04	0.05	0.05
VC1871	0.04	0.08	0.03	0.03
VC1872	0.04	0.02	0.08	0.06
VC1873	0.06	0.05	0.06	0.06
VC1874	0.08	0.10	0.06	0.04
VC1875	0.07	0.08	0.07	0.07
VC1876	0.05	0.04	0.06	0.05
VC1877	0.01	0.01	0.01	0.01
VC1878	0.06	0.06	0.05	0.06
VC1879	0.04	0.03	0.04	0.06
VC1879	0.02	0.01	0.04	0.04
VC1880	0.09	0.10	0.04	0.05
VC1881	0.07	0.08	0.04	0.04
VC1882	0.02	0.02	0.00	0.01
VC1883	0.11	0.10	0.05	0.05
VC1884	0.12	0.11	0.05	0.04
VC1885	0.10	0.11	0.05	0.07
VC1886	0.01	0.01	0.07	0.06
VC1887	0.10	0.10	0.04	0.03
VC1888	0.02	0.01	0.04	0.05
VC1889	0.13	0.13	0.05	0.04
VC1890	0.13	0.13	0.07	0.07
VC1891	0.04	0.04	0.04	0.05
VC1891	0.07	0.07	0.04	0.03
VC1892	0.11	0.10	-0.02	0.02
VC1893	0.15	0.14	0.02	0.04
VC1894	0.07	0.05	0.03	0.03
VC1895	0.01	0.02	0.03	0.00
VC1896	0.08	0.08	0.03	0.05

VC1897	0.10	0.09	0.00	0.00
VC1898	0.04	0.05	0.06	0.06
VC1899	0.12	0.10	-0.01	0.03
VC1900	0.03	0.03	0.07	0.03
VC1901	0.09	0.08	0.03	0.03
VC1902	0.16	0.13	0.02	0.02
VC1903	0.06	0.05	0.06	0.03
VC1904	0.10	0.09	0.00	0.01
VC1905	0.13	0.12	0.00	0.01
VC1906	0.14	0.12	0.00	0.02
VC1907	0.05	0.05	0.00	0.01
VC1908	0.06	0.07	0.08	0.06
VC1909	0.04	0.07	0.04	0.04
VC1910	0.04	0.07	0.04	0.03
VC1911	0.05	0.04	0.03	0.03
VC1912	0.06	0.03	0.06	0.09
VC1913	0.06	0.05	0.04	0.04
VC1914	0.04	0.05	0.03	0.03
VC1915	0.06	0.09	0.05	0.05
VC1916	0.04	0.04	0.08	0.07
VC1917	0.04	0.03	0.06	0.04
VC1918	0.06	0.07	0.04	0.03
VC1919	0.09	0.09	0.07	0.07
VC1920	0.05	0.06	0.06	0.07
VC1921	0.01	0.02	0.02	0.04
VC1922	0.06	0.05	0.05	0.05
VC1923	0.06	0.06	0.08	0.08
VC1924	0.06	0.05	0.05	0.02
VC1925	0.07	0.07	0.07	0.05
VC1926	0.04	0.04	0.10	0.09
VC1927	0.05	0.06	0.04	0.04
VC1928	0.03	0.03	0.08	0.06
VC1929	0.09	0.07	0.07	0.09
VC1930	0.05	0.06	0.04	0.04
VC1931	0.06	0.05	0.04	0.05
VC1932	0.02	0.02	0.02	0.04
VC1933	0.11	0.12	0.06	0.05
VC1934	0.10	0.11	0.01	0.02
VC1935	0.01	0.01	0.05	0.06
VC1936	0.02	0.02	0.04	0.05
VC1937	0.05	0.05	0.06	0.06
VC1938	0.03	0.04	0.04	0.07
VC1938	0.02	0.02	0.05	0.04

VC1939	0.03	0.04	0.05	0.05
VC1940	0.05	0.05	0.05	0.04
VC1941	0.06	0.05	0.04	0.05
VC1942	0.00	0.02	0.10	0.11
VC1943	0.04	0.05	0.04	0.05
VC1943	0.06	0.06	0.01	0.03
VC1944	0.06	0.07	0.08	0.08
VC1945	0.06	0.06	0.03	0.04
VC1946	0.05	0.08	0.03	0.05
VC1947	0.03	0.03	0.06	0.06
VC1948	0.05	0.06	0.04	0.05
VC1949	0.08	0.04	0.05	0.05
VC1950	0.03	0.03	0.06	0.05
VC1951	0.05	0.05	0.03	0.03
VC1952	0.04	0.06	0.04	0.04
VC1953	0.08	0.04	0.09	0.14
VC1954	0.02	0.02	0.03	0.04
VC1955	0.02	0.03	0.09	0.04
VC1956	0.04	0.03	0.04	0.03
VC1957	0.08	0.06	0.07	0.07
VC1958	0.06	0.06	0.03	0.03
VC1959	0.03	0.02	0.02	0.06
VC1960	0.04	0.06	0.04	0.04
VC1961	0.05	0.05	0.05	0.07
VC1962	0.01	0.02	0.08	0.07
VC1963	0.07	0.09	0.05	0.04
VC1964	0.08	0.08	0.06	0.04
VC1965	0.06	0.07	0.06	0.07
VC1966	0.04	0.03	0.01	0.02
VC1967	0.01	0.02	0.06	0.06
VC1968	0.06	0.07	0.06	0.06
VC1969	0.05	0.06	0.04	0.05
VC1970	0.02	0.02	0.02	0.02
VC1971	0.03	0.06	0.06	0.05
VC1972	0.08	0.07	0.04	0.04
VC1973	0.06	0.06	0.06	0.06
VC1974	0.06	0.07	0.06	0.05
VC1975	0.07	0.06	0.03	0.02
VC1976	0.01	0.03	0.03	0.04
VC1977	0.02	0.01	0.05	0.05
VC1978	0.02	0.02	0.05	0.06
VC1979	0.02	0.03	0.11	0.11
VC1980	0.03	0.02	0.06	0.06

VC1981	0.03	0.02	0.04	0.06
VC1982	0.06	0.08	0.03	0.03
VC1983	0.08	0.09	0.04	0.04
VC1984	0.03	0.04	0.04	0.02
VC1985	0.09	0.10	0.04	0.05
VC1986	0.03	0.05	0.08	0.05
VC1987	0.02	0.02	0.05	0.05
VC1988	0.05	0.05	0.06	0.04
VC1989	0.03	0.02	0.09	0.07
VC1990	0.05	0.05	0.05	0.04
VC1991	0.03	0.05	0.04	0.04
VC1992	0.04	0.04	0.07	0.06
VC1993	0.03	0.03	0.04	0.06
VC1994	0.05	0.04	0.04	0.04
VC1995	0.03	0.02	0.11	0.11
VC1996	0.05	0.05	0.04	0.03
VC1997	0.06	0.07	0.03	0.03
VC1998	0.07	0.07	0.03	0.02
VC1999	0.06	0.07	0.05	0.03
VC2000	0.03	0.05	0.06	0.06
VC2001	0.05	0.05	0.07	0.05
VC2002	0.01	0.01	0.05	0.05
VC2003	0.07	0.07	0.03	0.04
VC2004	0.06	0.07	0.05	0.04
VC2005	0.09	0.10	0.03	0.04
VC2006	0.06	0.03	0.05	0.04
VC2007	0.06	0.07	0.09	0.08
VC2008	0.05	0.07	0.05	0.04
VC2009	0.07	0.06	0.05	0.05
VC2010	0.06	0.06	0.05	0.06
VC2011	0.01	0.01	0.01	0.01
VC2012	0.03	0.04	0.05	0.03
VC2013	0.03	0.03	0.06	0.04
VC2014	0.09	0.10	0.02	0.03
VC2015	0.06	0.06	0.04	0.03
VC2016	0.04	0.04	0.02	0.02
VC2017	0.06	0.07	0.04	0.04
VC2018	0.08	0.07	0.02	0.02
VC2019	0.06	0.06	0.07	0.04
VC2021	0.06	0.09	0.06	0.05
VC2022	0.06	0.07	0.07	0.05
VC2023	0.04	0.04	0.05	0.05
VC2024	0.00	0.03	0.02	0.03

VC2025	0.04	0.04	0.06	0.06
VC2026	0.04	0.04	0.05	0.05
VC2027	0.04	0.04	0.05	0.07
VC2028	0.05	0.06	0.05	0.06
VC2029	0.05	0.05	0.03	0.04
VC2030	0.01	0.02	0.00	0.01
VC2031	0.00	0.02	0.05	0.04
VC2032	0.03	0.03	0.04	0.04
VC2033	0.05	0.07	0.08	0.09
VC2034	0.07	0.07	0.06	0.07
VC2035	0.04	0.05	0.07	0.06
VC2036	0.03	0.03	0.06	0.03
VC2037	0.09	0.09	0.05	0.07
VC2039	0.06	0.07	0.05	0.05
VC2040	0.06	0.05	0.06	0.06
VC2041	0.00	0.01	0.04	0.07
VC2042	0.10	0.07	0.04	0.06
VC2043	0.04	0.06	0.04	0.05
VC2044	0.05	0.06	0.06	0.07
VC2045	0.02	0.05	0.08	0.06
VC2046	0.04	0.05	0.02	0.04
VC2047	0.06	0.05	0.07	0.09
VC2048	0.03	0.03	0.02	0.02
VC2049	-0.01	0.01	0.04	0.03
VC2051	0.06	0.07	0.04	0.06
VC2052	0.01	0.02	0.05	0.05
VC2053	0.06	0.06	0.03	0.03
VC2054	0.00	0.02	0.03	0.05
VC2055	0.00	0.03	0.03	0.03
VC2056	0.01	0.03	0.01	0.05
VC2057	0.04	0.04	0.04	0.04
VC2058	0.05	0.03	0.04	0.06
VC2059	0.03	0.03	0.07	0.06
VC2060	0.03	0.02	0.05	0.04
VC2061	0.01	0.01	0.05	0.04
VC2062	0.03	0.04	0.04	0.05
VC2063	0.04	0.06	0.06	0.05
VC2064	0.03	0.02	0.05	0.05
VC2065	0.10	0.09	0.04	0.04
VC2066	0.04	0.04	0.21	0.22
VC2067	0.05	0.03	0.04	0.05
VC2068	0.00	0.01	0.03	0.03
VC2069	0.06	0.06	0.05	0.06

VC2070	0.02	0.01	0.05	0.05
VC2071	0.05	0.05	0.04	0.05
VC2072	0.07	0.05	0.05	0.04
VC2073	0.03	0.04	0.03	0.07
VC2074	0.06	0.05	0.02	0.01
VC2075	0.07	0.08	0.03	0.03
VC2076	0.08	0.06	0.08	0.06
VC2077	0.03	0.02	0.05	0.06
VC2078	0.11	0.12	0.04	0.03
VC2079	0.08	0.08	0.02	0.05
VC2080	0.03	0.05	0.04	0.04
VC2081	0.05	0.05	0.05	0.04
VC2082	0.06	0.08	0.04	0.03
VC2083	0.02	0.01	0.09	0.07
VC2084	0.02	0.02	0.03	0.03
VC2085	0.02	0.03	0.01	0.01
VC2086	0.04	0.04	0.01	0.03
VC2087	0.01	0.01	0.06	0.05
VC2088	0.03	0.03	0.07	0.05
VC2089	0.01	0.02	0.15	0.13
VC2090	-0.01	0.02	0.03	0.03
VC2091	0.04	0.04	0.05	0.04
VC2092	0.06	0.06	0.07	0.07
VC2093	0.05	0.06	0.03	0.04
VC2094	0.04	0.04	0.11	0.10
VC2095	0.04	0.05	0.16	0.14
VC2096	0.02	0.03	0.24	0.20
VC2097	0.04	0.04	0.12	0.11
VC2098	0.02	0.03	0.02	0.00
VC2099	0.03	0.02	0.00	0.00
VC2100	0.03	0.04	0.11	0.12
VC2101	0.06	0.06	0.03	0.04
VC2102	0.05	0.07	0.02	0.04
VC2103	0.02	0.01	0.06	0.05
VC2105	0.07	0.08	0.04	0.04
VC2106	0.03	0.03	0.01	0.02
VC2107	0.03	0.02	0.05	0.05
VC2108	0.01	0.03	0.05	0.06
VC2109	0.02	0.02	0.07	0.10
VC2110	0.08	0.05	0.04	0.04
VC2111	0.05	0.06	0.03	0.02
VC2112	0.02	0.03	0.06	0.06
VC2112	0.01	0.01	0.05	0.05

VC2113	0.06	0.06	0.03	0.03
VC2114	0.05	0.06	0.01	0.02
VC2115	0.07	0.05	0.04	0.06
VC2116	0.03	0.03	0.06	0.08
VC2117	0.04	0.05	0.03	0.05
VC2118	0.02	0.03	0.05	0.06
VC2119	0.04	0.03	0.05	0.03
VC2120	0.02	0.03	0.04	0.03
VC2121	0.04	0.04	0.08	0.06
VC2122	0.06	0.07	0.02	0.04
VC2123	0.00	0.00	0.04	0.05
VC2124	0.03	0.05	0.03	0.04
VC2125	0.04	0.04	0.02	0.04
VC2126	0.01	0.01	0.05	0.05
VC2127	0.03	0.03	0.04	0.04
VC2128	0.02	0.02	0.04	0.04
VC2129	0.07	0.08	0.03	0.03
VC2130	-0.01	0.04	0.05	0.04
VC2131	0.06	0.08	0.06	0.08
VC2132	0.06	0.05	0.05	0.04
VC2133	0.01	0.02	0.04	0.04
VC2134	0.02	0.02	0.07	0.05
VC2134	-0.02	0.00	0.04	0.04
VC2135	0.05	0.04	0.10	0.10
VC2136	0.02	0.02	0.04	0.05
VC2137	0.02	0.04	0.15	0.15
VC2138	0.05	0.07	0.06	0.07
VC2139	0.05	0.05	0.08	0.08
VC2140	0.01	0.02	0.04	0.04
VC2141	0.03	0.04	0.06	0.06
VC2142	0.05	0.03	0.03	0.14
VC2143	0.04	0.02	0.07	0.06
VC2144	0.02	0.02	0.09	0.09
VC2145	0.05	0.04	0.11	0.09
VC2146	0.00	0.03	0.00	0.01
VC2147	0.03	0.03	0.03	0.02
VC2148	0.03	0.04	0.04	0.03
VC2149	0.03	0.03	0.06	0.04
VC2150	0.02	0.01	0.06	0.07
VC2151	0.04	0.05	0.04	0.04
VC2152	0.05	0.02	0.08	0.07
VC2153	0.02	0.03	0.04	0.07
VC2154	0.05	0.06	0.03	0.03

VC2155	0.02	0.02	0.05	0.06
VC2156	0.03	0.04	0.08	0.06
VC2157	0.04	0.04	0.03	0.03
VC2158	0.05	0.06	0.06	0.06
VC2159	0.00	0.01	0.10	0.09
VC2160	0.04	0.07	0.08	0.10
VC2161	-0.01	0.00	0.07	0.09
VC2162	0.05	0.05	0.06	0.05
VC2163	0.05	0.06	0.05	0.05
VC2164	0.09	0.09	0.05	0.07
VC2165	0.06	0.06	0.09	0.08
VC2166	0.02	0.03	0.07	0.07
VC2167	0.04	0.04	0.06	0.06
VC2168	0.07	0.07	0.03	0.02
VC2169	0.04	0.05	0.05	0.05
VC2170	0.05	0.05	0.04	0.04
VC2171	0.05	0.05	0.04	0.05
VC2172	0.01	0.01	0.06	0.05
VC2174	0.07	0.07	0.03	0.03
VC2175	0.05	0.05	0.04	0.02
VC2176	0.04	0.05	0.04	0.04
VC2177	-0.01	-0.01	0.06	0.04
VC2178	0.06	0.06	0.04	0.02
VC2179	0.02	0.03	0.02	0.02
VC2180	0.02	0.02	0.08	0.04
VC2181	0.03	0.03	0.03	0.06
VC2182	0.03	0.05	0.04	0.04
VC2183	0.01	0.02	0.01	0.02
VC2184	0.15	0.08	0.02	0.02
VC2185	0.04	0.04	0.03	0.00
VC2186	0.08	0.08	0.06	0.02
VC2187	0.04	0.04	0.05	0.06
VC2188	0.03	0.03	0.06	0.09
VC2189	0.01	0.05	0.05	0.05
VC2190	0.07	0.04	0.05	0.07
VC2191	0.04	0.03	0.05	0.05
VC2192	0.03	0.03	0.04	0.05
VC2193	0.03	0.04	0.03	0.03
VC2194	0.03	0.03	0.04	0.03
VC2195	0.01	0.11	0.03	0.04
VC2196	0.03	0.04	0.04	0.03
VC2197	0.03	0.03	0.07	0.06
VC2198	0.05	0.05	0.05	0.05

VC2199	0.03	0.03	0.03	0.04
VC2200	0.02	0.03	0.05	0.06
VC2201	0.02	0.04	0.03	0.04
VC2202	0.03	0.07	0.05	0.04
VC2203	0.02	0.03	0.02	0.03
VC2204	0.06	0.07	0.04	0.03
VC2205	0.04	0.07	0.07	0.06
VC2206	0.03	0.10	0.05	0.04
VC2207	0.08	0.09	0.02	0.03
VC2208	0.02	0.02	0.01	0.01
VC2209	0.00	0.01	0.03	0.05
VC2210	0.03	0.04	0.04	0.04
VC2211	0.02	0.02	0.04	0.13
VC2212	0.01	0.02	0.07	0.09
VC2213	0.02	0.03	0.01	0.01
VC2214	0.01	0.01	0.00	0.01
VC2215	0.01	0.02	0.04	0.04
VC2216	0.06	0.06	0.04	0.03
VC2217	0.01	0.01	0.02	0.02
VC2218	0.09	0.08	0.02	0.03
VC2219	0.08	0.06	0.01	0.01
VC2220	0.02	0.03	0.00	0.01
VC2221	0.09	0.07	0.05	0.05
VC2222	0.07	0.07	0.07	0.08
VC2223	0.04	0.05	0.03	0.04
VC2224	0.02	0.02	0.01	0.02
VC2225	0.09	0.08	0.03	0.04
VC2226	0.05	0.06	0.06	0.04
VC2227	0.06	0.05	0.07	0.07
VC2228	0.09	0.08	0.02	0.02
VC2229	0.05	0.07	0.04	0.03
VC2230	0.06	0.06	0.06	0.07
VC2231	0.04	0.05	0.05	0.05
VC2232	0.05	0.08	0.06	0.06
VC2233	0.03	0.02	0.01	0.01
VC2234	0.05	0.06	0.08	0.05
VC2235	0.05	0.07	0.04	0.05
VC2236	0.14	0.13	0.08	0.08
VC2237	0.03	0.03	0.05	0.01
VC2238	0.08	0.08	0.09	0.07
VC2239	0.08	0.09	0.08	0.09
VC2240	0.05	0.06	0.05	0.04
VC2241	0.05	0.06	0.05	0.06

VC2242	0.03	0.03	0.09	0.08
VC2243	0.04	0.06	0.05	0.05
VC2244	0.05	0.06	0.05	0.06
VC2245	0.07	0.07	0.08	0.05
VC2246	0.05	0.06	0.03	0.04
VC2247	0.05	0.05	0.05	0.04
VC2248	0.07	0.07	0.09	0.10
VC2249	0.06	0.08	0.06	0.05
VC2250	0.04	0.04	0.04	0.04
VC2252	0.01	0.02	0.04	0.05
VC2253	0.01	0.02	0.05	0.04
VC2254	0.02	0.03	0.05	0.05
VC2255	0.01	0.02	0.01	0.01
VC2256	0.05	0.06	0.06	0.07
VC2258	0.02	0.02	0.05	0.06
VC2258	0.04	0.05	0.09	0.06
VC2259	0.09	0.09	0.05	0.04
VC2260	0.03	0.03	0.01	0.02
VC2261	0.06	0.07	0.07	0.07
VC2262	0.06	0.06	0.05	0.04
VC2263	0.04	0.09	0.05	0.03
VC2263	0.05	0.06	0.04	0.05
VC2264	0.05	0.05	0.09	0.05
VC2265	0.11	0.13	0.06	0.07
VC2266	0.03	0.05	0.05	0.06
VC2267	0.11	0.09	0.05	0.09
VC2268	0.08	0.07	0.11	0.07
VC2269	0.06	0.04	0.12	0.08
VC2270	0.05	0.05	0.08	0.07
VC2271	0.01	0.01	0.01	0.01
VC2272	0.08	0.06	0.05	0.05
VC2273	0.08	0.06	0.04	0.04
VC2274	0.04	0.04	0.07	0.06
VC2275	0.07	0.07	0.09	0.09
VC2276	0.10	0.11	0.06	0.08
VC2277	0.06	0.08	0.09	0.09
VC2278	0.03	0.05	0.01	0.03
VC2279	0.05	0.05	0.06	0.05
VC2280	0.08	0.07	0.13	0.12
VC2281	0.05	0.05	0.06	0.06
VC2282	0.00	0.02	0.00	0.04
VC2282	0.01	0.05	0.05	0.06
VC2283	0.12	0.15	0.07	0.07

VC2284	0.05	0.04	0.05	0.06
VC2285	-0.02	0.00	-0.01	-0.01
VC2286	0.03	0.05	0.07	0.08
VC2287	0.06	0.03	0.04	0.06
VC2288	0.06	0.06	0.00	0.03
VC2289	0.03	0.03	0.04	0.03
VC2290	0.09	0.07	0.06	0.06
VC2291	0.04	0.05	0.02	0.03
VC2292	0.04	0.05	0.06	0.06
VC2293	0.05	0.05	0.08	0.08
VC2294	0.03	0.03	0.05	0.05
VC2295	0.08	0.07	0.05	0.06
VC2296	0.05	0.06	0.09	0.09
VC2297	0.06	0.06	0.05	0.05
VC2298	0.09	0.07	0.08	0.10
VC2299	0.04	0.05	0.03	0.04
VC2300	0.05	0.06	0.06	0.05
VC2301	0.07	0.08	0.00	0.02
VC2302	0.05	0.06	0.09	0.06
VC2303	0.05	0.05	0.04	0.04
VC2304	0.03	0.03	0.05	0.04
VC2305	0.08	0.07	0.04	0.05
VC2306	0.04	0.05	0.04	0.04
VC2307	0.09	0.08	0.09	0.12
VC2308	0.04	0.04	0.04	0.06
VC2309	0.06	0.06	0.09	0.09
VC2310	0.04	0.04	0.05	0.06
VC2311	0.09	0.09	0.11	0.10
VC2312	0.06	0.06	0.08	0.10
VC2313	0.06	0.07	0.09	0.07
VC2314	0.05	0.04	0.06	0.05
VC2315	0.07	0.09	0.02	0.03
VC2316	0.04	0.04	0.08	0.07
VC2317	0.07	0.08	0.03	0.03
VC2317	0.05	0.05	0.02	0.03
VC2318	0.07	0.08	0.11	0.11
VC2319	-0.01	-0.02	0.04	0.04
VC2320	0.03	0.07	0.12	0.10
VC2321	0.05	0.05	0.05	0.05
VC2322	0.01	0.01	0.04	0.06
VC2323	0.09	0.07	0.05	0.05
VC2324	0.07	0.06	0.07	0.06
VC2325	0.05	0.04	0.05	0.07

VC2326	0.05	0.04	0.08	0.08
VC2327	0.06	0.06	0.06	0.08
VC2328	0.03	0.07	0.07	0.07
VC2329	0.03	0.03	0.08	0.03
VC2330	0.04	0.04	0.08	0.08
VC2331	0.06	0.05	0.03	0.02
VC2331	0.05	0.05	0.05	0.05
VC2332	0.04	0.04	0.08	0.07
VC2333	0.10	0.11	0.05	0.04
VC2334	0.06	0.06	0.04	0.04
VC2335	0.05	0.06	0.10	0.08
VC2336	0.04	0.04	0.06	0.10
VC2337	0.05	0.04	0.08	0.07
VC2338	0.01	0.01	0.05	0.05
VC2339	0.12	0.10	0.07	0.07
VC2340	0.09	0.07	0.08	0.07
VC2341	0.06	0.05	0.03	0.04
VC2342	0.03	0.05	0.04	0.05
VC2343	0.03	0.03	0.12	0.10
VC2344	0.62	0.65	0.58	0.55
VC2345	0.10	0.11	0.05	0.05
VC2346	0.09	0.09	0.08	0.09
VC2347	0.06	0.03	0.05	0.04
VC2348	0.06	0.05	0.08	0.07
VC2349	0.17	0.15	0.07	0.06
VC2350	0.11	0.12	0.08	0.06
VC2351	0.04	0.05	0.05	0.06
VC2352	0.05	0.04	0.07	0.07
VC2353	0.11	0.11	0.05	0.05
VC2354	0.05	0.06	0.12	0.12
VC2355	0.12	0.13	0.05	0.05
VC2356	0.02	0.05	0.01	0.01
VC2356	-0.01	0.03	0.05	0.04
VC2357	0.06	0.07	0.07	0.06
VC2358	0.01	0.01	0.00	0.00
VC2359	0.07	0.07	0.08	0.09
VC2360	0.05	0.07	0.04	0.05
VC2361	0.10	0.10	0.03	0.04
VC2362	0.08	0.09	0.06	0.05
VC2363	0.06	0.05	0.03	0.03
VC2364	0.01	0.01	0.04	0.04
VC2364.1	0.03	0.04	0.04	0.04
VC2364.1	0.06	0.05	0.04	0.04

VC2365	0.14	0.17	0.05	0.07
VC2366	0.13	0.13	0.03	0.03
VC2367	0.08	0.08	0.07	0.08
VC2368	0.12	0.10	0.08	0.08
VC2369	0.13	0.14	0.04	0.05
VC2370	0.23	0.27	0.23	0.24
VC2371	0.15	0.14	0.01	0.03
VC2372	0.11	0.11	0.03	0.02
VC2373	0.02	0.02	0.00	0.04
VC2373	0.01	0.01	0.05	0.06
VC2374	0.12	0.08	0.05	0.04
VC2376	0.03	0.02	0.02	0.02
VC2376	0.02	0.02	0.03	0.05
VC2377	0.04	0.04	0.08	0.07
VC2378	0.12	0.13	0.05	0.02
VC2379	0.10	0.10	0.01	0.00
VC2380	0.08	0.05	0.02	0.00
VC2381	0.04	0.04	0.02	0.01
VC2382	0.07	0.06	0.01	0.01
VC2383	0.06	0.06	0.07	0.06
VC2384	0.09	0.08	0.02	0.01
VC2385	0.04	0.04	0.08	0.06
VC2386	0.11	0.10	0.05	0.05
VC2387	0.10	0.12	0.01	0.01
VC2388	0.11	0.09	0.02	0.01
VC2389	0.03	0.03	0.01	0.03
VC2390	0.02	0.03	0.02	0.03
VC2391	0.10	0.09	0.01	0.00
VC2392	0.11	0.12	0.05	0.02
VC2393	0.05	0.06	0.04	0.05
VC2394	0.03	0.04	0.08	0.06
VC2395	0.20	0.18	-0.02	0.00
VC2396	0.09	0.08	0.00	0.02
VC2397	0.03	0.03	0.03	0.01
VC2398	0.03	0.03	0.03	0.04
VC2399	0.12	0.11	0.02	0.02
VC2400	0.00	0.01	0.01	0.02
VC2401	0.02	0.03	0.06	0.05
VC2402	0.04	0.03	0.04	0.03
VC2403	0.16	0.15	0.04	0.04
VC2404	0.02	0.04	0.05	0.04
VC2405	0.10	0.09	0.06	0.07
VC2406	0.08	0.08	0.05	0.05

VC2408	0.06	0.08	0.05	0.05
VC2409	0.10	0.09	-0.01	0.00
VC2410	0.05	0.06	0.05	0.04
VC2410	0.06	0.08	0.05	0.04
VC2411	0.07	0.06	0.04	0.04
VC2411	0.07	0.09	0.05	0.05
VC2412	0.05	0.04	0.02	0.03
VC2414	0.00	0.01	0.04	0.04
VC2415	0.11	0.10	0.02	0.02
VC2416	0.08	0.08	0.05	0.05
VC2417	0.05	0.04	0.02	0.03
VC2419	0.08	0.09	0.05	0.04
VC2420	0.08	0.05	0.05	0.04
VC2421	0.08	0.08	0.08	0.07
VC2422	0.06	0.05	0.08	0.07
VC2423	0.06	0.04	0.08	0.06
VC2424	0.05	0.04	0.01	0.02
VC2425	0.02	0.02	0.05	0.06
VC2426	0.03	0.03	0.03	0.03
VC2427	0.06	0.05	0.05	0.03
VC2428	0.05	0.06	0.10	0.10
VC2429	0.04	0.05	0.06	0.06
VC2430	0.16	0.20	0.04	0.05
VC2431	0.06	0.07	0.06	0.04
VC2432	0.10	0.09	0.13	0.10
VC2433	0.08	0.08	0.10	0.13
VC2434	0.10	0.07	0.09	0.05
VC2435	0.08	0.07	0.08	0.08
VC2436	0.08	0.05	0.08	0.05
VC2437	0.01	0.02	0.04	0.05
VC2438	0.04	0.02	0.03	0.03
VC2439	0.03	0.06	0.06	0.07
VC2440	0.02	0.02	0.05	0.06
VC2440	0.02	0.03	0.04	0.03
VC2441	0.07	0.05	0.06	0.06
VC2442	0.08	0.07	0.08	0.05
VC2443	0.07	0.07	0.08	0.06
VC2444	0.01	0.02	0.03	0.02
VC2445	0.00	0.02	0.02	0.04
VC2445	0.01	0.03	0.05	0.04
VC2446	0.06	0.06	0.08	0.07
VC2447	0.08	0.06	0.07	0.07
VC2448	0.03	0.03	0.00	0.01

VC2449	0.06	0.06	0.02	0.02
VC2450	0.04	0.04	0.03	0.05
VC2451	0.03	0.04	0.05	0.06
VC2452	0.10	0.11	0.05	0.05
VC2453	0.05	0.06	0.03	0.03
VC2454	-0.01	0.00	-0.01	0.00
VC2455	0.11	0.10	0.05	0.06
VC2456	0.06	0.07	0.06	0.06
VC2457	0.03	0.04	0.06	0.05
VC2458	0.05	0.06	0.12	0.09
VC2459	0.01	0.01	0.10	0.08
VC2460	0.07	0.06	0.05	0.04
VC2461	0.08	0.08	0.10	0.08
VC2462	0.05	0.06	0.05	0.05
VC2463	0.04	0.03	0.06	0.04
VC2464	0.01	0.01	0.10	0.09
VC2465	0.00	0.00	0.02	0.01
VC2466	0.02	0.02	0.07	0.05
VC2467	0.06	0.06	0.05	0.05
VC2468	0.04	0.03	0.07	0.04
VC2469	0.04	0.05	0.07	0.05
VC2470	0.03	0.03	0.03	0.04
VC2471	0.07	0.06	0.03	0.03
VC2472	0.02	0.04	0.05	0.07
VC2473	0.07	0.08	0.03	0.03
VC2474	0.03	0.04	0.06	0.05
VC2475	0.05	0.04	0.03	0.05
VC2476	0.06	0.05	0.02	0.04
VC2478	0.04	0.06	0.05	0.07
VC2479	0.05	0.04	0.06	0.04
VC2480	0.05	0.05	0.09	0.11
VC2481	0.05	0.03	0.03	0.05
VC2482	0.04	0.03	0.06	0.07
VC2483	0.06	0.08	0.06	0.05
VC2484	0.06	0.07	0.05	0.05
VC2485	0.05	0.04	0.05	0.04
VC2486	0.04	0.04	0.08	0.08
VC2487	0.05	0.06	0.03	0.03
VC2488	0.09	0.08	0.03	0.09
VC2489	0.03	0.04	0.03	0.04
VC2490	0.04	0.04	0.05	0.07
VC2491	0.04	0.03	0.06	0.04
VC2492	0.09	0.07	0.06	0.07

VC2493	0.16	0.04	0.05	0.05
VC2494	0.03	0.03	0.03	0.03
VC2495	0.05	0.05	0.07	0.08
VC2496	0.04	0.05	0.07	0.07
VC2497	0.03	0.03	0.08	0.07
VC2498	0.01	0.02	0.03	0.03
VC2499	0.03	0.02	0.06	0.03
VC2500	0.02	0.03	0.01	0.00
VC2501	0.03	0.04	0.09	0.09
VC2502	0.04	0.05	0.07	0.07
VC2503	0.05	0.06	0.05	0.05
VC2504	0.05	0.05	0.09	0.08
VC2505	0.07	0.06	0.05	0.03
VC2506	0.02	0.02	0.06	0.07
VC2507	0.02	0.01	0.04	0.04
VC2508	0.07	0.07	0.07	0.06
VC2509	0.06	0.06	0.04	0.03
VC2511	0.08	0.09	0.06	0.06
VC2512	0.06	0.07	0.07	0.06
VC2513	0.12	0.11	0.06	0.07
VC2514	0.09	0.09	0.12	0.12
VC2515	0.07	0.08	0.05	0.05
VC2516	0.05	0.06	0.04	0.03
VC2517	0.05	0.05	0.09	0.08
VC2518	0.06	0.05	0.03	0.03
VC2519	0.03	0.01	0.04	0.05
VC2520	0.07	0.07	0.05	0.06
VC2521	0.03	0.03	0.04	0.05
VC2522	0.05	0.05	0.06	0.07
VC2523	0.07	0.05	0.02	0.03
VC2524	0.04	0.04	0.03	0.03
VC2525	0.04	0.08	0.03	0.05
VC2527	0.02	0.00	0.05	0.04
VC2528	0.06	0.06	0.04	0.03
VC2529	0.14	0.11	0.21	0.12
VC2530	0.09	0.09	0.06	0.03
VC2531	0.07	0.04	0.05	0.06
VC2532	0.06	0.09	0.06	0.06
VC2534	0.04	0.02	0.05	0.05
VC2535	0.03	0.03	0.05	0.05
VC2536	0.07	0.08	0.04	0.03
VC2537	0.06	0.04	0.05	0.12
VC2538	0.04	0.05	0.09	0.05

VC2539	0.07	0.05	0.08	0.09
VC2540	0.05	0.09	0.05	0.06
VC2541	0.05	0.05	0.05	0.06
VC2542	0.05	0.05	0.05	0.05
VC2543	0.05	0.06	0.07	0.06
VC2544	0.07	0.05	0.08	0.07
VC2545	0.07	0.05	0.08	0.09
VC2546	0.07	0.07	0.05	0.03
VC2547	0.05	0.05	0.04	0.04
VC2547	0.01	0.04	0.04	0.03
VC2548	0.03	0.02	0.05	0.06
VC2549	0.04	0.03	0.08	0.09
VC2551	0.07	0.06	0.04	0.03
VC2552	0.08	0.09	0.05	0.07
VC2553	0.09	0.10	0.07	0.05
VC2554	0.03	0.03	0.06	0.07
VC2555	0.02	0.02	0.03	0.04
VC2557	0.06	0.05	0.03	0.03
VC2558	0.04	0.05	0.05	0.04
VC2559	0.04	0.04	0.02	0.02
VC2560	0.02	0.03	0.04	0.04
VC2561	0.04	0.04	0.03	0.04
VC2562	0.02	0.03	0.03	0.04
VC2563	0.03	0.04	0.06	0.06
VC2564	0.05	0.05	0.04	0.04
VC2565	0.05	0.06	0.06	0.05
VC2566	0.02	0.02	0.05	0.03
VC2567	0.03	0.05	0.04	0.04
VC2568	0.06	0.05	0.08	0.09
VC2569	0.06	0.06	0.05	0.05
VC2570	0.02	0.02	0.07	0.13
VC2571	0.04	0.05	0.06	0.04
VC2572	0.03	0.04	0.02	0.02
VC2573	0.02	0.03	0.02	0.02
VC2574	0.07	0.06	0.07	0.06
VC2575	0.06	0.07	0.06	0.08
VC2576	0.04	0.05	0.04	0.04
VC2578	0.08	0.08	0.06	0.07
VC2579	0.03	0.03	0.08	0.05
VC2580	0.07	0.07	0.05	0.05
VC2581	0.02	0.03	0.07	0.07
VC2582	0.03	0.03	0.04	0.04
VC2583	0.05	0.06	0.09	0.09

VC2584	0.03	0.04	0.03	0.03
VC2585	0.02	0.03	0.01	0.02
VC2586	0.02	0.02	0.07	0.05
VC2587	0.08	0.07	0.07	0.07
VC2588	0.09	0.06	0.04	0.04
VC2589	0.11	0.12	0.05	0.07
VC2590	0.05	0.06	0.03	0.04
VC2591	0.03	0.05	0.04	0.06
VC2592	0.04	0.04	0.05	0.06
VC2593	0.00	0.02	0.03	0.04
VC2594	0.03	0.02	0.04	0.07
VC2595	0.04	0.05	0.02	0.04
VC2596	0.02	0.02	0.06	0.01
VC2597	0.04	0.03	0.01	0.01
VC2598	0.00	0.02	0.04	0.08
VC2599	0.05	0.05	0.08	0.07
VC2600	0.06	0.05	0.02	0.03
VC2601	0.05	0.06	0.03	0.05
VC2602	0.04	0.06	0.04	0.04
VC2603	0.01	0.01	0.06	0.05
VC2604	-0.01	0.01	0.04	0.09
VC2605	0.08	0.09	0.08	0.07
VC2606	0.04	0.09	0.08	0.08
VC2607	0.06	0.07	0.05	0.05
VC2608	0.05	0.03	0.03	0.02
VC2609	0.07	0.05	0.04	0.07
VC2610	0.05	0.05	0.05	0.03
VC2611	0.05	0.05	0.05	0.05
VC2612	0.07	0.07	0.07	0.06
VC2613	0.05	0.06	0.05	0.04
VC2614	0.07	0.06	0.05	0.04
VC2615	0.08	0.06	0.07	0.07
VC2616	0.07	0.06	0.07	0.06
VC2617	0.04	0.04	0.06	0.05
VC2618	0.03	0.03	0.09	0.10
VC2619	0.05	0.05	0.05	0.05
VC2620	0.02	0.03	0.04	0.04
VC2621	0.01	0.02	0.06	0.06
VC2622	0.04	0.05	0.03	0.04
VC2623	0.05	0.05	0.06	0.02
VC2624	0.06	0.05	0.05	0.04
VC2625	0.04	0.03	0.09	0.08
VC2626	0.09	0.08	0.07	0.05

VC2627	0.04	0.03	0.02	0.02
VC2628	0.06	0.05	0.05	0.06
VC2629	0.03	0.03	0.06	0.05
VC2631	0.08	0.06	0.10	0.09
VC2632	0.02	0.01	0.05	0.04
VC2633	0.03	0.03	0.03	0.04
VC2634	0.03	0.05	0.05	0.05
VC2635	0.04	0.05	0.04	0.04
VC2636	0.01	0.00	0.01	0.04
VC2637	0.01	0.04	0.04	0.07
VC2638	0.05	0.05	0.12	0.13
VC2639	0.11	0.08	0.04	0.02
VC2640	0.07	0.07	0.04	0.04
VC2641	0.03	0.04	0.04	0.06
VC2642	0.05	0.04	0.16	0.17
VC2643	0.01	0.01	0.04	0.03
VC2644	0.06	0.06	0.05	0.05
VC2645	0.04	0.04	0.06	0.05
VC2646	0.04	0.05	0.05	0.05
VC2647	0.03	0.05	0.06	0.03
VC2648	0.10	0.07	0.01	0.04
VC2649	0.10	0.08	0.02	0.02
VC2650	0.05	0.05	0.10	0.10
VC2651	0.03	0.04	0.07	0.05
VC2652	0.08	0.06	0.06	0.04
VC2653	0.04	0.03	0.11	0.14
VC2654	0.00	0.00	0.08	0.05
VC2655	0.03	0.04	0.05	0.03
VC2656	0.02	0.00	0.06	0.07
VC2657	0.06	0.05	0.06	0.07
VC2658	0.03	0.02	0.04	0.07
VC2659	0.05	0.05	0.05	0.04
VC2660	0.05	0.05	0.09	0.05
VC2661	0.01	0.01	0.05	0.06
VC2662	0.01	0.01	0.05	0.07
VC2663	0.08	0.05	0.04	0.05
VC2664	0.06	0.06	0.06	0.06
VC2665	0.07	0.08	0.05	0.07
VC2666	0.05	0.05	0.07	0.03
VC2667	0.03	0.04	0.04	0.03
VC2668	0.03	0.04	0.05	0.04
VC2669	0.05	0.04	0.07	0.06
VC2670	0.04	0.04	0.01	0.01

VC2671	0.04	0.05	0.06	0.05
VC2672	0.05	0.05	0.08	0.07
VC2673	0.00	0.01	0.05	0.05
VC2674	0.05	0.06	0.06	0.05
VC2675	0.02	0.02	0.07	0.08
VC2676	0.02	0.02	0.04	0.04
VC2677	0.06	0.06	0.09	0.07
VC2678	0.10	0.11	0.05	0.04
VC2679	0.03	0.03	0.05	0.05
VC2680	0.05	0.05	0.07	0.03
VC2680	0.06	0.07	0.03	0.04
VC2681	0.04	0.05	0.05	0.04
VC2682	0.04	0.04	0.07	0.09
VC2683	0.04	0.05	0.04	0.05
VC2684	0.03	0.06	0.03	0.06
VC2685	0.06	0.07	0.06	0.06
VC2686	0.04	0.04	0.09	0.07
VC2687	0.06	0.08	0.05	0.05
VC2688	0.04	0.04	0.06	0.03
VC2689	0.06	0.07	0.03	0.06
VC2690	0.10	0.11	0.05	0.05
VC2691	0.05	0.04	0.07	0.07
VC2692	0.05	0.07	0.07	0.08
VC2693	0.00	0.03	0.06	0.06
VC2694	0.04	0.05	0.06	0.05
VC2695	0.05	0.06	0.09	0.08
VC2696	0.05	0.03	0.03	0.03
VC2697	0.00	0.01	0.01	0.00
VC2698	0.05	0.05	0.04	0.06
VC2699	0.04	0.03	0.03	0.04
VC2700	0.05	0.05	0.04	0.04
VC2701	0.04	0.05	0.04	0.05
VC2702	0.05	0.04	0.11	0.08
VC2703	0.02	0.01	0.04	0.05
VC2704	0.06	0.06	0.02	0.04
VC2705	-0.01	-0.01	0.05	0.04
VC2706	0.01	0.00	0.07	0.05
VC2708	0.02	0.01	0.04	0.06
VC2709	0.06	0.06	0.06	0.05
VC2710	0.05	0.05	0.06	0.07
VC2711	0.10	0.06	0.06	0.07
VC2712	0.01	0.03	0.04	0.05
VC2713	0.04	0.04	0.08	0.05

VC2714	0.02	0.05	0.06	0.04
VC2715	0.05	0.03	0.05	0.05
VC2716	0.09	0.07	0.07	0.06
VC2717	0.01	0.02	0.06	0.06
VC2718	0.08	0.08	0.02	0.01
VC2719	0.01	0.01	0.10	0.10
VC2720	0.05	0.06	0.06	0.05
VC2721	0.03	0.03	0.04	0.05
VC2722	0.02	0.06	0.06	0.05
VC2723	0.02	0.05	0.05	0.06
VC2724	0.02	0.03	0.00	0.00
VC2725	0.08	0.09	0.04	0.06
VC2726	0.11	0.08	0.04	0.05
VC2727	0.03	0.03	0.05	0.05
VC2728	0.05	0.06	0.06	0.07
VC2729	0.04	0.05	0.04	0.04
VC2730	0.04	0.04	0.06	0.03
VC2731	0.04	0.05	0.04	0.04
VC2732	0.05	0.06	0.04	0.03
VC2733	0.03	0.03	0.03	0.02
VC2734	0.02	0.03	0.04	0.04
VC2735	0.04	0.04	0.07	0.07
VC2736	0.03	0.04	0.05	0.04
VC2737	0.08	0.08	0.01	0.05
VC2738	0.05	0.06	0.04	0.05
VC2739	0.03	0.03	0.03	0.07
VC2740	0.08	0.09	0.06	0.08
VC2741	0.05	0.05	0.03	0.03
VC2742	0.03	0.04	0.05	0.05
VC2743	0.04	0.09	0.06	0.07
VC2744	0.07	0.08	0.06	0.04
VC2745	0.05	0.04	0.04	0.04
VC2746	0.06	0.06	0.04	0.04
VC2747	0.05	0.05	0.04	0.04
VC2748	0.00	0.03	0.05	0.08
VC2749	0.06	0.07	0.07	0.05
VC2750	-0.01	0.00	0.03	0.03
VC2751	0.04	0.03	0.04	0.05
VC2752	0.06	0.05	0.06	0.06
VC2754	0.06	0.07	0.06	-0.04
VC2755	0.05	0.05	0.07	0.07
VC2756	0.07	0.06	0.00	0.01
VC2757	0.08	0.06	0.01	0.01

VC2758	0.08	0.07	0.08	0.07
VC2759	0.02	0.02	0.00	0.02
VC2760	0.03	0.03	0.07	0.06
VC2761	0.02	0.02	0.04	0.05
VC2762	0.10	0.09	0.06	0.08
VC2763	0.03	0.03	0.08	0.06
VC2764	0.03	0.01	0.00	-0.01
VC2765	0.02	0.03	0.06	0.05
VC2767	0.04	0.04	0.03	0.02
VC2768	0.04	0.03	0.00	0.01
VC2769	0.09	0.03	0.07	0.07
VC2770	0.08	0.04	0.04	0.03
VC2771	0.05	0.05	0.05	0.05
VC2772	0.05	0.07	0.10	0.10
VC2773	0.02	0.03	0.04	0.08
VC2774	0.03	0.03	0.05	0.06
VC2775	0.04	0.03	0.06	0.07
VCA0001	0.10	0.05	0.05	0.04
VCA0002	0.02	0.02	0.04	0.04
VCA0003	0.05	0.03	0.07	0.08
VCA0004	0.03	0.04	0.06	0.07
VCA0005	0.02	0.03	0.07	0.07
VCA0006	0.03	0.03	0.02	0.02
VCA0007	0.03	0.04	0.11	0.08
VCA0008	0.04	0.04	0.02	0.02
VCA0009	0.03	0.03	0.03	0.04
VCA0010	0.04	0.03	0.03	0.02
VCA0011	0.02	0.04	0.05	0.05
VCA0012	0.06	0.06	0.05	0.05
VCA0013	0.01	0.04	0.06	0.06
VCA0014	0.04	0.04	0.06	0.06
VCA0016	0.11	0.05	0.04	0.05
VCA0017	0.05	0.06	0.06	0.07
VCA0018	0.03	0.04	0.05	0.04
VCA0019	0.00	0.02	0.06	0.08
VCA0020	0.05	0.05	0.05	0.04
VCA0021	0.03	0.02	0.04	0.03
VCA0022	0.03	0.01	0.03	0.04
VCA0023	0.03	0.03	0.13	0.11
VCA0024	0.03	0.01	0.03	0.03
VCA0025	0.02	0.02	0.02	0.03
VCA0026	0.02	0.03	0.07	0.06
VCA0027	0.07	0.05	0.07	0.06

VCA0028	0.04	0.09	0.05	0.05
VCA0029	0.04	0.06	0.08	0.09
VCA0030	0.06	0.07	0.02	0.07
VCA0031	0.08	0.09	0.03	0.03
VCA0032	0.05	0.07	0.07	0.06
VCA0033	0.04	0.06	0.05	0.04
VCA0034	0.03	0.05	0.04	0.06
VCA0035	0.06	0.09	0.06	0.06
VCA0036	0.15	0.15	0.09	0.05
VCA0037	0.09	0.12	0.06	0.07
VCA0038	0.04	0.05	0.05	0.04
VCA0039	0.03	0.08	0.04	0.06
VCA0040	0.06	0.08	0.06	0.06
VCA0041	0.06	0.06	0.05	0.05
VCA0042	0.58	0.62	0.49	0.55
VCA0043	0.05	0.06	0.08	0.08
VCA0044	0.03	0.07	0.04	0.05
VCA0046	0.03	0.04	0.06	0.06
VCA0047	0.08	0.08	0.07	0.05
VCA0048	0.06	0.12	0.04	0.04
VCA0049	0.04	0.04	0.02	0.00
VCA0050	0.11	0.08	0.04	0.04
VCA0051	0.02	0.01	0.06	0.08
VCA0052	0.04	0.04	0.04	0.05
VCA0053	0.04	0.07	0.06	0.07
VCA0054	0.03	0.05	0.08	0.07
VCA0055	0.05	0.06	0.08	0.06
VCA0056	0.05	0.08	0.06	0.05
VCA0057	0.10	0.10	0.11	0.11
VCA0058	0.07	0.08	0.07	0.05
VCA0060	0.06	0.09	0.04	0.04
VCA0061	0.04	0.04	0.06	0.06
VCA0062	0.04	0.05	0.04	0.03
VCA0062	0.04	0.04	0.06	0.06
VCA0063	0.06	0.09	0.03	0.03
VCA0064	0.03	0.03	0.05	0.06
VCA0065	0.06	0.05	0.05	0.04
VCA0066	0.05	0.04	0.04	0.04
VCA0067	0.04	0.05	0.07	0.05
VCA0068	0.03	0.03	0.06	0.05
VCA0069	0.06	0.07	0.02	0.03
VCA0069	0.05	0.06	0.05	0.05
VCA0070	0.04	0.05	0.09	0.07

VCA0071	0.15	0.13	0.19	0.22
VCA0072	0.07	0.07	0.11	0.09
VCA0073	0.06	0.05	0.09	0.04
VCA0074	0.00	0.02	0.06	0.01
VCA0075	0.02	0.02	0.05	0.05
VCA0076	0.03	0.03	0.02	0.05
VCA0077	0.04	0.03	0.03	0.03
VCA0078	0.04	0.05	0.02	0.01
VCA0079	0.06	0.06	0.07	-0.04
VCA0080	0.13	0.14	-0.01	-0.01
VCA0081	0.06	0.06	0.04	0.04
VCA0082	0.09	0.08	0.09	0.08
VCA0083	0.06	0.05	0.09	0.06
VCA0084	0.07	0.06	0.11	0.08
VCA0085	0.07	0.06	0.11	0.05
VCA0086	0.06	0.06	0.12	0.10
VCA0087	0.07	0.06	0.05	0.04
VCA0089	0.05	0.05	0.03	0.04
VCA0090	0.03	0.03	0.04	0.04
VCA0091	0.07	0.07	0.12	0.09
VCA0092	0.07	0.08	0.09	0.09
VCA0093	0.06	0.10	0.07	0.06
VCA0093	0.06	0.07	0.04	0.05
VCA0094	0.07	0.07	0.10	0.12
VCA0095	0.06	0.06	0.08	0.06
VCA0096	0.02	0.01	0.09	0.09
VCA0097	0.06	0.10	0.06	0.05
VCA0098	0.04	0.04	0.03	0.03
VCA0099	0.07	0.06	0.12	0.09
VCA0100	0.05	0.06	0.09	0.08
VCA0101	0.07	0.05	0.04	0.08
VCA0102	0.05	0.06	0.06	0.05
VCA0103	0.04	0.03	0.02	0.05
VCA0104	0.07	0.06	0.04	0.08
VCA0105	0.05	0.07	0.10	0.08
VCA0106	0.03	0.03	0.05	0.04
VCA0107	0.06	0.06	0.12	0.08
VCA0108	0.02	0.06	0.05	0.04
VCA0109	0.07	0.06	0.09	0.09
VCA0110	0.04	0.03	0.03	0.05
VCA0111	0.03	0.05	0.09	0.06
VCA0112	0.04	0.05	0.06	0.06
VCA0113	0.06	0.05	0.05	0.10

VCA0114	0.06	0.06	0.16	0.09
VCA0115	0.03	0.04	0.01	0.02
VCA0116	0.13	0.09	0.05	0.06
VCA0117	0.08	0.08	0.04	0.08
VCA0118	0.04	0.05	0.09	0.06
VCA0119	0.03	0.04	0.07	0.07
VCA0120	0.03	0.03	0.06	0.06
VCA0121	0.05	0.06	0.12	0.06
VCA0122	0.06	0.05	0.12	0.10
VCA0123	0.05	0.04	0.04	0.04
VCA0124	0.05	0.06	0.15	0.13
VCA0125	0.07	0.07	0.14	0.09
VCA0126	0.07	0.07	0.09	0.07
VCA0127	0.04	0.04	0.04	0.05
VCA0128	0.03	0.03	0.06	0.04
VCA0129	0.03	0.03	0.06	0.06
VCA0130	0.06	0.09	0.07	0.07
VCA0131	0.05	0.05	0.06	0.06
VCA0132	0.06	0.08	0.08	0.07
VCA0133	0.03	0.03	0.03	0.04
VCA0134	0.01	0.02	0.04	0.04
VCA0135	0.08	0.09	0.05	0.05
VCA0136	0.03	0.08	0.05	0.03
VCA0137	0.01	0.02	0.06	0.01
VCA0138	0.08	0.09	0.03	0.03
VCA0139	0.06	0.06	0.10	0.09
VCA0140	0.04	0.07	0.08	0.07
VCA0141	0.01	0.01	0.05	0.05
VCA0142	0.06	0.06	0.04	0.05
VCA0143	0.07	0.07	0.05	0.04
VCA0144	0.03	0.05	0.06	0.05
VCA0145	0.05	0.05	0.04	0.05
VCA0146	0.01	0.00	0.03	0.04
VCA0147	0.05	0.07	0.07	0.09
VCA0148	0.08	0.08	0.07	0.04
VCA0149	0.07	0.09	0.04	0.04
VCA0150	0.06	0.07	0.07	0.07
VCA0151	0.04	0.04	0.05	0.05
VCA0152	0.05	0.06	0.09	0.08
VCA0153	0.04	0.06	0.06	0.04
VCA0154	0.06	0.08	0.05	0.05
VCA0155	0.05	0.07	0.07	0.09
VCA0156	0.05	0.07	0.10	0.10

VCA0157	0.04	0.04	0.04	0.06
VCA0158	0.06	0.07	0.05	0.05
VCA0159	0.06	0.06	0.06	0.08
VCA0160	0.04	0.05	0.05	0.05
VCA0161	0.03	0.05	0.06	0.04
VCA0162	0.07	0.07	0.07	0.06
VCA0163	0.08	0.08	0.06	0.05
VCA0164	0.06	0.08	0.06	0.05
VCA0165	-0.04	-0.02	-0.01	0.01
VCA0166	0.06	0.07	0.06	0.04
VCA0167	0.05	0.05	0.03	0.04
VCA0168	0.04	0.05	0.04	0.06
VCA0171	0.07	0.04	0.04	0.04
VCA0172	0.06	0.08	0.09	0.10
VCA0173	0.07	0.07	0.08	0.06
VCA0174	0.05	0.05	0.09	0.08
VCA0175	0.05	0.06	0.07	0.06
VCA0176	0.12	0.12	0.05	0.06
VCA0177	0.06	0.07	0.09	0.06
VCA0178	0.10	0.09	0.05	0.05
VCA0179	0.04	0.05	0.09	0.09
VCA0180	0.06	0.06	0.05	0.05
VCA0181	0.05	0.08	0.06	0.07
VCA0182	0.08	0.09	0.06	0.05
VCA0183	0.07	0.06	0.12	0.07
VCA0184	0.05	0.06	0.06	0.06
VCA0185	0.06	0.07	0.05	0.05
VCA0186	0.05	0.05	0.04	0.03
VCA0187	0.06	0.07	0.06	0.04
VCA0188	0.03	0.05	0.04	0.03
VCA0189	0.04	0.04	0.06	0.03
VCA0190	0.05	0.04	0.03	0.05
VCA0191	0.01	0.04	0.07	0.06
VCA0192	0.00	-0.01	0.05	0.07
VCA0193	0.01	0.01	0.05	0.05
VCA0194	0.00	0.01	0.07	0.06
VCA0195	0.06	0.07	0.02	0.02
VCA0196	0.05	0.05	0.03	0.02
VCA0197	0.04	0.04	0.07	0.05
VCA0199	0.06	0.06	0.07	0.05
VCA0200	0.01	0.01	0.03	0.03
VCA0201	0.01	0.01	0.08	0.08
VCA0202	0.05	0.05	0.05	0.06

VCA0203	0.04	0.05	0.04	-0.09
VCA0204	0.06	0.06	0.08	0.08
VCA0205	0.03	0.05	0.05	0.04
VCA0206	0.10	0.04	0.10	0.07
VCA0207	0.04	0.04	0.09	0.09
VCA0208	0.03	0.03	0.04	0.05
VCA0209	0.05	0.02	0.09	0.07
VCA0210	0.11	0.09	0.27	0.23
VCA0211	0.00	0.01	0.05	0.06
VCA0212	0.00	0.01	0.03	0.04
VCA0213	0.03	0.02	0.06	0.05
VCA0214	0.00	0.01	0.04	0.04
VCA0214	-0.01	0.00	0.04	0.05
VCA0215	0.02	0.10	0.04	0.05
VCA0216	0.01	0.02	0.00	0.05
VCA0216	0.01	0.03	0.04	0.03
VCA0217	0.03	0.04	0.05	0.04
VCA0218	0.02	0.02	0.06	0.06
VCA0219	0.04	0.04	0.06	0.04
VCA0220	0.00	0.01	0.06	0.05
VCA0221	0.03	0.03	0.02	0.02
VCA0222	0.01	0.01	0.06	0.04
VCA0224	0.03	0.04	0.05	0.03
VCA0225	0.07	0.07	0.07	0.09
VCA0226	0.04	0.04	0.06	0.05
VCA0227	0.02	0.03	0.04	0.04
VCA0228	0.01	0.02	0.05	0.05
VCA0229	0.04	0.06	0.04	0.04
VCA0230	0.04	0.06	0.10	0.10
VCA0231	0.03	0.03	0.05	0.04
VCA0232	0.01	0.02	0.05	0.02
VCA0233	-0.02	0.01	0.05	0.05
VCA0233	0.01	0.01	0.06	0.05
VCA0234	0.03	0.04	0.03	0.04
VCA0235	0.05	0.05	0.06	0.06
VCA0236	0.03	0.03	0.04	0.02
VCA0237	0.05	0.01	0.06	0.05
VCA0238	0.03	0.01	0.05	0.05
VCA0239	0.05	0.05	0.10	0.10
VCA0240	0.03	0.03	0.08	0.07
VCA0241	0.02	0.03	0.07	0.07
VCA0242	0.04	0.05	0.13	0.10
VCA0243	0.03	0.04	0.05	0.05

VCA0244	0.05	0.05	0.06	0.06
VCA0245	0.04	0.05	0.04	0.04
VCA0246	0.09	0.09	0.04	0.04
VCA0247	0.00	0.00	0.07	0.06
VCA0248	-0.02	-0.01	0.04	0.02
VCA0249	-0.01	-0.01	0.06	0.04
VCA0250	0.02	0.02	0.06	0.04
VCA0251	0.04	0.06	0.02	0.02
VCA0252	0.05	0.07	0.05	0.06
VCA0253	0.05	0.06	0.04	0.04
VCA0255	0.01	0.02	0.05	0.05
VCA0256	0.07	0.06	0.06	0.06
VCA0258	0.05	0.05	0.05	0.07
VCA0259	0.08	0.06	0.03	0.02
VCA0260	0.07	0.07	0.08	0.04
VCA0262	0.05	0.10	0.04	0.04
VCA0263	0.07	0.05	0.08	0.09
VCA0264	0.02	0.03	0.05	0.05
VCA0265	0.03	0.03	0.05	0.05
VCA0266	0.03	0.13	0.04	0.04
VCA0267	0.02	0.03	0.04	0.03
VCA0268	0.02	0.03	0.04	0.02
VCA0269	0.05	0.06	0.04	0.04
VCA0270	0.03	0.03	0.02	0.08
VCA0271	0.04	0.04	0.05	0.05
VCA0272	0.05	0.05	0.05	0.03
VCA0273	0.06	0.07	0.07	0.02
VCA0274	0.04	0.03	0.04	0.04
VCA0275	0.07	0.08	0.04	0.03
VCA0276	0.05	0.04	0.04	0.04
VCA0277	0.04	0.04	0.06	0.05
VCA0278	0.03	0.05	0.04	0.04
VCA0279	0.05	0.06	0.07	0.07
VCA0280	0.03	0.03	0.03	0.04
VCA0281	0.01	0.02	0.04	0.04
VCA0282	0.02	0.03	0.01	0.03
VCA0283	0.05	0.06	0.04	0.06
VCA0284	0.07	0.07	0.04	0.07
VCA0285	0.07	0.08	0.04	0.03
VCA0286	0.07	0.06	0.04	0.02
VCA0287	0.03	0.02	0.09	0.08
VCA0288	0.08	0.07	0.05	0.06
VCA0289	0.08	0.07	0.04	0.04

VCA0290	0.04	0.05	0.07	0.07
VCA0291	0.06	0.07	0.05	0.05
VCA0292	0.07	0.05	0.04	0.04
VCA0294	0.07	0.07	0.05	0.04
VCA0295	0.07	0.06	0.02	0.05
VCA0296	0.10	0.10	0.03	0.05
VCA0297	0.07	0.06	0.02	0.03
VCA0298	0.07	0.07	0.08	0.08
VCA0299	0.10	0.09	0.07	0.06
VCA0300	0.09	0.07	0.05	0.02
VCA0301	0.09	0.07	0.10	0.09
VCA0303	0.07	0.08	0.05	0.04
VCA0304	0.08	0.07	0.14	0.16
VCA0305	0.01	0.03	0.06	0.06
VCA0306	0.07	0.07	0.06	0.06
VCA0307	0.03	0.02	0.05	0.06
VCA0307	-0.01	0.00	0.08	0.07
VCA0308	0.03	0.02	0.09	0.07
VCA0308	0.01	0.00	0.05	0.05
VCA0309	0.10	0.09	0.09	0.10
VCA0310	0.07	0.07	0.04	0.04
VCA0312	0.08	0.06	0.05	0.04
VCA0313	0.11	0.09	0.06	0.03
VCA0314	0.10	0.08	0.06	0.06
VCA0315	0.07	0.06	0.07	0.05
VCA0316	0.07	0.06	0.06	0.06
VCA0317	0.08	0.07	0.03	0.04
VCA0319	0.07	0.07	0.04	0.07
VCA0320	0.06	0.08	0.06	0.08
VCA0321	0.09	0.08	0.04	0.07
VCA0322	0.13	0.10	0.05	0.04
VCA0323	0.04	0.04	0.00	0.01
VCA0324	0.01	0.01	0.07	0.07
VCA0326	0.06	0.08	0.03	0.04
VCA0327	0.02	0.02	0.08	0.07
VCA0328	0.00	0.01	0.14	0.12
VCA0329	0.04	0.06	0.08	0.07
VCA0330	0.01	0.01	0.07	0.06
VCA0331	0.03	0.03	0.04	0.04
VCA0333	0.07	0.06	0.07	0.05
VCA0334	0.02	0.02	0.06	0.04
VCA0335	0.06	0.06	0.01	0.02
VCA0336	0.05	0.06	0.04	0.04

VCA0337	0.02	0.01	0.13	0.08
VCA0338	0.02	0.02	0.03	0.05
VCA0338	0.01	0.02	0.04	0.06
VCA0339	0.04	0.06	0.03	0.04
VCA0340	-0.01	-0.01	0.18	0.14
VCA0341	0.02	0.02	0.04	0.04
VCA0341	-0.02	-0.01	0.05	0.06
VCA0342	0.02	0.01	0.11	0.09
VCA0343	0.06	0.05	0.05	0.03
VCA0344	0.04	0.04	0.04	0.02
VCA0345	0.00	0.00	0.10	0.07
VCA0346	0.13	0.01	0.02	0.02
VCA0347	0.03	0.04	0.05	0.06
VCA0349	0.01	0.02	0.03	0.05
VCA0349	0.01	0.03	0.04	0.05
VCA0350	0.05	0.07	0.05	0.02
VCA0351	0.00	0.00	0.08	0.08
VCA0352	0.02	0.03	0.00	0.03
VCA0353	0.05	0.06	0.06	0.05
VCA0354	0.03	0.04	0.03	0.02
VCA0355	0.11	0.04	0.06	0.14
VCA0356	0.02	0.02	0.08	0.08
VCA0357	0.05	0.05	0.05	0.02
VCA0358	0.02	0.01	0.06	0.07
VCA0359	0.08	0.05	0.04	0.03
VCA0360	0.09	0.10	0.04	0.03
VCA0361	0.11	0.10	0.03	0.04
VCA0362	0.06	0.07	0.03	0.03
VCA0363	0.06	0.05	0.05	0.07
VCA0364	0.07	0.07	0.03	0.03
VCA0366	0.07	0.07	0.08	0.07
VCA0367	0.06	0.05	0.04	0.09
VCA0368	0.06	0.06	0.03	0.07
VCA0369	0.07	0.07	0.07	0.05
VCA0370	0.06	0.06	0.09	0.12
VCA0371	0.03	0.02	0.09	0.08
VCA0372	0.13	0.12	0.06	0.06
VCA0373	0.06	0.07	0.05	0.05
VCA0374	0.01	0.03	0.05	0.04
VCA0376	0.07	0.08	0.02	0.02
VCA0379	0.07	0.09	0.07	0.10
VCA0379	0.02	0.03	0.04	0.05
VCA0380	0.03	0.03	0.04	0.05

VCA0381	0.04	0.07	0.03	0.02
VCA0382	0.06	0.05	0.10	0.08
VCA0383	0.06	0.07	0.06	0.06
VCA0384	0.06	0.06	0.03	0.02
VCA0386	0.03	0.04	0.10	0.13
VCA0387	0.03	0.03	0.01	0.02
VCA0388	0.04	0.07	0.03	0.09
VCA0389	0.02	0.03	0.04	0.03
VCA0390	0.06	0.11	0.02	0.02
VCA0391	0.03	0.03	0.06	0.07
VCA0392	0.04	0.04	0.13	0.09
VCA0393	0.04	0.03	0.04	0.02
VCA0394	0.08	0.09	0.02	0.02
VCA0395	0.03	0.02	0.04	0.04
VCA0396	0.04	0.01	0.03	0.08
VCA0397	0.05	0.05	0.05	0.05
VCA0398	0.05	0.10	0.06	0.06
VCA0400	0.01	0.02	0.10	0.06
VCA0401	0.03	0.03	0.05	0.09
VCA0401	0.01	0.04	0.04	0.04
VCA0402	0.17	0.19	0.03	0.03
VCA0403	0.03	0.04	0.05	0.03
VCA0404	0.10	0.08	0.05	0.07
VCA0405	0.03	0.06	0.06	0.07
VCA0406	0.03	0.04	0.05	0.06
VCA0407	0.05	0.06	0.04	0.03
VCA0408	0.06	0.05	0.15	0.11
VCA0409	0.10	0.09	0.03	0.03
VCA0410	0.12	0.07	0.07	0.09
VCA0411	0.06	0.06	0.06	0.03
VCA0412	0.04	0.05	0.05	0.05
VCA0413	0.04	0.06	0.07	0.07
VCA0414	0.02	0.02	0.05	0.04
VCA0415	0.06	0.08	0.08	0.08
VCA0417	0.07	0.06	0.09	0.08
VCA0418	0.04	0.05	0.06	0.05
VCA0419	0.04	0.05	0.04	0.03
VCA0420	0.04	0.02	0.05	0.04
VCA0421	0.06	0.05	0.04	0.04
VCA0422	0.10	0.06	0.06	0.05
VCA0423	0.03	0.04	0.05	0.06
VCA0424	0.02	0.02	0.02	0.03
VCA0425	0.04	0.03	0.06	0.04

VCA0426	0.05	0.05	0.05	0.05
VCA0427	0.05	0.06	0.06	0.04
VCA0428	0.05	0.07	0.07	0.06
VCA0429	0.05	0.06	0.05	0.06
VCA0430	0.04	0.06	0.06	0.05
VCA0431	0.03	0.04	0.05	0.04
VCA0432	0.05	0.05	0.10	0.09
VCA0433	0.15	0.03	0.03	0.02
VCA0434	0.05	0.05	0.07	0.06
VCA0435	0.05	0.04	0.06	0.06
VCA0436	0.03	0.03	0.07	0.08
VCA0437	0.04	0.05	0.04	0.02
VCA0437	0.05	0.05	0.06	0.08
VCA0438	0.05	0.07	0.02	0.02
VCA0439	0.04	0.04	0.06	0.07
VCA0440	0.04	0.04	0.04	0.02
VCA0441	0.03	0.04	0.08	0.08
VCA0442	0.03	0.03	0.04	0.03
VCA0443	0.01	0.03	0.07	0.06
VCA0445	0.04	0.04	0.05	0.03
VCA0446	0.06	0.06	0.05	0.05
VCA0447	0.02	0.04	0.04	0.04
VCA0448	0.02	0.03	0.06	0.02
VCA0449	0.08	0.09	0.05	0.04
VCA0450	0.03	0.03	0.06	0.04
VCA0451	0.02	0.04	0.07	0.03
VCA0453	0.08	0.07	0.09	0.06
VCA0454	0.04	0.04	0.13	0.13
VCA0455	0.02	0.02	0.04	0.05
VCA0456	0.07	0.07	0.03	0.03
VCA0457	0.02	0.03	0.04	0.03
VCA0458	0.08	0.06	0.03	0.03
VCA0459	0.04	0.04	0.02	0.02
VCA0460	0.03	0.03	0.05	0.09
VCA0461	0.07	0.08	0.05	0.06
VCA0462	0.06	0.07	0.04	0.03
VCA0463	0.04	0.05	0.07	0.06
VCA0464	0.03	0.06	0.04	0.04
VCA0465	0.02	0.03	0.05	0.04
VCA0466	0.06	0.06	0.07	0.06
VCA0467	0.06	0.06	0.06	0.05
VCA0468	0.06	0.06	0.06	0.05
VCA0469	0.05	0.08	0.03	0.04

VCA0470	0.05	0.06	0.06	0.05
VCA0471	0.06	0.07	0.05	0.04
VCA0472	0.03	0.03	0.10	0.09
VCA0473	0.06	0.09	0.07	0.07
VCA0474	0.06	0.07	0.07	0.08
VCA0476	0.05	0.06	0.07	0.08
VCA0477	0.02	0.04	0.04	0.05
VCA0479	0.04	0.05	0.06	0.04
VCA0481	0.01	0.03	-0.02	-0.03
VCA0482	0.02	0.02	0.06	0.07
VCA0483	0.04	0.06	0.06	0.05
VCA0484	0.07	0.07	0.06	0.06
VCA0485	0.03	0.03	0.05	0.06
VCA0487	0.04	0.05	0.04	0.04
VCA0488	0.03	0.06	0.06	0.06
VCA0490	0.02	0.05	0.04	0.04
VCA0491	0.03	0.05	0.04	0.04
VCA0492	0.05	0.05	0.07	0.05
VCA0493	0.04	0.04	0.06	0.05
VCA0494	0.07	0.06	0.09	0.06
VCA0495	0.05	0.06	0.05	0.05
VCA0496	0.09	0.07	0.05	0.09
VCA0498	0.05	0.09	0.06	0.06
VCA0499	0.06	0.06	0.05	0.06
VCA0500	0.07	0.08	0.09	0.07
VCA0501	0.01	0.02	0.05	0.05
VCA0502	0.04	0.06	0.05	0.06
VCA0505	0.03	0.06	0.06	0.04
VCA0506	0.03	0.03	0.07	0.05
VCA0507	-0.01	0.00	0.03	0.05
VCA0508	0.01	0.03	0.05	0.05
VCA0509	0.02	0.03	0.05	0.04
VCA0510	0.03	0.03	0.07	0.05
VCA0511	0.04	0.04	0.07	0.06
VCA0512	0.04	0.05	0.04	0.06
VCA0513	0.03	0.03	0.05	0.07
VCA0514	0.06	0.08	0.03	0.02
VCA0515	0.08	0.10	0.03	0.03
VCA0516	0.02	0.01	0.06	0.08
VCA0517	-0.01	-0.01	0.04	0.06
VCA0518	0.03	0.03	0.07	0.08
VCA0519	0.00	0.01	0.05	0.04
VCA0520	0.03	0.01	0.02	0.04

VCA0521	0.09	0.05	0.07	0.08
VCA0522	0.09	0.08	0.07	0.06
VCA0523	0.03	0.03	0.06	0.06
VCA0524	0.07	0.06	0.03	0.03
VCA0525	0.09	0.09	0.00	0.01
VCA0526	0.03	0.05	0.02	0.02
VCA0527	0.03	0.02	0.08	0.08
VCA0528	0.03	0.03	0.06	0.09
VCA0529	0.00	0.01	0.06	0.05
VCA0530	0.03	0.04	0.04	0.05
VCA0531	0.05	0.04	0.05	0.04
VCA0532	0.04	0.05	0.04	0.03
VCA0533	0.02	0.02	0.04	0.06
VCA0534	0.02	0.05	0.05	0.05
VCA0535	0.04	0.04	0.06	0.06
VCA0538	0.03	0.03	0.07	0.07
VCA0539	0.03	0.04	0.17	0.12
VCA0540	0.00	0.00	0.05	0.05
VCA0541	0.09	0.08	0.03	0.03
VCA0542	0.03	0.02	0.06	0.05
VCA0543	0.02	0.03	0.09	0.08
VCA0546	0.04	0.05	0.15	0.14
VCA0547	0.09	0.08	0.04	0.04
VCA0548	0.07	0.08	0.01	0.05
VCA0549	0.05	0.05	0.15	0.14
VCA0550	0.01	0.01	0.15	0.14
VCA0551	0.04	0.02	0.03	0.04
VCA0552	0.05	0.05	0.07	0.07
VCA0553	0.04	0.03	0.05	0.04
VCA0554	0.02	0.00	0.04	0.04
VCA0555	0.04	0.06	0.01	0.02
VCA0556	0.04	0.02	0.04	0.03
VCA0557	-0.01	-0.01	-0.02	-0.01
VCA0558	0.03	0.05	0.03	0.03
VCA0559	-0.01	-0.01	0.03	0.03
VCA0560	0.01	0.00	0.06	0.06
VCA0561	0.07	0.10	0.05	0.05
VCA0562	0.05	0.06	0.04	0.05
VCA0563	0.02	0.03	0.04	0.04
VCA0564	0.02	0.02	0.04	0.05
VCA0565	0.02	0.03	0.06	0.06
VCA0566	0.06	0.07	0.04	0.02
VCA0567	0.04	0.04	0.08	0.12

VCA0568	0.06	0.07	0.05	0.05
VCA0569	0.08	0.07	0.04	0.05
VCA0570	0.08	0.08	0.07	0.04
VCA0571	0.04	0.04	0.02	0.09
VCA0572	0.05	0.06	0.06	0.05
VCA0573	0.07	0.07	0.06	0.05
VCA0574	0.04	0.04	0.05	0.05
VCA0575	0.11	0.11	0.08	0.07
VCA0576	0.02	0.03	0.04	0.05
VCA0577	0.09	0.08	0.03	0.02
VCA0578	0.04	0.05	0.03	0.04
VCA0579	0.07	0.05	0.06	0.03
VCA0580	0.03	0.03	0.02	0.04
VCA0581	0.03	0.03	0.03	0.06
VCA0582	0.04	0.06	0.06	0.06
VCA0583	0.04	0.03	0.04	0.02
VCA0584	0.08	0.06	0.05	0.05
VCA0585	0.04	0.05	0.02	0.04
VCA0586	0.07	0.05	0.08	0.11
VCA0587	0.08	0.08	0.07	0.06
VCA0588	0.06	0.05	0.05	0.04
VCA0589	0.02	0.02	0.00	0.01
VCA0590	0.02	0.03	0.04	0.03
VCA0591	0.04	0.06	0.04	0.06
VCA0592	0.06	0.07	0.04	0.04
VCA0593	0.56	0.55	0.58	0.52
VCA0594	0.04	0.05	0.05	0.06
VCA0595	0.06	0.07	0.08	0.05
VCA0596	0.06	0.06	0.06	0.05
VCA0597	0.04	0.05	0.02	0.02
VCA0598	0.05	0.06	0.06	0.04
VCA0599	0.05	0.07	0.07	0.07
VCA0600	0.10	0.08	0.06	0.06
VCA0601	0.03	0.03	0.05	0.08
VCA0602	0.00	0.03	0.04	0.03
VCA0603	0.06	0.09	0.11	0.07
VCA0604	0.04	0.05	0.03	0.04
VCA0605	0.02	0.01	0.06	0.06
VCA0606	0.13	0.06	0.08	0.09
VCA0607	0.09	0.09	0.07	0.06
VCA0608	0.03	0.04	0.04	0.04
VCA0609	0.05	0.06	0.04	0.05
VCA0610	0.04	0.07	0.05	0.05

VCA0611	0.06	0.07	0.02	0.04
VCA0612	0.05	0.07	0.03	0.03
VCA0613	0.07	0.07	0.05	0.04
VCA0614	0.05	0.06	0.06	0.09
VCA0615	0.03	0.06	0.04	0.06
VCA0616	0.04	0.04	0.04	0.05
VCA0617	0.06	0.07	0.05	0.05
VCA0618	0.08	0.04	0.05	0.05
VCA0619	0.04	0.02	0.08	0.05
VCA0620	0.06	0.06	0.11	0.09
VCA0621	0.10	0.11	0.05	0.11
VCA0622	0.07	0.06	0.05	0.05
VCA0623	0.09	0.08	0.08	0.06
VCA0624	0.04	0.04	0.05	0.16
VCA0626	0.06	0.06	0.09	0.06
VCA0627	0.05	0.05	0.05	0.05
VCA0628	0.01	0.02	0.03	0.06
VCA0629	0.05	0.05	0.04	0.04
VCA0630	0.09	0.07	0.13	0.11
VCA0631	0.08	0.10	0.10	0.08
VCA0632	0.07	0.08	0.03	0.04
VCA0633	0.03	0.03	0.08	0.06
VCA0634	0.10	0.08	0.07	0.09
VCA0635	0.07	0.08	0.09	0.07
VCA0636	0.05	0.06	0.07	0.08
VCA0637	0.05	0.06	0.06	0.07
VCA0638	0.02	0.03	0.04	0.04
VCA0639	0.08	0.05	0.07	0.04
VCA0640	0.07	0.10	0.09	0.09
VCA0641	0.08	0.06	0.10	0.13
VCA0642	0.08	0.07	0.09	0.08
VCA0644	0.06	0.06	0.11	0.05
VCA0645	0.06	0.10	0.08	0.07
VCA0646	0.05	0.06	0.04	0.05
VCA0647	0.07	0.07	0.10	0.09
VCA0648	0.05	0.05	0.04	0.03
VCA0649	0.08	0.08	0.11	0.08
VCA0650	0.05	0.06	0.04	0.05
VCA0651	0.05	0.04	0.06	0.04
VCA0652	0.07	0.06	0.06	0.07
VCA0653	0.05	0.04	0.07	0.05
VCA0654	0.04	0.07	0.13	0.10
VCA0655	0.07	0.07	0.05	0.05

VCA0656	0.06	0.05	0.07	0.08
VCA0657	0.10	0.10	0.03	0.03
VCA0658	0.05	0.04	0.05	0.05
VCA0659	0.06	0.05	0.06	0.08
VCA0660	0.05	0.06	0.06	0.05
VCA0661	0.06	0.05	0.06	0.07
VCA0662	0.06	0.05	0.06	0.06
VCA0663	0.04	0.03	0.04	0.03
VCA0664	0.05	0.04	0.04	0.07
VCA0665	0.06	0.07	0.07	0.07
VCA0666	0.05	0.06	0.04	0.02
VCA0667	0.05	0.05	0.05	0.04
VCA0668	0.04	0.04	0.03	0.03
VCA0669	0.05	0.06	0.07	0.07
VCA0670	0.08	0.09	0.14	0.16
VCA0671	0.03	0.03	0.10	0.10
VCA0672	0.05	0.06	0.02	0.03
VCA0673	0.05	0.04	0.06	0.06
VCA0674	0.02	0.02	0.07	0.06
VCA0675	0.04	0.04	0.03	0.03
VCA0676	0.04	0.06	0.05	0.05
VCA0677	0.05	0.03	0.09	0.09
VCA0678	0.02	0.02	0.04	0.06
VCA0678	0.01	0.01	0.05	0.04
VCA0679	0.06	0.07	0.08	0.07
VCA0680	0.06	0.05	0.07	0.06
VCA0681	0.54	0.62	0.61	0.62
VCA0682	0.06	0.06	0.04	0.05
VCA0683	0.06	0.06	0.07	0.05
VCA0684	0.03	0.04	0.07	0.07
VCA0685	0.07	0.06	0.08	0.12
VCA0686	0.05	0.06	0.05	0.05
VCA0687	0.04	0.05	0.09	0.08
VCA0688	0.07	0.06	0.03	0.03
VCA0689	0.04	0.04	0.11	0.10
VCA0690	0.04	0.04	0.08	0.07
VCA0691	0.05	0.05	0.07	0.14
VCA0692	0.01	0.04	0.02	0.04
VCA0693	0.00	0.01	0.02	0.02
VCA0694	0.06	0.05	0.08	0.06
VCA0695	0.04	0.03	0.07	0.11
VCA0696	0.07	0.04	0.03	0.03
VCA0696	0.03	0.03	0.02	0.03

VCA0697	0.01	0.01	0.10	0.09
VCA0698	0.07	0.06	0.03	0.03
VCA0699	0.05	0.05	0.08	0.06
VCA0700	0.05	0.05	0.05	0.05
VCA0701	0.05	0.06	0.06	0.06
VCA0702	0.09	0.10	0.11	0.09
VCA0703	0.05	0.04	0.06	0.04
VCA0704	0.05	0.04	0.08	0.07
VCA0705	0.03	0.04	0.03	0.04
VCA0706	0.03	0.03	0.05	0.05
VCA0707	0.03	0.03	0.13	0.12
VCA0708	0.05	0.04	0.06	0.04
VCA0709	0.02	0.02	0.03	0.03
VCA0710	0.08	0.07	0.05	0.06
VCA0711	0.08	0.05	0.04	0.07
VCA0712	0.10	0.09	0.07	0.06
VCA0713	0.06	0.05	0.07	0.07
VCA0714	0.08	0.07	0.05	0.05
VCA0715	0.04	0.05	0.06	0.07
VCA0716	0.04	0.02	0.07	0.05
VCA0717	0.03	0.05	0.04	0.14
VCA0718	0.07	0.08	0.03	0.03
VCA0719	0.12	0.13	0.05	0.05
VCA0720	0.01	0.01	0.14	0.12
VCA0721	0.06	0.07	0.04	0.06
VCA0722	0.12	0.14	0.06	0.05
VCA0723	0.04	0.02	0.06	0.05
VCA0724	0.03	0.04	0.02	0.02
VCA0724	0.01	0.05	0.07	0.04
VCA0725	0.05	0.06	0.06	0.06
VCA0726	0.04	0.08	0.04	0.03
VCA0727	0.04	0.06	0.04	0.05
VCA0728	0.05	0.06	0.06	0.05
VCA0729	0.10	0.07	0.06	0.06
VCA0730	0.04	0.04	0.05	0.05
VCA0730	0.01	-0.02	0.08	0.04
VCA0731	0.14	0.12	0.03	0.03
VCA0732	0.03	0.03	0.07	0.04
VCA0733	0.09	0.09	0.06	0.07
VCA0734	0.08	0.08	0.05	0.06
VCA0735	0.12	0.13	0.23	0.24
VCA0736	0.01	0.02	0.04	0.05
VCA0737	0.14	0.11	0.02	0.02

VCA0738	0.05	0.06	0.02	0.01
VCA0739	0.15	0.16	0.05	0.04
VCA0740	0.15	0.13	-0.01	0.01
VCA0741	0.09	0.08	0.05	0.04
VCA0742	0.06	0.06	0.03	0.05
VCA0743	0.13	0.12	0.02	0.01
VCA0744	0.11	0.12	0.12	0.13
VCA0745	0.02	0.03	0.04	0.03
VCA0746	0.12	0.11	0.04	0.01
VCA0747	0.07	0.05	0.04	0.03
VCA0748	0.12	0.12	0.02	0.04
VCA0749	0.12	0.09	0.02	0.01
VCA0750	0.07	0.07	0.05	0.05
VCA0750	0.07	0.07	0.03	0.05
VCA0751	0.09	0.09	-0.01	0.01
VCA0752	0.13	0.12	-0.01	0.00
VCA0753	0.08	0.06	0.04	0.04
VCA0754	0.08	0.07	0.00	0.01
VCA0755	0.10	0.09	0.03	0.02
VCA0756	0.10	0.10	0.00	0.02
VCA0757	0.12	0.12	0.01	0.01
VCA0758	0.12	0.09	0.00	0.01
VCA0759	0.13	0.11	0.01	0.00
VCA0760	0.15	0.12	0.01	0.01
VCA0761	0.12	0.09	0.02	0.02
VCA0762	0.05	0.06	0.05	0.06
VCA0763	0.10	0.10	0.07	0.07
VCA0764	0.06	0.05	0.05	0.05
VCA0765	0.13	0.10	0.03	0.01
VCA0766	0.15	0.13	-0.01	-0.01
VCA0767	0.08	0.09	0.03	0.02
VCA0768	0.13	0.13	0.02	0.02
VCA0769	0.12	0.11	0.00	0.00
VCA0770	0.06	0.05	0.06	0.05
VCA0770	0.06	0.06	0.04	0.05
VCA0771	0.06	0.07	0.05	0.04
VCA0772	0.10	0.07	0.02	0.02
VCA0773	0.09	0.10	0.08	0.08
VCA0774	0.05	0.04	0.04	0.04
VCA0775	0.03	0.03	0.06	0.07
VCA0776	0.02	0.02	0.05	0.05
VCA0777	0.06	0.06	0.06	0.04
VCA0778	0.09	0.07	0.08	0.05

VCA0779	0.04	0.03	0.01	0.01
VCA0780	0.08	0.09	0.03	0.04
VCA0781	0.05	0.06	0.03	0.03
VCA0782	0.04	0.05	0.08	0.06
VCA0783	0.05	0.04	0.04	0.03
VCA0784	0.09	0.06	0.06	0.06
VCA0785	0.04	0.05	0.00	-0.01
VCA0786	0.07	0.06	0.02	0.02
VCA0787	0.06	0.06	0.03	0.04
VCA0788	0.07	0.08	0.06	0.06
VCA0789	0.10	0.09	0.05	0.04
VCA0790	0.06	0.07	0.02	0.03
VCA0791	0.06	0.05	0.06	0.06
VCA0792	0.05	0.03	0.04	0.05
VCA0793	0.05	0.09	0.10	0.08
VCA0794	0.04	0.07	0.07	0.05
VCA0795	0.06	0.06	0.07	0.05
VCA0796	0.09	0.10	0.04	0.05
VCA0796	0.06	0.07	0.08	0.07
VCA0797	0.06	0.11	0.08	0.07
VCA0798	0.04	0.05	0.11	0.10
VCA0799	0.07	0.06	0.07	0.04
VCA0800	0.07	0.06	0.11	0.08
VCA0801	0.08	0.08	0.05	0.04
VCA0802	0.03	0.04	0.02	0.04
VCA0803	0.02	0.02	0.04	0.05
VCA0804	0.04	0.04	0.05	0.01
VCA0805	0.04	0.04	-0.02	-0.02
VCA0806	0.07	0.05	0.06	0.04
VCA0807	0.06	0.07	0.06	0.06
VCA0808	0.06	0.05	0.03	0.02
VCA0809	0.04	0.04	0.02	0.02
VCA0810	0.05	0.05	0.04	0.05
VCA0810	0.05	0.06	0.04	0.05
VCA0811	0.06	0.07	0.03	0.05
VCA0812	0.16	0.17	0.06	0.06
VCA0813	0.08	0.08	0.06	0.06
VCA0814	0.06	0.07	0.08	0.08
VCA0815	0.05	0.06	0.03	0.03
VCA0815	-0.03	0.00	0.02	0.04
VCA0816	0.05	0.08	0.04	0.05
VCA0816	0.05	0.07	0.04	0.05
VCA0817	0.05	0.06	0.06	0.07

VCA0819	0.09	0.09	0.06	0.05
VCA0820	0.02	0.02	0.09	0.08
VCA0821	0.05	0.05	0.04	0.05
VCA0822	0.09	0.10	0.01	0.05
VCA0823	0.07	0.06	0.05	0.05
VCA0824	0.01	0.03	0.04	0.05
VCA0824	0.01	0.03	0.04	0.04
VCA0825	0.06	0.07	0.05	0.08
VCA0826	0.06	0.07	0.05	0.04
VCA0826	0.06	0.06	0.04	0.04
VCA0827	0.12	0.11	0.05	0.05
VCA0828	0.05	0.06	0.08	0.09
VCA0830	0.01	0.01	0.04	0.04
VCA0831	0.03	0.04	0.06	0.06
VCA0832	0.06	0.03	0.06	0.07
VCA0833	0.05	0.04	0.05	0.06
VCA0834	0.05	0.03	0.08	0.06
VCA0835	0.03	0.05	0.03	0.05
VCA0836	0.03	0.02	0.04	0.06
VCA0836	0.01	0.01	0.05	0.05
VCA0837	0.05	0.05	0.09	0.13
VCA0838	0.06	0.05	0.08	0.07
VCA0839	0.02	0.02	0.06	0.07
VCA0840	0.10	0.10	0.06	0.08
VCA0841	0.05	0.06	0.09	0.09
VCA0842	0.05	0.05	0.03	0.03
VCA0842	0.05	0.06	0.05	0.05
VCA0843	0.11	0.10	0.09	0.09
VCA0844	0.05	0.06	0.03	0.03
VCA0845	0.04	0.05	0.05	0.05
VCA0846	0.08	0.06	0.06	0.08
VCA0847	0.01	0.02	0.04	0.04
VCA0848	0.01	0.01	-0.01	0.02
VCA0850	0.04	0.04	0.06	0.11
VCA0851	0.08	0.07	0.05	0.08
VCA0852	0.03	0.06	0.04	0.07
VCA0853	0.11	0.09	0.04	0.04
VCA0854	0.05	0.04	0.07	0.07
VCA0855	0.08	0.09	0.06	0.03
VCA0855	0.06	0.06	0.07	0.05
VCA0856	0.05	0.07	0.06	0.08
VCA0857	0.05	0.06	0.08	0.07
VCA0858	0.04	0.05	0.05	0.05

VCA0861	0.06	0.06	0.03	0.04
VCA0862	0.06	0.06	0.04	0.05
VCA0863	0.07	0.06	0.05	0.05
VCA0864	0.04	0.01	0.03	0.04
VCA0865	0.03	0.04	0.08	0.06
VCA0866	0.03	0.03	0.04	0.04
VCA0867	0.02	0.03	0.02	0.02
VCA0868	0.06	0.07	0.02	0.03
VCA0869	0.05	0.06	0.05	0.05
VCA0870	0.05	0.05	0.08	0.08
VCA0871	0.05	0.03	0.02	0.02
VCA0872	0.02	0.01	0.03	0.05
VCA0873	0.05	0.07	0.03	0.03
VCA0874	0.05	0.06	0.10	0.11
VCA0875	0.05	0.05	0.07	0.06
VCA0876	0.03	0.04	0.10	0.10
VCA0878	0.07	0.09	0.04	0.04
VCA0879	0.04	0.07	0.03	0.04
VCA0879	0.07	0.07	0.06	0.05
VCA0880	0.08	0.06	0.04	0.03
VCA0882	0.04	0.05	0.05	0.04
VCA0883	0.12	0.13	0.05	0.08
VCA0884	0.03	0.03	0.04	0.05
VCA0885	0.07	0.05	0.07	0.07
VCA0886	0.07	0.07	0.08	0.08
VCA0887	0.06	0.06	0.09	0.06
VCA0888	0.07	0.05	0.06	0.04
VCA0889	0.05	0.09	0.11	0.09
VCA0890	0.08	0.06	0.09	0.11
VCA0891	0.05	0.04	0.02	0.03
VCA0892	0.08	0.09	0.04	0.03
VCA0893	0.09	0.09	0.04	0.05
VCA0894	0.06	0.08	0.08	0.07
VCA0895	0.06	0.05	0.24	0.27
VCA0896	0.04	0.05	0.05	0.05
VCA0897	0.08	0.08	0.03	0.05
VCA0898	0.05	0.05	0.05	0.07
VCA0899	0.06	0.06	0.04	0.04
VCA0900	0.06	0.05	-0.03	-0.02
VCA0901	0.03	0.03	0.06	0.06
VCA0902	0.04	0.03	0.08	0.06
VCA0903	0.07	0.05	0.09	0.08
VCA0904	0.06	0.03	0.10	0.09

VCA0905	0.05	0.04	0.04	0.04
VCA0906	0.04	0.04	0.05	0.04
VCA0907	0.06	0.04	0.10	0.10
VCA0908	0.02	0.04	0.04	0.04
VCA0909	0.04	0.04	0.05	0.06
VCA0910	0.03	0.06	0.07	0.06
VCA0911	0.08	0.08	0.03	0.03
VCA0912	0.03	0.04	0.04	0.05
VCA0913	0.04	0.09	0.07	0.06
VCA0914	0.04	0.04	0.04	0.04
VCA0915	0.05	0.04	0.04	0.05
VCA0916	0.03	0.05	0.06	0.05
VCA0917	0.11	0.07	0.07	0.08
VCA0918	0.03	0.03	0.03	0.03
VCA0918	0.03	0.06	0.05	0.06
VCA0919	0.06	0.05	0.11	0.09
VCA0920	0.03	0.04	0.04	0.09
VCA0921	0.09	0.08	0.01	0.01
VCA0922	0.05	0.06	0.07	0.05
VCA0923	-0.01	-0.01	0.06	0.05
VCA0924	-0.01	-0.01	0.01	0.00
VCA0925	0.07	0.07	0.08	0.06
VCA0926	0.04	0.07	0.05	0.03
VCA0927	0.00	0.01	0.08	0.06
VCA0928	0.00	0.00	0.07	0.04
VCA0929	0.04	0.07	0.00	0.01
VCA0930	0.02	0.02	0.05	0.04
VCA0931	0.47	0.48	0.35	0.30
VCA0932	0.06	0.06	0.07	0.06
VCA0933	0.04	0.05	0.08	0.08
VCA0934	0.05	0.06	0.04	0.04
VCA0935	0.04	0.05	0.05	0.04
VCA0936	0.03	0.03	0.09	0.08
VCA0937	0.05	0.05	0.06	0.06
VCA0938	0.03	0.03	0.05	0.04
VCA0939	0.03	0.04	-0.01	-0.02
VCA0940	-0.01	0.02	0.04	0.07
VCA0941	0.07	0.08	0.06	0.08
VCA0942	0.07	0.06	0.03	0.03
VCA0943	0.03	0.03	0.04	0.04
VCA0944	0.04	0.03	0.04	0.05
VCA0945	0.02	0.02	0.02	0.19
VCA0946	0.05	0.05	0.03	0.04

VCA0947	0.01	0.01	0.06	0.23
VCA0948	0.08	0.07	0.03	0.04
VCA0949	0.05	0.06	0.02	0.02
VCA0950	0.08	0.07	0.02	0.04
VCA0951	0.02	0.01	0.03	0.04
VCA0952	0.07	0.07	0.10	0.08
VCA0953	0.04	0.06	0.02	0.04
VCA0954	0.05	0.06	0.05	0.05
VCA0955	0.00	0.00	0.03	0.07
VCA0956	0.00	-0.02	-0.01	0.00
VCA0957	0.06	0.06	0.04	0.03
VCA0958	0.04	0.04	0.05	0.05
VCA0959	0.12	0.07	0.06	0.05
VCA0960	0.05	0.03	0.06	0.08
VCA0961	0.04	0.05	0.03	0.05
VCA0962	0.05	0.04	0.05	0.06
VCA0963	0.01	0.01	0.16	0.04
VCA0964	0.01	0.02	0.04	0.03
VCA0965	0.00	0.01	0.11	0.14
VCA0966	0.03	0.02	0.05	0.06
VCA0967	0.06	0.07	0.03	0.04
VCA0968	0.07	0.07	0.07	0.06
VCA0969	0.07	0.08	0.05	0.07
VCA0970	0.03	0.03	0.04	0.07
VCA0971	0.03	0.03	0.03	0.05
VCA0972	0.05	0.06	0.07	0.09
VCA0973	0.07	0.08	0.07	0.05
VCA0974	0.02	0.03	0.04	0.03
VCA0975	0.03	0.03	0.05	0.05
VCA0976	0.01	0.02	0.04	0.04
VCA0977	0.04	0.05	0.06	0.05
VCA0979	0.02	0.04	0.06	0.04
VCA0980	0.02	0.00	0.04	0.05
VCA0981	0.04	0.04	0.05	0.04
VCA0982	0.01	0.01	0.07	0.05
VCA0983	0.03	0.03	0.04	0.05
VCA0984	0.03	0.07	0.06	0.04
VCA0985	0.02	0.02	0.04	0.04
VCA0986	0.02	0.02	0.06	0.05
VCA0987	0.03	0.05	0.04	0.06
VCA0988	0.03	0.03	0.04	0.05
VCA0989	0.03	0.04	0.04	0.04
VCA0990	0.03	0.03	0.07	0.07

VCA0991	0.07	0.11	0.05	0.06
VCA0992	0.04	0.07	0.09	0.10
VCA0993	0.06	0.06	0.09	0.09
VCA0994	0.05	0.07	0.07	0.06
VCA0995	0.05	0.08	0.07	0.06
VCA0996	0.04	0.04	0.04	0.03
VCA0997	0.04	0.04	0.06	0.05
VCA0998	0.06	0.05	0.09	0.07
VCA0999	0.05	0.07	0.10	0.09
VCA1000	0.06	0.07	0.03	0.02
VCA1001	0.08	0.11	0.06	0.05
VCA1002	0.03	0.04	0.02	0.02
VCA1003	0.05	0.07	0.08	0.06
VCA1004	0.03	0.04	0.07	0.06
VCA1005	0.02	0.05	0.06	0.05
VCA1006	0.04	0.04	0.09	0.07
VCA1007	0.05	0.07	0.06	0.07
VCA1008	0.02	0.03	0.06	0.07
VCA1009	0.05	0.06	0.07	0.04
VCA1009	0.06	0.06	0.04	0.04
VCA1010	0.12	0.13	0.06	0.07
VCA1011	0.03	0.07	0.06	0.05
VCA1012	0.07	0.12	0.06	0.04
VCA1013	0.08	0.16	0.13	0.10
VCA1014	0.04	0.13	0.03	0.03
VCA1014	0.06	0.07	0.04	0.05
VCA1015	0.03	0.02	0.09	0.09
VCA1016	0.04	0.06	0.03	0.02
VCA1017	0.03	0.04	0.06	0.06
VCA1018	0.04	0.04	0.06	0.05
VCA1019	0.05	0.03	0.04	0.03
VCA1019	0.05	0.05	0.04	0.03
VCA1021	0.04	0.05	0.07	0.08
VCA1024	0.06	0.06	0.07	0.05
VCA1025	0.08	0.10	0.07	0.08
VCA1026	0.05	0.06	0.05	0.05
VCA1027	0.05	0.11	0.06	0.05
VCA1028	0.04	0.04	0.06	0.02
VCA1029	0.07	0.03	0.02	0.03
VCA1030	0.06	0.05	0.05	0.05
VCA1031	0.01	0.05	0.02	0.03
VCA1032	0.08	0.10	0.08	0.10
VCA1033	0.08	0.05	0.06	0.10

VCA1034	0.06	0.06	0.06	0.04
VCA1035	0.03	0.05	0.06	0.06
VCA1037	0.01	0.06	0.04	0.05
VCA1038	0.03	0.04	0.06	0.06
VCA1039	0.02	0.02	0.04	0.03
VCA1040	0.03	0.03	0.04	0.06
VCA1041	0.06	0.07	0.06	0.05
VCA1042	0.00	0.01	0.08	0.08
VCA1043	0.03	0.03	0.04	0.05
VCA1044	0.08	0.08	0.05	0.09
VCA1045	0.07	0.07	0.05	0.04
VCA1046	0.08	0.08	0.07	0.10
VCA1047	0.07	0.08	0.08	0.10
VCA1048	0.08	0.07	0.04	0.05
VCA1049	0.03	0.03	0.04	0.04
VCA1050	0.09	0.07	0.18	0.13
VCA1051	0.05	0.08	0.05	0.06
VCA1052	0.03	0.04	0.07	0.07
VCA1053	0.04	0.04	0.04	0.06
VCA1054	0.05	0.06	0.06	0.09
VCA1055	0.03	0.02	0.04	0.06
VCA1056	0.05	0.05	-0.02	-0.01
VCA1057	0.05	0.05	0.05	0.06
VCA1058	0.04	0.03	0.08	0.10
VCA1059	0.06	0.06	0.04	0.04
VCA1060	0.07	0.08	0.06	0.09
VCA1061	0.05	0.05	0.03	0.04
VCA1062	0.04	0.05	0.06	0.08
VCA1063	0.05	0.05	0.06	0.04
VCA1064	0.05	0.04	0.04	0.05
VCA1065	0.07	0.08	0.05	0.06
VCA1065	0.08	0.05	0.05	0.05
VCA1066	0.07	0.05	0.05	0.05
VCA1067	0.07	0.07	0.03	0.02
VCA1068	-0.01	-0.02	0.08	0.07
VCA1069	0.06	0.05	0.06	0.04
VCA1070	0.03	0.03	0.09	0.08
VCA1071	0.03	0.04	0.06	0.06
VCA1072	0.06	0.05	0.01	0.03
VCA1073	0.06	0.05	0.05	0.04
VCA1074	0.06	0.07	0.14	0.16
VCA1075	0.02	0.02	0.04	0.04
VCA1076	0.04	0.04	0.06	0.06

VCA1077	0.06	0.07	0.03	0.04
VCA1078	0.03	0.03	0.04	0.03
VCA1079	0.08	0.08	0.02	0.04
VCA1080	0.03	0.03	0.06	0.05
VCA1081	0.08	0.10	0.04	0.03
VCA1083	0.61	0.61	0.54	0.58
VCA1084	0.04	0.03	0.04	0.06
VCA1085	0.06	0.06	0.05	0.04
VCA1086	0.08	0.09	0.06	0.06
VCA1087	0.08	0.09	0.06	0.07
VCA1088	0.04	0.03	0.04	0.04
VCA1089	0.02	0.05	0.05	0.05
VCA1090	0.06	0.07	0.04	0.04
VCA1091	0.04	0.06	0.05	0.06
VCA1092	0.04	0.03	0.12	0.09
VCA1093	0.06	0.05	0.05	0.06
VCA1094	0.04	0.05	0.00	-0.01
VCA1095	0.04	0.04	0.02	0.02
VCA1096	0.04	0.03	0.07	0.06
VCA1097	0.03	0.03	0.03	0.08
VCA1098	0.05	0.03	0.01	0.02
VCA1099	0.01	0.04	0.07	0.08
VCA1100	0.03	0.03	0.04	0.08
VCA1101	0.02	0.02	0.06	0.04
VCA1102	0.16	0.15	0.03	0.03
VCA1103	0.07	0.07	0.03	0.04
VCA1104	0.00	0.03	0.04	0.04
VCA1105	0.00	0.02	0.06	0.04
VCA1106	0.01	0.02	0.04	0.05
VCA1106	0.00	0.02	0.05	0.04
VCA1107	0.02	0.03	0.05	0.04
VCA1108	0.01	0.03	0.05	0.06
VCA1109	0.03	0.05	0.05	0.06
VCA1110	0.01	0.00	0.17	0.15
VCA1111	0.04	0.04	0.01	0.00
VCA1112	0.04	0.05	0.04	0.04
VCA1113	0.05	0.04	0.08	0.05
VCA1114	0.08	0.08	0.03	0.03
VCA1115	0.05	0.05	0.06	0.05

References

1. Payne, A.H. and Hales, D.B. (2004) Overview of steroidogenic enzymes in the pathway from cholesterol to active steroid hormones. *Endocr. Rev.*, **25**, 947-970.

2. Wurtman, R.J., Hefti, F. and Melamed, E. (1980) Precursor control of neurotransmitter synthesis. *Pharmacol. Rev.*, **32**, 315-335.

3. Sunahara, R.K., Dessauer, C.W. and Gilman, A.G. (1996) Complexity and diversity of mammalian adenylyl cyclases. *Annu. Rev. Pharmacol. Toxicol.*, **36**, 461-480.

4. Arias-Carrión, O. and Pŏppel, E. (2007) Dopamine, learning, and reward-seeking behavior. *Acta Neurobiol. Exp. (Wars)*, **67**, 481-488.

5. Nef, S. and Parada, L.F. (2000) Hormones in male sexual development. *Genes Dev.*, **14**, 3075-3086.

6. Görke, B. and Stülke, J. (2008) Carbon catabolite repression in bacteria: many ways to make the most out of nutrients. *Nat. Rev. Microbiol.*, **6**, 613-624.

7. Boolell, M., Allen, M.J., Ballard, S.A., Gepi-Attee, S., Muirhead, G.J., Naylor, A.M., Osterloh, I.H. and Gingell, C. (1996) Sildenafil: an orally active type 5 cyclic GMP-specific phosphodiesterase inhibitor for the treatment of penile erectile dysfunction. *Int. J. Impot. Res.*, **8**, 47-52.

8. Tyler, E.T. (1967) Antifertility agents. *Annu. Rev. Pharmacol.*, **7**, 381-398.

9. Murrough, J.W. (2012) Ketamine as a novel antidepressant: from synapse to behavior. *Clin. Pharmacol. Ther.*, **91**, 303-309.

10. Deutscher, J., Francke, C. and Postma, P.W. (2006) How phosphotransferase system-related protein phosphorylation regulates carbohydrate metabolism in bacteria. *Microbiol. Mol. Biol. Rev.*, **70**, 939-1031.

11. Meadow, N.D., Saffen, D.W., Dottin, R.P. and Roseman, S. (1982) Molecular cloning of the *crr* gene and evidence that it is the structural gene for IIIGlc, a phosphocarrier protein of the bacterial phosphotransferase system. *Proc. Natl. Acad. Sci. U S A*, **79**, 2528-2532.

12. Harwood, J.P., Gazdar, C., Prasad, C., Peterkofsky, A., Curtis, S.J. and Epstein, W. (1976) Involvement of the glucose enzymes II of the sugar phosphotransferase system in the regulation of adenylate cyclase by glucose in *Escherichia coli*. *J Biol. Chem.*, **251**, 2462-2468.

13. Park, Y.H., Lee, B.R., Seok, Y.J. and Peterkofsky, A. (2006) In vitro reconstitution of catabolite repression in *Escherichia coli*. *J. Biol. Chem.*, **281**, 6448-6454.

14. Emmer, M., deCrombrugghe, B., Pastan, I. and Perlman, R. (1970) Cyclic AMP receptor protein of *E. coli*: its role in the synthesis of inducible enzymes. *Proc. Natl. Acad. Sci. U S A*, **66**, 480-487.

15. Ebright, R.H., Ebright, Y.W. and Gunasekera, A. (1989) Consensus DNA site for the Escherichia coli catabolite gene activator protein (CAP): CAP exhibits a 450-fold higher affinity for the consensus DNA site than for the *E. coli lac* DNA site. *Nucleic Acids Res.*, **17**, 10295-10305.

16. Zheng, D., Constantinidou, C., Hobman, J.L. and Minchin, S.D. (2004) Identification of the CRP regulon using in vitro and in vivo transcriptional profiling. *Nucleic Acids Res.*, **32**, 5874-5893.

17. Epstein, W., Rothman-Denes, L.B. and Hesse, J. (1975) Adenosine 3':5'-cyclic monophosphate as mediator of catabolite repression in *Escherichia coli*. *Proc. Natl. Acad. Sci. U S A*, **72**, 2300-2304.

18. Pastan, I. and Perlman, R.L. (1968) The role of the lac promotor locus in the regulation of beta-galactosidase synthesis by cyclic 3',5'-adenosine monophosphate. *Proc. Natl. Acad. Sci. U S A*, **61**, 1336-1342.

19. Nakada, D. and Magasanik, B. (1964) The Roles of Inducer and Catabolite Repressor in the Synthesis of Beta-galactosidase by *Escherichia coli. J. Mol. Biol.*, **8**, 105-127.

20. Hantke, K., Winkler, K. and Schultz, J.E. (2011) *Escherichia coli* exports cyclic AMP via TolC. *J. Bacteriol.*, **193**, 1086-1089.

21. Imamura, R., Yamanaka, K., Ogura, T., Hiraga, S., Fujita, N., Ishihama, A. and Niki, H. (1996) Identification of the cpdA gene encoding cyclic 3',5'-adenosine monophosphate phosphodiesterase in *Escherichia coli*. *J. Biol. Chem.*, **271**, 25423-25429.

22. Sunahara, R.K. and Taussig, R. (2002) Isoforms of mammalian adenylyl cyclase: multiplicities of signaling. *Mol. Interv.*, **2**, 168-184.

23. Venkatakrishnan, A.J., Deupi, X., Lebon, G., Tate, C.G., Schertler, G.F. and Babu, M.M. (2013) Molecular signatures of G-protein-coupled receptors. *Nature*, **494**, 185-194.

24. Graziano, M.P., Casey, P.J. and Gilman, A.G. (1987) Expression of cDNAs for G proteins in Escherichia coli. Two forms of Gs alpha stimulate adenylate cyclase. *J. Biol. Chem.*, **262**, 11375-11381.

25. Taussig, R., Iñiguez-Lluhi, J.A. and Gilman, A.G. (1993) Inhibition of adenylyl cyclase by Gi alpha. *Science*, **261**, 218-221.

26. Tang, W.J. and Gilman, A.G. (1991) Type-specific regulation of adenylyl cyclase by G protein beta gamma subunits. *Science*, **254**, 1500-1503.

27. Iwami, G., Kawabe, J., Ebina, T., Cannon, P.J., Homcy, C.J. and Ishikawa, Y. (1995) Regulation of adenylyl cyclase by protein kinase A. *J. Biol. Chem.*, **270**, 12481-12484.

28. Skalhegg, B.S. and Tasken, K. (2000) Specificity in the cAMP/PKA signaling pathway. Differential expression,regulation, and subcellular localization of subunits of PKA. *Front. Biosci.*, **5**, D678-693.

29. Døskeland, S.O., Maronde, E. and Gjertsen, B.T. (1993) The genetic subtypes of cAMP-dependent protein kinase--functionally different or redundant? *Biochim. Biophys. Acta.*, **1178**, 249-258.

30. Lee, D.C., Carmichael, D.F., Krebs, E.G. and McKnight, G.S. (1983) Isolation of a cDNA clone for the type I regulatory subunit of bovine cAMP-dependent protein kinase. *Proc. Natl. Acad. Sci. U S A*, **80**, 3608-3612.

31. Clegg, C.H., Cadd, G.G. and McKnight, G.S. (1988) Genetic characterization of a brain-specific form of the type I regulatory subunit of cAMP-dependent protein kinase. *Proc. Natl. Acad. Sci. U S A*, **85**, 3703-3707.

32. Scott, J.D., Glaccum, M.B., Zoller, M.J., Uhler, M.D., Helfman, D.M., McKnight, G.S. and Krebs, E.G. (1987) The molecular cloning of a type II regulatory subunit of the cAMP-dependent protein kinase from rat skeletal muscle and mouse brain. *Proc. Natl. Acad. Sci. U S A*, **84**, 5192-5196.

33. Jahnsen, T., Hedin, L., Kidd, V.J., Beattie, W.G., Lohmann, S.M., Walter, U., Durica, J., Schulz, T.Z., Schiltz, E. and Browner, M. (1986) Molecular cloning, cDNA structure, and regulation of the regulatory subunit of type II cAMP-dependent protein kinase from rat ovarian granulosa cells. *J. Biol. Chem.*, **261**, 12352-12361.

34. Beebe, S.J., Oyen, O., Sandberg, M., Frøysa, A., Hansson, V. and Jahnsen, T. (1990) Molecular cloning of a tissue-specific protein kinase (C gamma) from human testis--representing a third isoform for the catalytic subunit of cAMP-dependent protein kinase. *Mol. Endocrinol.*, **4**, 465-475.

35. Solberg, R., Sandberg, M., Natarajan, V., Torjesen, P.A., Hansson, V., Jahnsen, T. and Taskén, K. (1997) The human gene for the regulatory subunit RI alpha of cyclic adenosine 3', 5'-monophosphate-dependent protein kinase: two distinct promoters provide differential regulation of alternately spliced messenger ribonucleic acids. *Endocrinology*, **138**, 169-181.

36. Uhler, M.D., Chrivia, J.C. and McKnight, G.S. (1986) Evidence for a second isoform of the catalytic subunit of cAMP-dependent protein kinase. *J. Biol. Chem.*, **261**, 15360-15363.

37. Uhler, M.D., Carmichael, D.F., Lee, D.C., Chrivia, J.C., Krebs, E.G. and McKnight, G.S. (1986) Isolation of cDNA clones coding for the catalytic subunit of mouse cAMP-dependent protein kinase. *Proc. Natl. Acad. Sci. U S A*, **83**, 1300-1304.

38. Thomis, D.C., Floyd-Smith, G. and Samuel, C.E. (1992) Mechanism of interferon action. cDNA structure and regulation of a novel splice-site variant of the catalytic subunit of human protein kinase A from interferon-treated human cells. *J. Biol. Chem.*, **267**, 10723-10728.

39. Cadd, G.G., Uhler, M.D. and McKnight, G.S. (1990) Holoenzymes of cAMP-dependent protein kinase containing the neural form of type I regulatory subunit have an increased sensitivity to cyclic nucleotides. *J. Biol. Chem.*, **265**, 19502-19506.

40. de Rooij, J., Zwartkruis, F.J., Verheijen, M.H., Cool, R.H., Nijman, S.M., Wittinghofer, A. and Bos, J.L. (1998) Epac is a Rap1 guanine-nucleotide-exchange factor directly activated by cyclic AMP. *Nature*, **396**, 474-477.

41. Kawasaki, H., Springett, G.M., Mochizuki, N., Toki, S., Nakaya, M., Matsuda, M., Housman, D.E. and Graybiel, A.M. (1998) A family of cAMP-binding proteins that directly activate Rap1. *Science*, **282**, 2275-2279.

42. Knox, A.L. and Brown, N.H. (2002) Rap1 GTPase regulation of adherens junction positioning and cell adhesion. *Science*, **295**, 1285-1288.

43. Nakamura, T. and Gold, G.H. (1987) A cyclic nucleotide-gated conductance in olfactory receptor cilia. *Nature*, **325**, 442-444.

44. Conti, M., Richter, W., Mehats, C., Livera, G., Park, J.Y. and Jin, C. (2003) Cyclic AMP-specific PDE4 phosphodiesterases as critical components of cyclic AMP signaling. *J. Biol. Chem.*, **278**, 5493-5496.

45. Conti, M. and Jin, S.L. (1999) The molecular biology of cyclic nucleotide phosphodiesterases. *Prog. Nucleic Acid Res. Mol. Biol.*, **63**, 1-38.

46. MacKenzie, S.J., Baillie, G.S., McPhee, I., Bolger, G.B. and Houslay, M.D. (2000) ERK2 mitogen-activated protein kinase binding, phosphorylation, and regulation of the PDE4D cAMP-specific phosphodiesterases. The involvement of COOH-terminal docking sites and NH2-terminal UCR regions. *J. Biol. Chem.*, **275**, 16609-16617.

47. Sette, C. and Conti, M. (1996) Phosphorylation and activation of a cAMP-specific phosphodiesterase by the cAMP-dependent protein kinase. Involvement of serine 54 in the enzyme activation. *J. Biol. Chem.*, **271**, 16526-16534.

48. DiSanto, M.E., Glaser, K.B. and Heaslip, R.J. (1995) Phospholipid regulation of a cyclic AMP-specific phosphodiesterase (PDE4) from U937 cells. *Cell Signal.*, **7**, 827-835.

49. Buck, J., Sinclair, M.L., Schapal, L., Cann, M.J. and Levin, L.R. (1999) Cytosolic adenylyl cyclase defines a unique signaling molecule in mammals. *Proc. Natl. Acad. Sci. U S A*, **96**, 79-84.

50. Edwards, H.V., Christian, F. and Baillie, G.S. (2012) cAMP: novel concepts in compartmentalised signalling. *Semin. Cell Dev. Biol.*, **23**, 181-190.

51. Ruehr, M.L., Russell, M.A., Ferguson, D.G., Bhat, M., Ma, J., Damron, D.S., Scott, J.D. and Bond, M. (2003) Targeting of protein kinase A by muscle A kinase-anchoring protein (mAKAP) regulates phosphorylation and function of the skeletal muscle ryanodine receptor. *J. Biol. Chem.*, **278**, 24831-24836.

52. Dodge, K.L., Khouangsathiene, S., Kapiloff, M.S., Mouton, R., Hill, E.V., Houslay, M.D., Langeberg, L.K. and Scott, J.D. (2001) mAKAP assembles a protein kinase A/PDE4 phosphodiesterase cAMP signaling module. *EMBO J.*, **20**, 1921-1930.

53. Kapiloff, M.S., Piggott, L.A., Sadana, R., Li, J., Heredia, L.A., Henson, E., Efendiev, R. and Dessauer, C.W. (2009) An adenylyl cyclase-mAKAPbeta signaling complex regulates cAMP levels in cardiac myocytes. *J. Biol. Chem.*, **284**, 23540-23546.

54. Zaccolo, M. and Pozzan, T. (2002) Discrete microdomains with high concentration of cAMP in stimulated rat neonatal cardiac myocytes. *Science*, **295**, 1711-1715.

55. Zaccolo, M., Magalhães, P. and Pozzan, T. (2002) Compartmentalisation of cAMP and Ca(2+) signals. *Curr. Opin. Cell Biol.*, **14**, 160-166.

56. Wolfgang, M.C., Lee, V.T., Gilmore, M.E. and Lory, S. (2003) Coordinate regulation of bacterial virulence genes by a novel adenylate cyclase-dependent signaling pathway. *Dev. Cell*, **4**, 253-263.

57. Yahr, T.L., Vallis, A.J., Hancock, M.K., Barbieri, J.T. and Frank, D.W. (1998) ExoY, an adenylate cyclase secreted by the *Pseudomonas aeruginosa* type III system. *Proc. Natl. Acad. Sci. U S A*, **95**, 13899-13904.

58. Lory, S., Wolfgang, M., Lee, V. and Smith, R. (2004) The multi-talented bacterial adenylate cyclases. *Int. J. Med. Microbiol.*, **293**, 479-482.

59. West, S.E., Sample, A.K. and Runyen-Janecky, L.J. (1994) The *vfr* gene product, required for *Pseudomonas aeruginosa* exotoxin A and protease production, belongs to the cyclic AMP receptor protein family. *J. Bacteriol.*, **176**, 7532-7542.

60. Smith, R.S., Wolfgang, M.C. and Lory, S. (2004) An adenylate cyclase-controlled signaling network regulates *Pseudomonas aeruginosa* virulence in a mouse model of acute pneumonia. *Infect. Immun.*, **72**, 1677-1684.

61. McCue, L.A., McDonough, K.A. and Lawrence, C.E. (2000) Functional classification of cNMP-binding proteins and nucleotide cyclases with implications for novel regulatory pathways in *Mycobacterium tuberculosis*. *Genome Res.*, **10**, 204-219.

62. Bai, G., Knapp, G.S. and McDonough, K.A. (2011) Cyclic AMP signalling in *mycobacteria*: redirecting the conversation with a common currency. *Cell Microbiol.*, **13**, 349-358.

63. Bai, G., McCue, L.A. and McDonough, K.A. (2005) Characterization of *Mycobacterium tuberculosis* Rv3676 (CRPMt), a cyclic AMP receptor protein-like DNA binding protein. *J. Bacteriol*, **187**, 7795-7804.

64. Nambi, S., Basu, N. and Visweswariah, S.S. (2010) cAMP-regulated protein lysine acetylases in *mycobacteria*. *J. Biol. Chem.*, **285**, 24313-24323.

65. Bai, G., Gazdik, M.A., Schaak, D.D. and McDonough, K.A. (2007) The *Mycobacterium bovis* BCG cyclic AMP receptor-like protein is a functional DNA binding protein in vitro and in vivo, but its activity differs from that of its *M. tuberculosis* ortholog, Rv3676. *Infect. Immun.*, **75**, 5509-5517.

66. Gazdik, M.A., Bai, G., Wu, Y. and McDonough, K.A. (2009) Rv1675c (*cmr*) regulates intramacrophage and cyclic AMP-induced gene expression in *Mycobacterium tuberculosis*-complex *mycobacteria*. *Mol. Microbiol.*, **71**, 434-448.

67. Shenoy, A.R., Sreenath, N., Podobnik, M., Kovacevic, M. and Visweswariah, S.S. (2005) The Rv0805 gene from *Mycobacterium tuberculosis* encodes a 3',5'-cyclic nucleotide phosphodiesterase: biochemical and mutational analysis. *Biochemistry*, **44**, 15695-15704.

68. Lowrie, D.B., Jackett, P.S. and Ratcliffe, N.A. (1975) *Mycobacterium microti* may protect itself from intracellular destruction by releasing cyclic AMP into phagosomes. *Nature*, **254**, 600-602.

69. Agarwal, N., Lamichhane, G., Gupta, R., Nolan, S. and Bishai, W.R. (2009) Cyclic AMP intoxication of macrophages by a *Mycobacterium tuberculosis* adenylate cyclase. *Nature*, **460**, 98-102.

70. Bai, G., Schaak, D.D. and McDonough, K.A. (2009) cAMP levels within *Mycobacterium tuberculosis* and *Mycobacterium bovis* BCG increase upon infection of macrophages. *FEMS Immunol. Med. Microbiol.*, **55**, 68-73.

71. Egli, M., Gessner, R.V., Williams, L.D., Quigley, G.J., van der Marel, G.A., van Boom, J.H., Rich, A. and Frederick, C.A. (1990) Atomic-resolution structure of the cellulose synthase regulator cyclic diguanylic acid. *Proc. Natl. Acad. Sci. U S A*, **87**, 3235-3239.

72. Ross, P., Weinhouse, H., Aloni, Y., Michaeli, D., Weinberger-Ohana, P., Mayer, R., Braun, S., de Vroom, E., van der Marel, G.A., van Boom, J.H. *et al.* (1987) Regulation of cellulose synthesis in Acetobacter xylinum by cyclic diguanylic acid. *Nature*, **325**, 279-281.

73. Amikam, D. and Benziman, M. (1989) Cyclic diguanylic acid and cellulose synthesis in *Agrobacterium tumefaciens*. *J. Bacteriol.*, **171**, 6649-6655.

74. Mayer, R., Ross, P., Weinhouse, H., Amikam, D., Volman, G., Ohana, P., Calhoon, R.D., Wong, H.C., Emerick, A.W. and Benziman, M. (1991) Polypeptide composition of bacterial cyclic diguanylic acid-dependent cellulose synthase and the occurrence of immunologically crossreacting proteins in higher plants. *Proc. Natl. Acad. Sci. U S A*, **88**, 5472-5476.

75. Tal, R., Wong, H.C., Calhoon, R., Gelfand, D., Fear, A.L., Volman, G., Mayer, R., Ross, P., Amikam, D., Weinhouse, H. *et al.* (1998) Three *cdg* operons control cellular turnover of cyclic di-GMP in *Acetobacter xylinum*: genetic organization and occurrence of conserved domains in isoenzymes. *J. Bacteriol.*, **180**, 4416-4425.

76. Pei, J. and Grishin, N.V. (2001) GGDEF domain is homologous to adenylyl cyclase. *Proteins*, **42**, 210-216.

77. Paul, R., Weiser, S., Amiot, N.C., Chan, C., Schirmer, T., Giese, B. and Jenal, U. (2004) Cell cycle-dependent dynamic localization of a bacterial response regulator with a novel di-guanylate cyclase output domain. *Genes Dev.*, **18**, 715-727.

78. Römling, U., Galperin, M.Y. and Gomelsky, M. (2013) Cyclic di-GMP: the first 25 years of a universal bacterial second messenger. *Microbiol. Mol. Biol. Rev.*, **77**, 1-52.

79. Galperin, M.Y., Nikolskaya, A.N. and Koonin, E.V. (2001) Novel domains of the prokaryotic two-component signal transduction systems. *FEMS Microbiol. Lett.*, **203**, 11-21.

80. Kulasakara, H., Lee, V., Brencic, A., Liberati, N., Urbach, J., Miyata, S., Lee, D.G., Neely, A.N., Hyodo, M., Hayakawa, Y. *et al.* (2006) Analysis of *Pseudomonas aeruginosa* diguanylate cyclases and phosphodiesterases reveals a role for bis-(3'-5')-cyclic-GMP in virulence. *Proc. Natl. Acad. Sci. U S A*, **103**, 2839-2844.

81. Solano, C., Garcia, B., Latasa, C., Toledo-Arana, A., Zorraquino, V., Valle, J., Casals, J., Pedroso, E. and Lasa, I. (2009) Genetic reductionist approach for dissecting individual roles of GGDEF proteins within the c-di-GMP signaling network in *Salmonella*. *Proc. Natl. Acad. Sci. U S A*, **106**, 7997-8002.

82. Massie, J.P., Reynolds, E.L., Koestler, B.J., Cong, J.P., Agostoni, M. and Waters, C.M. (2012) Quantification of high-specificity cyclic diguanylate signaling. *Proc. Natl. Acad. Sci. U S A*, **109**, 12746-12751.

83. Sommerfeldt, N., Possling, A., Becker, G., Pesavento, C., Tschowri, N. and Hengge, R. (2009) Gene expression patterns and differential input into curli fimbriae regulation of all GGDEF/EAL domain proteins in *Escherichia coli*. *Microbiology*, **155**, 1318-1331.

84. Chan, C., Paul, R., Samoray, D., Amiot, N., Giese, B., Jenal, U. and Schirmer, T. (2004) Structural basis of activity and allosteric control of diguanylate cyclase. *Proc. Natl. Acad. Sci. U S A*, **101**, 17084-17089.

85. Paul, R., Abel, S., Wassmann, P., Beck, A., Heerklotz, H. and Jenal, U. (2007) Activation of the diguanylate cyclase PleD by phosphorylation-mediated dimerization. *J. Biol. Chem.*, **282**, 29170-29177.

86. Christen, B., Christen, M., Paul, R., Schmid, F., Folcher, M., Jenoe, P., Meuwly, M. and Jenal, U. (2006) Allosteric control of cyclic di-GMP signaling. *J. Biol. Chem.*, **281**, 32015-32024.

87. Lee, S.Y., Cho, H.S., Pelton, J.G., Yan, D., Berry, E.A. and Wemmer, D.E. (2001) Crystal structure of activated CheY. Comparison with other activated receiver domains. *J. Biol. Chem.*, **276**, 16425-16431.

88. Wassmann, P., Chan, C., Paul, R., Beck, A., Heerklotz, H., Jenal, U. and Schirmer, T. (2007) Structure of $BeF3^-$ -modified response regulator PleD: implications for diguanylate cyclase activation, catalysis, and feedback inhibition. *Structure*, **15**, 915-927.

89. Hickman, J., Tifrea, D. and Harwood, C. (2005) A chemosensory system that regulates biofilm formation through modulation of cyclic diguanylate levels. *Proc. Natl. Acad. Sci. U S A*, **102**, 14422-14427.

90. Güvener, Z.T. and Harwood, C.S. (2007) Subcellular location characteristics of the *Pseudomonas aeruginosa* GGDEF protein, WspR, indicate that it produces cyclic-di-GMP in response to growth on surfaces. *Mol. Microbiol.*, **66**, 1459-1473.

91. De, N., Navarro, M.V., Raghavan, R.V. and Sondermann, H. (2009) Determinants for the activation and autoinhibition of the diguanylate cyclase response regulator WspR. *J. Mol. Biol.*, **393**, 619-633.

92. Draper, J., Karplus, K. and Ottemann, K.M. (2011) Identification of a chemoreceptor zinc-binding domain common to cytoplasmic bacterial chemoreceptors. *J. Bacteriol.*, **193**, 4338-4345.

93. Zähringer, F., Lacanna, E., Jenal, U., Schirmer, T. and Boehm, A. (2013) Structure and signaling mechanism of a zinc-sensory diguanylate cyclase. *Structure*, **21**, 1149-1157.

94. Tischler, A.D. and Camilli, A. (2004) Cyclic diguanylate (c-di-GMP) regulates *Vibrio cholerae* biofilm formation. *Mol. Microbiol.*, **53**, 857-869.

95. Tamayo, R., Tischler, A.D. and Camilli, A. (2005) The EAL domain protein VieA is a cyclic diguanylate phosphodiesterase. *J. Biol. Chem.*, **280**, 33324-33330.

96. Christen, M., Christen, B., Folcher, M., Schauerte, A. and Jenal, U. (2005) Identification and characterization of a cyclic di-GMP-specific phosphodiesterase and its allosteric control by GTP. *J. Biol. Chem.*, **280**, 30829-30837.

97. Hengge, R. (2009) Principles of c-di-GMP signalling in bacteria. *Nat. Rev. Microbiol.*, **7**, 263-273.

98. Schmidt, A.J., Ryjenkov, D.A. and Gomelsky, M. (2005) The ubiquitous protein domain EAL is a cyclic diguanylate-specific phosphodiesterase: enzymatically active and inactive EAL domains. *J. Bacteriol.*, **187**, 4774-4781.

99. Barends, T.R., Hartmann, E., Griese, J.J., Beitlich, T., Kirienko, N.V., Ryjenkov, D.A., Reinstein, J., Shoeman, R.L., Gomelsky, M. and Schlichting, I. (2009) Structure and mechanism of a bacterial light-regulated cyclic nucleotide phosphodiesterase. *Nature*, **459**, 1015-1018.

100. Sundriyal, A., Massa, C., Samoray, D., Zehender, F., Sharpe, T., Jenal, U. and Schirmer, T. (2014) Inherent regulation of EAL domain-catalyzed hydrolysis of second messenger c-di-GMP. *J. Biol. Chem.*.

101. Ryan, R., Fouhy, Y., Lucey, J., Crossman, L., Spiro, S., He, Y., Zhang, L., Heeb, S., Cámara, M., Williams, P. *et al.* (2006) Cell-cell signaling in *Xanthomonas campestris* involves an HD-GYP domain protein that functions in cyclic di-GMP turnover. *Proc. Natl. Acad. Sci. U S A*, **103**, 6712-6717.

102. Stelitano, V., Giardina, G., Paiardini, A., Castiglione, N., Cutruzzolà, F. and Rinaldo, S. (2013) C-di-GMP hydrolysis by *Pseudomonas aeruginosa* HD-GYP phosphodiesterases: analysis of the reaction mechanism and novel roles for pGpG. *PLoS One*, **8**, e74920.

103. Ryan, R.P., McCarthy, Y., Andrade, M., Farah, C.S., Armitage, J.P. and Dow, J.M. (2010) Cell-cell signal-dependent dynamic interactions between HD-GYP and GGDEF domain proteins mediate virulence in *Xanthomonas campestris*. *Proc. Natl. Acad. Sci. U S A*, **107**, 5989-5994.

104. Miner, K.D., Klose, K.E. and Kurtz, D.M. (2013) An HD-GYP cyclic di-guanosine monophosphate phosphodiesterase with a non-heme diiron-carboxylate active site. *Biochemistry*, **52**, 5329-5331.

105. Bellini, D., Caly, D.L., McCarthy, Y., Bumann, M., An, S.Q., Dow, J.M., Ryan, R.P. and Walsh, M.A. (2014) Crystal structure of an HD-GYP domain cyclic-di-GMP phosphodiesterase reveals an enzyme with a novel trinuclear catalytic iron centre. *Mol. Microbiol.*, **91**, 26-38.

106. Seshasayee, A.S., Fraser, G.M. and Luscombe, N.M. (2010) Comparative genomics of cyclic-di-GMP signalling in bacteria: post-translational regulation and catalytic activity. *Nucleic Acids Res.*, **38**, 5970-5981.

107. Ferreira, R.B., Antunes, L.C., Greenberg, E.P. and McCarter, L.L. (2008) *Vibrio parahaemolyticus* ScrC modulates cyclic dimeric GMP regulation of gene expression relevant to growth on surfaces. *J. Bacteriol.*, **190**, 851-860.

108. Tarutina, M., Ryjenkov, D.A. and Gomelsky, M. (2006) An unorthodox bacteriophytochrome from *Rhodobacter sphaeroides* involved in turnover of the second messenger c-di-GMP. *J. Biol. Chem.*, **281**, 34751-34758.

109. Duerig, A., Abel, S., Folcher, M., Nicollier, M., Schwede, T., Amiot, N., Giese, B. and Jenal, U. (2009) Second messenger-mediated spatiotemporal control of protein degradation regulates bacterial cell cycle progression. *Genes Dev.*, **23**, 93-104.

110. Hobley, L., Fung, R.K., Lambert, C., Harris, M.A., Dabhi, J.M., King, S.S., Basford, S.M., Uchida, K., Till, R., Ahmad, R. *et al.* (2012) Discrete cyclic di-GMP-dependent control of bacterial predation versus axenic growth in *Bdellovibrio bacteriovorus*. *PLoS Pathog.*, **8**, e1002493.

111. Petters, T., Zhang, X., Nesper, J., Treuner-Lange, A., Gomez-Santos, N., Hoppert, M., Jenal, U. and Søgaard-Andersen, L. (2012) The orphan histidine protein kinase SgmT is a c-di-GMP receptor and regulates composition of the extracellular matrix together with the orphan DNA binding response regulator DigR in *Myxococcus xanthus*. *Mol. Microbiol.*, **84**, 147-165.

112. Kazmierczak, B.I., Lebron, M.B. and Murray, T.S. (2006) Analysis of FimX, a phosphodiesterase that governs twitching motility in *Pseudomonas aeruginosa*. *Mol. Microbiol.*, **60**, 1026-1043.

113. Rao, F., Qi, Y., Chong, H., Kotaka, M., Li, B., Li, J., Lescar, J., Tang, K. and Liang, Z. (2009) The functional role of a conserved loop in EAL domain-based cyclic di-GMP-specific phosphodiesterase. *J. Bacteriol.*, **191**, 4722-4731.

114. Navarro, M.V., De, N., Bae, N., Wang, Q. and Sondermann, H. (2009) Structural analysis of the GGDEF-EAL domain-containing c-di-GMP receptor FimX. *Structure*, **17**, 1104-1116.

115. Qi, Y., Chuah, M.L., Dong, X., Xie, K., Luo, Z., Tang, K. and Liang, Z.X. (2011) Binding of cyclic diguanylate in the non-catalytic EAL domain of FimX induces a long-range conformational change. *J. Biol. Chem.*, **286**, 2910-2917.

116. Huang, B., Whitchurch, C.B. and Mattick, J.S. (2003) FimX, a multidomain Protein Connecting Environmental Signals to Twitching Motility in *Pseudomonas aeruginosa. J. Bacteriol.*, **185**, 7068-7076.

117. Newell, P.D., Monds, R.D. and O'Toole, G.A. (2009) LapD is a bis-(3',5')-cyclic dimeric GMP-binding protein that regulates surface attachment by *Pseudomonas fluorescens* Pf0-1. *Proc. Natl. Acad. Sci. U S A*, **106**, 3461-3466.

118. Minasov, G., Padavattan, S., Shuvalova, L., Brunzelle, J.S., Miller, D.J., Baslé, A., Massa, C., Collart, F.R., Schirmer, T. and Anderson, W.F. (2009) Crystal structures of YkuI and its complex with second messenger cyclic Di-GMP suggest catalytic mechanism of phosphodiester bond cleavage by EAL domains. *J. Biol. Chem.*, **284**, 13174-13184.

119. Newell, P.D., Boyd, C.D., Sondermann, H. and O'Toole, G.A. (2011) A c-di-GMP effector system controls cell adhesion by inside-out signaling and surface protein cleavage. *PLoS Biol.*, **9**, e1000587.

120. Navarro, M.V., Newell, P.D., Krasteva, P.V., Chatterjee, D., Madden, D.R., O'Toole, G.A. and Sondermann, H. (2011) Structural basis for c-di-GMP-mediated inside-out signaling controlling periplasmic proteolysis. *PLoS Biol.*, **9**, e1000588.

121. Amikam, D. and Galperin, M.Y. (2006) PilZ domain is part of the bacterial c-di-GMP binding protein. *Bioinformatics*, **22**, 3-6.

122. Ryjenkov, D.A., Simm, R., Romling, U. and Gomelsky, M. (2006) The PilZ domain is a receptor for the second messenger c-di-GMP: the PilZ domain protein YcgR controls motility in enterobacteria. *J. Biol. Chem.*, **281**, 30310-30314.

123. Chin, K.H., Lee, Y.C., Tu, Z.L., Chen, C.H., Tseng, Y.H., Yang, J.M., Ryan, R.P., McCarthy, Y., Dow, J.M., Wang, A.H. *et al.* (2010) The cAMP receptor-like protein CLP is a novel c-di-GMP receptor linking cell-cell signaling to virulence gene expression in *Xanthomonas campestris*. *J. Mol. Biol.*, **396**, 646-662.

124. Simm, R., Morr, M., Kader, A., Nimtz, M. and Romling, U. (2004) GGDEF and EAL domains inversely regulate cyclic di-GMP levels and transition from sessility to motility. *Mol. Microbiol.*, **53**, 1123-1134.

125. Remminghorst, U. and Rehm, B.H. (2006) Alg44, a unique protein required for alginate biosynthesis in *Pseudomonas aeruginosa*. *FEBS Lett.*, **580**, 3883-3888.

126. Merighi, M., Lee, V.T., Hyodo, M., Hayakawa, Y. and Lory, S. (2007) The second messenger bis-(3'-5')-cyclic-GMP and its PilZ domain-containing receptor Alg44 are required for alginate biosynthesis in *Pseudomonas aeruginosa*. *Mol. Microbiol.*, **65**, 876-895.

127. Pratt, J.T., Tamayo, R., Tischler, A.D. and Camilli, A. (2007) PilZ domain proteins bind cyclic diguanylate and regulate diverse processes in *Vibrio cholerae*. *J. Biol. Chem.*, **282**, 12860-12870.

128. Christen, M., Christen, B., Allan, M.G., Folcher, M., Jeno, P., Grzesiek, S. and Jenal, U. (2007) DgrA is a member of a new family of cyclic diguanosine monophosphate receptors and controls flagellar motor function in *Caulobacter crescentus*. *Proc. Natl. Acad. Sci. U S A*, **104**, 4112-4117.

129. McCarthy, Y., Ryan, R.P., O'Donovan, K., He, Y.Q., Jiang, B.L., Feng, J.X., Tang, J.L. and Dow, J.M. (2008) The role of PilZ domain proteins in the virulence of *Xanthomonas campestris pv. campestris*. *Mol. Plant Pathol.*, **9**, 819-824.

130. Freedman, J., Rogers, E., Kostick, J., Zhang, H., Iyer, R., Schwartz, I. and Marconi, R. (2010) Identification and molecular characterization of a cyclic-di-GMP effector protein, PlzA (BB0733): additional evidence for the existence of a functional cyclic-di-GMP regulatory network in the Lyme disease spirochete, *Borrelia burgdorferi*. *FEMS Immunol. Med. Microbiol.*, **58**, 285-294.

131. Wilksch, J.J., Yang, J., Clements, A., Gabbe, J.L., Short, K.R., Cao, H., Cavaliere, R., James, C.E., Whitchurch, C.B., Schembri, M.A. *et al.* (2011) MrkH, a novel c-di-GMP-dependent transcriptional activator, controls Klebsiella pneumoniae biofilm formation by regulating type 3 fimbriae expression. *PLoS Pathog.*, **7**, e1002204.

132. Pultz, I.S., Christen, M., Kulasekara, H.D., Kennard, A., Kulasekara, B. and Miller, S.I. (2012) The response threshold of *Salmonella* PilZ domain proteins is determined by their binding affinities for c-di-GMP. *Mol. Microbiol.*, **86**, 1424-1440.

133. Zorraquino, V., García, B., Latasa, C., Echeverz, M., Toledo-Arana, A., Valle, J., Lasa, I. and Solano, C. (2013) Coordinated cyclic-di-GMP repression of *Salmonella* motility through YcgR and cellulose. *J. Bacteriol.*, **195**, 417-428.

134. Russell, M.H., Bible, A.N., Fang, X., Gooding, J.R., Campagna, S.R., Gomelsky, M. and Alexandre, G. (2013) Integration of the second messenger c-di-GMP into the chemotactic signaling pathway. *MBio*, **4**, e00001-00013.

135. Barnhart, D.M., Su, S. and Farrand, S.K. (2014) A signaling pathway involving the diguanylate cyclase CelR and the response regulator DivK controls cellulose synthesis in *Agrobacterium tumefaciens*. *J. Bacteriol.*, **196**, 1257-1274.

136. Dambach, M.D. and Winkler, W.C. (2009) Expanding roles for metabolite-sensing regulatory RNAs. *Curr Opin Microbiol*, **12**, 161-169.

137. Tucker, B.J. and Breaker, R.R. (2005) Riboswitches as versatile gene control elements. *Curr Opin Struct Biol*, **15**, 342-348.

138. Sudarsan, N., Lee, E.R., Weinberg, Z., Moy, R.H., Kim, J.N., Link, K.H. and Breaker, R.R. (2008) Riboswitches in eubacteria sense the second messenger cyclic di-GMP. *Science*, **321**, 411-413.

139. Lee, E., Baker, J., Weinberg, Z., Sudarsan, N. and Breaker, R. (2010) An allosteric self-splicing ribozyme triggered by a bacterial second messenger. *Science*, **329**, 845-848.

140. Nielsen, H. and Johansen, S.D. (2009) Group I introns: Moving in new directions. *RNA Biol.*, **6**, 375-383.

141. Smith, K.D., Lipchock, S.V., Ames, T.D., Wang, J., Breaker, R.R. and Strobel, S.A. (2009) Structural basis of ligand binding by a c-di-GMP riboswitch. *Nat Struct. Mol. Biol.*, **16**, 1218-1223.

142. Smith, K.D., Lipchock, S.V., Livingston, A.L., Shanahan, C.A. and Strobel, S.A. (2010) Structural and biochemical determinants of ligand binding by the c-di-GMP riboswitch. *Biochemistry*, **49**, 7351-7359.

143. Smith, K.D., Shanahan, C.A., Moore, E.L., Simon, A.C. and Strobel, S.A. (2011) Structural basis of differential ligand recognition by two classes of bis-(3'-5')-cyclic dimeric guanosine monophosphate-binding riboswitches. *Proc. Natl. Acad. Sci. U S A*, **108**, 7757-7762.

144. Smith, K.D., Lipchock, S.V. and Strobel, S.A. (2012) Structural and biochemical characterization of linear dinucleotide analogues bound to the c-di-GMP-I aptamer. *Biochemistry*, **51**, 425-432.

145. Shanahan, C.A., Gaffney, B.L., Jones, R.A. and Strobel, S.A. (2013) Identification of c-di-GMP derivatives resistant to an EAL domain phosphodiesterase. *Biochemistry*, **52**, 365-377.

146. Wood, S., Ferré-D'Amaré, A.R. and Rueda, D. (2012) Allosteric tertiary interactions preorganize the c-di-GMP riboswitch and accelerate ligand binding. *ACS Chem. Biol.*, **7**, 920-927.

147. Gu, H., Furukawa, K. and Breaker, R.R. (2012) Engineered allosteric ribozymes that sense the bacterial second messenger cyclic diguanosyl 5'-monophosphate. *Anal. Chem.*, **84**, 4935-4941.

148. Hickman, J.W. and Harwood, C.S. (2008) Identification of FleQ from *Pseudomonas aeruginosa* as a c-di-GMP-responsive transcription factor. *Mol. Microbiol.*, **69**, 376-389.

149. Friedman, L. and Kolter, R. (2003) Genes involved in matrix formation in *Pseudomonas aeruginosa* PA14 biofilms. *Mol. Microbiol.*, **51**, 675-690.

150. Friedman, L. and Kolter, R. (2004) Two genetic loci produce distinct carbohydrate-rich structural components of the *Pseudomonas aeruginosa* biofilm matrix. *J. Bacteriol.*, **186**, 4457-4465.

151. Baraquet, C., Murakami, K., Parsek, M.R. and Harwood, C.S. (2012) The FleQ protein from *Pseudomonas aeruginosa* functions as both a repressor and an activator to control gene expression from the pel operon promoter in response to c-di-GMP. *Nucleic Acids Res.*, **40**, 7207-7218.

152. Baraquet, C. and Harwood, C.S. (2013) Cyclic diguanosine monophosphate represses bacterial flagella synthesis by interacting with the Walker A motif of the enhancer-binding protein FleQ. *Proc. Natl. Acad. Sci. U S A*, **110**, 18478-18483.

153. Goodman, A.L., Kulasekara, B., Rietsch, A., Boyd, D., Smith, R.S. and Lory, S. (2004) A signaling network reciprocally regulates genes associated with acute infection and chronic persistence in *Pseudomonas aeruginosa*. *Dev Cell*, **7**, 745-754.

154. Lee, V.T., Matewish, J.M., Kessler, J.L., Hyodo, M., Hayakawa, Y. and Lory, S. (2007) A cyclic-di-GMP receptor required for bacterial exopolysaccharide production. *Mol. Microbiol.*, **65**, 1474-1484.

155. Whitney, J.C., Colvin, K.M., Marmont, L.S., Robinson, H., Parsek, M.R. and Howell, P.L. (2012) Structure of the cytoplasmic region of PelD, a degenerate diguanylate cyclase receptor that regulates exopolysaccharide production in *Pseudomonas aeruginosa*. *J. Biol. Chem.*, **287**, 23582-23593.

156. Li, Z., Chen, J.H., Hao, Y. and Nair, S.K. (2012) Structures of the PelD cyclic diguanylate effector involved in pellicle formation in *Pseudomonas aeruginosa* PAO1. *J. Biol. Chem.*, **287**, 30191-30204.

157. Leduc, J.L. and Roberts, G.P. (2009) Cyclic di-GMP allosterically inhibits the CRP-like protein (Clp) of *Xanthomonas axonopodis pv. citri*. *J. Bacteriol.*, **191**, 7121-7122.

158. de Crecy-Lagard, V., Glaser, P., Lejeune, P., Sismeiro, O., Barber, C.E., Daniels, M.J. and Danchin, A. (1990) A *Xanthomonas campestris pv. campestris* protein similar to catabolite activation factor is involved in regulation of phytopathogenicity. *J. Bacteriol.*, **172**, 5877-5883.

159. He, Y.W., Ng, A.Y., Xu, M., Lin, K., Wang, L.H., Dong, Y.H. and Zhang, L.H. (2007) *Xanthomonas campestris* cell-cell communication involves a putative nucleotide receptor protein Clp and a hierarchical signalling network. *Mol. Microbiol.*, **64**, 281-292.

160. Srivastava, D., Hsieh, M.L., Khataokar, A., Neiditch, M.B. and Waters, C.M. (2013) Cyclic di-GMP inhibits *Vibrio cholerae* motility by repressing induction of transcription and inducing extracellular polysaccharide production. *Mol. Microbiol.*, **90**, 1262-1276.

161. Lim, B., Beyhan, S., Meir, J. and Yildiz, F. (2006) Cyclic-diGMP signal transduction systems in *Vibrio cholerae*: modulation of rugosity and biofilm formation. *Mol. Microbiol.*, **60**, 331-348.

162. Beyhan, S., Bilecen, K., Salama, S., Casper-Lindley, C. and Yildiz, F. (2007) Regulation of rugosity and biofilm formation in *Vibrio cholerae*: comparison of VpsT and VpsR regulons and epistasis analysis of vpsT, vpsR, and hapR. *J. Bacteriol.*, **189**, 388-402.

163. Beyhan, S., Odell, L.S. and Yildiz, F.H. (2008) Identification and characterization of cyclic diguanylate signaling systems controlling rugosity in *Vibrio cholerae*. *J. Bacteriol.*, **190**, 7392-7405.

164. Shikuma, N.J., Fong, J.C. and Yildiz, F.H. (2012) Cellular levels and binding of c-di-GMP control subcellular localization and activity of the *Vibrio cholerae* transcriptional regulator VpsT. *PLoS Pathog.*, **8**, e1002719.

165. Srivastava, D., Harris, R.C. and Waters, C.M. (2011) Integration of cyclic di-GMP and quorum sensing in the control of vpsT and aphA in *Vibrio cholerae*. *J. Bacteriol.*, **193**, 6331-6341.

166. Krasteva, P.V., Fong, J.C., Shikuma, N.J., Beyhan, S., Navarro, M.V., Yildiz, F.H. and Sondermann, H. (2010) *Vibrio cholerae* VpsT regulates matrix production and motility by directly sensing cyclic di-GMP. *Science*, **327**, 866-868.

167. Bush, M. and Dixon, R. (2012) The role of bacterial enhancer binding proteins as specialized activators of σ54-dependent transcription. *Microbiol. Mol. Biol. Rev.*, **76**, 497-529.

168. He, M., Ouyang, Z., Troxell, B., Xu, H., Moh, A., Piesman, J., Norgard, M.V., Gomelsky, M. and Yang, X.F. (2011) Cyclic di-GMP is essential for the survival of the lyme disease spirochete in ticks. *PLoS Pathog.*, **7**, e1002133.

169. He, M., Zhang, J.J., Ye, M., Lou, Y. and Yang, X.F. (2014) Cyclic Di-GMP receptor PlzA controls virulence gene expression through RpoS in *Borrelia burgdorferi*. *Infect. Immun.*, **82**, 445-452.

170. Kostick, J.L., Szkotnicki, L.T., Rogers, E.A., Bocci, P., Raffaelli, N. and Marconi, R.T. (2011) The diguanylate cyclase, Rrp1, regulates critical steps in the enzootic cycle of the Lyme disease spirochetes. *Mol. Microbiol.*, **81**, 219-231.

171. Pitzer, J.E., Sultan, S.Z., Hayakawa, Y., Hobbs, G., Miller, M.R. and Motaleb, M.A. (2011) Analysis of the *Borrelia burgdorferi* cyclic-di-GMP-binding protein PlzA reveals a role in motility and virulence. *Infect. Immun.*, **79**, 1815-1825.

172. Tischler, A.D., Lee, S.H. and Camilli, A. (2002) The *Vibrio cholerae vieSAB* locus encodes a pathway contributing to cholera toxin production. *J. Bacteriol.*, **184**, 4104-4113.

173. Tischler, A.D. and Camilli, A. (2005) Cyclic diguanylate regulates *Vibrio cholerae* virulence gene expression. *Infect. Immun.*, **73**, 5873-5882.

174. Lewin, B. (2007) *Cells*. Jones and Bartlett Publishers, Scudbury, MA.

175. Schirmer, T. and Jenal, U. (2009) Structural and mechanistic determinants of c-di-GMP signalling. *Nat. Rev. Microbiol.*, **7**, 724-735.

176. Jacobson, K.A. and Boeynaems, J.M. (2010) P2Y nucleotide receptors: promise of therapeutic applications. *Drug Discov. Today*, **15**, 570-578.

177. Feist, A.M., Herrgård, M.J., Thiele, I., Reed, J.L. and Palsson, B. (2009) Reconstruction of biochemical networks in microorganisms. *Nat. Rev. Microbiol.*, **7**, 129-143.

178. Kafsack, B.F. and Llinás, M. (2010) Eating at the table of another: metabolomics of host-parasite interactions. *Cell Host Microbe*, **7**, 90-99.

179. Horai, H., Arita, M., Kanaya, S., Nihei, Y., Ikeda, T., Suwa, K., Ojima, Y., Tanaka, K., Tanaka, S., Aoshima, K. *et al.* (2010) MassBank: a public repository for sharing mass spectral data for life sciences. *J. Mass Spectrom.*, **45**, 703-714.

180. Saito, K. and Matsuda, F. (2010) Metabolomics for functional genomics, systems biology, and biotechnology. *Annu. Rev. Plant Biol.*, **61**, 463-489.

181. Nirenberg, M. and Leder, P. (1964) RNA Codewords and Protein Synthesis. The Effect of Trinucleotides Upon the Binding of SRNA to Ribosomes. *Science*, **145**, 1399-1407.

182. Northup, J.K., Sternweis, P.C., Smigel, M.D., Schleifer, L.S., Ross, E.M. and Gilman, A.G. (1980) Purification of the regulatory component of adenylate cyclase. *Proc. Natl. Acad. Sci. U S A*, **77**, 6516-6520.

183. Wong, I. and Lohman, T.M. (1993) A double-filter method for nitrocellulose-filter binding: application to protein-nucleic acid interactions. *Proc. Natl. Acad. Sci. U S A*, **90**, 5428-5432.

184. Sturtevant, J.M. (1974) Some applications of calorimetry in biochemistry and biology. *Annu. Rev. Biophys. Bioeng.*, **3**, 35-51.

185. Alfthan, K. (1998) Surface plasmon resonance biosensors as a tool in antibody engineering. *Biosens. Bioelectron.*, **13**, 653-663.

186. Vuignier, K., Schappler, J., Veuthey, J.L., Carrupt, P.A. and Martel, S. (2010) Drug-protein binding: a critical review of analytical tools. *Anal. Bioanal. Chem.*, **398**, 53-66.

187. Zhu, H. and Snyder, M. (2003) Protein chip technology. *Curr. Opin. Chem. Biol.*, **7**, 55-63.

188. Zhu, H., Klemic, J.F., Chang, S., Bertone, P., Casamayor, A., Klemic, K.G., Smith, D., Gerstein, M., Reed, M.A. and Snyder, M. (2000) Analysis of yeast protein kinases using protein chips. *Nat. Genet.*, **26**, 283-289.

189. Zhu, H., Bilgin, M., Bangham, R., Hall, D., Casamayor, A., Bertone, P., Lan, N., Jansen, R., Bidlingmaier, S., Houfek, T. *et al.* (2001) Global analysis of protein activities using proteome chips. *Science*, **293**, 2101-2105.

190. Jones, R.B., Gordus, A., Krall, J.A. and MacBeath, G. (2006) A quantitative protein interaction network for the ErbB receptors using protein microarrays. *Nature*, **439**, 168-174.

191. Merighi, M., Lee, V., Hyodo, M., Hayakawa, Y. and Lory, S. (2007) The second messenger bis-(3'-5')-cyclic-GMP and its PilZ domain-containing receptor Alg44 are required for alginate biosynthesis in *Pseudomonas aeruginosa*. *Mol. Microbiol.*, **65**, 876-895.

192. Zubay, G., Schwartz, D. and Beckwith, J. (1970) Mechanism of activation of catabolite-sensitive genes: a positive control system. *Proc. Natl. Acad. Sci. U S A*, **66**, 104-110.

193. Ninfa, A.J. and Magasanik, B. (1986) Covalent modification of the glnG product, NRI, by the glnL product, NRII, regulates the transcription of the glnALG operon in Escherichia coli. *Proc. Natl. Acad. Sci. U S A*, **83**, 5909-5913.

194. Camilli, A. and Bassler, B.L. (2006) Bacterial small-molecule signaling pathways. *Science*, **311**, 1113-1116.

195. Boehm, A., Kaiser, M., Li, H., Spangler, C., Kasper, C.A., Ackermann, M., Kaever, V., Sourjik, V., Roth, V. and Jenal, U. (2010) Second messenger-mediated adjustment of bacterial swimming velocity. *Cell*, **141**, 107-116.

196. Paul, K., Nieto, V., Carlquist, W.C., Blair, D.F. and Harshey, R.M. (2010) The c-di-GMP binding protein YcgR controls flagellar motor direction and speed to affect chemotaxis by a "backstop brake" mechanism. *Mol. Cell*, **38**, 128-139.

197. Chen, W., Kuolee, R. and Yan, H. (2010) The potential of 3',5'-cyclic diguanylic acid (c-di-GMP) as an effective vaccine adjuvant. *Vaccine*, **28**, 3080-3085.

198. Kulasekara, H.D., Ventre, I., Kulasekara, B.R., Lazdunski, A., Filloux, A. and Lory, S. (2005) A novel two-component system controls the expression of Pseudomonas aeruginosa fimbrial cup genes. *Mol. Microbiol.*, **55**, 368-380.

199. Lee, V., Matewish, J., Kessler, J., Hyodo, M., Hayakawa, Y. and Lory, S. (2007) A cyclic-di-GMP receptor required for bacterial exopolysaccharide production. *Mol. Microbiol.*, **65**, 1474-1484.

200. Galperin, M.Y. (2005) A census of membrane-bound and intracellular signal transduction proteins in bacteria: bacterial IQ, extroverts and introverts. *BMC Microbiol.*, **5**, 35.

201. Knickerbocker, T., Chen, J.R., Thadhani, R. and MacBeath, G. (2007) An integrated approach to prognosis using protein microarrays and nonparametric methods. *Mol. Syst. Biol.*, **3**, 123.

202. MacBeath, G. (2002) Protein microarrays and proteomics. *Nat. Genet.*, **32**, 526-532.

203. Fields, S. and Song, O. (1989) A novel genetic system to detect protein-protein interactions. *Nature*, **340**, 245-246.

204. Velmurugan, K., Chen, B., Miller, J.L., Azogue, S., Gurses, S., Hsu, T., Glickman, M., Jacobs, W.R., Porcelli, S.A. and Briken, V. (2007) *Mycobacterium tuberculosis nuoG* is a virulence gene that inhibits apoptosis of infected host cells. *PLoS Pathog.*, **3**, e110.

205. White, L.A. and Kellogg, D.S. (1965) An improved fermentation medium for Neisseria gonorrhoeae and other *Neisseria*. *Health Lab. Sci.*, **2**, 238-241.

206. Galperin, M.Y., Natale, D.A., Aravind, L. and Koonin, E.V. (1999) A specialized version of the HD hydrolase domain implicated in signal transduction. *J Mol. Microbiol. Biotechnol.*, **1**, 303-305.

207. Aldridge, P., Paul, R., Goymer, P., Rainey, P. and Jenal, U. (2003) Role of the GGDEF regulator PleD in polar development of *Caulobacter crescentus*. *Mol. Microbiol.*, **47**, 1695-1708.

208. Nesper, J., Reinders, A., Glatter, T., Schmidt, A. and Jenal, U. (2012) A novel capture compound for the identification and analysis of cyclic di-GMP binding proteins. *J. Proteomics*, **75**, 4874-4878.

209. Roelofs, K.G., Wang, J., Sintim, H.O. and Lee, V.T. (2011) Differential radial capillary action of ligand assay for high-throughput detection of protein-metabolite interactions. *Proc. Natl. Acad. Sci. U S A*, **108**, 15528-15533.

210. Kitagawa, M., Ara, T., Arifuzzaman, M., Ioka-Nakamichi, T., Inamoto, E., Toyonaga, H. and Mori, H. (2005) Complete set of ORF clones of *Escherichia coli* ASKA library (a complete set of E. coli K-12 ORF archive): unique resources for biological research. *DNA Res.*, **12**, 291-299.

211. Camus, J.C., Pryor, M.J., Médigue, C. and Cole, S.T. (2002) Re-annotation of the genome sequence of *Mycobacterium tuberculosis* H37Rv. *Microbiology*, **148**, 2967-2973.

212. Deng, W., Burland, V., Plunkett, G., Boutin, A., Mayhew, G.F., Liss, P., Perna, N.T., Rose, D.J., Mau, B., Zhou, S. *et al.* (2002) Genome sequence of *Yersinia pestis* KIM. *J. Bacteriol.*, **184**, 4601-4611.

213. Rolfs, A., Montor, W.R., Yoon, S.S., Hu, Y., Bhullar, B., Kelley, F., McCarron, S., Jepson, D.A., Shen, B., Taycher, E. *et al.* (2008) Production and sequence validation of a complete full length ORF collection for the pathogenic bacterium *Vibrio cholerae*. *Proc. Natl. Acad. Sci. U S A*, **105**, 4364-4369.

214. Hartley, J.L., Temple, G.F. and Brasch, M.A. (2000) DNA cloning using in vitro site-specific recombination. *Genome Res.*, **10**, 1788-1795.

215. Kapust, R.B. and Waugh, D.S. (1999) *Escherichia coli* maltose-binding protein is uncommonly effective at promoting the solubility of polypeptides to which it is fused. *Protein Sci.*, **8**, 1668-1674.

216. Hunter, J.L., Severin, G.B., Koestler, B.J. and Waters, C.M. (2014) The *Vibrio cholerae* diguanylate cyclase VCA0965 has an AGDEF active site and synthesizes cyclic di-GMP. *BMC Microbiol.*, **14**, 22.

217. Hammer, B.K. and Bassler, B.L. (2009) Distinct sensory pathways in *Vibrio cholerae* El Tor and classical biotypes modulate cyclic dimeric GMP levels to control biofilm formation. *J. Bacteriol.*, **191**, 169-177.

218. Rao, F., Qi, Y., Chong, H.S., Kotaka, M., Li, B., Li, J., Lescar, J., Tang, K. and Liang, Z.X. (2009) The functional role of a conserved loop in EAL domain-based cyclic di-GMP-specific phosphodiesterase. *J. Bacteriol.*, **191**, 4722-4731.

219. Waters, C.M., Lu, W., Rabinowitz, J.D. and Bassler, B.L. (2008) Quorum sensing controls biofilm formation in *Vibrio cholerae* through modulation of cyclic di-GMP levels and repression of *vpsT*. *J. Bacteriol.*, **190**, 2527-2536.

220. Liu, X., Beyhan, S., Lim, B., Linington, R.G. and Yildiz, F.H. (2010) Identification and characterization of a phosphodiesterase that inversely regulates motility and biofilm formation in *Vibrio cholerae*. *J. Bacteriol.*, **192**, 4541-4552.

221. Pratt, J.T., McDonough, E. and Camilli, A. (2009) PhoB regulates motility, biofilms, and cyclic di-GMP in *Vibrio cholerae*. *J. Bacteriol.*, **191**, 6632-6642.

222. Tamayo, R., Schild, S., Pratt, J.T. and Camilli, A. (2008) Role of cyclic Di-GMP during el tor biotype *Vibrio cholerae* infection: characterization of the in vivo-induced cyclic Di-GMP phosphodiesterase CdpA. *Infect. Immun.*, **76**, 1617-1627.

223. Marsh, J.W. and Taylor, R.K. (1999) Genetic and transcriptional analyses of the *Vibrio cholerae* mannose-sensitive hemagglutinin type 4 pilus gene locus. *J. Bacteriol.*, **181**, 1110-1117.

224. Hsiao, A., Liu, Z., Joelsson, A. and Zhu, J. (2006) *Vibrio cholerae* virulence regulator-coordinated evasion of host immunity. *Proc. Natl. Acad. Sci. U S A*, **103**, 14542-14547.

225. Watnick, P.I., Fullner, K.J. and Kolter, R. (1999) A role for the mannose-sensitive hemagglutinin in biofilm formation by *Vibrio cholerae* El Tor. *J. Bacteriol.*, **181**, 3606-3609.

226. Watnick, P.I. and Kolter, R. (1999) Steps in the development of a *Vibrio cholerae* El Tor biofilm. *Mol. Microbiol.*, **34**, 586-595.

227. Moorthy, S. and Watnick, P.I. (2004) Genetic evidence that the *Vibrio cholerae* monolayer is a distinct stage in biofilm development. *Mol. Microbiol.*, **52**, 573-587.

228. Chiavelli, D.A., Marsh, J.W. and Taylor, R.K. (2001) The mannose-sensitive hemagglutinin of *Vibrio cholerae* promotes adherence to zooplankton. *Appl. Environ. Microbiol.*, **67**, 3220-3225.

229. Klose, K.E., Novik, V. and Mekalanos, J.J. (1998) Identification of multiple sigma54-dependent transcriptional activators in *Vibrio cholerae*. *J. Bacteriol.*, **180**, 5256-5259.

230. Prouty, M.G., Correa, N.E. and Klose, K.E. (2001) The novel sigma54- and sigma28-dependent flagellar gene transcription hierarchy of *Vibrio cholerae*. *Mol. Microbiol.*, **39**, 1595-1609.

231. Dong, T.G. and Mekalanos, J.J. (2012) Characterization of the RpoN regulon reveals differential regulation of T6SS and new flagellar operons in *Vibrio cholerae* O37 strain V52. *Nucleic Acids Res*, **40**, 7766-7775.

232. Rao, N.N. and Torriani, A. (1990) Molecular aspects of phosphate transport in *Escherichia coli. Mol. Microbiol.*, **4**, 1083-1090.

233. Wanner, B.L. (1996) Signal transduction in the control of phosphate-regulated genes of *Escherichia coli*. *Kidney Int.*, **49**, 964-967.

234. Kornberg, A., Rao, N.N. and Ault-Riché, D. (1999) Inorganic polyphosphate: a molecule of many functions. *Annu. Rev. Biochem.*, **68**, 89-125.

235. Shi, X., Rao, N.N. and Kornberg, A. (2004) Inorganic polyphosphate in Bacillus cereus: motility, biofilm formation, and sporulation. *Proc. Natl. Acad. Sci. U S A*, **101**, 17061-17065.

236. Shi, T., Fu, T. and Xie, J. (2011) Polyphosphate deficiency affects the sliding motility and biofilm formation of *Mycobacterium smegmatis*. *Curr. Microbiol.*, **63**, 470-476.

237. Zhang, H., Rao, N.N., Shiba, T. and Kornberg, A. (2005) Inorganic polyphosphate in the social life of *Myxococcus xanthus*: motility, development, and predation. *Proc. Natl. Acad. Sci. U S A*, **102**, 13416-13420.

238. Malde, A., Gangaiah, D., Chandrashekhar, K., Pina-Mimbela, R., Torrelles, J.B. and Rajashekara, G. (2014) Functional characterization of exopolyphosphatase/guanosine pentaphosphate phosphohydrolase (PPX/GPPA) of *Campylobacter jejuni*. *Virulence*, **5**.

239. Kuchma, S.L., Griffin, E.F. and O'Toole, G.A. (2012) Minor pilins of the type IV pilus system participate in the negative regulation of swarming motility. *J. Bacteriol.*, **194**, 5388-5403.

240. O'Toole, G.A. and Kolter, R. (1998) Flagellar and twitching motility are necessary for *Pseudomonas aeruginosa* biofilm development. *Mol. Microbiol.*, **30**, 295-304.

241. Burrows, L.L. (2012) *Pseudomonas aeruginosa* twitching motility: type IV pili in action. *Annu. Rev. Microbiol.*, **66**, 493-520.

242. Ryan, R.P., McCarthy, Y., Kiely, P.A., O'Connor, R., Farah, C.S., Armitage, J.P. and Dow, J.M. (2012) Dynamic complex formation between HD-GYP, GGDEF and PilZ domain proteins regulates motility in *Xanthomonas campestris*. *Mol. Microbiol.*, **86**, 557-567.

243. Guzzo, C.R. and Farah, C.S. (2009) Expression, crystallization and preliminary crystallographic analysis of PilZ(XAC1133) from *Xanthomonas axonopodis pv. citri*. *Acta. Crystallogr. Sect. F. Struct. Biol. Cryst. Commun.*, **65**, 304-306.

244. Guzzo, C.R., Dunger, G., Salinas, R.K. and Farah, C.S. (2013) Structure of the PilZ-FimXEAL-c-di-GMP Complex Responsible for the Regulation of Bacterial Type IV Pilus Biogenesis. *J. Mol. Biol.*, **425**, 2174-2197.

245. Peabody, C.R., Chung, Y.J., Yen, M.R., Vidal-Ingigliardi, D., Pugsley, A.P. and Saier, M.H. (2003) Type II protein secretion and its relationship to bacterial type IV pili and archaeal flagella. *Microbiology*, **149**, 3051-3072.

246. Turner, L.R., Lara, J.C., Nunn, D.N. and Lory, S. (1993) Mutations in the consensus ATP-binding sites of XcpR and PilB eliminate extracellular protein secretion and pilus biogenesis in *Pseudomonas aeruginosa*. *J. Bacteriol.*, **175**, 4962-4969.

247. Turner, L.R., Olson, J.W. and Lory, S. (1997) The XcpR protein of *Pseudomonas aeruginosa* dimerizes via its N-terminus. *Mol. Microbiol.*, **26**, 877-887.

248. Robien, M.A., Krumm, B.E., Sandkvist, M. and Hol, W.G. (2003) Crystal structure of the extracellular protein secretion NTPase EpsE of *Vibrio cholerae*. *J. Mol. Biol.*, **333**, 657-674.

249. Camberg, J.L. and Sandkvist, M. (2005) Molecular analysis of the *Vibrio cholerae* type II secretion ATPase EpsE. *J. Bacteriol.*, **187**, 249-256.

250. Camberg, J.L., Johnson, T.L., Patrick, M., Abendroth, J., Hol, W.G. and Sandkvist, M. (2007) Synergistic stimulation of EpsE ATP hydrolysis by EpsL and acidic phospholipids. *EMBO J.*, **26**, 19-27.

251. Patrick, M., Korotkov, K.V., Hol, W.G. and Sandkvist, M. (2011) Oligomerization of EpsE coordinates residues from multiple subunits to facilitate ATPase activity. *J. Biol. Chem.*, **286**, 10378-10386.

252. Lu, C., Turley, S., Marionni, S.T., Park, Y.J., Lee, K.K., Patrick, M., Shah, R., Sandkvist, M., Bush, M.F. and Hol, W.G. (2013) Hexamers of the type II secretion ATPase GspE from *Vibrio cholerae* with increased ATPase activity. *Structure*, **21**, 1707-1717.

253. Benach, J., Swaminathan, S.S., Tamayo, R., Handelman, S.K., Folta-Stogniew, E., Ramos, J.E., Forouhar, F., Neely, H., Seetharaman, J., Camilli, A. *et al.* (2007) The structural basis of cyclic diguanylate signal transduction by PilZ domains. *EMBO J.*, **26**, 5153-5166.

254. Corrigan, R.M., Campeotto, I., Jeganathan, T., Roelofs, K.G., Lee, V.T. and Gründling, A. (2013) Systematic identification of conserved bacterial c-di-AMP receptor proteins. *Proc. Natl. Acad. Sci. U S A*, **110**, 9084-9089.

255. Rual, J.F., Hill, D.E. and Vidal, M. (2004) ORFeome projects: gateway between genomics and omics. *Curr. Opin. Chem. Biol.*, **8**, 20-25.

256. Martzen, M.R., McCraith, S.M., Spinelli, S.L., Torres, F.M., Fields, S., Grayhack, E.J. and Phizicky, E.M. (1999) A biochemical genomics approach for identifying genes by the activity of their products. *Science*, **286**, 1153-1155.

257. MacBeath, G. and Schreiber, S.L. (2000) Printing proteins as microarrays for high-throughput function determination. *Science*, **289**, 1760-1763.

258. Zhu, H. and Snyder, M. (2001) Protein arrays and microarrays. *Curr. Opin. Chem. Biol.*, **5**, 40-45.

259. Schild, S., Tamayo, R., Nelson, E.J., Qadri, F., Calderwood, S.B. and Camilli, A. (2007) Genes induced late in infection increase fitness of *Vibrio cholerae* after release into the environment. *Cell Host Microbe*, **2**, 264-277.

260. Beyhan, S., Tischler, A.D., Camilli, A. and Yildiz, F.H. (2006) Transcriptome and phenotypic responses of *Vibrio cholerae* to increased cyclic di-GMP level. *J. Bacteriol.*, **188**, 3600-3613.

261. Pittard, J., Camakaris, H. and Yang, J. (2005) The TyrR regulon. *Mol. Microbiol.*, **55**, 16-26.

262. Guzzo, C.R., Salinas, R.K., Andrade, M.O. and Farah, C.S. (2009) PILZ protein structure and interactions with PILB and the FIMX EAL domain: implications for control of type IV pilus biogenesis. *J. Mol. Biol.*, **393**, 848-866.

263. Jain, R., Behrens, A.J., Kaever, V. and Kazmierczak, B.I. (2012) Type IV pilus assembly in *Pseudomonas aeruginosa* over a broad range of cyclic di-GMP concentrations. *J. Bacteriol.*, **194**, 4285-4294.

264. McLaughlin, L.S., Haft, R.J. and Forest, K.T. (2012) Structural insights into the Type II secretion nanomachine. *Curr. Opin. Struct. Biol.*, **22**, 208-216.

265. de Crombrugghe, B., Busby, S. and Buc, H. (1984) Cyclic AMP receptor protein: role in transcription activation. *Science*, **224**, 831-838.

266. Garges, S. and Adhya, S. (1985) Sites of allosteric shift in the structure of the cyclic AMP receptor protein. *Cell*, **41**, 745-751.

267. Gunasekera, A., Ebright, Y.W. and Ebright, R.H. (1992) DNA sequence determinants for binding of the *Escherichia coli* catabolite gene activator protein. *J. Biol. Chem.*, **267**, 14713-14720.

268. Green, N. M. (1963) AVIDIN. 1. The Use of (14-C)Biotin for Kinetic Studies and for Assay. *Biochem. J.*, **89**, 585-591.

269. Pastan, I. and Perlman, R. (1970) Cyclic adenosine monophosphate in bacteria. *Science*, **169**, 339-344.

270. Adhya, S. and Miller, W. (1979) Modulation of the two promoters of the galactose operon of *Escherichia coli*. *Nature*, **279**, 492-494.

271. Irani, M.H., Orosz, L. and Adhya, S. (1983) A control element within a structural gene: the gal operon of *Escherichia coli*. *Cell*, **32**, 783-788.

272. Busby, S., Aiba, H. and de Crombrugghe, B. (1982) Mutations in the *Escherichia coli* operon that define two promoters and the binding site of the cyclic AMP receptor protein. *J. Mol. Biol.*, **154**, 211-227.

273. Meiklejohn, A.L. and Gralla, J.D. (1985) Entry of RNA polymerase at the *lac* promoter. *Cell*, **43**, 769-776.

274. Riggs, A.D., Reiness, G. and Zubay, G. (1971) Purification and DNA-binding properties of the catabolite gene activator protein. *Proc. Natl. Acad. Sci. U S A*, **68**, 1222-1225.

275. Fried, M.G. and Crothers, D.M. (1984) Equilibrium studies of the cyclic AMP receptor protein-DNA interaction. *J. Mol. Biol.*, **172**, 241-262.

276. Fried, M.G. and Crothers, D.M. (1984) Kinetics and mechanism in the reaction of gene regulatory proteins with DNA. *J. Mol. Biol.*, **172**, 263-282.

277. Fried, M. and Crothers, D.M. (1981) Equilibria and kinetics of lac repressor-operator interactions by polyacrylamide gel electrophoresis. *Nucleic Acids Res.*, **9**, 6505-6525.

278. Garner, M.M. and Revzin, A. (1981) A gel electrophoresis method for quantifying the binding of proteins to specific DNA regions: application to components of the *Escherichia coli* lactose operon regulatory system. *Nucleic Acids Res.*, **9**, 3047-3060.

279. Revzin, A., Ceglarek, J.A. and Garner, M.M. (1986) Comparison of nucleic acid-protein interactions in solution and in polyacrylamide gels. *Anal. Biochem.*, **153**, 172-177.

280. Savery, N.J., Lloyd, G.S., Kainz, M., Gaal, T., Ross, W., Ebright, R.H., Gourse, R.L. and Busby, S.J. (1998) Transcription activation at Class II CRP-dependent promoters: identification of determinants in the C-terminal domain of the RNA polymerase alpha subunit. *EMBO J.*, **17**, 3439-3447.

281. Iyer, V.R., Horak, C.E., Scafe, C.S., Botstein, D., Snyder, M. and Brown, P.O. (2001) Genomic binding sites of the yeast cell-cycle transcription factors SBF and MBF. *Nature*, **409**, 533-538.

282. Ren, B., Robert, F., Wyrick, J.J., Aparicio, O., Jennings, E.G., Simon, I., Zeitlinger, J., Schreiber, J., Hannett, N., Kanin, E. *et al.* (2000) Genome-wide location and function of DNA binding proteins. *Science*, **290**, 2306-2309.

283. Grainger, D.C., Hurd, D., Harrison, M., Holdstock, J. and Busby, S.J. (2005) Studies of the distribution of *Escherichia coli* cAMP-receptor protein and RNA polymerase along the *E. coli* chromosome. *Proc. Natl. Acad. Sci. U S A*, **102**, 17693-17698.

284. Wiseman, T., Williston, S., Brandts, J.F. and Lin, L.N. (1989) Rapid measurement of binding constants and heats of binding using a new titration calorimeter. *Anal. Biochem.*, **179**, 131-137.

285. Pockrand, I., Swalen, J.D., Gordon, J.G. and Philpott, M.R. (1978) Surface plasmon spectroscopy of organic monolayer assemblies. *Surface Sci.*, **74**, 237-244.

286. Bondeson, K., Frostell-Karlsson, A., Fägerstam, L. and Magnusson, G. (1993) Lactose repressor-operator DNA interactions: kinetic analysis by a surface plasmon resonance biosensor. *Anal. Biochem.*, **214**, 245-251.

287. Winkler, W.C., Cohen-Chalamish, S. and Breaker, R.R. (2002) An mRNA structure that controls gene expression by binding FMN. *Proc. Natl. Acad. Sci. U S A*, **99**, 15908-15913.

288. Winkler, W., Nahvi, A. and Breaker, R.R. (2002) Thiamine derivatives bind messenger RNAs directly to regulate bacterial gene expression. *Nature*, **419**, 952-956.

289. Nahvi, A., Barrick, J.E. and Breaker, R.R. (2004) Coenzyme B12 riboswitches are widespread genetic control elements in prokaryotes. *Nucleic Acids Res.*, **32**, 143-150.

290. Epshtein, V., Mironov, A.S. and Nudler, E. (2003) The riboswitch-mediated control of sulfur metabolism in bacteria. *Proc. Natl. Acad. Sci. U S A*, **100**, 5052-5056.

291. Waters, L.S. and Storz, G. (2009) Regulatory RNAs in bacteria. *Cell*, **136**, 615-628.

292. Hannon, G.J. and Rossi, J.J. (2004) Unlocking the potential of the human genome with RNA interference. *Nature*, **431**, 371-378.

293. Lu, Y., Shi, W., Qin, J. and Lin, B. (2010) Fabrication and characterization of paper-based microfluidics prepared in nitrocellulose membrane by wax printing. *Anal Chem*, **82**, 329-335.

294. Revzin, A., Ceglarek, J.A. and Garner, M.M. (1986) Comparison of nucleic acid-protein interactions in solution and in polyacrylamide gels. *Anal. Biochem.*, **153**, 172-177.

295. Düvel, J., Bertinetti, D., Möller, S., Schwede, F., Morr, M., Wissing, J., Radamm, L., Zimmermann, B., Genieser, H.G., Jänsch, L. *et al.* (2012) A chemical proteomics approach to identify c-di-GMP binding proteins in *Pseudomonas aeruginosa*. *J. Microbiol. Methods*, **88**, 229-236.

296. Wang, J., Zhou, J., Donaldson, G.P., Nakayama, S., Yan, L., Lam, Y.F., Lee, V.T. and Sintim, H.O. (2011) Conservative change to the phosphate moiety of cyclic diguanylic monophosphate remarkably affects its polymorphism and ability to bind DGC, PDE, and PilZ proteins. *J. Am. Chem. Soc.*, **133**, 9320-9330.

297. Zhou, J., Watt, S., Wang, J., Nakayama, S., Sayre, D.A., Lam, Y.F., Lee, V.T. and Sintim, H.O. (2013) Potent suppression of c-di-GMP synthesis via I-site allosteric inhibition of diguanylate cyclases with 2'-F-c-di-GMP. *Bioorg. Med. Chem.*, **21**, 4396-4404.

298. Donaldson, G.P., Roelofs, K.G., Luo, Y., Sintim, H.O. and Lee, V.T. (2012) A rapid assay for affinity and kinetics of molecular interactions with nucleic acids. *Nucleic Acids Res.*, **40**, e48.

299. Paul, K., Nieto, V., Carlquist, W.C., Blair, D.F. and Harshey, R.M. (2010) The c-di-GMP binding protein YcgR controls flagellar motor direction and speed to affect chemotaxis by a "backstop brake" mechanism. *Mol. Cell*, **38**, 128-139.

300. Fang, X. and Gomelsky, M. (2010) A post-translational, c-di-GMP-dependent mechanism regulating flagellar motility. *Mol. Microbiol.*, **76**, 1295-1305.

301. Wolfe, A.J. and Berg, H.C. (1989) Migration of bacteria in semisolid agar. *Proc. Natl. Acad. Sci. U S A*, **86**, 6973-6977.

302. Alm, R.A., Bodero, A.J., Free, P.D. and Mattick, J.S. (1996) Identification of a novel gene, pilZ, essential for type 4 fimbrial biogenesis in *Pseudomonas aeruginosa*. *J. Bacteriol.*, **178**, 46-53.

303. Hazes, B. and Frost, L. (2008) Towards a systems biology approach to study type II/IV secretion systems. *Biochim. Biophys. Acta.*, **1778**, 1839-1850.

304. Ayers, M., Howell, P.L. and Burrows, L.L. (2010) Architecture of the type II secretion and type IV pilus machineries. *Future Microbiol.*, **5**, 1203-1218.

305. Chiang, P. and Burrows, L.L. (2003) Biofilm formation by hyperpiliated mutants of *Pseudomonas aeruginosa*. *J. Bacteriol.*, **185**, 2374-2378.

306. Chiang, P., Habash, M. and Burrows, L.L. (2005) Disparate subcellular localization patterns of *Pseudomonas aeruginosa* Type IV pilus ATPases involved in twitching motility. *J. Bacteriol.*, **187**, 829-839.

307. Chiang, P., Sampaleanu, L.M., Ayers, M., Pahuta, M., Howell, P.L. and Burrows, L.L. (2008) Functional role of conserved residues in the characteristic secretion NTPase motifs of the *Pseudomonas aeruginosa* type IV pilus motor proteins PilB, PilT and PilU. *Microbiology*, **154**, 114-126.

308. Ball, G., Chapon-Hervé, V., Bleves, S., Michel, G. and Bally, M. (1999) Assembly of XcpR in the cytoplasmic membrane is required for extracellular protein secretion in *Pseudomonas aeruginosa*. *J. Bacteriol.*, **181**, 382-388.

309. Ball, G., Durand, E., Lazdunski, A. and Filloux, A. (2002) A novel type II secretion system in Pseudomonas aeruginosa. *Mol. Microbiol.*, **43**, 475-485.

310. Wozniak, D.J. and Ohman, D.E. (1991) *Pseudomonas aeruginosa* AlgB, a two-component response regulator of the NtrC family, is required for *algD* transcription. *J. Bacteriol.*, **173**, 1406-1413.

311. Leech, A.J., Sprinkle, A., Wood, L., Wozniak, D.J. and Ohman, D.E. (2008) The NtrC family regulator AlgB, which controls alginate biosynthesis in mucoid Pseudomonas aeruginosa, binds directly to the *algD* promoter. *J. Bacteriol.*, **190**, 581-589.

312. Peabody, D.S. (1993) The RNA binding site of bacteriophage MS2 coat protein. *EMBO J.*, **12**, 595-600.

313. Keryer-Bibens, C., Barreau, C. and Osborne, H.B. (2008) Tethering of proteins to RNAs by bacteriophage proteins. *Biol. Cell*, **100**, 125-138.

314. Shtatland, T., Gill, S.C., Javornik, B.E., Johansson, H.E., Singer, B.S., Uhlenbeck, O.C., Zichi, D.A. and Gold, L. (2000) Interactions of iRNA with bacteriophage MS2 coat protein: genomic SELEX. *Nucleic Acids Res.*, **28**, E93.

315. Pesavento, C. and Hengge, R. (2009) Bacterial nucleotide-based second messengers. *Curr. Opin. Microbiol.*, **12**, 170-176.

316. Gomelsky, M. (2011) cAMP, c-di-GMP, c-di-AMP and now cGMP: bacteria use them all! *Mol. Microbiol.*, **79**, 562-565.

317. Davies, B.W., Bogard, R.W., Young, T.S. and Mekalanos, J.J. (2012) Coordinated regulation of accessory genetic elements produces cyclic di-nucleotides for *V. cholerae* virulence. *Cell*, **149**, 358-370.

318. Sun, L., Wu, J., Du, F., Chen, X. and Chen, Z.J. (2013) Cyclic GMP-AMP synthase is a cytosolic DNA sensor that activates the type I interferon pathway. *Science*, **339**, 786-791.

319. Yin, Q., Tian, Y., Kabaleeswaran, V., Jiang, X., Tu, D., Eck, M.J., Chen, Z.J. and Wu, H. (2012) Cyclic di-GMP sensing via the innate immune signaling protein STING. *Mol. Cell*, **46**, 735-745.

320. Wu, J., Sun, L., Chen, X., Du, F., Shi, H., Chen, C. and Chen, Z.J. (2013) Cyclic GMP-AMP is an endogenous second messenger in innate immune signaling by cytosolic DNA. *Science*, **339**, 826-830.

321. Zhang, X., Shi, H., Wu, J., Sun, L., Chen, C. and Chen, Z.J. (2013) Cyclic GMP-AMP containing mixed phosphodiester linkages is an endogenous high-affinity ligand for STING. *Mol. Cell*, **51**, 226-235.

322. Shang, F., Xue, T., Sun, H., Xing, L., Zhang, S., Yang, Z., Zhang, L. and Sun, B. (2009) The *Staphylococcus aureus* GGDEF domain-containing protein, GdpS, influences protein A gene expression in a cyclic diguanylic acid-independent manner. *Infect. Immun.*, **77**, 2849-2856.

323. Holland, L.M., O'Donnell, S.T., Ryjenkov, D.A., Gomelsky, L., Slater, S.R., Fey, P.D., Gomelsky, M. and O'Gara, J.P. (2008) A staphylococcal GGDEF domain protein regulates biofilm formation independently of cyclic dimeric GMP. *J. Bacteriol.*, **190**, 5178-5189.

324. Ude, S., Arnold, D.L., Moon, C.D., Timms-Wilson, T. and Spiers, A.J. (2006) Biofilm formation and cellulose expression among diverse environmental *Pseudomonas* isolates. *Environ. Microbiol.*, **8**, 1997-2011.

325. Brouillette, E., Hyodo, M., Hayakawa, Y., Karaolis, D.K. and Malouin, F. (2005) 3',5'-cyclic diguanylic acid reduces the virulence of biofilm-forming *Staphylococcus aureus* strains in a mouse model of mastitis infection. *Antimicrob. Agents Chemother.*, **49**, 3109-3113.

326. Johnson, J.G. and Clegg, S. (2010) Role of MrkJ, a phosphodiesterase, in type 3 fimbrial expression and biofilm formation in *Klebsiella pneumoniae*. *J. Bacteriol.*, **192**, 3944-3950.

327. Karaolis, D.K., Cheng, K., Lipsky, M., Elnabawi, A., Catalano, J., Hyodo, M., Hayakawa, Y. and Raufman, J.P. (2005) 3',5'-Cyclic diguanylic acid (c-di-GMP) inhibits basal and growth factor-stimulated human colon cancer cell proliferation. *Biochem. Biophys. Res. Commun.*, **329**, 40-45.